PRECLINICAL CHARACTERIZATION OF TRAUMATIC BRAIN INJURY PATHOPHYSIOLOGY AND ASSOCIATED FUNCTIONAL OUTCOMES

by

HOLLY A. KINDER

(Under the Direction of Franklin D. West)

ABSTRACT

Traumatic brain injury (TBI) is a leading cause of long-term disability and death in the United States. Young children are particularly susceptible to sustaining a concussive TBI as the result of a fall, and it is well established that TBI at a young age can lead to short- and long-term functional deficits in learning and memory, behavior, and motor function. The development of functional deficits may be attributed to damage to cortical regions, sub-cortical white matter, or major limbic structures such as the hippocampus, either as a result of primary or secondary injury mechanisms. The secondary injury cascade, usually characterized by pathophysiologic changes like blood brain barrier damage, decreased cerebral blood flow, astrogliosis, and microglia activation, leads to neuronal death, axonal injury, white matter disruption and ultimately, the development of functional impairments. Currently, there are no Food and Drug Administration (FDA)-approved therapies for TBI that demonstrate significant neuroprotective or restorative effects that mitigate the development of functional deficits. Therefore, it is of interest to study TBI pathophysiology and corresponding functional responses in large animal models like the pig that may have more similar responses to injury and greater predictive power in identifying potential therapeutics. The objectives of these studies were to 1) develop a piglet

TBI model and characterize pathophysiologic mechanisms in response to injury severity and time course, and 2) assess changes in cognition, behavior, and motor function as a result of TBI.

INDEX WORDS: Traumatic Brain Injury, Cognition, Behavior, Motor Function

PRECLINICAL CHARACTERIZATION OF TRAUMATIC BRAIN INJURY PATHOPHYSIOLOGY AND ASSOCIATED FUNCTIONAL OUTCOMES

by

HOLLY A. KINDER

B.S.A., University of Georgia, 2012

A Dissertation Submitted to the Graduate Faculty of The University of Georgia in Partial Fulfillment of the Requirements for the Degree

DOCTOR OF PHILOSOPHY

ATHENS, GEORGIA

2017

PRECLINICAL CHARACTERIZATION OF TRAUMATIC BRAIN INJURY PATHOPHYSIOLOGY AND ASSOCIATED FUNCTIONAL OUTCOMES

by

HOLLY A. KINDER

Major Professor:	Franklin D. West
Committee:	Steven L. Stice
	Elizabeth W. Howerth
	Simon R. Platt

Electronic Version Approved:

Suzanne Barbour
Dean of the Graduate School
The University of Georgia
August 2017

ACKNOWLEDGEMENTS

First and foremost, I have to thank my boss, my mentor, and my friend, Franklin West, for his support and guidance these last 5 years. It's certainly been a journey! Who could predict that it would take us almost 4 years to complete Aim 1 of your master plan because, you know, science. You've gone above and beyond the call of duty for a mentor, and I'll never be able to thank you enough for molding me into the scientist that I am today. Your passion for science is contagious, and I thank you for sharing it with me and so many others. Thank you from the bottom of my heart for truly being the world's best boss. To Emily, you are the only person I can happily share an office with every single day for 5 years. Thank you for laughing at my jokes no matter how stupid they are, for "winging it" through far too many experiments with me, for your support and advice, and most importantly, for your friendship. It's been a joy incessantly teasing Frank with you (Frank pullin' a Frank!) and optimizing all the things. Science Soul Mates for life! Thank you to my other committee members Dr. Steve Stice, Dr. Buffy Howerth, and Dr. Simon Platt for all your help and guidance and for being so invested in my research. Thank you to the amazing past and present West lab members- Jessica, Vivian, Erin, Beth, Madelaine, Kelly, and Monika- for your help and encouragement #westlabisthebestlab. To my fiancée Danny, thank you for your unwavering love and support, for always pushing me forward, for buying me lots of Panera Bread and organic food while I was studying for my qualifying exams, and for making me so incredibly happy. To my Mom, thank you for being the glue of our family and for lots and lots of long phone calls. To my dad, thank you for supporting all of my life goals. And to my siblings Kevin and Kelli, thank you for the laughs and love.

TABLE OF CONTENTS

Page

CHAPTER 1

INTRODUCTION

Traumatic brain injury (TBI) is a leading cause of death and long-term disability. Approximately 1.7 million people sustain a TBI in the United States each year, and at least 5.3 million people are living with a long-term disability as a result of a TBI [1]. The most common causes of TBI include falls, motor vehicle accidents, assaults, blast-induced head injuries, and sports-related concussions [2]. TBI can be classified by injury type, generally designated as focal or diffuse, although elements of both are common for most head injuries [3, 4]. TBI can also be classified by injury severity using either length of loss of consciousness or the Glasgow Coma Scale (GCS) that categorizes TBI as either mild (GCS ≥ 13), moderate (GCS 9-12), or severe (GCS ≤ 8) [5]. The moment of injury, referred to as the primary injury, results in immediate mechanical strain on neuronal or glial cells, the vasculature, and axons as a result of direct physical impact or acceleration-deceleration shear forces [6]. Immediately following the primary injury, a series of systemic and cellular responses lead to the initiation of secondary injury responses. Systemically, TBI can lead to the formation of edema, increases in intracranial pressure, decreases in cerebral blood flow, and disruption of hemodynamic autoregulatory responses, resulting in dysregulated metabolism and ischemia [6]. This leads to further blood brain barrier and cellular membrane damage, glutamate excitotoxicity, calcium overload, mitochondrial dysfunction, activation of astrocytes and microglia, ROS production, and secretion of pro-inflammatory cytokines and chemokines [6, 7]. Ultimately, this cascade of secondary

events contributes to axonal injury, white matter disruption, neurodegeneration and development of functional deficits [7, 8].

After TBI, many people suffer from functional impairments in the short-term and/or long-term [9]. This is especially true for children after sustaining a TBI at an early age, as they may initially exhibit few to no functional impairments immediately after injury. However, TBI can disrupt normal developmental processes during a critical period of brain growth and maturation, leading to significant functional impairments later in life [10]. Functional impairments associated with TBI include disruption of cognitive processes like learning and memory [11], behavior problems like depression, anxiety, and attention deficit hyperactive disorder [12], or motor function deficits that affect gross movement, fine motor control, and gait [13]. Both age at injury and injury severity have been found to correlate with the presence and persistence of functional outcomes. Children who sustain a TBI at a young age are more susceptible to developing long-term functional deficits [14], and severe TBI in both children and adults is associated with poorer functional outcomes [15, 16].

However, our understanding of the pathophysiological and functional outcomes associated with TBI are still limited, which is likely a major contributing factor to the reason no effective Food and Drug Administration (FDA)-approved treatment currently exists for TBI [17]. Experimental animal models of TBI, especially rodent TBI models, have yielded critical insight into TBI sequelae, providing much of our mechanistic understanding of the cellular, tissue, and functional changes associated with TBI [18]. However, a significant disadvantage of rodent models may be their lack of translatability in developing effective therapeutic intervention strategies given their smaller brain size, lissencephalic brain structure, and lack of significant white matter compared to the human brain [19]. The pig possesses a number of key similarities

to humans that suggest that it may be more appropriate for modeling TBI and developing more translational, therapeutically relevant intervention strategies and treatments [20]. The pig brain is large, gyrencephalic, and has proportionally more white matter than gray matter, much like the human brain [21]. A number of different types of TBI models have been developed that recapitulate different elements of TBI including the controlled cortical impact (CCI) model. The CCI TBI model produces a focal, reproducible injury that allows for control of injury location and injury severity [22]. It has been shown to produce many of the key physiologic and secondary injury responses associated with focal TBI in pigs [23, 24]. However, there remain many important unanswered questions pertaining to the spatial-temporal responses of TBI pathology, lesion size, edema formation, and white matter disruption in pig CCI models. Additionally, few studies have examined cognitive and motor function deficits in pigs after TBI, and fewer still that correlate functional deficits with histopathology.

The studies that comprise this dissertation sought to characterize TBI pathophysiology and functional responses in a more translatable pig CCI model using a number of innovative techniques such as longitudinal magnetic resonance imaging (MRI), quantitative histological analysis, behavior testing, and gait analysis. These studies were designed to test the following hypotheses: 1) increasing TBI severity results in a scalable brain injury at the cellular and tissue levels that corresponds with the development of gait deficits; 2) TBI contributes to changes in lesion size, edema accumulation, white matter integrity, cerebral blood flow, and neurometabolite concentrations that can be tracked longitudinally using MRI and correlated with histopathological analysis; 3) pigs are capable of performing a series of behavioral tests that provide a comprehensive assessment of piglet behavior and cognition; and 4) TBI results in cognitive, behavioral, and motor function deficits that correlate with histopathology

References

1. Langlois, J.A., Rutland-Brown, W., Thomas, K.E., *Traumatic brain injury in the United States: Emergency deparment visits, hospitalizations, and deaths.* Atlanta, GA: Centers for Disease Control and Prevention, National Center for Injury Prevention and Control, 2006.
2. Maas, A.I., N. Stocchetti, and R. Bullock, *Moderate and severe traumatic brain injury in adults.* Lancet Neurol, 2008. **7**(8): p. 728-41.
3. Marklund, N. and L. Hillered, *Animal modelling of traumatic brain injury in preclinical drug development: where do we go from here?* Br J Pharmacol, 2011. **164**(4): p. 1207-29.
4. Andriessen, T.M., B. Jacobs, and P.E. Vos, *Clinical characteristics and pathophysiological mechanisms of focal and diffuse traumatic brain injury.* J Cell Mol Med, 2010. **14**(10): p. 2381-92.
5. Teasdale, G. and B. Jennett, *Assessment of coma and impaired consciousness. A practical scale.* Lancet, 1974. **2**(7872): p. 81-4.
6. Walker, K.R. and G. Tesco, *Molecular mechanisms of cognitive dysfunction following traumatic brain injury.* Front Aging Neurosci, 2013. **5**: p. 29.
7. Sajja, V.S., N. Hlavac, and P.J. VandeVord, *Role of Glia in Memory Deficits Following Traumatic Brain Injury: Biomarkers of Glia Dysfunction.* Front Integr Neurosci, 2016. **10**: p. 7.
8. Kou, Z. and P.J. VandeVord, *Traumatic white matter injury and glial activation: from basic science to clinics.* Glia, 2014. **62**(11): p. 1831-55.
9. Rabinowitz, A.R. and H.S. Levin, *Cognitive sequelae of traumatic brain injury.* Psychiatr Clin North Am, 2014. **37**(1): p. 1-11.

10. Babikian, T. and R. Asarnow, *Neurocognitive outcomes and recovery after pediatric TBI: meta-analytic review of the literature.* Neuropsychology, 2009. **23**(3): p. 283-96.

11. Lowther, J.L. and J. Mayfield, *Memory functioning in children with traumatic brain injuries: a TOMAL validity study.* Arch Clin Neuropsychol, 2004. **19**(1): p. 105-18.

12. Li, L. and J. Liu, *The effect of pediatric traumatic brain injury on behavioral outcomes: a systematic review.* Dev Med Child Neurol, 2013. **55**(1): p. 37-45.

13. Kuhtz-Buschbeck, J.P., et al., *Analyses of gait, reaching, and grasping in children after traumatic brain injury.* Arch Phys Med Rehabil, 2003. **84**(3): p. 424-30.

14. Anderson, V.A., et al., *Functional memory skills following traumatic brain injury in young children.* Pediatr Rehabil, 1999. **3**(4): p. 159-66.

15. Anderson, V.A., et al., *Understanding predictors of functional recovery and outcome 30 months following early childhood head injury.* Neuropsychology, 2006. **20**(1): p. 42-57.

16. de Guise, E., et al., *Prediction of behavioural and cognitive deficits in patients with traumatic brain injury at an acute rehabilitation setting.* Brain Inj, 2017: p. 1-8.

17. Jain, K.K., *Neuroprotection in traumatic brain injury.* Drug Discov Today, 2008. **13**(23-24): p. 1082-9.

18. Xiong, Y., A. Mahmood, and M. Chopp, *Animal models of traumatic brain injury.* Nat Rev Neurosci, 2013. **14**(2): p. 128-42.

19. Ahmad, A.S., et al., *Considerations for the Optimization of Induced White Matter Injury Preclinical Models.* Front Neurol, 2015. **6**: p. 172.

20. Duhaime, A.C., *Large animal models of traumatic injury to the immature brain.* Dev Neurosci, 2006. **28**(4-5): p. 380-7.

21. Lind, N.M., et al., *The use of pigs in neuroscience: modeling brain disorders.* Neurosci Biobehav Rev, 2007. **31**(5): p. 728-51.

22. Osier, N.D., J.R. Korpon, and C.E. Dixon, *Controlled Cortical Impact Model*, in *Brain Neurotrauma: Molecular, Neuropsychological, and Rehabilitation Aspects*, F.H. Kobeissy, Editor. 2015: Boca Raton (FL).

23. Manley, G.T., et al., *Controlled cortical impact in swine: pathophysiology and biomechanics.* J Neurotrauma, 2006. **23**(2): p. 128-39.

24. Alessandri, B., et al., *Moderate controlled cortical contusion in pigs: effects on multi-parametric neuromonitoring and clinical relevance.* J Neurotrauma, 2003. **20**(12): p. 1293-305.

CHAPTER 2

LITERATURE REVIEW:

THE PIG AS A PRECLINICAL TBI MODEL: CURRENT MODELS, FUNCTIONAL OUTCOME MEASURES, AND TRANSLATIONAL DETECTION STRATEGIES [1]

[1]Kinder, H.A., Baker, E.W., West, F.D. To be submitted to *Journal of Neurotrauma.*

Abstract

Traumatic brain injury (TBI) is a major contributor of long-term disability and a leading cause of death worldwide. A TBI can be caused by focal or diffuse injuries like falls, automobile accidents, or being struck by an object. A series of secondary injury cascades can contribute to cell death and tissue loss, and ultimately, to the development of functional impairments. However, there are currently no treatments for TBI. As a result, a number of experimental TBI models have been developed to recapitulate TBI injury mechanisms and to test the efficacy of potential therapeutics at improving TBI outcomes. In particular, the pig brain follows a similar pattern of development and is closer in size, structure, and composition to the human brain, making it an ideal large animal model to study TBI pathophysiology and functional outcomes. This review will focus on the shared characteristics between humans and pigs that make them ideal for modeling TBI and will review the 3 most common pig TBI models- the diffuse axonal injury model, the controlled cortical impact model, and the fluid percussion model. It will also review current advances in functional outcome assessment measures and other non-invasive, translational TBI detection and measurement tools like biomarker analysis and magnetic resonance imaging. Finally, it will review the effectiveness of several therapeutic intervention strategies utilized in pig TBI models to provide neuroprotection after injury.

Introduction

Traumatic brain injury (TBI) is a leading cause of long-term disability and death. It has been estimated that as many as 1.7 million people sustain a TBI annually in the United States, and almost one third of all head injuries occur among children aged 0 to 14 [1]. TBI can be caused by a multitude of factors such as falls, blast waves, motor vehicle accidents, rapid acceleration and deceleration, or penetration of a foreign object [2]. Brain injuries are generally considered focal or diffuse in nature, but may oftentimes involve elements of both, such as a focal contusion with associated diffuse axonal injury [3]. TBI can lead to immediate and sustained impairments in physiologic and hemodynamic responses that perpetuate secondary injury progression, which is characterized by the release of pro-inflammatory cytokines, chemokines, free radicals, mitochondria dysfunction, and oxidative stress that contribute to cell death, axonal degeneration, tissue necrosis, and ultimately, functional impairments [4, 5]. Although current management strategies aimed at reducing physiologic damage after TBI have vastly improved survivability outcomes, there are currently no effective Food and Drug Administration (FDA)-approved treatments that offer neuroprotection and/or regeneration after injury [6, 7].

Animal models of TBI have proven indispensable in characterizing the pathophysiology of injury progression and in developing effective management strategies [8]. Large animal models, such as the pig, are ideal given their similar brain size, structure, composition, and development [9]. In particular, pigs have a similar white to gray matter ratio to humans, unlike the more commonly studied rodent models [10]. White and gray matter have different mechanical properties, and thus respond differently to injury [11]. Given the propensity for TBI to contribute to widespread white matter damage in humans, shifted focus to large animal models

with a comparable myelination pattern and white matter composition will be paramount in developing more effective, translational treatments for TBI in both juvenile and adult populations [12, 13].

A number of diverse, experimental models of TBI have been developed in pigs to recapitulate and study different aspects of human brain injury [14]. For example, the diffuse axonal injury model uses a rotational head device to achieve an acceleration-deceleration injury that produces traumatic axonal injury and widespread white matter damage [15]. The controlled cortical impact model produces a focal injury characterized by significant cellular damage and death at the injury site [16]. The fluid percussion injury contains elements of both diffuse and focal TBI and leads to significant physiologic impairments, hemorrhage, and cell death [17]. Studies using pig TBI models have provided important evidence detailing TBI pathophysiology and potential therapeutic targets.

TBI can lead to significant functional impairments that can affect cognition, motor function, and overall quality of life [18-21]. Cognitive deficits generally correlate with injury severity. Mild TBI is typically associated with few, if any, cognitive deficits that typically resolve within three months in human patients [22, 23]. Although, there is some evidence of a small cohort of patients that experience persistent cognitive impairments even after mild TBI [24]. Moderate to severe TBI is associated with more complex and persistent cognitive deficits that can remain unresolved for months to even years after injury [25]. Similarly, motor function deficits have been found to correlate with injury severity and can impair both fine and gross motor function abilities [26]. Increased interest in studying functional changes after TBI in animal models has led to a small number of pig TBI studies that assess functional outcomes [27, 28]. Although the field is lacking in well-validated behavioral measures to assess neurocognitive

and motor function changes in pig TBI models, these initial studies show the importance of identifying and characterizing functional outcome measures after experimental TBI in large animal models.

In this review, we will discuss the similarities of pig and human neurodevelopment, brain anatomy and physiology, immune, and functional characteristics that make the pig ideal for use as a large animal model. In addition, we will discuss three major pig TBI models- the diffuse axonal injury model, the controlled cortical impact model, and the fluid percussion model. Last, we will review the limited, albeit important, initial studies that performed neurobehavioral testing in pig TBI models to assess cognitive and motor function changes.

Advantages of Large Animal Models

Piglet neurodevelopment

The potential benefit of using pigs to model human neurodevelopment has long been known [29]. Early studies in the late 1960s by Dickerson and Dobbing investigated the prenatal and postnatal growth and chemical development of the pig central nervous system [30]. They found that the pig brain experienced a rapid increase in brain growth between 50 days before birth to about 40 days after birth. Analysis of changes in brain composition before and after birth yielded a substantial decrease in water content immediately following birth coupled with increases in cholesterol and total phosphorus- which is composed of mainly lipid phosphorus- suggesting an increase in myelination in the weeks after birth. In subsequent studies, Dobbing and Sands showed the pig and human brain exhibit a similar time course of development, or brain growth spurt, that transiently spans both the prenatal and postnatal periods [31]. They showed that the pig brain at birth has reached 25% of its adult brain weight, and similarly, the

human infant brain has reached 27% of its adult brain weight at birth. This is in contrast to other commonly used animal species such as the rhesus monkey whom exhibits a significant brain growth spurt prenatally and thus has reached 76% of its adult brain weight at birth, or the rat who exhibits a significant brain growth spurt postnatally and is only born with 12% of its adult brain weight. A study by Conrad et al. provided supporting evidence of similarities in brain growth between pigs and humans using longitudinal magnetic resonance imaging (MRI) from 2 to 24 weeks of age [32]. They showed that the pig brain undergoes substantial brain growth during the postnatal period, with the most rapid period of growth occurring at about 4 weeks of age when the brain is at ~50% of maximum volume. These studies suggest that piglets may be an ideal model to investigate the effect of early life insults, like TBI, on brain development and growth.

A recent study by Costine et al. described the subventricular zone (SVZ) in immature pigs and found it similar to humans [33]. The piglet ventricular SVZ (vSVZ) has dense populations of doublecortin (DCX) positive neuroblasts and the abventricular SVZ (aSVZ) contains DCX neuroblasts organized into distinct chains that decrease in density with age. Like the human infant brain, neuroblasts migrate from the SVZ to populate multiple brain regions during the early postnatal period. The piglet is also an ideal model to study the response of neuroblast populations at the SVZ after injury [33, 34]. Similar to humans, after TBI migrating neuroblasts have been identified in cavitated lesions of the gyral gray and white matter [34]. TBI has also been found to lead to alterations in normal postnatal neuroblast populations, demonstrated by increased neuroblast density in the external capsule compared to normal animals [34]. It is of interest for future studies to further elucidate the implications of these injury-induced changes in neuroblast behavior to contribute to either repair mechanisms and/or

disruption of normal developmental processes that can ultimately lead to the chronic effects of TBI.

A number of studies have investigated changes in myelination in the pig brain during brain maturation, noting a similar time course of myelination compared to humans [35-37]. Fang et al. used MRI and histological analysis to show that myelination in the pig brain increases through adolescence up to 6 months of age when the pig reaches sexual maturity [38]. Similarly, in humans myelination can continue through adolescence and even into early adulthood [39]. This period of myelination is critical for normal brain function and is therefore recognized as being a vulnerable period in development [40]. For example, nutritional deficiencies in piglets at an early age can lead to reduced brain cell density and brain growth as well as reduced cholesterol levels, indicative of disruption of normal myelination [41, 42]. Brain injury such as TBI can also contribute to widespread white matter damage in young children that can lead to long-term neurological deficits [43]. Despite the high prevalence of rodents used to model TBI, the myelination pattern of rodents in different from that of humans with significant differences in both the time scale of myelination and total amount of white matter [44]. White and gray matter have been found to have different mechanical properties- gray matter has less anisotropy and is stiffer compared to white matter which has more anisotropy and is less stiff [45]. Therefore, use of an animal model like the pig with a similar white to gray matter ratio is ideal for modeling TBI.

Anatomical, Physiologic, Immunologic Characteristic of Pigs

The pig possesses a number of advantageous characteristics that make it suitable for modeling brain disorders like TBI. The size, organization, and composition of the pig brain is

similar to that of the human brain. Compared to the adult human brain that weighs between 1,300-1,400g, the adult pig brain, depending on breed, weighs between 80-180g [46]. This is in vast contrast to the mature rat or mouse brain that weights approximately 2 and 0.5g, respectively [47]. Brain size is important in modeling TBI such that injury type, location, or severity leads to appropriate injury responses that are similar to that of human TBI. For example, in rodents, the hippocampus is more vulnerable to focal cortical injury due to the small size of the brain combined with the location and more superior orientation of the hippocampus [48, 49]. This is in contrast to the human and pig brain in which the hippocampus lies more ventrally within the temporal lobe and thus more protected from injury [48, 49].

The organization of the pig brain resembles that of the human brain. The pig brain, like the human brain, is gyrencephalic and follows a similar gyral pattern [46]. The rodent brain, however, lacks gyri and sulci, and is thus lissencephalic in nature. The volume of the prefrontal cortex in the Göttingen minipig constitutes 24% of the neocortex and 10% of total brain volume which is comparable to humans [50]. The dorsal striatum of the pig brain is split by the internal capsule into two distinct structures- the caudate nucleus and the putamen; in comparison, the rodent brain contains a single caudate-putamen structure [51, 52]. The pig hippocampus has been well described and has been found to be structurally more similar to the human hippocampus than the rodent, having a degree of encephalization that lies between rodent and primate [49]. A number of descriptive, comparative anatomical studies have been performed for the pig brain thalamus, hypothalamus, hypothalamic nuclei [53-55], brainstem structures [56, 57], and the cerebellum [58]. Similar to humans, sensory cortices such as the motor cortex [59] and the somatosensory cortex [60] are arranged somatotopically. The anatomy and organization of the

brain is important in modeling TBI as it effects the brain regions injured, vascular responses, and ultimately, the short- and/or long-term clinical effects of the injury [14].

Pigs have an immune system and inflammatory responses more similar to humans after injury, which is important in studying the sequela of TBI and identifying potential neuroprotective targets [61-63]. An immunological comparison between humans, pigs, and rodents revealed that, compared to mice, the pig immune system is more similar to humans for over 80% of immune system variables compared. However, compared to the pig, the mouse immune system is more similar to humans for less than 10% of variables [64]. In addition, the pig immune system appears to have a more human-like inflammatory response to immune challenge. Dawson et al. found that pig macrophage polarization to interferon-γ (IFN-γ) and lipopolysaccharide (LPS) reveal predominately human-like responses [61]. These data suggest that the pig may be ideal for measuring inflammatory responses after TBI and for identifying potential neuroprotective targets that mitigate inflammation.

Pig Traumatic Brain Injury Models

Experimental models of TBI have been developed to study different types of injury, temporal pathophysiological mechanisms, and functional outcomes as well as to evaluate potential therapies with the goal of translating preclinical findings to a clinical setting (**Table 2.1**). We will review the major modalities and strategies used to assess TBI pathophysiology, functional outcomes, and response to therapeutic intervention for the three most widely used pig TBI models- the diffuse axonal injury model, the controlled cortical impact model, and the fluid percussion model (**Figure 2.1**).

Diffuse Axonal Injury Model

Diffuse axonal injury (DAI) in humans occurs as result of damage to axons in brain neural tracts, specifically in major white matter tracks and can lead to significant morbidity and even mortality [65]. DAI is caused by acceleration and deceleration inertial forces that lead to disruption of neurofilament subunits within the axonal cytoskeleton [65]. Rather than being a diffuse, widespread injury as its name implies, this type of injury is best characterized as being multifocal. Given the restriction of DAI to axons of white matter tracts, it is often described as traumatic axonal injury (TAI) [66]. DAI is generated by a rotational injury by securing an animal's head in a rotational acceleration injury apparatus that can produce either single [67] or repetitive [68, 69] impulsive rotation in either the coronal[70], axial [67], horizontal [71], and sagittal [71] planes. Injury severity can be controlled by manipulating the acceleration velocity to generate either mild, moderate, or severe injury [72, 73].

DAI in humans can often lead to temporary or sustained loss of consciousness and apnea and can influence systemic physiologic responses [65, 74]. Similarly, rotational head injury in pigs can result in immediate loss of consciousness [67, 75]. Presence and length of loss of consciousness has found to be dependent on direction of rotational acceleration and number of rotations. Browne et al. demonstrated that rotational injury in the axial but not coronal plane results in loss of consciousness [73]. Eucker et al. similarly observed no loss of consciousness after rotational injury in the coronal plane, but also showed that rotational injury in the sagittal and horizontal planes did result in loss of consciousness [71]. Friess et al. showed that repetitive rotational injury led to a significant increase in duration of unconscious time compared to sham animals when rotational injury is 24 hours apart, but not 7 days apart [69]. The incidence of apnea, characterized as cessation of breathing or reduced respiratory effort resulting in arterial

oxygen saturation (SaO_2) <90% was significantly increased after axial [67], sagittal, and horizontal [71] rotational injury in piglets and is dependent on injury severity [72].

Rotational injury can lead to physiologic impairments like elevated intracranial pressure (ICP), decreased cerebral blood flow (CBF), decreased cerebral perfusion pressure (CPP), decreased brain tissue oxygenation ($PbtO_2$), and elevated lactate-pyruvate (LPR) ratio [71, 75], but mean heartrate, body temperature, respiratory rate, arterial blood gas appear to remain largely unaffected [67, 72, 73]. Rotational injury can also contribute in amplitude suppression in EEG recordings [72]. Physiologic responses have also been found to correlate with neuropathology [75].

Rotational injury in pig models have the hallmark neuropathological deficit of diffuse axonal injury in major white matter tracks typical of human patients [66]. Morphologically, traumatically damaged axons in pigs exhibit terminal clubbing (retraction balls) and swelling [15, 76]. The inertial forces of rotational injury disrupt cytoplasm flow, leading to intraaxonal damage to neurofilament subunits that impair the axonal cytoskeleton [65]. Neurofilament proteins then disassemble, dephosphorylate, and accumulate in damaged axons [77]. Accumulation of large neurofilament proteins in the pig brain therefore provides convincing evidence of axonal damage within white matter tracks as a result of injury [67, 72]. The extent of traumatic axonal damage has also been found to correlate with age, such that younger piglets demonstrate a higher density of injured axons in the cerebrum compared to adults after comparable rotational injury [67]. Accumulation of ß-APP in damaged axons is another hallmark of diffuse injury and has been found to be correlated with injury severity [72, 78]. In addition, accumulation of amyloid-beta (Aß) and tau proteins have also been observed after rotational injury suggesting a link between traumatic brain injury and the initiation of the

neurodegenerative process [79, 80]. The direction of head motion appears to play a role in the pathology of DAI. Browne et al. showed that axial plane injury, but not coronal plane injury, resulted in degenerative neurons in the cortex and hippocampus and greater accumulation of neurofilament protein in damaged axons [73]. Eucker et al. similarly showed that horizontal and sagittal head rotation but not coronal rotation resulted in significantly higher ß-APP accumulation.

Rotational injury may also contribute to neuroinflammatory pathways such as astrogliosis [15], and microglia activation [81], and may produces substantial subarachnoid hemorrhage [68, 71, 72, 82, 83]. Furthermore, younger newborn pigs have been found to be more susceptible to intracranial hemorrhage and axonal injury than older piglets, providing further evidence that younger brains are more sensitive to injury [83].

Controlled Cortical Impact Model

As opposed to inertial acceleration-deceleration forces that produce diffuse brain injury, impact forces produce a focal injury that can potentially lead to skull fracture, disruption and hemorrhage of the cortical surface, and contusions [14]. Impact forces occur when the head comes in contact with a hard surface or object. Falls, for example, account for almost 35% of all sustained head injuries and over 50% of sustained head injuries between children aged 0-14 years [1]. Head injuries incurred from a fall may certainly involve elements of both diffuse and focal TBI, and as a result may be studied in conjunction [84], but it is of interest to experimentally isolate and study the pathophysiological and functional elements of focal injury. As such, the controlled cortical impact (CCI) model is a widely utilized and well-validated experimental focal injury model [85]. A CCI device consists of an impactor tip that is attached to

a shaft that is accelerated by either a pneumatic piston or electromechanical actuator [85]. Precise, quantitative control over CCI parameters such as velocity, dwell time, and depth of depression allow for scaled manipulation of TBI severity [86]. In addition, injury location can be targeted to specific brain regions such as the frontal cortex [16, 87] or the parietal cortex [88-90]. As a result, CCI can produce graded cellular, tissue, physiologic, and functional responses to TBI.

Mild to severe TBI can lead to immediate disruption of physiologic responses and impaired autoregulatory function, generally as a function of injury severity [91]. Similarly, physiologic responses after CCI in pigs have been shown to be sensitive to injury severity, ranging from minor alterations [89] to significant impairments [88, 90]. Interestingly, Durham et al. observed a significant decrease in CBF in 1 month and 4 month old pigs, but a significant increase in CBF in 5 day old pigs, which the authors suggest may provide some protection from early ischemia after injury [92]. However, no other physiologic changes were noted. However, moderate CCI in adult pigs has been shown to lead to significant physiologic impairments that result in decreases in CPP and $ptiO_2$ coupled with significant increases in ICP, glutamate, and lactate [88, 90]. Manley et al. qualitatively assessed physiologic changes after scaled CCI, finding substantial increases in ICP and HR and trending decreases in MAP and CPP that correlated with increased injury severity [16].

In humans, a head injury produced by a significant impact force will often lead to the development of a focal lesion. Duhaime et al. showed that the lesion volumes of adolescent (4 month old) and toddler (1 month old) pigs were significantly larger than infant (5-day old) pigs in response to proportionally identical injury, suggesting that vulnerability to mechanical trauma increases progressively during maturation. [89]. In addition to age, gender may also play a

contributing role in lesion size for young pigs; 1 month old male pigs developed significantly larger lesions than male 5 day old pigs, but this effect was not seen in females [93].

CCI results in a number of clinically relevant histopathological outcomes that include but are not limited to gross pathological changes such as hemorrhages, swelling/edema, and midline shift, and histopathological changes such as neuronal cell damage/death and inflammation [16, 90]. Semi quantitative means to assess histological changes after CCI include generation of an injury score that scores relative hemorrhage, cell appearance, and cell injury in white and gray matter specific regions [90] or a lesion index that scores intracerebral bleeding, subarachnoid hemorrhage, intensity of edema, and surface contusion [88]. Quantitative approaches to assess histological changes after CCI in pigs is limited, but two recent studies by the Duhaime group quantitatively analyzed the proliferation of DCX+ neuroblasts at the subventricular zone and their ability to migrate to white and gray matter specific regions and to target the lesion site [33, 34]. Further histological studies are needed in pig CCI models that more quantitatively assess secondary injury mechanisms that contribute to cell death, astrogliosis, microglia activation, and white matter disruption with enhanced spatial and temporal acuity.

Fluid Percussion Injury Model

Fluid percussion injury (FPI) has elements of both diffuse and focal injury. There are two main types of FPI- medial or lateral. A medial injury is applied at the midline, along the sagittal sutures between bregma and lambda, producing a more widespread diffuse injury, and a lateral injury is applied over the cerebral cortex at the parietal cortex, producing a slightly more focal injury targeted to one side of the brain [94]. To generate the injury, a craniotomy is performed to expose the underlying, intact dura. Then using a fluid percussion device, a pendulum strikes the

piston of a reservoir of fluid, generating a fluid pressure pulse that impacts the extradural space producing a brief displacement of brain tissue [8]. Injury severity corresponds to the strength of the pressure pulse and results in graded morphological and pathophysiological changes [95].

In the immature pig, FPI has been well established to contribute to age-dependent hemodynamic effects [17]. Armstead showed that moderate FPI decreased systemic arterial blood pressure in the newborn piglet but increased in the juvenile piglet [96]. Pial arteries constricted to a greater extent, regional cerebral blood flow remained restricted for a longer period of time, and cerebral oxygenation, an index of metabolism, was transiently increased and followed by a prolonged decrease in newborn piglets compared to juvenile piglets [96]. In addition, upregulation of endothelin-1 activity after FPI has been found to contribute to adenosine triphosphate (ATP)-sensitive potassium (K+) channel impairments that are age-dependent, leading to impaired hypotensive cerebral autoregulation [97-100]. Further, disruption of cerebral hemodynamics after injury may be due to impairments in N-methyl-D-aspartate (NMDA) receptor mediated vascular dilation, which has also been found to be age-dependent [101]. Recent evidence has shown that the dopaminergic system may be sensitive to TBI. Acute increases in dopamine (DA) can have potentially neurotoxic effects and has been shown to play a role in the pathogenesis of neuronal injury, potentially through the production of free radicals [102]. Measurement of aromatic amino acid decarboxylase (AADC) levels, an indicator of DA activity, has been shown to be upregulated in newborn piglets but not juvenile piglets after FPI [102]. Disruption of cholinergic neurotransmission, evident by increased acetylcholine esterase (AchE) activity [103] and reduced muscarinic Ach receptor density [104], has been observed after FPI, leading to depressed cholinergic transmission that can ultimately contribute to the development of functional impairments.

FPI in humans also activates secondary injury mechanisms common to DAI and CCI including inflammation, apoptosis, and necrotic cell death [105]. Similarly, immunohistological analyses after FPI have revealed hemorrhage [106], neuronal necrosis in the cortex [100, 106] and hippocampus [107, 108] as well as dramatic increases in Iba-1+ microglia with extended processes that contacted APP+ proximal axonal swellings [109].

Functional Measures in Pigs

Changes in Cognition, Behavior, and Motor Function after TBI

TBI is well known to contribute to cognitive deficits in both children and adults [25]. TBI location and severity appear are important in determining the impaired cognitive processes and whether the effects are short-term, long-term, or both [110, 111]. The age of the patient at the time of injury is also an important predictor of outcome following TBI. Children who sustain a TBI at a younger age are more likely to develop cognitive dysfunction, likely as a result of disruption of the normal developmental processes during a critical time period of brain maturation [18, 112]. TBI can also contribute to motor function deficits that can affect different aspects of fine motor control and gait [113, 114]. Similarly, TBI has been found to contribute to impairments in motor function that correlate with injury severity and age [115, 116]. Therefore, it is of interest to study the sequelae of neurocognitive and motor function changes in experimental models of TBI to elucidate mechanisms of injury on cognitive responses and to test the ability of potential therapeutics to mitigate cognitive impairments. To date, a large number of rodent studies have investigated cognitive changes after TBI [117-121]. However, functional testing is extremely limited in pig models of TBI, despite a number of key similarities between

humans and pigs that make them ideal for studying functional brain responses to injury and potential treatments [46].

To date only a limited number of studies have performed a comprehensive assessment of neurobehavioral functional changes after TBI in pigs. Friess et al. first utilized several behavioral tests, namely a modified open field test, a glass barrier task, a food cover task, and a balance beam test after mild and moderate rotational injury in piglets [27]. The open field test, a general measure of ambulation and exploratory behaviors, was slightly modified to contain both static and interactive objects placed throughout the arena to further gauge a higher level of cortical-striatal-pallidal sensory processing. In addition, a male littermate was also added to the arena to assess social behaviors. For the glass barrier task, which provides a measure of problem-solving, pigs had to learn to navigate around a glass barrier to reach a food reward. Piglets performed a food cover task in which piglets had to learn to find and access a food reward located under an opaque lid, which provides a measure of non-visual object discrimination learning. Last, for the balance beam test pigs had to walk along a balance beam to a food reward without any foot slips or falls [27]. No cognitive deficits for any behavior tests were observed in mild TBI animals. They found moderately injured pigs exhibited limited changes in open field behavior, although injured pigs spent significantly less time sniffing the walls of the arena than sham pigs. In the glass barrier task and food cover tasks injured pigs had significantly higher failure rates than sham pigs early on the first day of testing only. No deficits in motor function were observed in the balance beam test [27]. The results of this study showed only few significant changes in cognition that were generally transient in nature.

In a follow up study, Friess et al. subjected piglets to either single or repetitive (24 hours and 1 week) rotational injury and assessed cognitive function after injury using the open field

test, glass barrier task, food cover task, and balance beam test [69]. In addition, piglets performed a T-maze task in which they had to locate a food reward in a T-shaped maze during a training, test, and reversal phase and during a challenge phase when a novel object was placed in the arena. Compared to sham animals, no significant differences were observed in either injury group for the open field test, food cover task, and balance beam test. They noted a trend for repetitively injured piglets to have longer latencies to the food reward after reward reversal in the T-maze test. They also found that repetitive injury after 24 hours resulted in significantly higher failure rates of the glass barrier task on day 1 [69]. In an effort to reduce variability within groups, they developed a cognitive composite dysfunction (CCD) score comprised of several behavioral outcomes with the most consistent responses of the sham animals (T-maze training failure rate, T-maze intra-maze change time in contact with novel object, latency to food reward for T-maze normal trials and T-maze reversal trials, sniffing the walls from open field testing). They found that cognitive composite dysfunction scores correlated well with percent white matter injury (0.83) and were significantly higher after repetitive TBI than single TBI [69].

The effectiveness of folic acid to provide neuroprotection and improve functional recovery was assessed after moderate rotational injury in piglets [122]. Functional recovery was assessed using the open field test, glass barrier task, food cover task, T-maze task, and balance beam test in combination with the cognitive composite dysfunction score. Though most measures were not significant, significant functional improvements in folic acid treated animals was noted in open field exploration, CCD score, and time to complete the balance beam task on day 1, suggesting folic acid could potentially contribute to early but transient cognitive and motor function improvements [122].

Noting the presence of high variability and possible lack of sensitivity of these tests, Sullivan et al. made a series of changes to several behavior tests to improve their reliability and sensitivity [28, 123]. First, Sullivan et al. used improved open field measures to assess locomotion and exploratory behaviors after injury to explore the effect of rotational direction (axial vs. sagittal) on cognitive function [123]. They tracked the pig's location within 9 zones in the open field arena and assigned a zone position sequence which they used to calculate four different measures of specific aspects of the pig's locomotion around the arena: P_{DIAG} (stationary vs. mobile), Shannon entropy (No zone preference vs. zone preference), first order mutual information (zone position sequence is stable vs. rapidly changing), and Lempel-Ziv Complexity (random travel vs. structured travel). P_{DIAG} measures indicated that pigs with sagittal rotation injury had a significantly greater level of inactivity after injury and Lempel-Ziv Complexity measures showed that pigs with sagittal rotation injury had less random use of the open field arena than pigs with axial rotation injury [123].

Next, using the updated open field test and improved measures for the T-maze and balance beam tests, Sullivan et al. assessed cognitive changes after rotational injury in the sagittal plane in piglets [28]. To improve the sensitivity of the T-maze test, visual discrimination cues were added to each arm of the T maze, an image with three large dots at the arm with a food reward and an image with a single large dot at the arm with no reward. To improve the balance beam test, the beam was inclined and pigs were also given a motor proficiency score (MPS) that ranged from gait abnormalities on every run (score o 0) to no gait abnormalities on all runs (score of 4) [28]. Injured pigs showed a significant increase in P_{DIAG}, indicative of less activity in the open field, spent more time at the old food location after reversal in the T-maze test, possibly due to deficits in visual cue based learning, and MPS was significantly lower for injured pigs

compared to sham pigs on day 1. A more sensitive composite porcine disability score (PDS) was developed using a number of different significant metrics from behavior testing that showed small but persistent impairments in cognition and motor function and that correlated with percent axonal injury [28].

Additional behavior testing paradigms are limited in pig TBI models. Olson et al. found disturbances in daytime and nighttime activity in piglets after diffuse and focal brain injury by outfitting piglets with jackets containing tri-axial accelerometers to measure movement of the thorax [124]. Oldland et al. used a Treat Retrieval Test to evaluate the ability of adult pigs to recognize a food-containing bin when presented with three identical bins [125]. Animals were graded on a scale of -1 (animal opens another bin) to +4 (animal opens the correct bin without approaching either of the other two bins). The Alam group has assessed functional changes after CCI adult pigs using a Neurological Severity Score (NSS) and cognitive performance using a food retrieval task in color coded boxes after treatment with valproic acid [126] or lyophilized or fresh frozen plasma [127]. The NSS is a 32-point scale (where zero is no deficit and 32 is severe deficits) that measures level of consciousness, behavior, appetite, standing position, head position, utterance, gait, and motor function. For the food retrieval task, pigs were taught to retrieval a food reward from a specific colored box that was accessible without opening any of the other boxes. This test is a measure of memory retention, recall, color recognition, spatial memory, and prioritization. Treatment with either valproic acid, lyophilized plasma, or fresh frozen plasma resulted in significantly reduced NSS scores and significantly fewer testing sessions to reach proficiency at the food retrieval task comparted to saline treated animals [126, 127]. Future studies are needed to validate existing behavior tests used in pigs after TBI as well

as new, improved methods to assess different aspects of cognition with improved reliability and temporal sensitivity.

Development of Translational TBI Detection Tools and Therapies in Pig Models

Pig Biomarkers for TBI

Evaluation of serum biomarkers as a means to more easily and rapidly assess TBI severity, predict prognosis, and test the effectiveness of therapeutic intervention has gained interest in recent years in clinical settings, prompting the search for enhanced, more sensitive biomarkers [128]. The effectiveness of the peripheral blood biomarkers neuron-specific enolase (NSE), myelin basic protein (MBP), and S100B were tested in pigs of varying ages 15 mins, 1, 4, and 7 days after CCI injury [129]. Only NSE was significantly elevated after CCI, although the predictive power of NSE alone was noted to be only poor to fair.

Kilbaugh et al. assessed peripheral whole blood for mitochondrial DNA (mtDNA) copy number and found that mean relative mtDNA copy numbers increased significantly after CCI, suggesting that this approach may be an ideal means to assess mitochondria bioenergetics dysfunction and to non-invasively identify presence of brain injury [130]. Recent evidence suggests that mitochondria dysfunction may be a major contributor of the secondary injury cascade after TBI [131]. Mitochondria play a pivotal role in energy metabolism in normal functioning cells. However, brain injury can lead to higher energy demands for cell repair that damaged mitochondria cannot meet [131]. Excessive Ca uptake leads to mitochondrial damage, potentiating excitotoxicity, ROS generation, and depletion of ATP, which can ultimately lead to cell death [131]. A number of studies have begun to examine mitochondrial response to injury in

pig CCI models to further elucidate the bioenergetic response to injury [130, 132, 133] and to test the ability of therapeutic interventions to improve mitochondrial function [134].

Magnetic Resonance Imaging (MRI)

Human MRI studies have found that lesion volume is a critical predictor of outcome after TBI [135]. Given the clinical significance of MRI, it is of interest to study the time-course of lesion development and progression after injury in pigs to further elucidate TBI sequelae and to test the effectiveness of potential therapeutics. However, only a limited number of MRI studies have been performed in pig TBI models. Using a DAI pig model, both conventional MRI and high field proton magnetic resonance spectroscopy (MRS), which provides a measure of neurometabolic changes as a result of TBI, were performed, and no abnormalities were detected with conventional MRI [136, 137]. However, spectroscopy results revealed a significant decrease in N-acetylaspartate/creatine (NAA/Cre), which may reflect neuronal and axonal damage [136, 137]. McGowan et al. performed magnetization transfer imaging (MTI) after DAI which generates quantitative magnetization transfer ratio (MTR) maps that identify regions with axonal injury. They found significant reduction of MTR in thus demonstrating the presence of diffuse axonal pathology. Using a pig CCI model. Duhaime et al. measured lesion volume using T1, T2-weighted, and FLAIR sequences, although lesion volume was found to be generally larger when measured with T2-weighted or FLAIR sequences [138, 139]. Magnetic resonance spectroscopy (MRS), was also utilized in this study, but the authors note that due to number of limitations including hemorrhage, skull thickness, and fat content, results were highly variable. In addition, they noted presence of restricted diffusion at the injury site using diffusion weighted imaging (DWI), but no further quantitative analyses were provided [138]. MRI results were correlated

with histological analysis allowing for improved temporal, spatial, and microscopic assessment of the lesion site. Functional magnetic resonance imaging (fMRI) has also been utilized in a piglet CCI model to assess recovery in the somatosensory cortex over time [140]. Additional temporal MRI studies are needed in both piglet and adult pig CCI models to gain greater insight into the pathophysiologic responses of injury and how they might contribute to lesion progression and functional outcomes.

Development of Therapeutic Strategies and Pharmacologic Agents in TBI Pigs

Several neuroprotective therapeutic approaches have been tested in pig DAI models. Polyethylene glycol prevented β-APP accumulation in the medial cortex, hippocampus, thalamus, medial lemniscus, and medial longitudinal fasciculus [141]. Folic acid treatment after rotational injury resulted in early functional improvements, but the treatment effect was only observed short-term and had no effect on axonal injury [122]. Administration of the vasoconstrictor phenylephrine was used to maintain cerebral perfusion pressure within normal range at either 70 mm Hg or 40 mm Hg [142]. Phenylephrine treatment resulted in significantly smaller injury volumes, and improved lactate/pyruvate ratios [142]. However, treatment with the vasopressor norepinephrine was shown to contribute to higher brain tissue oxygenation than phenylephrine [143]. Recently, a case study was performed by Margulies et al. using a preclinical trial design to target an optimum dose and test the effectiveness of Cyclosporin A. Cyclosporin A was found to meet a "positive outcome" effectiveness evaluation, which provides a qualitative assessment of efficacy [134].

A number of physiologic measurement techniques and therapeutic interventions strategies have been tested in pig CCI models. For example, the placement of tissue oxygen

probes either distal or proximal to the injury site were found to differentially measure brain tissue oxygen tension, suggesting clinical interpretations of brain tissue oxygen measurements should take into consideration probe placement relative to the injury site [87]. As a potential therapeutic strategy, application of an internal jugular vein compression collar was found to significantly reduce hemorrhage after CCI [144]. TBI in humans may be accompanied by other associated extra-cranial injuries like significant blood loss which can lead to hemorrhagic shock (HS) and hypotension, and markedly worsen outcomes [145]. Developing effective intervention strategies are critical for reducing morbidity and mortality rates. The Alam group has carried out a number of studies using a combined CCI and hemorrhagic shock approach to study the effectiveness of several therapeutic interventions, including hetastarch, Hextend vs. fresh frozen plasma [146], isotonic sodium chloride solution vs. hetastarch [147], Hextend vs. valproic acid, fresh frozen plasma vs. lyophilized plasma [148], normal saline vs. normal saline and valproic acid [126] as well as a model of TBI and polytrauma (blood loss, rib fracture, soft-tissue damage, and liver injury) to assess treatment with fresh frozen plasma [149] and lyophilized plasma[127]. Treatment with fresh frozen plasma, valproic acid, and lyophilized plasma were shown to significantly reduce lesion size and swelling.

The pig fluid percussion model has also been used to assess the ability of neuroprotective therapeutics to reduce injury responses. Administration of mutant tissue plasminogen activator (tPA) tPA- s481A [150] or combined glucagon and plasminogen activator inhibitor-1 derived peptide (PAI-1DP), an inhibitor of endogenous tPA [151], reduced glutamate excitotoxicity and reduced vasoconstriction; Recombinant factor VIIa (rFVIIa) reduced neuronal necrosis and intracranial hemorrhage [106]; Vasoactive agents dopamine [152] and norepinephrine [107] improved cerebral perfusion pressure and cerebral autoregulation; Polyethylene glycol telomere

B (PEG-TB), which lyses pro-thrombotic and pro-inflammatory microparticles (MP) released endogenously after injury, reduced hippocampal neuronal cell loss and protected cerebrovasodilation during hypotension [108]. Taken together, these studies show the value of using the pig TBI model to assess the ability of potential therapeutic interventions to mitigate injury responses of both focal and diffuse TBI.

Conclusion

Despite the high prevalence of TBI in adults and young children, we are still limited in our understanding of the pathophysiology and functional responses associated with TBI and how to best treat and restore lost function. Animal modeling provides the ability to break TBI down into more specific components, to tease apart the biggest contributors to injury progression, and to test the ability of potential treatments to mitigate injury. Pigs, in particular, are well suited to model TBI given their similarities to humans. Additional studies in pigs, particularly in regards to characterizing and improving affected cognitive processes and motor impairments, are vital in pushing the field towards the ultimate goal of restoring total function after TBI.

References

1. Langlois, J.A., Rutland-Brown, W., Thomas, K.E., *Traumatic brain injury in the United States: Emergency deparment visits, hospitalizations, and deaths.* Atlanta, GA: Centers for Disease Control and Prevention, National Center for Injury Prevention and Control, 2006.
2. Maas, A.I., N. Stocchetti, and R. Bullock, *Moderate and severe traumatic brain injury in adults.* Lancet Neurol, 2008. **7**(8): p. 728-41.
3. Andriessen, T.M., B. Jacobs, and P.E. Vos, *Clinical characteristics and pathophysiological mechanisms of focal and diffuse traumatic brain injury.* J Cell Mol Med, 2010. **14**(10): p. 2381-92.
4. Kenney, K., et al., *Cerebral Vascular Injury in Traumatic Brain Injury.* Exp Neurol, 2016. **275 Pt 3**: p. 353-66.
5. Ichkova, A., et al., *Vascular impairment as a pathological mechanism underlying long-lasting cognitive dysfunction after pediatric traumatic brain injury.* Neurochem Int, 2017.
6. Chakraborty, S., B. Skolnick, and R.K. Narayan, *Neuroprotection Trials in Traumatic Brain Injury.* Curr Neurol Neurosci Rep, 2016. **16**(4): p. 29.
7. Jain, K.K., *Neuroprotection in traumatic brain injury.* Drug Discov Today, 2008. **13**(23-24): p. 1082-9.
8. Xiong, Y., A. Mahmood, and M. Chopp, *Animal models of traumatic brain injury.* Nat Rev Neurosci, 2013. **14**(2): p. 128-42.
9. Lind, N.M., et al., *The use of pigs in neuroscience: modeling brain disorders.* Neurosci Biobehav Rev, 2007. **31**(5): p. 728-51.

10. Zhang, K. and T.J. Sejnowski, *A universal scaling law between gray matter and white matter of cerebral cortex.* Proc Natl Acad Sci U S A, 2000. **97**(10): p. 5621-6.

11. Elkin, B.S., A. Ilankova, and B. Morrison, *Dynamic, regional mechanical properties of the porcine brain: indentation in the coronal plane.* J Biomech Eng, 2011. **133**(7): p. 071009.

12. Gale, S.D., et al., *Nonspecific white matter degeneration following traumatic brain injury.* J Int Neuropsychol Soc, 1995. **1**(1): p. 17-28.

13. Johnson, V.E., et al., *Inflammation and white matter degeneration persist for years after a single traumatic brain injury.* Brain, 2013. **136**(Pt 1): p. 28-42.

14. Duhaime, A.C., *Large animal models of traumatic injury to the immature brain.* Dev Neurosci, 2006. **28**(4-5): p. 380-7.

15. Smith, D.H., et al., *Characterization of diffuse axonal pathology and selective hippocampal damage following inertial brain trauma in the pig.* J Neuropathol Exp Neurol, 1997. **56**(7): p. 822-34.

16. Manley, G.T., et al., *Controlled cortical impact in swine: pathophysiology and biomechanics.* J Neurotrauma, 2006. **23**(2): p. 128-39.

17. Armstead, W.M., *Age-dependent cerebral hemodynamic effects of traumatic brain injury in newborn and juvenile pigs.* Microcirculation, 2000. **7**(4): p. 225-35.

18. Anderson, V.A., et al., *Functional memory skills following traumatic brain injury in young children.* Pediatr Rehabil, 1999. **3**(4): p. 159-66.

19. Anderson, V., et al., *Predictors of cognitive function and recovery 10 years after traumatic brain injury in young children.* Pediatrics, 2012. **129**(2): p. e254-61.

20. Williams, G., et al., *Incidence of gait abnormalities after traumatic brain injury.* Arch Phys Med Rehabil, 2009. **90**(4): p. 587-93.

21. Koskinen, S., *Quality of life 10 years after a very severe traumatic brain injury (TBI): the perspective of the injured and the closest relative.* Brain Inj, 1998. **12**(8): p. 631-48.

22. Mathias, J.L. and J.L. Coats, *Emotional and cognitive sequelae to mild traumatic brain injury.* J Clin Exp Neuropsychol, 1999. **21**(2): p. 200-15.

23. Belanger, H.G., et al., *Factors moderating neuropsychological outcomes following mild traumatic brain injury: a meta-analysis.* J Int Neuropsychol Soc, 2005. **11**(3): p. 215-27.

24. Roe, C., et al., *Post-concussion symptoms after mild traumatic brain injury: influence of demographic factors and injury severity in a 1-year cohort study.* Disabil Rehabil, 2009. **31**(15): p. 1235-43.

25. Rabinowitz, A.R. and H.S. Levin, *Cognitive sequelae of traumatic brain injury.* Psychiatr Clin North Am, 2014. **37**(1): p. 1-11.

26. Kuhtz-Buschbeck, J.P., et al., *Sensorimotor recovery in children after traumatic brain injury: analyses of gait, gross motor, and fine motor skills.* Dev Med Child Neurol, 2003. **45**(12): p. 821-8.

27. Friess, S.H., et al., *Neurobehavioral functional deficits following closed head injury in the neonatal pig.* Exp Neurol, 2007. **204**(1): p. 234-43.

28. Sullivan, S., et al., *Improved behavior, motor, and cognition assessments in neonatal piglets.* J Neurotrauma, 2013. **30**(20): p. 1770-9.

29. Glauser, E.M., *Advantages of piglets as experimental animals in pediatric research.* Exp Med Surg, 1966. **24**(2): p. 181-90.

30. Dickerson, J.W.T. and J. Dobbing, *Prenatal and Postnatal Growth and Development of the Central Nervous System of the Pig.* Proceedings of the Royal Society of London. Series B. Biological Sciences, 1967. **166**(1005): p. 384-395.

31. Dobbing, J. and J. Sands, *Comparative aspects of the brain growth spurt.* Early Hum Dev, 1979. **3**(1): p. 79-83.

32. Conrad, M.S., R.N. Dilger, and R.W. Johnson, *Brain growth of the domestic pig (Sus scrofa) from 2 to 24 weeks of age: a longitudinal MRI study.* Dev Neurosci, 2012. **34**(4): p. 291-8.

33. Costine, B.A., et al., *The subventricular zone in the immature piglet brain: anatomy and exodus of neuroblasts into white matter after traumatic brain injury.* Dev Neurosci, 2015. **37**(2): p. 115-30.

34. Taylor, S.R., et al., *Neuroblast Distribution after Cortical Impact Is Influenced by White Matter Injury in the Immature Gyrencephalic Brain.* Front Neurosci, 2016. **10**: p. 387.

35. Flynn, T.J., *Developmental changes of myelin-related lipids in brain of miniature swine.* Neurochem Res, 1984. **9**(7): p. 935-45.

36. Pond, W.G., et al., *Perinatal ontogeny of brain growth in the domestic pig.* Proc Soc Exp Biol Med, 2000. **223**(1): p. 102-8.

37. Prensky, A.L., et al., *The lipid composition of the cerebral hemisphere of the miniature pig (Sus scrofa) during development.* Comp Biochem Physiol B, 1971. **39**(4): p. 725-38.

38. Fang, M., et al., *Myelination of the pig's brain: a correlated MRI and histological study.* Neurosignals, 2005. **14**(3): p. 102-8.

39. Giedd, J.N., et al., *Brain development during childhood and adolescence: a longitudinal MRI study.* Nat Neurosci, 1999. **2**(10): p. 861-3.

40. Davison, A., *Biochemical, morphological and functional changes in the developing brain.* Biochemical Correlates of Brain Structure and Function, 1977: p. 1-13.

41. Dickerson, J.W., J. Dobbin, and R.A. McCance, *The effect of undernutrition on the postnatal development of the brain and cord in pigs.* Proc R Soc Lond B Biol Sci, 1967. **166**(1005): p. 396-408.

42. Mudd, A.T. and R.N. Dilger, *Early-Life Nutrition and Neurodevelopment: Use of the Piglet as a Translational Model.* Adv Nutr, 2017. **8**(1): p. 92-104.

43. Genc, S., et al., *Recovery of White Matter following Pediatric Traumatic Brain Injury Depends on Injury Severity.* J Neurotrauma, 2017. **34**(4): p. 798-806.

44. Norton, W.T. and S.E. Poduslo, *Myelination in rat brain: changes in myelin composition during brain maturation.* J Neurochem, 1973. **21**(4): p. 759-73.

45. Prange, M.T. and S.S. Margulies, *Regional, directional, and age-dependent properties of the brain undergoing large deformation.* J Biomech Eng, 2002. **124**(2): p. 244-52.

46. Gieling, E.T., et al., *The pig as a model animal for studying cognition and neurobehavioral disorders.* Curr Top Behav Neurosci, 2011. **7**: p. 359-83.

47. Hofman, M.A., *Size and shape of the cerebral cortex in mammals. I. The cortical surface.* Brain Behav Evol, 1985. **27**(1): p. 28-40.

48. Strange, B.A., et al., *Functional organization of the hippocampal longitudinal axis.* Nat Rev Neurosci, 2014. **15**(10): p. 655-69.

49. Holm, I.E. and M.J. West, *Hippocampus of the domestic pig: a stereological study of subdivisional volumes and neuron numbers.* Hippocampus, 1994. **4**(1): p. 115-25.

50. Jelsing, J., et al., *The prefrontal cortex in the Gottingen minipig brain defined by neural projection criteria and cytoarchitecture.* Brain Res Bull, 2006. **70**(4-6): p. 322-36.

51. Matsas, R., A.J. Kenny, and A.J. Turner, *An immunohistochemical study of endopeptidase-24.11 ("enkephalinase") in the pig nervous system.* Neuroscience, 1986. **18**(4): p. 991-1012.

52. Felix, B., et al., *Stereotaxic atlas of the pig brain.* Brain Res Bull, 1999. **49**(1-2): p. 1-137.

53. Campos-Ortega, J.A., *The distribution of retinal fibres in the brain of the pig.* Brain Res, 1970. **19**(2): p. 306-12.

54. Szteyn, S., et al., *The stereotaxic configuration of hypothalamus nerve centres in the pig.* Anat Anz, 1980. **147**(1): p. 12-32.

55. Junge, D., *[The topography and cytoarchitectonic of the diencephalon of the cow (Bos taurus var. domesticus L.). II. The internal structure of the diencephalon of the cow (Bos taurus var. domesticus L.) (author's transl)].* Anat Anz, 1977. **141**(5): p. 478-97.

56. Freund, E., *[Cytoarchitectonics of the mesencephalon and pons in the domestic pig (Sus scrofa domestica)].* Anat Anz, 1969. **125**(4): p. 345-62.

57. Otabe, J.S. and A. Horowitz, *Morphology and cytoarchitecture of the red nucleus of the domestic pig (Sus scrofa).* J Comp Neurol, 1970. **138**(3): p. 373-89.

58. Larsell, O., *The development of the cerebellum of the pig.* Anat Rec, 1954. **118**(1): p. 73-107.

59. Breazile, J.E., Swafford, B.C.; Thompson, W.D., *Study of the motor cortex of the domestic pig.* Amer J Veterinary Res, 1966. **27**(120): p. 1369-1373.

60. Craner, S.L. and R.H. Ray, *Somatosensory cortex of the neonatal pig: I. Topographic organization of the primary somatosensory cortex (SI).* J Comp Neurol, 1991. **306**(1): p. 24-38.

61. Dawson, H.D., et al., *An in-depth comparison of the porcine, murine and human inflammasomes; lessons from the porcine genome and transcriptome.* Vet Microbiol, 2017. **202**: p. 2-15.

62. Dawson, H.D., et al., *Structural and functional annotation of the porcine immunome.* BMC Genomics, 2013. **14**: p. 332.

63. Fairbairn, L., et al., *The mononuclear phagocyte system of the pig as a model for understanding human innate immunity and disease.* J Leukoc Biol, 2011. **89**(6): p. 855-71.

64. Schook, L., et al., *Swine in biomedical research: creating the building blocks of animal models.* Anim Biotechnol, 2005. **16**(2): p. 183-90.

65. Meythaler, J.M., et al., *Current concepts: diffuse axonal injury-associated traumatic brain injury.* Arch Phys Med Rehabil, 2001. **82**(10): p. 1461-71.

66. Wang, H.C. and Y.B. Ma, *Experimental models of traumatic axonal injury.* J Clin Neurosci, 2010. **17**(2): p. 157-62.

67. Raghupathi, R. and S.S. Margulies, *Traumatic axonal injury after closed head injury in the neonatal pig.* J Neurotrauma, 2002. **19**(7): p. 843-53.

68. Raghupathi, R., et al., *Traumatic axonal injury is exacerbated following repetitive closed head injury in the neonatal pig.* J Neurotrauma, 2004. **21**(3): p. 307-16.

69. Friess, S.H., et al., *Repeated traumatic brain injury affects composite cognitive function in piglets.* J Neurotrauma, 2009. **26**(7): p. 1111-21.

70. Ross, D.T., et al., *Distribution of forebrain diffuse axonal injury following inertial closed head injury in miniature swine.* Exp Neurol, 1994. **126**(2): p. 291-9.

71. Eucker, S.A., et al., *Physiological and histopathological responses following closed rotational head injury depend on direction of head motion.* Exp Neurol, 2011. **227**(1): p. 79-88.

72. Ibrahim, N.G., et al., *Physiological and pathological responses to head rotations in toddler piglets.* J Neurotrauma, 2010. **27**(6): p. 1021-35.

73. Browne, K.D., et al., *Mild traumatic brain injury and diffuse axonal injury in swine.* J Neurotrauma, 2011. **28**(9): p. 1747-55.

74. Vieira, R.C., et al., *Diffuse Axonal Injury: Epidemiology, Outcome and Associated Risk Factors.* Front Neurol, 2016. **7**: p. 178.

75. Friess, S.H., et al., *Neurocritical care monitoring correlates with neuropathology in a swine model of pediatric traumatic brain injury.* Neurosurgery, 2011. **69**(5): p. 1139-47; discussion 1147.

76. McGowan, J.C., et al., *Diffuse axonal pathology detected with magnetization transfer imaging following brain injury in the pig.* Magn Reson Med, 1999. **41**(4): p. 727-33.

77. Chen, X.H., et al., *Evolution of neurofilament subtype accumulation in axons following diffuse brain injury in the pig.* J Neuropathol Exp Neurol, 1999. **58**(6): p. 588-96.

78. Johnson, V.E., W. Stewart, and D.H. Smith, *Axonal pathology in traumatic brain injury.* Exp Neurol, 2013. **246**: p. 35-43.

79. Smith, D.H., et al., *Accumulation of amyloid beta and tau and the formation of neurofilament inclusions following diffuse brain injury in the pig.* J Neuropathol Exp Neurol, 1999. **58**(9): p. 982-92.

80. Chen, X.H., et al., *Long-term accumulation of amyloid-beta, beta-secretase, presenilin-1, and caspase-3 in damaged axons following brain trauma.* Am J Pathol, 2004. **165**(2): p. 357-71.

81. Wofford, K.L., et al., *Rapid neuroinflammatory response localized to injured neurons after diffuse traumatic brain injury in swine.* Exp Neurol, 2017. **290**: p. 85-94.

82. Coats, B., et al., *Finite element model predictions of intracranial hemorrhage from non-impact, rapid head rotations in the piglet.* Int J Dev Neurosci, 2012. **30**(3): p. 191-200.

83. Weeks, D., et al., *Influences of developmental age on the resolution of diffuse traumatic intracranial hemorrhage and axonal injury.* J Neurotrauma, 2014. **31**(2): p. 206-14.

84. Zhang, J., et al., *Hemostatic and neuroprotective effects of human recombinant activated factor VII therapy after traumatic brain injury in pigs.* Exp Neurol, 2008. **210**(2): p. 645-55.

85. Osier, N. and C.E. Dixon, *The Controlled Cortical Impact Model of Experimental Brain Trauma: Overview, Research Applications, and Protocol.* Methods Mol Biol, 2016. **1462**: p. 177-92.

86. Osier, N.D., J.R. Korpon, and C.E. Dixon, *Controlled Cortical Impact Model*, in *Brain Neurotrauma: Molecular, Neuropsychological, and Rehabilitation Aspects*, F.H. Kobeissy, Editor. 2015: Boca Raton (FL).

87. Hawryluk, G.W., et al., *Brain tissue oxygen tension and its response to physiological manipulations: influence of distance from injury site in a swine model of traumatic brain injury.* J Neurosurg, 2016. **125**(5): p. 1217-1228.

88. Meissner, A., et al., *Effects of a small acute subdural hematoma following traumatic brain injury on neuromonitoring, brain swelling and histology in pigs.* Eur Surg Res, 2011. **47**(3): p. 141-53.

89. Duhaime, A.C., et al., *Maturation-dependent response of the piglet brain to scaled cortical impact.* J Neurosurg, 2000. **93**(3): p. 455-62.

90. Alessandri, B., et al., *Moderate controlled cortical contusion in pigs: effects on multi-parametric neuromonitoring and clinical relevance.* J Neurotrauma, 2003. **20**(12): p. 1293-305.

91. Toth, P., et al., *Traumatic brain injury-induced autoregulatory dysfunction and spreading depression-related neurovascular uncoupling: Pathomechanisms, perspectives, and therapeutic implications.* Am J Physiol Heart Circ Physiol, 2016. **311**(5): p. H1118-H1131.

92. Durham, S.R., et al., *Age-related differences in acute physiologic response to focal traumatic brain injury in piglets.* Pediatr Neurosurg, 2000. **33**(2): p. 76-82.

93. Missios, S., et al., *Scaled cortical impact in immature swine: effect of age and gender on lesion volume.* J Neurotrauma, 2009. **26**(11): p. 1943-51.

94. Kabadi, S.V., et al., *Fluid-percussion-induced traumatic brain injury model in rats.* Nat Protoc, 2010. **5**(9): p. 1552-63.

95. Sullivan, H.G., et al., *Fluid-percussion model of mechanical brain injury in the cat.* J Neurosurg, 1976. **45**(5): p. 521-34.

96. Armstead, W.M. and C.D. Kurth, *Different cerebral hemodynamic responses following fluid percussion brain injury in the newborn and juvenile pig.* J Neurotrauma, 1994. **11**(5): p. 487-97.

97. Armstead, W.M., *Role of endothelin-1 in age-dependent cerebrovascular hypotensive responses after brain injury.* Am J Physiol, 1999. **277**(5 Pt 2): p. H1884-94.

98. Armstead, W.M., *Age-dependent impairment of K(ATP) channel function following brain injury.* J Neurotrauma, 1999. **16**(5): p. 391-402.

99. Armstead, W.M. and C.W. Kreipke, *Endothelin-1 is upregulated after traumatic brain injury: a cross-species, cross-model analysis.* Neurol Res, 2011. **33**(2): p. 133-6.

100. Armstead, W.M. and R. Raghupathi, *Endothelin and the neurovascular unit in pediatric traumatic brain injury.* Neurol Res, 2011. **33**(2): p. 127-32.

101. Armstead, W.M., *NMDA and age dependent cerebral hemodynamics after traumatic brain injury.* Exp Toxicol Pathol, 2004. **56**(1-2): p. 75-81.

102. Walter, B., et al., *Age-dependent effects of severe traumatic brain injury on cerebral dopaminergic activity in newborn and juvenile pigs.* J Neurotrauma, 2004. **21**(8): p. 1076-89.

103. Donat, C.K., et al., *Effects of lateral fluid percussion injury on cholinergic markers in the newborn piglet brain.* Int J Dev Neurosci, 2010. **28**(1): p. 31-8.

104. Donat, C.K., et al., *Alterations of cholinergic receptors and the vesicular acetylcholine transporter after lateral fluid percussion injury in newborn piglets.* Neuropathol Appl Neurobiol, 2010. **36**(3): p. 225-36.

105. Werner, C. and K. Engelhard, *Pathophysiology of traumatic brain injury.* Br J Anaesth, 2007. **99**(1): p. 4-9.

106. Kim, B., et al., *Use of recombinant factor VIIa (rFVIIa) as pre-hospital treatment in a swine model of fluid percussion traumatic brain injury.* J Emerg Trauma Shock, 2014. **7**(2): p. 102-11.

107. Armstead, W.M., J. Riley, and M.S. Vavilala, *Preferential Protection of Cerebral Autoregulation and Reduction of Hippocampal Necrosis With Norepinephrine After Traumatic Brain Injury in Female Piglets.* Pediatr Crit Care Med, 2016. **17**(3): p. e130-7.

108. Bohman, L.E., et al., *Microparticles Impair Hypotensive Cerebrovasodilation and Cause Hippocampal Neuronal Cell Injury after Traumatic Brain Injury.* J Neurotrauma, 2016. **33**(2): p. 168-74.

109. Lafrenaye, A.D., et al., *Microglia processes associate with diffusely injured axons following mild traumatic brain injury in the micro pig.* J Neuroinflammation, 2015. **12**: p. 186.

110. Kinnunen, K.M., et al., *White matter damage and cognitive impairment after traumatic brain injury.* Brain, 2011. **134**(Pt 2): p. 449-63.

111. Novack, T.A., et al., *Outcome after traumatic brain injury: pathway analysis of contributions from premorbid, injury severity, and recovery variables.* Arch Phys Med Rehabil, 2001. **82**(3): p. 300-5.

112. Babikian, T. and R. Asarnow, *Neurocognitive outcomes and recovery after pediatric TBI: meta-analytic review of the literature.* Neuropsychology, 2009. **23**(3): p. 283-96.

113. Williams, G., et al., *Spatiotemporal deficits and kinematic classification of gait following a traumatic brain injury: a systematic review.* J Head Trauma Rehabil, 2010. **25**(5): p. 366-74.

114. Kuhtz-Buschbeck, J.P., et al., *Analyses of gait, reaching, and grasping in children after traumatic brain injury.* Arch Phys Med Rehabil, 2003. **84**(3): p. 424-30.

115. Beretta, E., et al., *Assessment of gait recovery in children after Traumatic Brain Injury.* Brain Inj, 2009. **23**(9): p. 751-9.

116. Katz-Leurer, M., et al., *Balance abilities and gait characteristics in post-traumatic brain injury, cerebral palsy and typically developed children.* Dev Neurorehabil, 2009. **12**(2): p. 100-5.

117. Ajao, D.O., et al., *Traumatic brain injury in young rats leads to progressive behavioral deficits coincident with altered tissue properties in adulthood.* J Neurotrauma, 2012. **29**(11): p. 2060-74.

118. Kamper, J.E., et al., *Juvenile traumatic brain injury evolves into a chronic brain disorder: behavioral and histological changes over 6months.* Exp Neurol, 2013. **250**: p. 8-19.

119. Hamm, R.J., et al., *Cognitive deficits following traumatic brain injury produced by controlled cortical impact.* J Neurotrauma, 1992. **9**(1): p. 11-20.

120. Peterson, T.C., et al., *A behavioral and histological comparison of fluid percussion injury and controlled cortical impact injury to the rat sensorimotor cortex.* Behav Brain Res, 2015. **294**: p. 254-63.

121. Tucker, L.T., A.H. Fu, and J.T. McCabe, *Performance of male and female C57BL/6J mice on motor and cognitive tasks commonly used in pre-clinical traumatic brain injury research.* J Neurotrauma, 2015.

122. Naim, M.Y., et al., *Folic acid enhances early functional recovery in a piglet model of pediatric head injury.* Dev Neurosci, 2010. **32**(5-6): p. 466-79.

123. Sullivan, S., et al., *Behavioral deficits and axonal injury persistence after rotational head injury are direction dependent.* J Neurotrauma, 2013. **30**(7): p. 538-45.

124. Olson, E., et al., *Alterations in Daytime and Nighttime Activity in Piglets after Focal and Diffuse Brain Injury.* J Neurotrauma, 2016. **33**(8): p. 734-40.

125. Odland, R.M., et al., *Efficacy of reductive ventricular osmotherapy in a swine model of traumatic brain injury.* Neurosurgery, 2012. **70**(2): p. 445-54; discussion 455.

126. Halaweish, I., et al., *Addition of low-dose valproic acid to saline resuscitation provides neuroprotection and improves long-term outcomes in a large animal model of combined traumatic brain injury and hemorrhagic shock.* J Trauma Acute Care Surg, 2015. **79**(6): p. 911-9; discussion 919.

127. Georgoff, P.E., et al., *Resuscitation with Lyophilized Plasma Is Safe and Improves Neurological Recovery in a Long-Term Survival Model of Swine Subjected to Traumatic Brain Injury, Hemorrhagic Shock, and Polytrauma.* J Neurotrauma, 2017.

128. Berger, R.P., P.M. Kochanek, and M.C. Pierce, *Biochemical markers of brain injury: could they be used as diagnostic adjuncts in cases of inflicted traumatic brain injury?* Child Abuse Negl, 2004. **28**(7): p. 739-54.

129. Costine, B.A., et al., *Neuron-specific enolase, but not S100B or myelin basic protein, increases in peripheral blood corresponding to lesion volume after cortical impact in piglets.* J Neurotrauma, 2012. **29**(17): p. 2689-95.

130. Kilbaugh, T.J., et al., *Peripheral Blood Mitochondrial DNA as a Biomarker of Cerebral Mitochondrial Dysfunction following Traumatic Brain Injury in a Porcine Model.* PLoS One, 2015. **10**(6): p. e0130927.

131. Cheng, G., et al., *Mitochondria in traumatic brain injury and mitochondrial-targeted multipotential therapeutic strategies.* Br J Pharmacol, 2012. **167**(4): p. 699-719.

132. Kilbaugh, T.J., et al., *Cyclosporin A preserves mitochondrial function after traumatic brain injury in the immature rat and piglet.* J Neurotrauma, 2011. **28**(5): p. 763-74.

133. Kilbaugh, T.J., et al., *Mitochondrial bioenergetic alterations after focal traumatic brain injury in the immature brain.* Exp Neurol, 2015. **271**: p. 136-44.

134. Margulies, S.S., et al., *Establishing a Clinically Relevant Large Animal Model Platform for TBI Therapy Development: Using Cyclosporin A as a Case Study.* Brain Pathol, 2015. **25**(3): p. 289-303.

135. Chastain, C.A., et al., *Predicting outcomes of traumatic brain injury by imaging modality and injury distribution.* J Neurotrauma, 2009. **26**(8): p. 1183-96.

136. Cecil, K.M., et al., *High-field proton magnetic resonance spectroscopy of a swine model for axonal injury.* J Neurochem, 1998. **70**(5): p. 2038-44.

137. Smith, D.H., et al., *Magnetic resonance spectroscopy of diffuse brain trauma in the pig.* J Neurotrauma, 1998. **15**(9): p. 665-74.

138. Duhaime, A.C., et al., *Magnetic resonance imaging studies of age-dependent responses to scaled focal brain injury in the piglet.* J Neurosurg, 2003. **99**(3): p. 542-8.

139. Grate, L.L., et al., *Traumatic brain injury in piglets of different ages: techniques for lesion analysis using histology and magnetic resonance imaging.* J Neurosci Methods, 2003. **123**(2): p. 201-6.

140. Duhaime, A.C., et al., *Functional magnetic resonance imaging of the primary somatosensory cortex in piglets.* J Neurosurg, 2006. **104**(4 Suppl): p. 259-64.

141. Koob, A.O. and R.B. Borgens, *Polyethylene glycol treatment after traumatic brain injury reduces beta-amyloid precursor protein accumulation in degenerating axons.* J Neurosci Res, 2006. **83**(8): p. 1558-63.

142. Friess, S.H., et al., *Early cerebral perfusion pressure augmentation with phenylephrine after traumatic brain injury may be neuroprotective in a pediatric swine model.* Crit Care Med, 2012. **40**(8): p. 2400-6.

143. Friess, S.H., et al., *Differing effects when using phenylephrine and norepinephrine to augment cerebral blood flow after traumatic brain injury in the immature brain.* J Neurotrauma, 2015. **32**(4): p. 237-43.

144. Sindelar, B., et al., *Effect of Internal Jugular Vein Compression on Intracranial Hemorrhage in a Porcine Controlled Cortical Impact Model.* J Neurotrauma, 2016.

145. Siegel, J.H., *The effect of associated injuries, blood loss, and oxygen debt on death and disability in blunt traumatic brain injury: the need for early physiologic predictors of severity.* J Neurotrauma, 1995. **12**(4): p. 579-90.

146. Jin, G., et al., *Traumatic brain injury and hemorrhagic shock: evaluation of different resuscitation strategies in a large animal model of combined insults.* Shock, 2012. **38**(1): p. 49-56.

147. Jin, G., et al., *Pharmacologic resuscitation for hemorrhagic shock combined with traumatic brain injury.* J Trauma Acute Care Surg, 2012. **73**(6): p. 1461-70.

148. Imam, A.M., et al., *Early treatment with lyophilized plasma protects the brain in a large animal model of combined traumatic brain injury and hemorrhagic shock.* J Trauma Acute Care Surg, 2013. **75**(6): p. 976-83.

149. Imam, A., et al., *Fresh frozen plasma resuscitation provides neuroprotection compared to normal saline in a large animal model of traumatic brain injury and polytrauma.* J Neurotrauma, 2015. **32**(5): p. 307-13.

150. Armstead, W.M., et al., *tPA-S481A prevents neurotoxicity of endogenous tPA in traumatic brain injury.* J Neurotrauma, 2012. **29**(9): p. 1794-802.

151. Armstead, W.M., et al., *Combination therapy with glucagon and a novel plasminogen activator inhibitor-1-derived peptide enhances protection against impaired cerebrovasodilation during hypotension after traumatic brain injury through inhibition of ERK and JNK MAPK.* Neurol Res, 2012. **34**(6): p. 530-7.

152. Armstead, W.M., J. Riley, and M.S. Vavilala, *Dopamine prevents impairment of autoregulation after traumatic brain injury in the newborn pig through inhibition of Up-regulation of endothelin-1 and extracellular signal-regulated kinase mitogen-activated protein kinase.* Pediatr Crit Care Med, 2013. **14**(2): p. e103-11.

Table 2.1. Overview of pig TBI preclinical studies using either a diffuse axonal injury model, controlled cortical impact model, or fluid percussion model. Physiologic responses, MRI, histopathological, and functional assessments as well as treatment strategies are listed where applicable. ICP, intracranial pressure; CBF, cerebral blood flow; CPP, cerebral perfusion pressure; LPR, lactate-pyruvate ratio; pO_2, partial pressure O_2; EEG, electroencephalogram; PtiO2, brain tissue oxygen; MABP, mean arterial blood pressure; MTI, magnetic transfer imaging; MRS, magnetic resonance spectroscopy; DWI, diffusion-weighted imaging; fMRI, functional magnetic resonance imaging; β-APP, beta-amyloid precursor protein; Aβ Protein, amyloid beta protein; tPA-s481A, tissue plasminogen activator- s481A; PAI-1DP, plasminogen activator inhibitor-1 derived peptide; rFVIIa, recombinant factor VIIa; PEG-TB, Polyethylene glycol telomere B

TBI Model	Physiologic Responses	MRI	Histopathology	Functional Outcomes	Treatments
Diffuse Axonal Injury	• Loss of consciousness [67, 69, 71, 73, 75] • Apnea [67, 71, 72] • ICP [71, 75] • CBF [71] • CPP [75] • LPR [75] • pO_2 [71, 73] • EEG [72]	• T1-weighted [76] • T2-weighted [76] • MTI [76] • MRS [136, 137]	• Terminal Clubbing and Swelling [15, 76] • NF Protein [67, 72, 73] • β-APP Plaques [71, 72] • Aβ and Tau Proteins [79, 80] • Neuronal Loss [71, 73] • Microglia Activation [81] • Astrogliosis [15] • Hemorrhage [67, 71, 72, 82, 83]	• Open Field Test [27, 28, 69, 122, 123] • Glass Barrier Task [27, 69, 122] • Food Cover Task [27, 69, 122] • T-maze Test [28, 69, 122] • Balance Beam Test [27, 69, 122] • Inclined Balance Beam Test [28] • Daytime/Nighttime Activity [124]	• Polyethylene Glycol [141] • Folic Acid [122] • Phenylephrine [142] • Norepinephrine [143] • Cyclosporin A [132, 134]
Controlled Cortical Impact Injury	• CBF [92] • ICP [16, 88, 90] • CPP [16, 88, 90] • $PtiO_2$ [88, 90] • Lactate [88, 90] • LPR [90] • MABP [16, 88, 90]	• T1-weighted [138, 140] • T2-weighted [138, 140] • FLAIR [138, 140] • MRS [138] • DWI [138] • fMRI [140]	• Neuronal Loss [16, 88-90] • Hemorrhage [16, 88-90] • Swelling/edema [16, 88] • Midline Shift [16] • Astrogliosis [89] • Neuroblast Proliferation and migration [33, 34]	• NSS [126, 127] • Treat Retrieval Task [125-127]	• Cyclosporin A [134] • Jugular vein compression collar [144] • Hetastarch, Hextend [146-148] • Valproic Acid [126, 148] • Fresh frozen plasma [146, 148, 149] • Lyophilized Plasma [127, 148] • Isotonic sodium chloride solution [147]
Fluid Percussion Injury	• MABP [43] • Pial Artery constriction [43] • CBF [43] • Cerebral oxygenation [43] • Cerebral autoregulation [44-47]		• Neuronal Loss [47-50] • Hemorrhage [48] • Microglia Activation [51] • APP+ Proximal Axonal Swellings [51]		• tPA-s481A [52] • PAI-1DP [53] • rFVIIa [48] • Dopamine [54] • Norepinephrine [49] • PEG-TB [50]

Figure 2.1. A comprehensive strategy for assessing the effects of TBI on neurodevelopment and behavior in piglets. Physiologic assessments, behavior testing, magnetic resonance imaging, tissue and histological analyses provide a platform with which test hypothesis about TBI pathophysiology, functional outcomes, and response to therapeutic intervention. ICP, intracranial pressure; CBF, cerebral blood flow; CPP, cerebral perfusion pressure; MABP, mean arterial blood pressure; DWI, diffusion-weighted imaging; MRS, magnetic resonance spectroscopy. Image adapted from Conrad et al. [55]

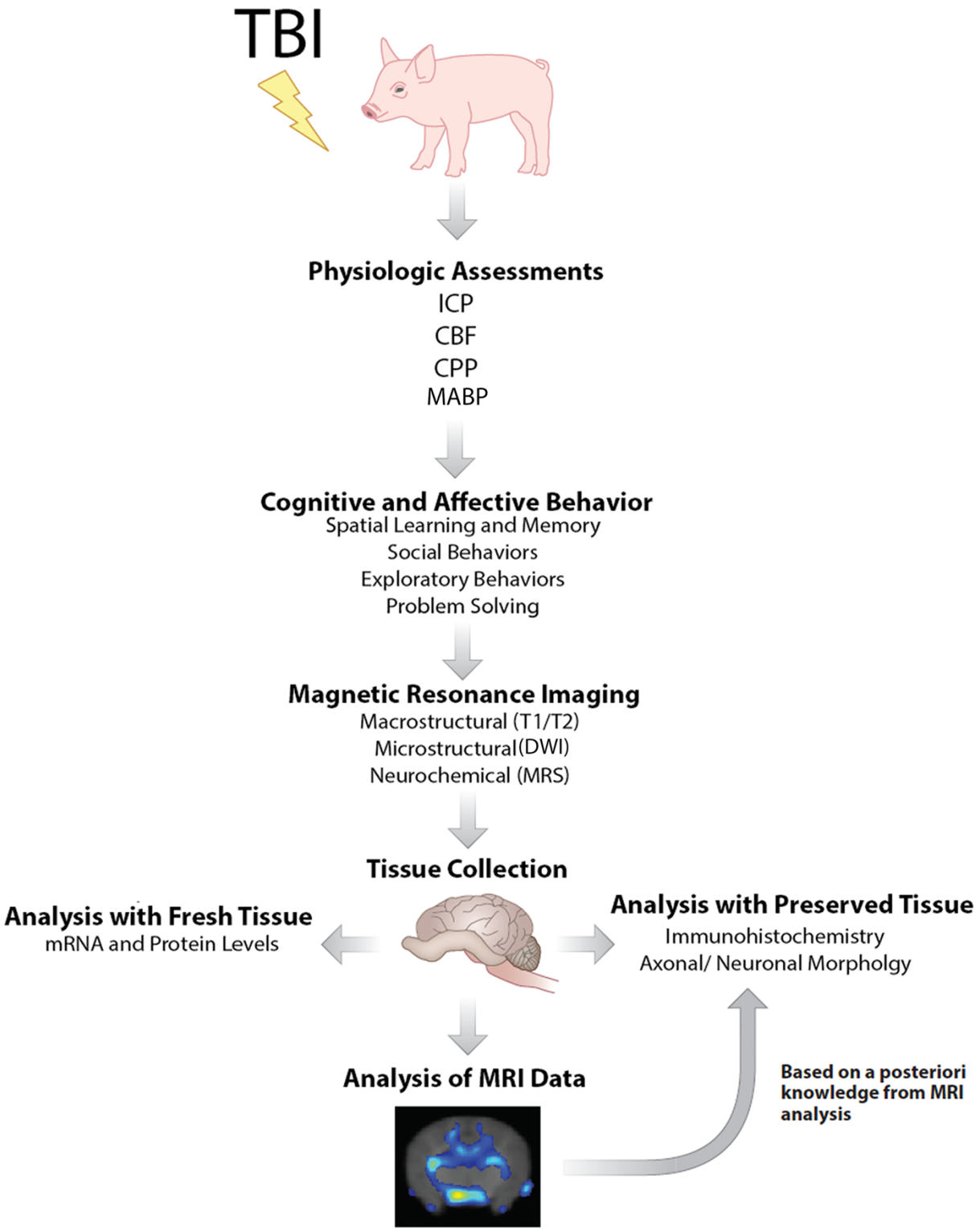
TBI
Physiologic Assessments
ICP
CBF
CPP
MABP
Cognitive and Affective Behavior
Spatial Learning and Memory
Social Behaviors
Exploratory Behaviors
Problem Solving
Magnetic Resonance Imaging
Macrostructural (T1/T2)
Microstructural(DWI)
Neurochemical (MRS)
Tissue Collection
Analysis with Fresh Tissue
mRNA and Protein Levels
Analysis with Preserved Tissue
Immunohistochemistry
Axonal/ Neuronal Morpholgy
Analysis of MRI Data
Based on a posteriori knowledge from MRI analysis

CHAPTER 3

CONTROLLED CORTICAL IMPACT RESULTS IN SCALABLE INJURY IN A PIGLET TRAUMATIC BRAIN INJURY MODEL[1]

[1]Kinder, H.A. and Baker, E.W., Hutcheson, J.M., Duberstein, K.J., Platt, S.R., Howerth, E.W., West, F.W. To be submitted to *Journal of Neurotrauma*

Abstract

Traumatic brain injury (TBI) is a major cause of death and long-term disability in the United States, and children who sustain TBI at a young age may suffer long-term deficits in cognition, behavior, and/or motor function. A number of preclinical animal models have been developed in an effort to recapitulate injury mechanisms and identify potential therapeutics. However, the lack of restorative treatments for TBI has led to considerable criticism of current preclinical therapeutic development strategies, namely the translatability of widely-used rodent models to human patients. The use of large animal models, such as the pig, with more comparable brain anatomy and physiology to humans may enhance the translational capacity of current preclinical animal models. The objective of this study was to develop and characterize a scaled piglet TBI model with quantitative pathological features at the cellular, tissue, and functional level that become more prominent with increasing TBI severity. TBI was produced by controlled cortical impact (CCI) in toddler-aged Landrace piglets with impact velocity and depth of depression set to 2m/s;6mm, 4m/s;6mm, 4m/s;12mm, or 4m/s;15mm resulting in scaled neural injury. Quantitative gait analysis was performed pre-TBI and 1, 3, and 7 days post-TBI, and piglets were sacrificed 7 days post-TBI. Increasing impact parameters correlated to increases in lesion size and the extent of neuronal loss, intracerebral hemorrhage, gliosis, and white matter damage as well as motor function deficits. The piglet TBI model described here could serve as a translational platform for studying TBI sequelae across injury severities and identifying novel therapeutics.

Introduction

In the United States, traumatic brain injury (TBI) results in an estimated 2,174 deaths and 473,947 emergency department visits among children aged 0-14 years annually [1]. Falls account for approximately 50.2% of all sustained TBIs for children, and the rate of fall-related TBIs is highest among children aged 0-4 year (839 per 100,000) [1]. Further, pediatric TBI accounts for more than $1 billion in total hospital charges annually [2]. Although adolescent brains are believed to be more "plastic" and thus more adept to recover and restore function after injury, recent evidence has shown that children who sustain a TBI at a younger age may suffer long-term neurological consequences such as impairments in cognition, behavior, and motor function [3-7]. At present, a number of management strategies are utilized to monitor and alter critical aspects affecting TBI outcomes including intracranial pressure, cerebral oxygenation, cerebral edema, and cerebrovascular injury after pediatric TBI, which may substantially decrease hospital stays and mortality rates [8]. Treatment options are restricted to techniques such as hyperosmolar therapy, temperature control, cerebrospinal fluid drainage, barbiturate therapy, decompressive craniectomy, and antiseizure prophylaxis that aim to reduce secondary brain insults [9]. However, these treatments have little influence on reducing long-term functional deficits [10-12].

Numerous experimental animal models have been developed in an effort to recapitulate the primary and secondary injury aspects of a human TBI and, in turn, have helped delineate many of the biomechanical, cellular, molecular, and functional responses of TBI that cannot be studied in a clinical setting [13]. In rodents, one of the most widely used and studied TBI models is the controlled cortical impact (CCI) model. CCI allows for precise, quantitative control over parameters that affect injury severity such as velocity, depth of depression, and tip diameter [14].

CCI can be manipulated to produce injuries ranging from mild to severe and is highly reproducible [15]. The ability to control injury severity allows researchers to produce gradable tissue damage, functional impairments, provide a means to better account for the variation in pathologies observed in TBI patients, and most importantly, develop appropriate treatment strategies [14]. Magnetic resonance imaging (MRI) studies in pediatric TBI patients have revealed that lesion size, gray and white matter disruption, and brain atrophy can be influenced by injury severity [16]. Functional deficits, such as cognition and motor function, have been documented to vary according to injury severity in children after TBI [17, 18]. To address this, scaled CCI in rodent models has been used to characterize the effects of injury severity on histopathological changes and behavioral and motor responses after injury and consequently, to identify potential therapeutic targets [19-23]. Despite promising preclinical results in rodent studies utilizing a wide range of therapeutics, there is no Food and Drug Administrative (FDA) approved treatment that promotes functional recovery in humans [24-26]. Given the significant impact of TBI, particularly in children who are at a critical period of brain development, the lack of effective treatments has led to considerable criticism of the use of rodents as a translational model [27, 28].

The pig, having similarities in brain anatomy and physiology to humans, may provide a significant advantage in modeling TBI and testing the safety and efficacy of novel therapeutics. The human brain is gyrencephalic and is comprised of >60% white matter [29, 30]. The gyrencephalic piglet brain has been found to mirror the pediatric brain in terms of size, development, and neuroinflammatory response, and is also comprised of >60% white matter [31-34]. However, the lissencephalic rodent brain is 650 times smaller than the human brain and is composed of only 14% of the relative white matter volume of humans [30, 35-37]. Given the

propensity for TBI to contribute to widespread white matter damage in human patients, the use of a large animal model with comparable white matter composition is critical to more closely recapitulate the human pathology [38]. Despite pressure to pursue more large animal models of TBI, limited progress has been made in the field. No study has been performed to directly assess the effect of scaled changes in velocity and depth of depression on cellular dynamics and motor function in a CCI piglet model [39, 40].

The purpose of this study was to develop and characterize a scaled piglet TBI model by manipulating CCI severity and measuring corresponding changes at the cellular, tissue and functional levels. CCI severity was controlled by manipulating either velocity, depth of depression, or both. Lesion size and histological analysis were assessed to measure changes at the tissue and cellular level and were found to correlate with injury severity. Finally, spatial-temporal gait analysis was performed to assess changes in motor function and was found to respond as a function of increasing injury severity. The development of a piglet TBI model with pathological and functional changes that mirror human TBI patients can be used in future studies to serve as a platform for the testing of novel therapeutics.

Materials and Methods

All work performed in this study was done in accordance with the University of Georgia Institutional Animal Care and Use Committee guidelines.

Animals

Sixteen commercially bred Landrace-cross piglets of mixed sex and 3 weeks of age were obtained from the University of Georgia Swine Unit 1 week prior to surgery. Piglets were group housed and fed a nutritionally complete starter diet ad libitum. Room temperature was maintained at 26°C with a 12h light/dark cycle and an overhead heat lamp provided supplemental heat. All animals were feed restricted overnight prior to surgery but had free access to water.

Surgical Preparation

Piglets underwent surgery at 4 weeks of age. Anesthesia was induced using 5% vaporized isoflurane in oxygen utilizing a surgical mask. After induction, anesthesia was maintained at 2-3% vaporized isoflurane in oxygen. Continuous physiological monitoring of heart rate, respiration rate, and rectal temperature was performed every 5 minutes after induction of anesthesia. The skin was prepared in a routine manner for sterile surgery using Betadine and 70% alcohol. The surgical site was draped in a standard fashion. A left-sided skin incision approximately 4cm in length was made over the top of the cranium. An air drill (Brasseler, USA) was used to produce a circular craniectomy approximately 20mm in diameter at the left posterior junction of the coronal and sagittal sutures. Care was taken to avoid disruption of the dura mater and underlying cortical surface.

Controlled Cortical Impact

Concussive TBI was generated through the use of a specialized controlled cortical impactor (CCI) device designed by our lab in collaboration with the University of Georgia Instrument Design and Fabrication Shop (Athens, GA). Impactor design was modeled after the design of Manley et al. [40]. Briefly, the impactor is comprised of a small-bore, double-acting, pneumatic cylinder with a piston. The cylinder is mounted to an adjustable frame that can be angled to the curvature of the piglet's skull. A 15-mm impactor tip with beveled edges is attached to the lower end of the threaded rod. The upper end of the rod is attached to the transducer core of a linear voltage differential transducer (LVDT). Fine-tuning the flow of pressurized gas to the pneumatic piston controls the velocity of the impactor. Velocity is calculated from the time/displacement curve measured by the LVDT and recorded by the computerized data acquisition system DAQ Central. In addition, a CLICK® Series Programmable Logic Controller (PLC) is used to regulate the dwell time of the impactor rod.

Following surgical preparation, the piglet was secured to the CCI frame and the impactor tip was positioned over the craniectomy site. For this initial study, we chose to assess the effects of a scaled injury by manipulating either the velocity or depth of depression, or both. Piglets were divided into four groups defined by the impact parameters in which TBI was induced: 2m/s impact velocity with 6mm depth of depression (n=4), 4m/s impact velocity with 6mm depth of depression (n=4), 4m/s impact velocity with 12mm depth of depression (n=4), and 4m/s impact velocity with 15mm depth of depression (n=4). The dwell time was held constant at 400ms for all animals.

After injury, the surgery site was flushed with sterile saline and the skin was re-apposed with surgical staples. Banamine (1.1 mg/kg IM) and Butorphanol (0.2 mg/kg IM) was

administered postoperatively for pain management, and Ceftiofur Sodium (Naxcel®; 4 mg/kg IM) was administered as an antibiotic. Anesthesia was discontinued and piglets were allowed to recover until ambulatory before being returned to their home pens. Piglets were monitored every 8 hours for the next 24 hours and any abnormal neurological behaviors were recorded.

Gait Analysis

One week prior to surgery, piglets were individually placed in a semi-circular gait analysis track in a separate climate-controlled room for gait track familiarization and training. Piglets were familiarized to the testing room and trained to move down the track for 3 days prior to data collection. After training, each piglet was video recorded on 3 separate days prior to TBI surgery to obtain pre-TBI gait measurements. Piglets were also evaluated on days 1, 3, and 7 post-TBI. Gait analysis was performed as previously described [41]. Briefly, 2 high speed GigEye Ethernet Cameras (IDS Imaging Development Systems, Obersulm, Germany) set to capture footage (70 frames per second) of each side of the pig in profile view were synchronized through an IDS computer driver. Piglets were recorded as they walked through the straight portion of the semi-circular track, where they were video recorded as they moved perpendicular to the 2 synchronized cameras recording each side of the piglet. Piglets were moved through the track until 5 usable repetitions were obtained. Video data was analyzed using Kinovea software (Kinovea open source project, www.kinovea.org) to obtain swing time, stance time, stride velocity, and 2-limb versus 3-limb support measurements.

Lesion Size Assessment

One week post-TBI, piglets were deeply anesthetized using 5% vaporized isoflurane in oxygen and euthanized via CO_2 inhalation. After euthanasia, brains were removed, sectioned into 5mm coronal slices, and fixed in 10% buffered formalin for lesion size measurement and histology. For lesion size measurement, serial 5mm coronal sections were scanned with a Canon CanoScan 8800F. Lesion size was measured using ImagePro Plus software (Media Cybernetics, Rockville, MD). The value obtained from each coronal section was multiplied by 5 to account for brain section depth, and measurements for each section were combined to obtain total lesion volume. Total lesion volumes were compared to the contralateral cerebral hemisphere.

Histology

Representative sections from each animal were collected, routinely processed, embedded in paraffin, sectioned at 4 μm, and stained with hematoxylin and eosin to evaluate the lesion microscopically. Additional sections were stained by immunohistochemistry for glial fibrillary acidic protein (GFAP; 1:4000; mouse; Biogenex), Olig2 (1:400; rabbit; Genetex), and neuronal nuclei (NeuN; 1:500, guinea pig, Millipore) as previously described [42]. . Heat induced antigen retrieval was performed for GFAP, Olig2, and NeuN using citrate buffer at pH6 (DAKO). Detection was performed using biotinylated anti-mouse (GFAP; Biocare), anti-guinea pig (NeuN; Biogenex), or anti-rabbit (Olig2; Biocare) antibodies, and a streptavidin label (4plus Streptavidin HRP or AP label; Biocare), and 3,3'-Diaminobenzidine (DAB) as the chromogen (DAKO). All sections were counterstained with hematoxylin. For quantification, a perilesional ROI was defined, which included dorsal and dorsolateral gyri (cingulate, marginal, suprasylvian and sylvian and/or ectosylvian), and 5 fields were imaged per section using an Olympus BX41

light microscope (Center Valley, PA). Utilizing ImagePro Plus software, the percentage of cells positive for NeuN and Olig2 were manually counted and GFAP was quantified by relative threshold value.

Statistics

Data was analyzed with SAS version 9.3 (Cary, NC) and statistical significances between groups were determined by two-way analysis of variance followed by post-hoc Tukey's Pair-Wise comparisons. Treatments where p-values were ≤ 0.05 were considered to be significantly different.

Results

Lesion volume is correlated to increased impact velocity and depth of depression

To determine if impact velocity and depth of depression had an effect on lesion size, piglet brain tissue underwent volumetric assessment after injury. Piglets in the 2m/s; 6mm group (velocity and depth, respectively) had minor brain lesions. However, when impact velocity was increased to 4m/s while maintaining a 6mm depth of depression, there was a greater than 50-fold increase in brain lesion volume ($2.29mm^3 \pm 2.29mm^3$ vs. $124.70mm^3 \pm 47.18\ mm^3$, respectively) and a significant ($p<0.05$) increase in lesion volume compared to the contralateral hemisphere (**Figure 3.1A-B, E**). Furthermore, when depth of depression was increased to 12mm and 15mm while maintaining the impact velocity at 4m/s, lesion volume continued to increase ($944.0mm^3 \pm 417.49$mm and $1236.15mm^3 \pm 240.94mm^3$, respectively) and remained significantly ($p<0.05$) larger than the contralateral side (**Figure 3.1C-D, E**). Taken together, these results indicate there was a clear positive correlation between lesion volume and velocity and depth of depression.

Histopathology reveals correlative increase in lesion size in response to scaled injury

In the 2m/s; 6mm group, microscopic changes were subtle. Tips of gyri (marginal, suprasylvian, and/or sylvian) at the lesion site had increased cellularity (gliosis) in both cortex and white matter and rare shrunken necrotic cortical neurons. Mild fibrosis of the leptomeninges overlying the lesion site was present (**Figure 3.2A**). Immunohistochemistry for GFAP revealed mild multifocal astrocytosis/astrogliosis in the involved cortex and underlying white matter (**Figure 3.3A**), but no subjective change in oligodendrocytes were present on Olig2 staining (**Figure 3.4I**). The 4m/s; 6mm group had more extensive changes, although similar to the 2m/s; 6mm group in that changes were primarily at the tips of gyri (marginal, suprasylvian, and sylvian) at the lesion site. This was characterized by more extensive neuronal necrosis and loss, reactive vessels, sometimes with mild perivascular cuffing by lymphocytes and plasma cells, and hypercellularity of both cortex and white matter in the involved area due to gliosis and infiltrating gitter cells. Unlike the 2m/s; 6mm group, some animals had shallow tracks filled with hemorrhage and/or gitter cells in the area of impact. In addition, there were hemorrhage, hemosiderin laden macrophages, mild perivascular cuffing by lymphocytes and plasma cells, and fibrosis in the overlying leptomeninges (**Figure 3.2B**). By immunohistochemistry, there was increased staining for GFAP around the lesion site (**Figure 3.3B**), but no discernable change in oligodendrocytes were present in Olig2 staining (**Figure 3.4I**). In the 4m/s; 12mm group, changes were more severe and were present in all the dorsolateral gyri (marginal, suprasylvian, and sylvian) and sometimes the cingulate gyrus. The immediate area of impact was disrupted deep into the white matter and mostly replaced with hemorrhage and macrophages containing hemosiderin. Surrounding the impact tract, adjacent cortex and white matter was hypercellular

and the white matter, down to the lateral ventricle, had extensive degenerative changes consisting of axonal and myelin degeneration. The overlying leptomeninges were thickened by hemorrhage and an infiltration of macrophages, lymphocytes, neutrophils, and fibroblasts (**Figure 3.2C**). There was a diffuse increase in staining for GFAP (astrocytosis/astrogliosis) surrounding the impact tract (**Figure 3.3C**), but numbers of cells staining for Olig2 did not appear increased (**Figure 3.4I**). The 4m/s; 15mm group had the most severe changes also involving the dorsolateral gyri (marginal, suprasylvian, and sylvian) and the cingulate gyrus. The lesion site was characterized by a large, deep tract of tissue necrosis and loss, often extending to the lateral ventricle and disrupting the ependymal lining, which was filled with hemorrhage and gitter cells. The tract was immediately surrounded by hemosiderin/hematoidin-laden gitter cells and a layer of gliosis with reactive vessels. Severe gliosis extended into the surrounding gyri and white matter, and the white matter had degenerative changes consisting of swollen axons and myelin degeneration. The overlying meninges were thickened by hemorrhage, infiltration of hemosiderin-laden macrophages, lymphocytes, plasma cells, and fibrosis. In one animal, the contralateral marginal gyrus had a large deep tract that extended to the ventricle and was filled with hemorrhage (**Figure 3.2D**). Surrounding the impact tract there was severe, diffuse staining for GFAP (astrocytosis/astrogliosis, **Figure 3.3D**), and slightly increased numbers of Olig2 stained cells in the white matter (**Figure 3.4I**).

Immunohistochemistry reveals correlative loss of neurons and increased gliosis in response to scaled injury

Immunohistochemical analysis was performed on the perilesional region to assess changes in the number of neurons, astrocytes, and oligodendrocytes as a result of increasing TBI

severity. A similar anatomical region on the contralateral hemisphere was utilized as the control to account for individual variability of basal neural cell numbers. First, staining for the neuron marker (NeuN) was used to quantify the number of mature neurons around the site of impact compared to the contralateral side. In the 2m/s; 6mm group, the lesion site was comprised of 37.76% ± 3.58% NeuN+ cells compared to 45.37% ± 2.69% NeuN+ cells on the contralateral hemisphere, indicating a decrease in NeuN+ cells around the lesion site, although not statistically significant (**Figure 3.4C**). The disparity of percent NeuN+ cells between the ipsilateral and contralateral hemispheres became more pronounced when impact velocity was increased to 4m/s and furthermore when depth of depression was increased. In the 4m/s; 6mm group, there was a significant ($p<0.01$) decrease in NeuN+ cells around the lesion site compared to the corresponding contralateral side (32.38% ± 1.59% vs. 42.05% ± 1.95%, **Figure 3.4C)**. There was also a significant ($p<0.01$) reduction in NeuN+ cells around the lesion site compared to the contralateral hemisphere in the 4m/s; 12mm group (29.33% ± 3.51% vs. 46.41% ± 1.62%, **Figure 3.4A-C**). Lastly, the most discernable decrease in NeuN reactivity around the lesion site was evident in the 4m/s; 15mm group where there were only 24.75% ± 2.72% NeuN+ cells in contrast to 45.01% ± 0.69% NeuN+ cells on the contralateral side ($p<0.0001$, **Figure 3.4C**). Taken together, there was a negative correlation in percentage of mature neurons around the lesion site as velocity and depth of depression was increased.

The dynamic changes in astrocyte numbers around the lesion site was determined by staining for GFAP and compared to the corresponding area on the contralateral hemisphere. A similar pattern observed for NeuN reactivity emerged for GFAP in the mildest, 2m/s; 6mm group; a minimal increase in GFAP reactivity was present around the lesion site comparable to the contralateral side (threshold value 1079.8 ± 454 vs. 1012.45 ± 359.38, **Figure 3.4F**).

However, as injury severity increased, the disparity between GFAP reactivity around the lesion site compared to the contralateral side became more distinct. The 4m/s;6mm group had a significant ($p<0.05$) increase in GFAP reactivity around the lesion site compared to the same anatomical region on the contralateral hemisphere (threshold value 1530.55 ± 224.28 vs. 690.65 ± 102.32, **Figure 3.4F**). The 4m/s; 12mm group also had a significant ($p<0.01$) upregulation of GFAP around the lesion site compared to the contralateral side (threshold value 1592.1±177.51 vs. 803.85 ± 63.81, **Figure 3.4E-F**). Lastly, the 4m/s; 15mm group, the most severe group, had the strongest statistical difference ($p<0.001$) between the ipsilateral and the contralateral sides (1511.47±31.17 vs. 913.8 ± 104.42, **Figure 3.4F**). Therefore, activation of astrocytes, and thus astrogliosis/astrocytosis, becomes more pronounced as velocity and depth of depression is increased.

Lastly, we quantified the number of oligodendrocytes around the lesion site compared to the contralateral side utilizing staining for Olig2, which labels both mature oligodendrocytes and oligodendrocyte precursor cells. There was no significant difference in Olig2 positive cells around the lesion site compared to the contralateral side in the 2m/s; 6mm group (29.64% ± 6.54% vs. 26.1% ± 1.80%, **Figure 3.4I**), the 4m/s; 6mm group (22.86% ± 3.31% vs. 34.39% ± 2.31%, **Figure 3.4I**), the 4m/s; 12mm group (29.14% ± 3.98% vs. 35.16% ± 4.49%, **Figure 3.4G-I**), or the 4m/s; 15mm group (26.17% ± 2.38% vs. 33.15% ± 6.51%, **Figure 3.4G**). Thus, oligodendrocyte numbers did not vary in response to changes in injury severity compared to the contralateral hemisphere.

Motor deficits become more pronounced with increasing impact velocity and depth of depression

To measure potential deficits in motor function, gait analysis was performed first before TBI to serve as a baseline and then 1, 3, and 7 days post-TBI. Changes in swing time, stance time, stride velocity, 2-limb support, and 3-limb support were assessed as a function of increasing impact velocity and depth of depression using Kinovea gait analysis software (**Figure 3.5A**). Stance time, represented as the percentage of time spent in the stance phase compared to the swing phase for one full stride cycle, was used to assess whether a shift occurred in the amount of time spent in stance phase compared to swing phase after TBI. For both the 2m/s; 6mm and 4m/s; 6mm groups, animals spent approximately half their stride in stance phase pre-TBI (47.6% ± 1.7% and 47.18% ± 0.63%, **Figure 3.5B**). Stance time remained unchanged at all time-points after TBI, indicating consistent stance:swing ratio throughout the study. However, the 4m/s; 12mm group demonstrated a significant ($p<0.001$) increase in percent stance time and spent almost 20% more time in stance phase 1 day post-TBI as compared to pre-TBI (62.07% ± 2.93% vs. 43.04% ±1.1%, **Figure 3.5B**). A significant ($p<0.01$) increase in percent stance time persisted through both 3 and 7 days post-TBI (61.62% ± 1.58% and 56.07% ± 3.22%, **Figure 3.5B**). Further, the 4m/s; 15mm group also displayed significant ($p<0.0001$) increases in percent stance time and spent almost 18% more time in stance phase 1 day post-TBI as compared to pre-TBI (62.765% ± 0.40% vs. 45.25% ± 0.65%, **Figure 3.5B**). Animals maintained a significantly ($p<0.001$) increased percent stance time at both 3 and 7 days post-TBI (58.59% ±2.10% and 59.36% ±1.70%, **Figure 3.5B**). Taken together, this data suggests that increasing both velocity and depth of depression to 12 or 15mm results in a shift in the stance:swing ratio such that animals spend more time in stance phase during one stride cycle.

Stride velocity, or the time to complete one stride cycle, was used as a measure to detect changes in rate of movement after TBI. Stride velocity remained largely unaffected through all post-TBI time points for both the 2m/s; 6mm and 4m/s; 6mm groups compared to pre-TBI assessment (1.76m/s ± 0.11m/s and 1.58m/s ± 0.04m/s, **Figure 3.5C**). However, stride velocity was significantly ($p<0.001$) slower for the 4m/s;12mm group 1 day post-TBI as compared to pre-TBI (0.68m/s ±0.14m/s vs. 1.77m/s ±0.10m/s), and remained slower both 3 and 7 days post-TBI (1.05m/s ±0.36m/s, 1.02m/s ±0.24m/s), although day 3 and 7 results did not reach significance (**Figure 3.5C**). However, stride velocity was significantly ($p<0.001$) slower for the 4m/s;15mm group 1, 3 and 7 days post-TBI (0.69m/s ±0.05m/s, 0.95m/s ±0.12m/s, and 0.87m/s ±0.01m/s, respectively) as compared to pre-TBI (1.64m/s ± 0.02m/s, **Figure 3.5C**). These results indicate that stride velocity was reduced as a result of increasing TBI severity.

2-limb support, or the time spent on two limbs during a stride cycle, was assessed to determine if pigs shift to 3-limb support which would suggest a decrease in balance and a need for additional support post-TBI. Percent of time spent in 2-limb support remained relatively unchanged for both the 2m/s; 6mm and 4m/s; 6mm groups after TBI for all time points as compared to pre-TBI (100% ± 0.11%, 100% ± 0.30%, **Figure 3.5D**). For the 4m/s; 12mm group, percent time spent in 2-limb support decreased 1 and 3 days post-TBI as compared to pre-TBI (73.79% ± 9.79% and 68.65% ± 9.79% vs. 100% ± 9.79%, respectively), although these results did not reach significance. However, percent 2-limb support significantly ($p<0.05$) decreased by almost 46% 7 days post-TBI as compared to pre-TBI (54.04% ± 9.79% vs. 100% ± 9.79%, **Figure 3.5D**). The 4m/s; 15mm group's percent time spent in 2-limb support significantly ($p<0.001$) decreased by almost 34% 1 day post-TBI as compared to pre-TBI (66.39% ± 5.82% vs. 100% ± 5.82%, **Figure 3.5D**). Interestingly, time spent in 2-limb support continued to

decrease over time, as opposed to stance time and stride velocity where small increments of improvement were noted at 3 and 7 days post-TBI. Percent 2-limb support significantly decreased by almost 38% 3 days post-TBI and by almost 54% 7 days post-TBI compared to pre-TBI (61.86 ± 5.82% and 46.51 ± 5.82% vs. 100% ± 5.82% respectively, $p<0.05$, **Figure 3.5D**). Taken together, this data suggests that uninjured animals and injured animals with a more mild TBI typically relied on only 2-limb support, but that increasing velocity and depth of depression resulted in a shift from 2-limb-only support to a combination of 2-and 3-limb support.

Discussion

In this study, we characterize a scaled piglet TBI model generated using an open skull CCI approach in which the histopathological and functional response to injury increases as a function of cortical impact speed and depth of depression. Increasing the velocity and depth of depression of impact contributed to significant increases in lesion volume 1 week post-TBI. Affected regions demonstrated macro- and microcellular changes in the brain, such as mild damage, mostly in the cortex at the tips of gyri, characterized by neuronal necrosis and mild astrocytosis/astrogliosis in more mildly affected groups to large tracts of necrosis, neuroparenchymal loss, and often hemorrhage extending from the meningeal surface to the ventricle with degeneration in the surrounding white matter and intense astrocytosis/astrogliosis in the more severely affected groups. Most importantly, functional changes were observed that corresponded with TBI severity. Gait biomechanic analysis revealed progressive motor function deficits in stance time, stride velocity, and limb support as CCI parameters increased. These changes are consistent with human TBI outcomes. These results suggest that this piglet TBI model may be an ideal model for use in future studies aimed at further elucidating the

complexities of TBI pathophysiology, time course, and functional responses, and may have greater predictive power of the efficacy of potential therapeutics.

We chose to utilize a CCI to generate a TBI as this approach has proven to be reliable and repeatable in both rodent and pig models [43]. The surgical approach is relatively quick and takes less than 1 hour from initial skin incision to final closure. This procedure resulted in no deaths, even in our most severe group despite all pigs exhibiting significant neurological impairments. We developed our CCI device after the design of Manley et al. using a gas driven pneumatic piston to allow for the precise control of the impact parameters, thus giving us the ability to manipulate injury severity [40]. It has been well established that manipulation of velocity, depth of depression, and dwell time either individually or in combination can affect injury severity.

We took several factors in to account when selecting each combination of impact parameters that would best produce features of human TBI. First, a dwell time of 400ms was selected for all groups, similar to previous reports [39, 40, 44, 45]. Duhaime et al. developed a piglet TBI model at three different maturational stages at 5 days, 1 month, and 4 months of age [39]. Depth of depression for 5-day, 1-month, and 4-month old animals varied from 5mm, 6mm, and 7mm, respectively, and velocity was held constant at 1.7m/s for all maturation stages [39]. Similarly, in this study, we used 1 month old piglets and selected a velocity of 2m/s and a depth of depression of 6mm as our initial CCI parameters to achieve a small focal contusion. Interestingly, despite a slightly faster velocity and a larger impactor tip diameter, we observed a smaller lesion than Duhaime et al. However, this may be attributed to their slightly different CCI approach in which injury does not occur as a result of the force of the impactor tip striking the brain, but instead from displacement of the tip resting on the cortical surface. Similar to Duhaime

et al., the 2m/s; 6mm group exhibited no gait abnormalities in our study. We next increased velocity to 4m/s similar to the velocity of a CCI model reported by Jin et al. [46]. Again, no motor deficits were observed in the 4m/s; 6mm group; however, we did observe a significant focal contusion with many histopathological hallmarks of TBI. Next, we held velocity constant at 4m/s but increased depth of depression to 12mm and 15mm similar to Manley et al. who developed a scaled CCI model in adult pigs (38-42kg) by fixing velocity at 3.5m/s and varied depth of depression from 9mm, 10mm, 11mm, or 12mm [40]. In addition, Meissner et al. measured neuromonitoring parameters and histological changes in an adult pig CCI model produced with a 2.5m/s velocity and a 9mm depth of depression and Maytar et al. assessed autoregulatory responses in a piglet CCI model with a 3m/s velocity a 6mm and 10mm depth of depression which they classified as moderate and severe, respectively [47, 48]. These previous studies influenced our decision to manipulate depth of depression to a much higher value in order to achieve histopathological and functional deficits with increased severity. Manley et al. did not report any functional deficits, however if they were present they cite lack of functional neurological outcome measures as an explanation [40]. As such, we present the first piglet CCI study to report and quantify functional motor deficits.

Given that there is no common scoring system that has been adopted to assess injury severity for any experimental animal species, like the Glasgow Coma Scale used in human TBI patients, we hesitate to classify our injury outcomes as either mild, moderate, or severe [13]. However, in this study we have achieved a range of injuries in which histopathological and functional changes correlate with severity, such that comparatively among groups outcomes range from mild to severe, similar to scaled studies in rodents [19, 22, 49].

In the present study, we assessed changes in lesion size in order to determine the extent of tissue damage as a result of increasing TBI severity. Human MRI studies have found that lesion volume is a critical predictor of outcome after TBI and that lesion volume directly correlates with long-term functional outcomes using multiple clinical scales [50, 51]. In addition, lesion size, characterized by the number of affected brain regions, correlates with the extent of motor deficits and affects the time of recovery [7]. We found a direct relationship between TBI severity and lesion size such that for each increase in CCI parameters, lesion volume was increased. It can also be noted that in this study, similar to humans, we observed a clear correlation between lesion size and motor deficits. The 4m/s; 12mm and 4m/s; 15mm groups with the largest lesion volumes exhibited the greatest impairments in gait. Previous studies have outlined a similar approach in pigs where serial sections were used to assess lesion volume [39, 52]. Previous reports of lesion analysis using histology and MRI and found that although not exact, histological assessment of lesion volume was comparable to MRI volumetric analysis [42, 53]. Future studies will benefit from MRI analyses to assess more specific changes within the lesion site such as cytotoxic or vasogenic edema, swelling, white matter disruption, and reduced cerebral blood flow after brain trauma.

In this report we provide both a qualitative and quantitative assessment of histological changes across groups. H&E stained brain slices were reviewed by a board certified veterinary pathologist and assessed for specific pathological hallmarks of TBI commonly observed in humans [54]. Histological assessment revealed increasing damage with increasing velocity and depth of impact. Low velocity and depth of depression resulted in a small superficial cortical focus of subtle damage characterized by neuronal necrosis and reactive gliosis. As velocity increased cortical damage and gliosis became more widespread, although still relatively

superficial, with associated hemorrhage, necrosis, and vascular reaction, as well as underlying white matter changes. As the depth of depression increased, associated lesions became large tracts of necrosis, tissue loss, and hemorrhage extending deep into the cerebrum often down to the ventricle. These larger lesions were surrounded by a more intense gliosis and vascular reaction, and more severe white matter degeneration. Similarly, scaled CCI in adult pigs has been shown to result in increased presence of vascular congestion and decreased loss of normal cytoarchitecture that corresponded with depth of depression [40]. In addition, TBI in the immature pig has revealed similar pathological features such as the presence of necrosis, hemorrhage, neuronal loss, and reactive gliosis at the site of injury [39, 52, 55].

Histological changes have been quantitatively evaluated using a numerical scoring system that ranks the severity of specific pathological features of TBI [44, 45]. However, a limited number of studies provide a direct quantification of changes of the relative number of specific cells types in the brain after CCI in pigs. Costine et al. evaluated the relative number of migrating DCX+ neuroblasts in the white matter after scaled cortical impact in piglets at different maturational stages, and Taylor et al., in a follow-up study, measured the distribution of DCX+, BrdU+ and DCX+/BrdU+ neuroblasts in the white matter from the subventricular zone to the site of injury. However, quantification of changes in neurons, astrocytes, and oligodendrocytes, three major cell types of the brain, after TBI in a pig brain is lacking. Therefore, in the current study, immunohistological staining was performed with the well-established markers NeuN, GFAP, and Olig2 to assess of the relative number of neurons, astrocytes, and oligodendrocytes, respectively, in the perilesional area 1 week post-TBI.

NeuN is a DNA-binding, neuron-specific protein expressed in post-mitotic neurons [56]. NeuN staining of human TBI-affected brain tissue has been shown to decrease at or near the site

of injury as a result of neuronal cell death [57]. In addition, rodent TBI studies reveal similar loss of neurons in response to injury and have been found to be sensitive to injury severity [19, 58, 59]. In our piglet TBI model, based on NeuN staining, the percent of mature neurons was significantly reduced for all groups except for the most mild, 2m/s; 6mm group, suggesting that neurons are sensitive to increasing TBI severity in this model.

GFAP, a cytoskeletal astrocytic marker, is well documented to measure astrocyte proliferation (astrocytosis) and hypertrophy (astrogliosis) after TBI [60, 61]. Reactive astrocytes grow in size, proliferate, and migrate to the site of injury where they release neurotrophic factors, promoting tissue repair [62]. However, astrocytosis and astrogliosis can also contribute to glial scar formation which can be detrimental to axonal regrowth and, ultimately, can contribute to neurodegeneration and the development of functional deficits [63]. GFAP expression is typically most highly upregulated at the site of the lesion and becomes less prominent in the perilesioned area in humans [57, 64]. Scaled injury in rodent models has shown that GFAP expression corresponds with injury severity [20]. Globally, we observed substantial astrocytosis and astrogliosis at and near the site of the lesion for the 4m/s; 6mm, 4m/s; 12mm, and 4m/s; 15mm groups and, in accordance, noted a significant upregulation of GFAP expression for these groups.

Lastly, Olig2, a basic helix loop helix (bHLH) transcription factor, is expressed in a number of different cell types including oligodendrocyte precursor cells and mature oligodendrocytes [65]. Oligodendrocytes are responsible for the myelination of axons. TBI in humans results in the death of mature oligodendrocytes followed by increases in oligodendrocyte precursor cells [66]. These dynamic changes may influence white matter function following TBI. Rodent TBI studies report similar changes in oligodendrocyte numbers in response to injury [67, 68]. Interestingly, the present study did not observe either increases or decreases in

oligodendrocytes in response to injury; however, there has been limited research on oligodendrocyte activity in the highly myelinated pig brain after TBI. Future studies may benefit from looking at changes in myelin basic protein (MBP) to assess direct changes in white matter composition as a result of TBI.

Children who sustain a TBI may develop impairments in motor proficiency. Several studies have evaluated motor deficits after TBI in children using quantitative gait analysis and found that children may exhibit deficits in spatiotemporal gait parameters [7, 18, 69]. Our group has previously developed a highly sensitive approach to assess changes in spatiotemporal gait parameters in a middle cerebral artery occlusion (MCAO) ischemic stroke pig model using high speed video cameras [70]. We present for the first time gait analysis performed in a piglet CCI model to assess impairments in motor function. We measured the response of stance percent, stride velocity, and limb support as a function of TBI severity. 4m/s; 12mm and 4m/s; 15mm groups exhibited significant deficits in stance percent at all time-points post-TBI, similar to TBI-affected children [71]. Increased overall stance percent may be explained by two reasons. First, the amount of time the pig spends in swing time may be reduced in an effort to hasten ground contact to begin the stance phase during which the pig is better able to stabilize its weight distribution. Second, limb weakness on the affected right side may limit the amount of propulsive forces needed to initiate and maintain the swing phase, resulting in a reduction of the time the hoof spends off the ground. Reduced stride velocity is one of the most common motor deficits observed as a result of moderate or severe TBI in children [71, 72]. Stride velocity was significantly reduced for the 4m/s; 12mm group 1 day post-TBI, and at all time-points for the 4m/s; 15mm group. Similar to human studies, pigs were given the option to move at a self-selected pace. We observed that normal piglets natural gait of choice is a run, during which 2

limbs support the entire stride cycle. However, post-TBI pigs that sustained a more severe TBI exhibited a preference to travel at either a slow run or even walk during which 3 limbs support a portion of the stride cycle. Therefore, we sought to measure the shift from 2-limb support to 3-limb support as a result of TBI. We found that there was a significant shift in 2-limb support to 3-limb support for the 4m/s; 12mm group 7 days post-TBI, and at all time-points for the 4m/s; 15mm group. This data suggests that the pigs altered both their speed of travel and their gait support as a result of TBI. Similar results were observed in rodent TBI studies that evaluated changes in gait [73, 74]. These findings indicate injury severity influences functional outcomes and that, similar to children, more moderately to severely affected animals develop motor deficits.

Conclusion

In this study, we developed and characterized a piglet CCI traumatic brain injury model. The piglet has several key similarities to children in both neuroanatomy and brain development making it more translational than traditional rodent models. Manipulating CCI parameters resulted in a reproducible, scalable injury with increasing lesion volume. The lesion site increased from a small superficial focus of neuronal necrosis and gliosis in the mildest impact to a large deep tract of necrosis and tissue loss with marked astrogliosis/astrocytosis and more extensive white matter changes in the more severe impacts. TBI produced motor impairments in gait that correlated with injury severity. This piglet TBI model is ideal to study the short and long-term responses of TBI in a more human-like model and to study the potential of novel diagnostics and therapeutics to translate successfully to human patients.

Acknowledgements and Disclosures

We would like to thank Richard Utley and Kelly Parham for their animal assistance; Vivian Lau and Lisa Reno for their surgical expertise and support; Mary Kate Mehegan for her assistance with animal work and tissue analysis; and Daniela Lorenco for her statistical analysis assistance. Financial support was provided by the University of Georgia Office of the Vice President for Research.

The authors have no conflicts of interest.

References

1. Langlois, J.A., Rutland-Brown, W., Thomas, K.E., *Traumatic brain injury in the United States: Emergency department visits, hospitalizations, and deaths.* Atlanta, GA: Centers for Disease Control and Prevention, National Center for Injury Prevention and Control, 2006.
2. Schneier, A.J., et al., *Incidence of pediatric traumatic brain injury and associated hospital resource utilization in the United States.* Pediatrics, 2006. **118**(2): p. 483-92.
3. Stiles, J., *Neural plasticity and cognitive development.* Dev Neuropsychol, 2000. **18**(2): p. 237-72.
4. Anderson, V., et al., *Functional plasticity or vulnerability after early brain injury?* Pediatrics, 2005. **116**(6): p. 1374-82.
5. Anderson, V., et al., *Predictors of cognitive function and recovery 10 years after traumatic brain injury in young children.* Pediatrics, 2012. **129**(2): p. e254-61.
6. Li, L. and J. Liu, *The effect of pediatric traumatic brain injury on behavioral outcomes: a systematic review.* Dev Med Child Neurol, 2013. **55**(1): p. 37-45.
7. Beretta, E., et al., *Assessment of gait recovery in children after Traumatic Brain Injury.* Brain Inj, 2009. **23**(9): p. 751-9.
8. Fakhry, S.M., et al., *Management of brain-injured patients by an evidence-based medicine protocol improves outcomes and decreases hospital charges.* J Trauma, 2004. **56**(3): p. 492-9; discussion 499-500.
9. Allen, K.A., *Pathophysiology and Treatment of Severe Traumatic Brain Injuries in Children.* J Neurosci Nurs, 2016. **48**(1): p. 15-27; quiz E1.

10. Maas, A.I., B. Roozenbeek, and G.T. Manley, *Clinical trials in traumatic brain injury: past experience and current developments.* Neurotherapeutics, 2010. **7**(1): p. 115-26.

11. Xiong, Y., A. Mahmood, and M. Chopp, *Emerging treatments for traumatic brain injury.* Expert Opin Emerg Drugs, 2009. **14**(1): p. 67-84.

12. Stein, D.G., R.I. Geddes, and E.A. Sribnick, *Recent developments in clinical trials for the treatment of traumatic brain injury.* Handb Clin Neurol, 2015. **127**: p. 433-51.

13. Xiong, Y., A. Mahmood, and M. Chopp, *Animal models of traumatic brain injury.* Nat Rev Neurosci, 2013. **14**(2): p. 128-42.

14. Kobeissy, F.H., *Brain neurotrauma : molecular, neuropsychological, and rehabilitation aspects*. Frontiers in neuroengineering. 2015, Boca Raton: CRC Press, Taylor & Francis Group. xxviii, 697 pages.

15. Romine, J., X. Gao, and J. Chen, *Controlled cortical impact model for traumatic brain injury.* J Vis Exp, 2014(90): p. e51781.

16. Bigler, E.D., et al., *Heterogeneity of brain lesions in pediatric traumatic brain injury.* Neuropsychology, 2013. **27**(4): p. 438-51.

17. Anderson, V.A., et al., *Recovery of memory function following traumatic brain injury in pre-school children.* Brain Inj, 2000. **14**(8): p. 679-92.

18. Kuhtz-Buschbeck, J.P., et al., *Analyses of gait, reaching, and grasping in children after traumatic brain injury.* Arch Phys Med Rehabil, 2003. **84**(3): p. 424-30.

19. Fox, G.B., et al., *Sustained sensory/motor and cognitive deficits with neuronal apoptosis following controlled cortical impact brain injury in the mouse.* J Neurotrauma, 1998. **15**(8): p. 599-614.

20. Saatman, K.E., et al., *Differential behavioral and histopathological responses to graded cortical impact injury in mice.* J Neurotrauma, 2006. **23**(8): p. 1241-53.

21. Yu, S., et al., *Severity of controlled cortical impact traumatic brain injury in rats and mice dictates degree of behavioral deficits.* Brain Res, 2009. **1287**: p. 157-63.

22. Washington, P.M., et al., *The effect of injury severity on behavior: a phenotypic study of cognitive and emotional deficits after mild, moderate, and severe controlled cortical impact injury in mice.* J Neurotrauma, 2012. **29**(13): p. 2283-96.

23. Zhao, Z., et al., *Comparing the predictive value of multiple cognitive, affective, and motor tasks after rodent traumatic brain injury.* J Neurotrauma, 2012. **29**(15): p. 2475-89.

24. Xiong, Y., A. Mahmood, and M. Chopp, *Neurorestorative treatments for traumatic brain injury.* Discov Med, 2010. **10**(54): p. 434-42.

25. Buki, A., D.O. Okonkwo, and J.T. Povlishock, *Postinjury cyclosporin A administration limits axonal damage and disconnection in traumatic brain injury.* J Neurotrauma, 1999. **16**(6): p. 511-21.

26. Riess, P., et al., *Transplanted neural stem cells survive, differentiate, and improve neurological motor function after experimental traumatic brain injury.* Neurosurgery, 2002. **51**(4): p. 1043-52; discussion 1052-4.

27. Kolb, B., R. Gibb, and G. Gorny, *Cortical plasticity and the development of behavior after early frontal cortical injury.* Dev Neuropsychol, 2000. **18**(3): p. 423-44.

28. Johnson, V.E., et al., *Animal models of traumatic brain injury.* Handb Clin Neurol, 2015. **127**: p. 115-28.

29. Kandel, E.R., *Principles of neural science*. 5th ed. 2013, New York: McGraw-Hill. l, 1709 p.

30. Ahmad, A.S., et al., *Considerations for the Optimization of Induced White Matter Injury Preclinical Models.* Front Neurol, 2015. **6**: p. 172.

31. Thomas, J.M. and J.L. Beamer, *Age-weight relationships of selected organs and body weight for miniature swine.* Growth, 1971. **35**(3): p. 259-72.

32. Coppoletta, J.M. and S.B. Wolbach, *Body Length and Organ Weights of Infants and Children: A Study of the Body Length and Normal Weights of the More Important Vital Organs of the Body between Birth and Twelve Years of Age.* Am J Pathol, 1933. **9**(1): p. 55-70.

33. Pond, W.G., et al., *Perinatal ontogeny of brain growth in the domestic pig.* Proc Soc Exp Biol Med, 2000. **223**(1): p. 102-8.

34. Flynn, T.J., *Developmental changes of myelin-related lipids in brain of miniature swine.* Neurochem Res, 1984. **9**(7): p. 935-45.

35. Lind, N.M., et al., *The use of pigs in neuroscience: modeling brain disorders.* Neurosci Biobehav Rev, 2007. **31**(5): p. 728-51.

36. Zhang, K. and T.J. Sejnowski, *A universal scaling law between gray matter and white matter of cerebral cortex.* Proc Natl Acad Sci U S A, 2000. **97**(10): p. 5621-6.

37. Fairbairn, L., et al., *The mononuclear phagocyte system of the pig as a model for understanding human innate immunity and disease.* J Leukoc Biol, 2011. **89**(6): p. 855-71.

38. Gale, S.D., et al., *Nonspecific white matter degeneration following traumatic brain injury.* J Int Neuropsychol Soc, 1995. **1**(1): p. 17-28.

39. Duhaime, A.C., et al., *Maturation-dependent response of the piglet brain to scaled cortical impact.* J Neurosurg, 2000. **93**(3): p. 455-62.

40. Manley, G.T., et al., *Controlled cortical impact in swine: pathophysiology and biomechanics.* J Neurotrauma, 2006. **23**(2): p. 128-39.

41. Duberstein, K.J., et al., *Gait analysis in a pre- and post-ischemic stroke biomedical pig model.* Physiol Behav, 2014. **125**: p. 8-16.

42. Platt, S.R., et al., *Development and characterization of a Yucatan miniature biomedical Pig permanent middle cerebral artery occlusion stroke model.* Exp Transl Stroke Med, 2014. **6**(1): p. 5.

43. Osier, N. and C.E. Dixon, *The Controlled Cortical Impact Model of Experimental Brain Trauma: Overview, Research Applications, and Protocol.* Methods Mol Biol, 2016. **1462**: p. 177-92.

44. Alessandri, B., et al., *Moderate controlled cortical contusion in pigs: effects on multi-parametric neuromonitoring and clinical relevance.* J Neurotrauma, 2003. **20**(12): p. 1293-305.

45. Sindelar, B., et al., *Effect of Internal Jugular Vein Compression on Intracranial Hemorrhage in a Porcine Controlled Cortical Impact Model.* J Neurotrauma, 2016.

46. Jin, G., et al., *Traumatic brain injury and hemorrhagic shock: evaluation of different resuscitation strategies in a large animal model of combined insults.* Shock, 2012. **38**(1): p. 49-56.

47. Meissner, A., et al., *Effects of a small acute subdural hematoma following traumatic brain injury on neuromonitoring, brain swelling and histology in pigs.* Eur Surg Res, 2011. **47**(3): p. 141-53.

48. Mytar, J., et al., *Static autoregulation is intact early after severe unilateral brain injury in a neonatal Swine model.* Neurosurgery, 2012. **71**(1): p. 138-45.

49. Markgraf, C.G., et al., *Injury severity and sensitivity to treatment after controlled cortical impact in rats.* J Neurotrauma, 2001. **18**(2): p. 175-86.

50. Chastain, C.A., et al., *Predicting outcomes of traumatic brain injury by imaging modality and injury distribution.* J Neurotrauma, 2009. **26**(8): p. 1183-96.

51. Pierallini, A., et al., *Correlation between MRI findings and long-term outcome in patients with severe brain trauma.* Neuroradiology, 2000. **42**(12): p. 860-7.

52. Missios, S., et al., *Scaled cortical impact in immature swine: effect of age and gender on lesion volume.* J Neurotrauma, 2009. **26**(11): p. 1943-51.

53. Grate, L.L., et al., *Traumatic brain injury in piglets of different ages: techniques for lesion analysis using histology and magnetic resonance imaging.* J Neurosci Methods, 2003. **123**(2): p. 201-6.

54. McGinn, M.J. and J.T. Povlishock, *Cellular and molecular mechanisms of injury and spontaneous recovery.* Handb Clin Neurol, 2015. **127**: p. 67-87.

55. Duhaime, A.C., et al., *Magnetic resonance imaging studies of age-dependent responses to scaled focal brain injury in the piglet.* J Neurosurg, 2003. **99**(3): p. 542-8.

56. Wolf, H.K., et al., *NeuN: a useful neuronal marker for diagnostic histopathology.* J Histochem Cytochem, 1996. **44**(10): p. 1167-71.

57. Buritica, E., et al., *Changes in calcium-binding protein expression in human cortical contusion tissue.* J Neurotrauma, 2009. **26**(12): p. 2145-55.

58. Gobbel, G.T., et al., *Diffuse alterations in synaptic protein expression following focal traumatic brain injury in the immature rat.* Childs Nerv Syst, 2007. **23**(10): p. 1171-9.

59. Ajao, D.O., et al., *Traumatic brain injury in young rats leads to progressive behavioral deficits coincident with altered tissue properties in adulthood.* J Neurotrauma, 2012. **29**(11): p. 2060-74.

60. Middeldorp, J. and E.M. Hol, *GFAP in health and disease.* Prog Neurobiol, 2011. **93**(3): p. 421-43.

61. Burda, J.E., A.M. Bernstein, and M.V. Sofroniew, *Astrocyte roles in traumatic brain injury.* Exp Neurol, 2016. **275 Pt 3**: p. 305-15.

62. Ziebell, J.M. and M.C. Morganti-Kossmann, *Involvement of pro- and anti-inflammatory cytokines and chemokines in the pathophysiology of traumatic brain injury.* Neurotherapeutics, 2010. **7**(1): p. 22-30.

63. Sajja, V.S., N. Hlavac, and P.J. VandeVord, *Role of Glia in Memory Deficits Following Traumatic Brain Injury: Biomarkers of Glia Dysfunction.* Front Integr Neurosci, 2016. **10**: p. 7.

64. Harish, G., et al., *Characterization of traumatic brain injury in human brains reveals distinct cellular and molecular changes in contusion and pericontusion.* J Neurochem, 2015. **134**(1): p. 156-72.

65. Gaber, Z.B. and B.G. Novitch, *All the embryo's a stage, and Olig2 in its time plays many parts.* Neuron, 2011. **69**(5): p. 833-5.

66. Flygt, J., et al., *Human Traumatic Brain Injury Results in Oligodendrocyte Death and Increases the Number of Oligodendrocyte Progenitor Cells.* J Neuropathol Exp Neurol, 2016. **75**(6): p. 503-15.

67. Dent, K.A., et al., *Oligodendrocyte birth and death following traumatic brain injury in adult mice.* PLoS One, 2015. **10**(3): p. e0121541.

68. Lotocki, G., et al., *Oligodendrocyte vulnerability following traumatic brain injury in rats.* Neurosci Lett, 2011. **499**(3): p. 143-8.

69. Kuhtz-Buschbeck, J.P., et al., *Sensorimotor recovery in children after traumatic brain injury: analyses of gait, gross motor, and fine motor skills.* Dev Med Child Neurol, 2003. **45**(12): p. 821-8.

70. Duberstein, K.J., et al., *Gait analysis in a pre- and post-ischemic stroke biomedical pig model.* Physiology & Behavior, 2014. **125**: p. 8-16.

71. Ochi, F., et al., *Temporal-spatial feature of gait after traumatic brain injury.* J Head Trauma Rehabil, 1999. **14**(2): p. 105-15.

72. Katz-Leurer, M., et al., *The effect of variable gait modes on walking parameters among children post severe traumatic brain injury and typically developed controls.* NeuroRehabilitation, 2011. **29**(1): p. 45-51.

73. Sashindranath, M., M. Daglas, and R.L. Medcalf, *Evaluation of gait impairment in mice subjected to craniotomy and traumatic brain injury.* Behav Brain Res, 2015. **286**: p. 33-8.

74. Neumann, M., et al., *Assessing gait impairment following experimental traumatic brain injury in mice.* J Neurosci Methods, 2009. **176**(1): p. 34-44.

Figure 3.1. Lesion Volume is Correlated to Increased Impact Velocity and Depth of Depression. Piglet brains were coronally sectioned and imaged for lesion size measurement. Brains that received a CCI of 2m/s; 6mm exhibited little to no visible lesion (**A**) while measurable lesions were seen in the 4m/s; 6mm, 4m/s; 12mm, and 4m/s; 15mm groups (outlined by dotted line, **B-D**, respectively). Lesion size of each brain was quantified and average lesion volume of each group showed that piglets receiving 4m/s; 6mm, 4m/s; 12mm, and 4m/s; 15mm impact velocity; depth of depression exhibited significant brain lesion 1 week post-TBI that was scaled in severity (**E**). * indicates significant difference compared to contralateral side at $p<0.05$.

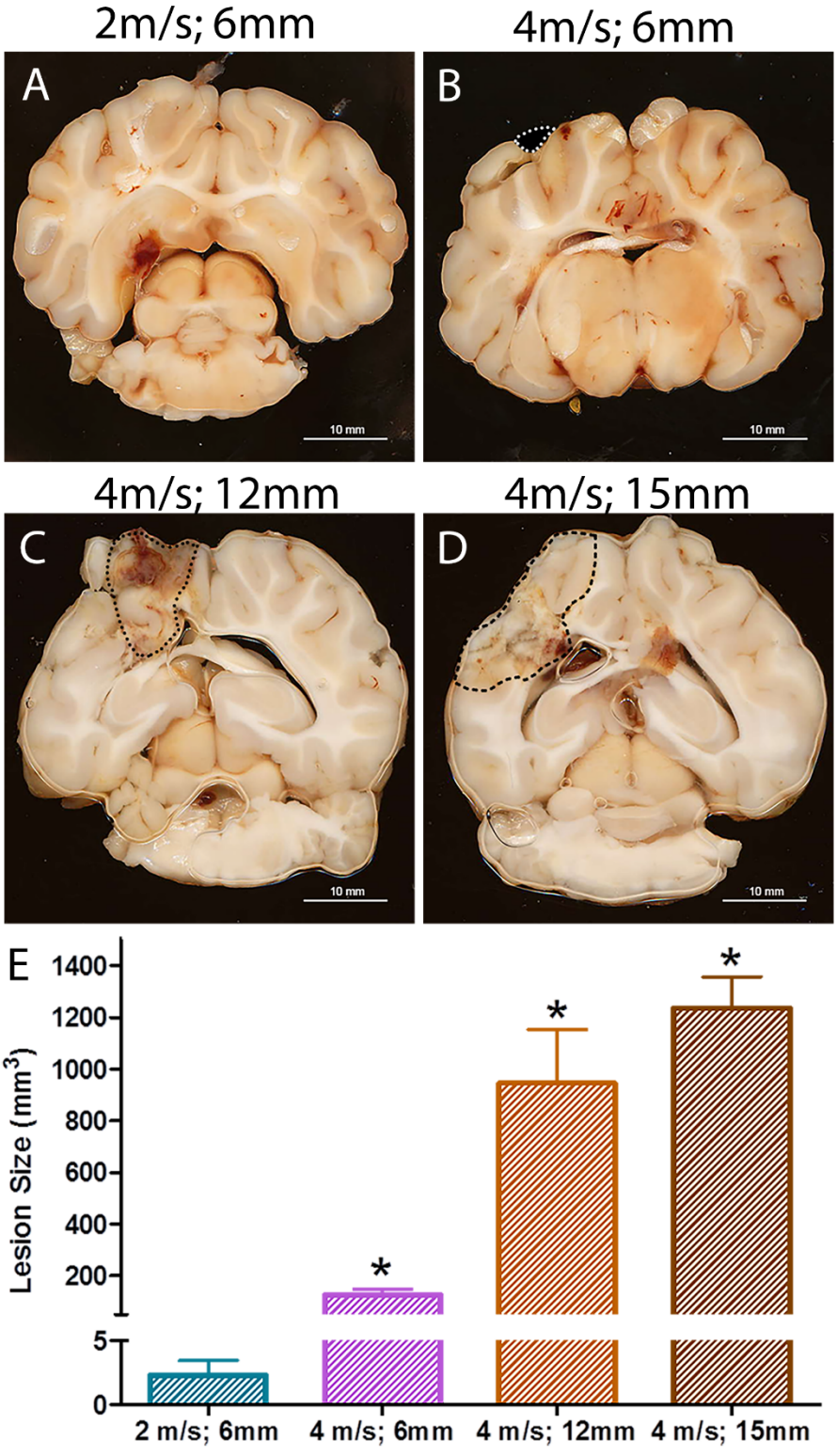
2m/s; 6mm
4m/s; 6mm
A
B
10 mm
10 mm
4m/s; 12mm
4m/s; 15mm
C
D
10 mm
10 mm
E
Lesion Size (mm3)
1400
1200
1000
800
600
400
200
5
0
*
*
*
2 m/s; 6mm
4 m/s; 6mm
4 m/s; 12mm
4 m/s; 15mm

Figure 3.2. **Histopathology Reveals Correlative Increase in Lesion Size in Response to Scaled Injury.** Hematoxylin and eosin staining of piglets impacted at 2m/s; 6mm (**A**), 4m/s; 6mm (**B**), 4m/s; 12mm (**C**), and 4m/s; 15mm (**D**). For 2m/s; 6mm, impact lesion is subtle and corresponds to focus of increased GFAP staining in Figure 3A at arrow. Note area of decreased cellularity in the cortex under the slightly fibrotic leptomeninges (F) and roughly between the *s. Decreased cellularity is due to shrunken eosinophilic necrotic neurons (see inset). Inset: Higher magnification showing necrotic neurons (arrows mark some but not all) in area of decreased cellularity (**A**). For 4m/s; 6mm, impact lesion is more extensive spanning multiple gyri but still relatively superficial. Note the expansion and severe cellularity due to gliosis of the cortex (C) of two gyri. There are also to tracts (T) of tissue loss that contain small numbers of gitter cells. Hemorrhage (H) is present in the leptomeninges in the sulcus between the gyri (**B**). For 4m/s; 12 mm, impact lesion is severe and extends deep into the cerebrum almost through the ependymal lining the lateral ventricle (**E**). The large tract (delineated by double headed arrow) is filled with necrotic debris and hemorrhage (H). The surrounding neuroparenchyma is highly cellular due to gliosis (G) (**C**). For 4m/s; 15mm, impact lesion is severe and extends deep into the cerebrum disrupting the ependymal and into the ventricle (V). The large tract (delineated by thicker double headed arrow) is filled with necrotic debris and hemorrhage (H) surrounded by a thick layer of infiltration gitter cells (*s with thinner double headed arrows denoting thickness). Inset: Higher magnification showing infiltrating gitter cells at *s (**D**). Scale bars: **A**, 1mm; **B-D**, 2mm. Insets taken at 400x.

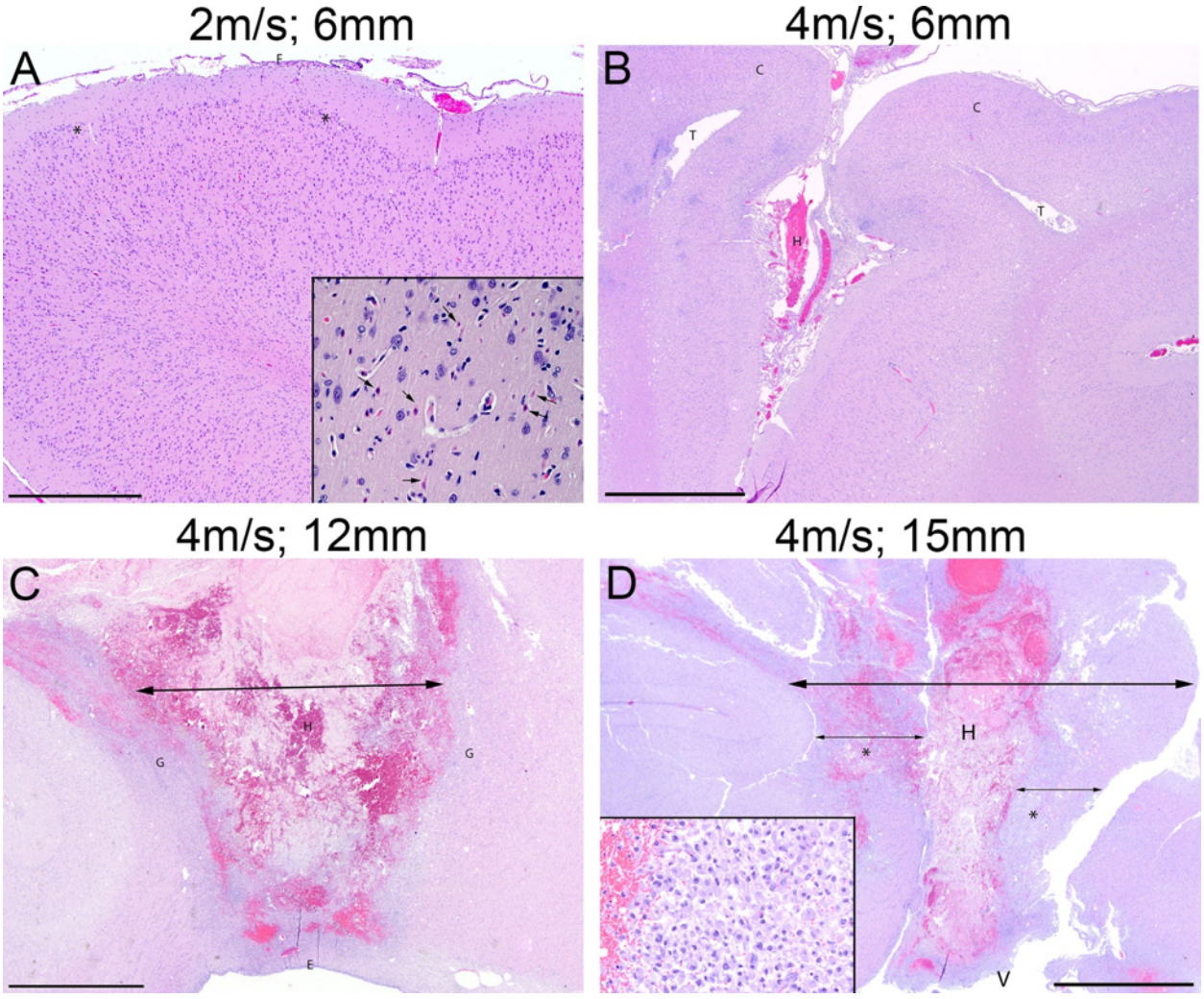
2m/s; 6mm
A
4m/s; 6mm
B
C
T
H
4m/s; 12mm
C
G
E
4m/s; 15mm
D
H
V

Figure 3.3. TBI Severity Corresponds to Increased Astrocytosis and Astrogliosis. Staining of GFAP+ reactive astrocytes in coronal sections of piglets impacted at 2m/s; 6mm (**A**), 4m/s; 6mm (**B**), 4m/s; 12mm (**C**), and 4m/s; 15mm (**D**). For 2m/s; 6mm, the cerebral cortex at the tip of one dorsolateral gyrus has a small focal area of mildly increased staining for GFAP at the lesion site, (arrow, **A**). For 4m/s; 6mm, the cerebral cortex at the tips of several dorsolateral gyri (marginal, suprasylvian, sylvian) has more extensive and moderately intense staining for GFAP at the lesion site (between arrows, **B**). For 4m/s; 12 mm, there is a large non-stained area of neuroparenchymal damage (D) at the lesion site that is surrounded by marked intense staining for GFAP of both cortical and white matter of the surrounding gyri, including the cingulate gyrus (C). For 4m/s; 15mm, there is an extensive area of neuroparenchymal damage and loss (D and L, respectively) at the lesion site with markedly intense staining for GFAP in the surrounding cortical and white matter (**D**). Scale bar is 10mm.

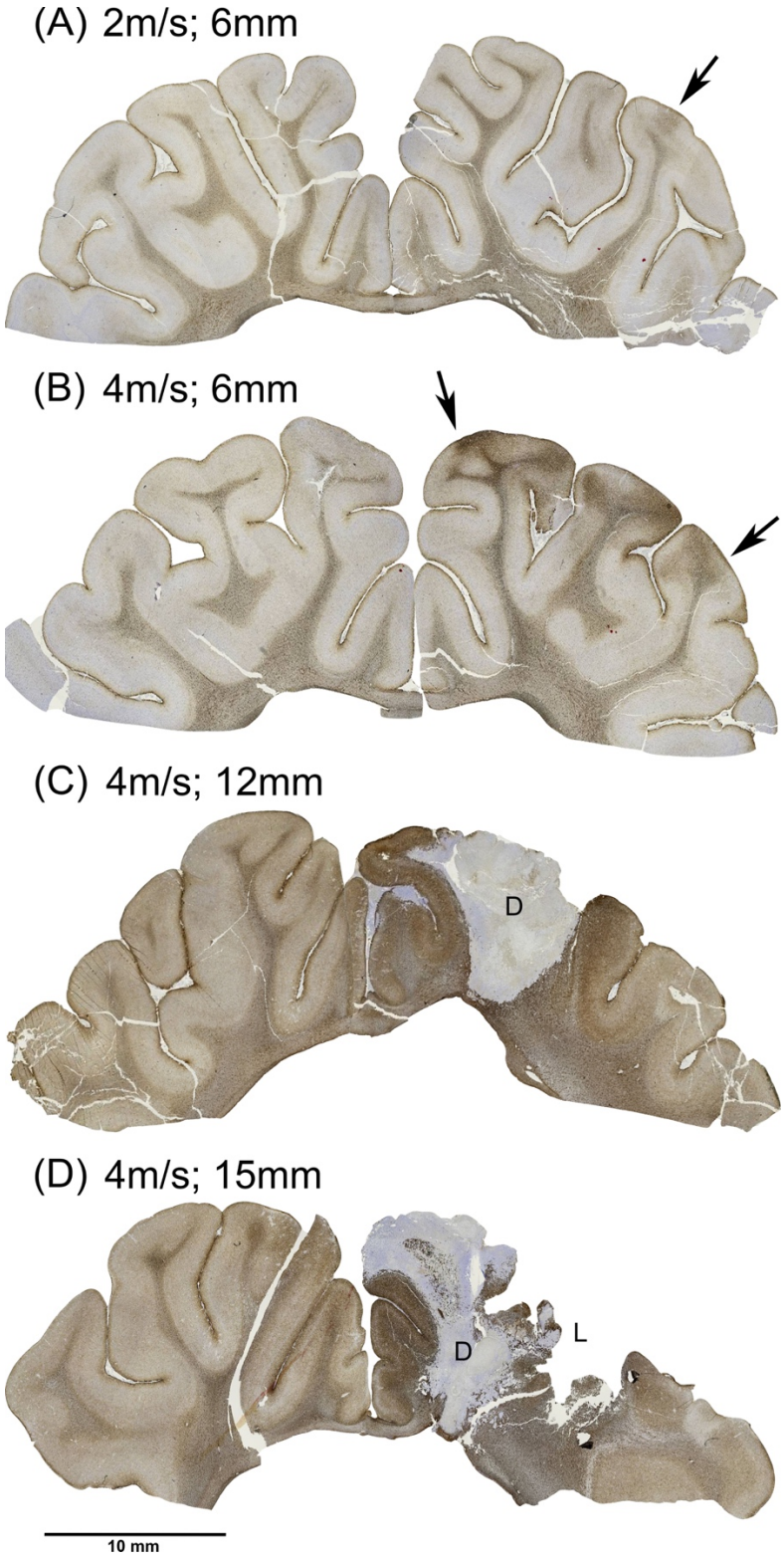
(A) 2m/s; 6mm
(B) 4m/s; 6mm
(C) 4m/s; 12mm
D
(D) 4m/s; 15mm
D
L
10 mm

Figure 3.4. TBI Severity Corresponds to Loss of NeuN+ Neurons and Upregulation of GFAP+ Astrocytes. Representative images of NeuN expression in 4m/s;12mm uninjured (**A**) and injured (**B**) hemispheres. NeuN expression was significantly reduced in the ipsilateral hemisphere compared to the contralateral hemisphere in the 4m/s; 6mm, 4m/s; 12mm, and 4m/s; 15mm groups 7 days post-TBI (**C**). Representative image of GFAP expression in 4m/s;12mm uninjured (**D**) injured (**E**) hemispheres. GFAP expression was significantly increased in the ipsilateral hemisphere compared to the contralateral hemisphere in the 4m/s; 6mm, 4m/s; 12mm, and 4m/s; 15mm groups 7 days post-TBI (**F**). Representative image of Olig2 expression in 4m/s; 12mm uninjured (**G**) and injured (**H**) hemispheres. Olig2 expression was unchanged in the ipsilateral hemisphere compared to the contralateral hemisphere in the for all groups 7 days post-TBI (**I**).
* indicates significant difference compared to contralateral side at $p<0.05$.

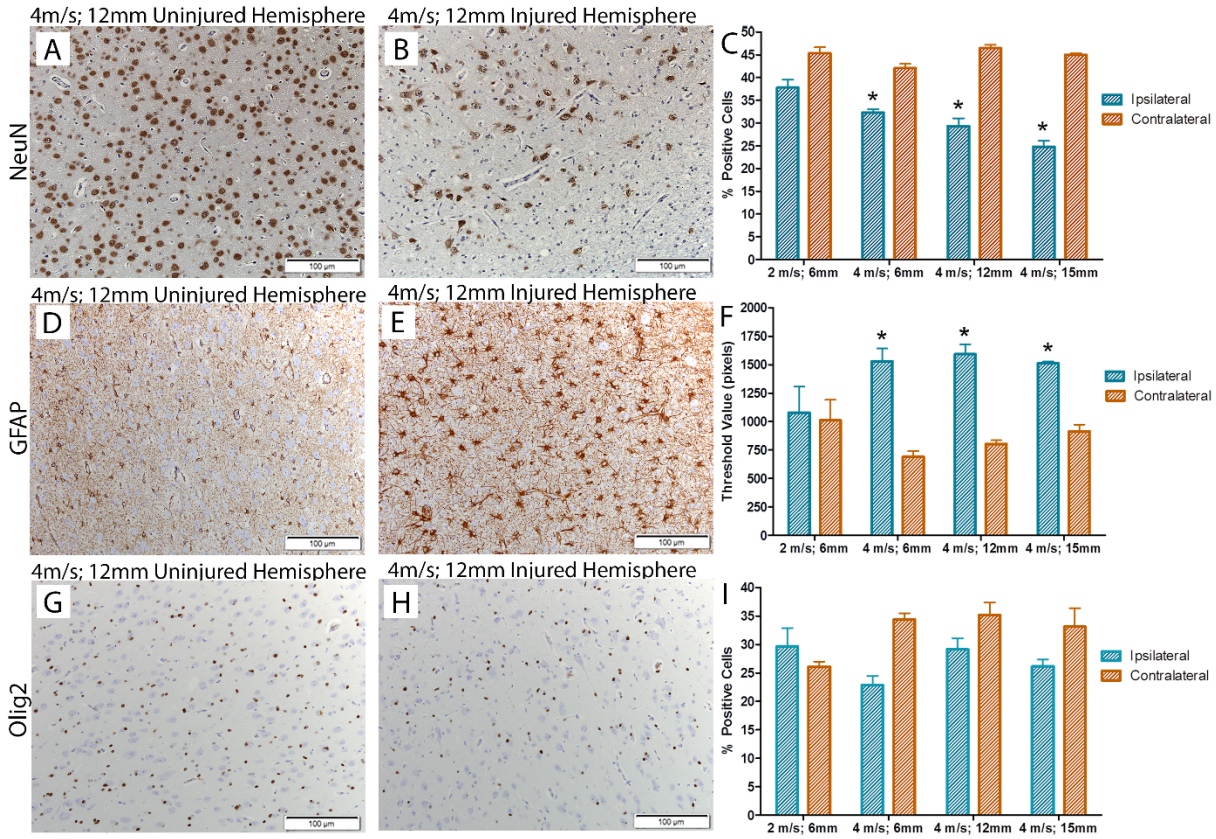
4m/s; 12mm Uninjured Hemisphere
4m/s; 12mm Injured Hemisphere
NeuN
A
B
C
% Positive Cells
Ipsilateral
Contralateral
2 m/s; 6mm
4 m/s; 6mm
4 m/s; 12mm
4 m/s; 15mm
GFAP
D
E
F
Threshold Value (pixels)
Olig2
G
H
I

Figure 3.5. Piglets that Received a TBI with a Depth of Depression of 12mm or 15mm Demonstrate Significant Motor Deficits that Persisted 7 days Post-TBI. Gait videos were analyzed in Kinovea software frame by frame for changes in stance time, swing time, stride velocity, 2-limb support, and 3-limb support (**A**). Piglets that received a TBI with a 4m/s impact velocity and either 12mm or 15mm depth of depression demonstrate a significant increase in stance time at 1, 3, and 7 days post-TBI (**B**). Piglets that received a TBI with a 12mm depth of depression showed a significant decrease in stride velocity 1 day post-TBI, and piglets that received a TBI with a 15mm depth of depression showed a significant decrease in stride velocity 1, 3, and 7 days post-TBI (**C**). Piglets that received a TBI with a 12mm depth of depression demonstrated a significant decrease in 2-limb support at 7 days post-TBI, while piglets that received a TBI with a 15mm TBI demonstrated a significant decrease in 2-limb support at 1, 3, and 7 days post-TBI (**D**). No significant changes in motor function were observed for any gait parameters in piglets that received a TBI with a depth of depression of 6mm at either 2m/s or 4m/s velocity. % stance time is represented as the percent of time spent in stance phase of the stride compared to the swing phase of the stride, and % 2-limb support is represented as the percent of time spent in 2-limb support compared to 3-limb support during a full stride cycle. * indicates significant difference compared to pre-TBI at $p<0.05$.

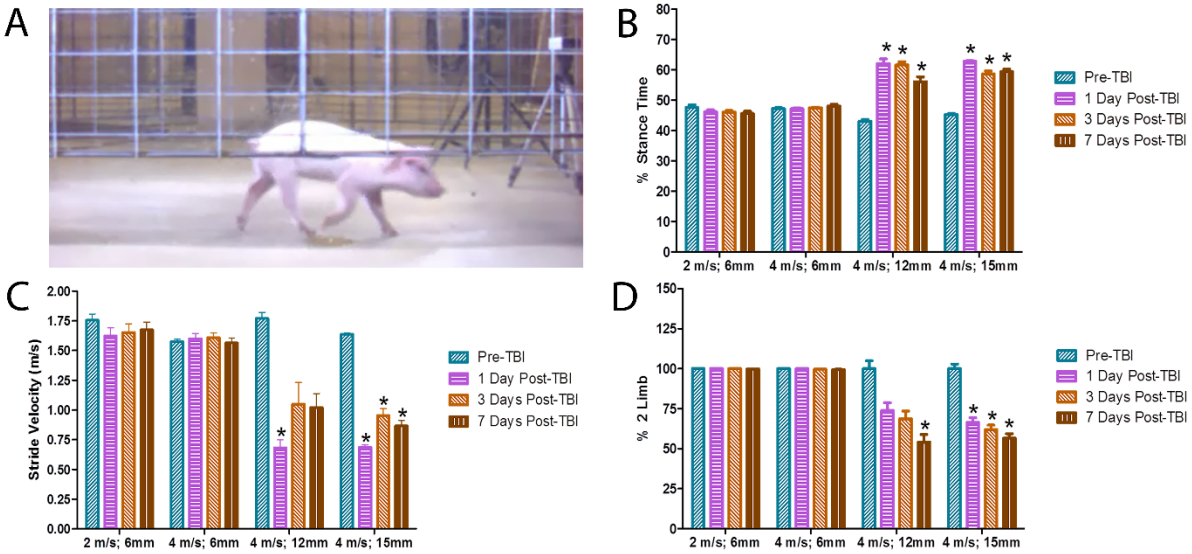
A
B
% Stance Time
2 m/s; 6mm
4 m/s; 6mm
4 m/s; 12mm
4 m/s; 15mm
Pre-TBI
1 Day Post-TBI
3 Days Post-TBI
7 Days Post-TBI
C
Stride Velocity (m/s)
D
% 2 Limb

CHAPTER 4

LONGITUDINAL MAGNETIC RESONANCE IMAGING AND HISTOLOGICAL ASSESSMENT OF TRAUMATIC BRAIN INJURY PATHOLOGY IN A PIGLET MODEL[1]

[1]Kinder, H.A. and Baker, E.W., Wang, S., Fleischer, C.C., Wendzik, M.N., Howerth, E.W., Duberstein, K.J., Mao, H., Platt, S.R., West, F.W.
To be submitted to *Journal of Neurotrauma.*

Abstract

Approximately 1.7 million people sustain a traumatic brain injury (TBI) in the United States each year. Despite the socioeconomic burden and hundreds of clinical trials, there remains to be no treatment to restore neurological function after TBI. Experts have repeatedly emphasized that the lack of translatability of preclinical models to human patients remains to be a major challenge facing TBI therapeutic development. Compared to the widely-used rodent model, pigs may be an ideal large animal model of TBI as they share key neuroanatomical similarities with humans. The objective of this study was to longitudinally assess TBI pathophysiology using multiparametric magnetic resonance imaging (MRI) and histological approaches in a piglet model. TBI was produced by controlled cortical impact (CCI) in Landrace piglets. MRI was performed 24 hours and 12 weeks post-TBI, and a subset of animals were sacrificed 24 hours, 1 week, 4 weeks, and 12 weeks post-TBI for histological analysis. TBI resulted in temporal changes in lesion size, white matter integrity, cerebral blood flow, and metabolism measured through T2-weighted imaging, diffusion weighted imaging (DWI), diffusion tensor imaging (DTI), arterial spin labeling (ASL), and proton magnetic resonance spectroscopy (^{1}H MRS), respectively, which correlated with histological evidence of neuronal loss, astrogliosis, microglia activation, and oligodendrocyte pathology. Taken together, this study illustrates the distinct time course of TBI pathoanatomic features at the cellular and tissue level up to 12 weeks post-TBI in a translational piglet TBI model, which can be used to study TBI injury and recovery mechanisms for application to the clinical setting.

Introduction

In the United States, of the approximately 1.7 million people who sustain a traumatic brain injury (TBI) each year, almost one third occur among children aged 0 to 14 [1]. The initial TBI insult causes immediate physical damage to neurons, glial cells, white matter tracts, and the blood brain barrier (BBB) [2]. A complex secondary injury sequela rapidly ensues post-primary injury characterized by the release of pro-inflammatory cytokines, chemokines, and free-radicals leading to vasogenic and cytotoxic edema, and ultimately, additional cell death and tissue necrosis [3]. Despite a vast number of promising neuroprotective therapies developed in rodent TBI models, there are currently no Food and Drug Administration (FDA)-approved treatments for TBI [4]. The heterogeneous and complex nature of TBI coupled with the use of small animal models may be a major contributor of the current translational gap from pre-clinical to clinical outcomes [5]. Improved characterization of TBI sequela in a more translational large animal model may yield promising insight in potential therapeutic targets and may provide a platform with which to test the efficacy of potential therapeutics.

Juvenile pigs may be an ideal large animal model of TBI as they share key similarities to human adolescents. Piglets exhibit a similar pattern of brain development and growth [6-8]. As a result, piglets have been used as a model to study neurodevelopmental outcomes influenced by pediatric nutrition as well as models of cognition and brain disorders [9-11]. Furthermore, the piglet brain follows a similar pattern of neurogenesis and migration of neuroblasts from the subventricular zone as human infants [12, 13], a similar time course of brain myelination [14], and possesses a comparable innate immunity [15]. These critical developmental parallels make piglets the ideal model to study the effects of TBI on neurodevelopment and the potential of novel therapeutic interventions [16].

Magnetic resonance imaging (MRI) has emerged as a powerful clinical and preclinical tool with high sensitivity and specificity for detection of complex pathoanatomic and pathophysiologic changes [17]. The use of noninvasive MRI modalities is highly advantageous as it allows for longitudinal assessment of TBI progression [17]. MRI is capable of providing highly detailed information about the spatiotemporal progression of structural changes resulting from TBI, such as lesion size, tissue volumetrics, and midline shift [18-20]. A major hallmark of focal TBI in the acute and sub-acute stages is the accumulation of cerebral edema. MRI is sensitive to microstructural changes and can thus identify predominate vasogenic or cytotoxic edema, which may indicate BBB compromise or ischemia, respectively [21, 22]. Cerebral edema accumulation can induce a series of secondary injury cascades, including decreased cerebral blood flow and neuronal dysfunction. MRI can create quantitative blood flow maps to track changes in cerebral blood flow [23], and localized *in vivo* proton magnetic resonance spectroscopy (^{1}H MRS) provides highly specific information regarding dynamic changes in cell metabolism by measuring small fluctuations in neurometabolite concentrations, including N-acetylaspartate (NAA), choline (Cho), creatine (Cr), myo-inositol (Ins), glutamate-glutamine (Glx), and lactate (Lac) after TBI [24, 25]. Furthermore, TBI primary or secondary injury mechanisms can contribute to widespread white matter damage. MRI provides an excellent measure of axonal damage and reflects changes in white matter integrity over time [26]. Experimental animal models of TBI have demonstrated the utility of correlating changes in MR signal and histological outcome [27-29]. However, there are few MRI studies with complementary histological changes that track the time course of TBI pathophysiology in a piglet TBI model [30]. Therefore, the combined use of multiparametric MRI and histopathological assessment in a piglet TBI model to study key TBI pathoanatomic and

pathophysiologic changes may lead to improved clinical translatability and may augment the predictive potential of novel therapeutic interventions.

The purpose of this study was to longitudinally assess the pathophysiology of TBI using a multiparametric quantitative MRI and histology approach in a piglet TBI model. Here we show evidence of spatio-temporal changes in lesion size, diffusion, white matter integrity, cerebral blood flow, and metabolism after TBI using T2-weighted, DWI, DTI, ASL, and ^{1}H MRS imaging, respectively. Complementary histological results show evidence of neuronal loss, increases in astrogliosis and microglia activity, and transient changes in oligodendrocytes. These results demonstrate the utility of measuring TBI sequelae in a more human-like piglet TBI model as a means to identify potential treatment targets and to test the efficacy of therapeutic interventions.

Materials and Methods

All work in this study was performed in accordance with the University of Georgia Institutional Animal Care and Use Committee guidelines.

Animals

Eighteen commercially bred, castrated male pigs were born at the Large Animal Research Unit at the University of Georgia. Piglets were weaned at 3 weeks of age, group housed, and fed a nutritionally complete starter diet ad libitum. After 4 weeks, pigs were fed a nutritionally complete grower diet ad libitum. All animals underwent surgical procedures between 4-5 weeks of age. Room temperature was maintained at 26°C with a 12h light/dark cycle and an overhead

heat lamp provided supplemental heat until 4 weeks of age. Feed was restricted the night prior to surgery but all animals had free access to water at all times.

Surgical Preparation and Controlled Cortical Impact

Piglets were anesthetized with 5% vaporized isoflurane mixed with oxygen with a surgical mask and maintained between 2.5-3% isoflurane through all surgical procedures. Temperature, heart rate, and respiration rate were monitored every 5-10 minutes for the duration of surgery. The surgical site was prepared in a routine manner using Betadine and 70% ethanol and covered with a sterile drape. A left-sided incision approximately 4cm in length was made at the top of the cranium to expose the underlying skull. A craniectomy was performed using an air drill (Brassler, USA) at the left anterior junction of the coronal and sagittal sutures, approximately 20mm in diameter, to expose the underlying dura.

The piglet was secured in a controlled cortical impactor (CCI) device (University of Georgia Instrument Design and Fabrication Shop; Athens, GA), previously described [31]. A 15mm impactor tip was positioned over the intact dura and a TBI was induced with the following parameters: 4m/s velocity, 9mm depth of depression, 400ms dwell time. After injury, the surgical site was flushed with sterile saline and the skin was re-apposed with surgical suture. Banamine (2.2mg/kg) and Butorphanol (0.2mg/kg) were administered for analgesia and Oxytetracycline (19.8mg/kg) was administered as an antibiotic for 5 days. Anesthesia was discontinued and piglets were allowed to breath oxygen until recovered. Once ambulatory, piglets were placed back in their home pens and monitored daily for health or signs of abnormal neurological behaviors.

For this study, we aimed to assess the time-course of cellular and tissue changes after TBI. Therefore, piglets were separated into 4 groups based on sacrifice date: 1 day (n=4), 1 week (n=4), 4 weeks (n=4), and 12 weeks (n=6) post-TBI.

Magnetic Resonance Imaging

Magnetic resonance imaging (MRI) was performed 24 hours and 12 weeks post-TBI on a Siemens TIM Trio 3.0 Tesla whole-body MR scanner using a 12-channel phased array head coil. Under the same anesthesia protocol used for CCI, MRI of the cranium was performed with the animal positioned in dorsal recumbency. Standard multiplanar MR brain imaging series at the coronal, horizontal, and sagittal planes were acquired including T2-weighted, T2-weighted fluid attenuated inversion recovery (FLAIR), diffusion-weighted imaging (DWI), diffusion tensor imaging (DTI), arterial spin labeling (ASL), and magnetic resonance spectroscopy (^{1}H MRS).

T2-weighted images were analyzed using OsiriX software (Pixmeo, Bernex, Switzerland). For volumetric analysis, T2-weighted images were utilized to measure the area of the lesion, ipsilateral (injured) hemisphere, and contralateral (uninjured) hemisphere at the levels containing abnormal tissue. Area and slice thickness were combined to obtain total lesion and hemisphere volumes. T2-weighted images were also used to measure midline shift. Midline shift was defined as the maximal horizontal displacement of the septum pellucidum in relation to the midline [32, 33]. The distance from the septum pellucidum to the outer border of the cortex was measured for each hemisphere, and midline shift was calculated using the formula "midline shift = (total diameter/2) – contralateral diameter."

Apparent diffusion coefficient (ADC) maps were obtained for each slice from the DW images. Mean ADC values were calculated with NIH ImageJ software at the lesion site by

manually outlining the region of interest (ROI) based on corresponding T2-weighted images for each slice with apparent lesion. Corresponding ROIs were drawn in a symmetrical site in the contralateral hemisphere to serve as an internal control. Mean ADC was obtained by calculating the average signal intensity across all slices. All ADC values are reported as 10^{-3} mm^2/s.

Fractional anisotropy (FA) maps and color-coded FA maps were generated from DT images. ROIs were drawn at the internal capsule and corpus callosum on one representative slice per animal using NIH ImageJ software at the ipsilateral and contralateral side of the injury. FA values are expressed as percent decrease of signal intensity compared to the contralateral side for each animal.

For ASL, two dimensional images were obtained from each brain slice, and cerebral blood flow (CBF) was calculated with NIH ImageJ software at the lesion site by manually outlining an ROI based on T2-weighted images. Corresponding ROIs were drawn in a symmetrical site in the contralateral hemisphere to serve as an internal control. All values were expressed as a percentage decrease of signal intensity compared to the contralateral hemisphere for each animal.

For ^1H MRS, a point-resolved spectroscopy (PRESS) sequence was used to acquire single-voxel spectra in the ipsilateral and contralateral hemispheres with the following parameters (repetition time (TR)=1800 ms; echo time (TE)=136 ms; averages=160; complex data points = 1024; bandwidth=1200 Hz; voxel size= 12x12x12 mm^3). ^1H MRS data were processed with LCModel (version 6.3-1L) [34]. Spectra were analyzed from 4 to 0.2 ppm, and metabolite concentrations were determined in the frequency domain with an 18 metabolite gamma-simulated basis set. Due to variations in total creatine concentration between hemispheres and over time, metabolite concentrations were compared qualitatively within scan

session to control for inter-scan session variations. A number of limitations including small cerebral volume, increased lipid layer near the skull, and substantial hemorrhage at the lesion site prevented quantitative comparisons between ipsilateral and contralateral hemispheres and between time points. However, a case study was performed using a single animal at 24 hours post-TBI to demonstrate that changes in neurometabolites can be measured in a piglet TBI model using ^{1}H MRS.

Histology

Pigs were euthanized 24 hours, 1 week, 4 weeks, and 12 weeks post-TBI. After euthanasia, the brains were removed, coronally sectioned, and fixed in 10% buffered formalin for immunohistochemical analysis. After fixation, a section of the ipsilateral hemisphere from each animal at the level of the lesion site was routinely processed, embedded in paraffin, and stained with antibodies specific to NeuN (Millipore, 1:500), GFAP (Biogenex, 1:4000), Olig2 (Genetex, 1:400), and Iba1 (Wako, 1:8000). Heat induced antigen retrieval was performed for all antibodies using citrate buffer at pH6 (DAKO). Detection was performed utilizing biotinylated antibodies and a streptavidin label (4plus Streptavidin HRP, Biocare) followed by an HRP label and DAB chromagen (DAKO). All sections were lightly counterstained with hematoxylin. Four healthy animals of a similar age that received no CCI surgery were processed as described above to serve as a baseline for quantification of cellular changes compared to normal control animals. Microscopic inspection and imaging was performed on a light microscope utilizing SPOT Imaging v5.2 software (Sterling Heights, MI). For quantification, an ROI in the perilesional area was drawn including the dorsal and dorsolateral gyri (cingulate, marginal, suprasylvian and sylvian and/or ectosylvian), and five fields were imaged per animal. For NeuN and Olig2,

positive and negative cells were manually counted using the cell counter plugin on ImageJ 2.0 and the percentage of NeuN+ and Olig2+ cells was determined [35]. For GFAP and Iba1, the total area of immunoreactivity corresponding to increased optical density was determined by ImageJ 2.0 software. All histological data was expressed as a percentage of normal control animals.

Statistics

Quantitative data was analyzed by two-way analysis of variance (ANOVA) and post-hoc Tukey's Pair-Wise comparisons to determine statistical significance between groups using SAS version 9.4 (Cary, NC). Groups where p-values were ≤ 0.05 were considered to be significantly different.

Results

CCI results in cerebral lesioning, significant parenchymal swelling followed by atrophy

First, we assessed cerebral lesioning and changes in hemisphere volume at 24 hours and 12 weeks post-TBI. At 24 hours post-TBI, distinct parenchymal lesioning comprised of both hyper- and hypointense regions was present on T2-weighted images (**Figure 4.1A**). At 12 weeks post-TBI, the lesion site was hyperintense on T2-weighted images, and the ipsilateral hemisphere had undergone parenchymal tissue atrophy resulting in an enlarged and distorted lateral ventricle (**Figure 4.1B**). There was no significant change in lesion size between 24 hours post-TBI and 12 weeks post-TBI (3.44 ± 0.52 cm^3 and 1.95 ± 0.44 cm^3, respectively) (**Figure 4.1C**). Since the pigs increase approximately 7-fold in size over the course of the study, the percentage of the total volume of tissue that contained lesion was calculated to account for changes in brain size. The

percentage of tissue volume comprised of lesion was significantly ($p<0.05$) decreased 12 weeks post-TBI compared to 24 hours post-TBI (9.40% ± 2.21% vs. 18.58% ± 1.83%, respectively) (**Figure 4.1D**). In addition, we assessed the volumetric ratio of the ipsilateral hemisphere (left hemisphere, LH) and the contralateral hemisphere (right hemisphere, RH) where a normal brain with equal volume between hemispheres would exhibit a LH:RH ratio of 1.0. At 24 hours post-TBI, the LH:RH ratio was significantly ($p<0.001$) increased compared to normal which indicates substantial parenchymal swelling in the ipsilateral hemisphere. At 12 weeks post-TBI, the LH:RH ratio was significantly ($p<0.0001$) decreased compared to normal indicating that the ipsilateral hemisphere has undergone parenchymal atrophy. Furthermore, there was a significant ($p<0.0001$) decrease in LH:RH ratio at 12 weeks post-TBI compared to 24 hours post-TBI (0.90 ± 0.01 vs. 1.17 ± 0.03, respectively) (**Figure 4.1E**). Together, this data illustrates a correlative decrease in both lesion size and ipsilateral hemisphere volume by 12 weeks post-TBI.

CCI results in cerebral midline shift indicative of brain swelling and atrophy

In human patients, the magnitude of midline shift is correlated with poor outcome after TBI [36]. The degree of midline shift was calculated at the level of the septum pellucidum at 24 hours and 12 weeks post-TBI. At 24 hours post-TBI, the midline was shifted 1.22 ± 0.68 mm toward the contralateral hemisphere which is indicative of parenchymal tissue swelling in the ipsilateral hemisphere (**Figure 4.2A, C**). Conversely, midline was significantly ($p<0.0001$) shifted 2.98 ± 0.29 mm toward the ipsilateral hemisphere at 12 weeks post-TBI (**Figure 4.2B, C**). Furthermore, there was a significant ($p<0.0001$) change in midline shift between 24 hours and 12 weeks post-TBI (1.22 ± 0.68mm and -2.98 ± 0.29 mm, respectively) (**Figure 4.2C**). Taken together, this data demonstrates that changes in midline shift supports the observed

hemisphere volumetric changes and further corroborates parenchymal swelling at 24 hours post-TBI followed by substantial tissue atrophy by 12 weeks post-TBI.

TBI leads to vasogenic and cytotoxic edema at the lesion site and disruption of white matter integrity

ADC maps were generated from diffusion weighted (DW) images to measure diffusivity changes at the lesion site and to distinguish between vasogenic and cytotoxic edema accumulation. A representative T2-weighted image demonstrates the presence of a focal lesion **(Figure 4.3A)** and a corresponding ADC map shows heterogeneous contrast of hyperintense vasogenic edema and hypointense cytotoxic edema accumulation at the lesion site **(Figure 4.3B)** at 24 hours post-TBI. Despite the heterogeneous nature of TBI, mean ADC at the lesion site was significantly ($p< 0.001$) increased 24 hours post-TBI compared to the contralateral side ($0.968 \pm .179$ vs. 0.862 ± 0.113, respectively) (**Figure 4.3I**). At 12 weeks post-TBI a representative T2-weighted image shows a substantial reduction in lesion size **(Figure 4.3C)**. However, a corresponding ADC map shows a focal region with a significant ($p< 0.0001$) increase in ADC hyperintensity compared to the contralateral side as well as compared to the ADC of the ipsilateral side 24 hours post-TBI ($1.563 \pm .613$ vs. $0.951.38 \pm 0.008$ and 0.862 ± 0.113, respectively) (**Figure 4.3D, I**), likely as a result of gliosis or cyst formation [27, 37]. These results indicate that both vasogenic and cytotoxic edema occur together in traumatized tissue, but mean ADC reflects that vasogenic edema is most prominent 24 hours post-TBI. However, late ADC increases at 12 weeks post-TBI can be attributed to gliosis and/or cystic formation as a result of tissue necrosis.

Diffusion tensor imaging (DTI) was performed to assess changes in white matter integrity after TBI. Representative fractional anisotropy (FA) maps demonstrate disruption of white matter tracts 24 hours **(Figure 4.3E)** and 12 weeks post-TBI **(Figure 4.3G)**. Representative color-coded FA maps show directional changes of white matter fibers 24 hours **(Figure 4.3F)** and 12 weeks post-TBI **(Figure 4.3H)**. FA values at the ipsilateral internal capsule were significantly ($p < 0.01$) decreased compared to the contralateral side at 24 hours and 12 weeks post-TBI (-15.19 ± 3.48% and -15.74 ± 0.881%, respectively) (**Figure 4.3J**). Similarly, FA values at the ipsilateral corpus callosum were significantly ($p< 0.05$) decreased compared to the contralateral side at 24 hours and 12 weeks post-TBI (-10.51 ± 2.12% and -11.056 ± 4.149%, respectively; **Figure 4.3J**). These results suggest that TBI can lead to rapid loss of white matter integrity in the internal capsule and corpus callosum at 24 hours post-TBI that is sustained for up 12 weeks post-TBI.

Cerebral blood flow is decreased at the lesion site post-CCI

Arterial spin labeling (ASL) was performed to assess whether CCI affected cerebral blood flow (CBF) at the lesion site. CBF was calculated at both the lesion site and a comparable area on the contralateral hemisphere. CBF at the lesion site was expressed as a percent change compared to CBF on the contralateral hemisphere with changes closer to 0% being more similar to normal tissue. There was a significant ($p<0.005$) decrease in CBF at both 24 hours and 12 weeks post-TBI at the lesion site compared to the contralateral hemisphere (-54.17% ± 7.12% and -30.73% ± 6.38%, respectively) (**Figure 4.4A-C**). However, there was a significant ($p<0.05$) recovery in CBF by 12 weeks post-TBI compared to 24 hours post-TBI (-30.73% ± 6.38% vs. -54.17% ± 7.12%; **Figure 4.4C**). This data indicates that although deficits in CBF are sustained

through 12 weeks post-TBI compared to normal tissue, initial impairments in CBF at 24 hours post-TBI are improved by 12 weeks.

TBI leads to changes in neurometabolite concentration 24 hours post-TBI

Magnetic resonance spectroscopy (^{1}H MRS) has the ability to identify changes in brain metabolites enabling characterization of injury and recovery. However, it has yet to be attempted in a pig neural injury model. As this is a novel assessment tool in pigs, we attempted a ^{1}H MRS case study in a single pig at 24 hours post-TBI. Sample ^{1}H MRS spectra were acquired from ipsilateral and contralateral voxels in a single subject. Changes in the healthy neuron marker NAA, the cellularity marker Cho, the energy marker Cr, the glial cell marker Ins, the amino acid marker Glx and the inflammatory marker Lac were assessed 24 hours post-TBI. Relative concentrations of NAA, Cho, Cr, Ins, and Glx were within a normal range in the contralateral hemisphere 24 hours post-TBI **(Figure 4.5A)**. However, decreases in NAA, Cho, Cr, Ins, and Glx as well as an increase in Lac were observed in the ipsilateral hemisphere **(Figure 4.5B)**. These results suggest that in a single animal, ^{1}H MRS can detect a number of neurometabolic changes that accompany TBI after 24 hours.

Histological analysis reveals neuronal loss, gliosis, and neuroinflammation correlative to observed tissue-level deficits

Parenchymal tissues underwent histological assessment to characterize cellular changes in the perilesional cortex after TBI including neuronal loss, astrogliosis, oligodendrocyte loss/proliferation, and microglial activation. To this end, we quantified NeuN+ neurons, GFAP+ astrocytes, Olig2+ oligodendrocytes, and Iba1+ microglia at 24 hours, 1 week, 4 weeks, and 12

weeks post-TBI and data was expressed as a percentage compared to normal where values closer to 100% being more similar to normal control animals. There was no difference in the number of neurons in the perilesional cortex 24 hours post-TBI compared to normal control animals. However, there was a significant ($p<0.01$) decrease in neurons at 1 week post-TBI compared to 24 hours post-TBI (72.49% ± 4.08% vs. 95.47% ± 2.47%, respectively) and normal control animals. Significant ($p<0.005$) neuronal loss was sustained through 4 weeks and 12 weeks post-TBI (64.26% ± 8.42% and 62.31% ± 0.48%, respectively) (**Figure 4.6A-D**). Conversely, we found a significant ($p<0.0005$) increase in astrocytes from 24 hours to 12 weeks post-TBI compared to normal control animals. Furthermore, there was a significant ($p<0.005$) increase in astrocyte reactivity at 1 week post-TBI compared to 24 hours post-TBI (204.87% ± 0.58% vs. 123.79% ± 3.68%, respectively), 4 weeks post-TBI compared to 1 week post-TBI (255.09% ± 9.79% vs. 204.87% ± 0.58%, respectively), and 12 weeks post-TBI compared to 4 weeks post-TBI (966.75% ± 7.98% vs. 255.09% ± 9.79%, respectively; **Figure 4.6E-H**). This demonstrates progressive increases in astrogliosis beginning 24 hours post-TBI through 12 weeks post-TBI. There was no difference in oligodendrocyte number at 24 hours post-TBI compared to normal control animals. However, there was a significant ($p<0.05$) decline in the number of oligodendrocytes at 1 week and 4 weeks post-TBI compared to normal control animals (67.62% ± 11.32% and 66.51% ± 9.13%, respectively). In contrast, there was a significant ($p<0.005$) increase in the number of oligodendrocytes in the perilesional cortex at 12 weeks post-TBI compared to both 4 weeks post-TBI (112.89% ± 1.94% vs. 66.51% ± 9.13%, respectively) and normal control animals, which indicates that oligodendrocyte proliferation occurs between 4 weeks and 12 weeks post-TBI (**Figure 4.6I-L**). Initially there was a significant ($p<0.05$) decline in the number of microglia in the perilesional cortex 24 hours post-TBI compared to normal

control animals. However, there was a significant ($p<0.05$) increase in microglia number at 1 week and 4 weeks post-TBI compared to normal control animals (130.74% ± 13.11% and 153.64% ± 13.98%, respectively). Furthermore, there was a significant ($p<0.0001$) increase in microglia abundance at 12 weeks post-TBI compared to both 4 weeks post-TBI (861.46% ± 15.45% vs. 153.64 ± 13.98%, respectively) and normal control animals, demonstrating sustained microglia activation beginning 1 week post-TBI through 12 weeks post-TBI (**Figure 4.6M-P**).

Discussion

Despite the prevalence of TBI and numerous clinical trials, there are few therapeutic options available to combat the tissue loss that leads to devastating functional deficits [4]. This may be due in part to the lack of translational animal models to optimize treatment strategies for clinical application. Here we combine translational multiparametric MRI and ^{1}H MRS approaches with histology to characterize TBI pathology in a piglet model. At 24 hours post-TBI, substantial parenchymal swelling due to both vasogenic and cytotoxic edema accumulation lead to increased ipsilateral hemisphere volume and midline shift with evidence of disturbed CBF and brain metabolism. Despite the edema heterogeneity present at 24 hours post-TBI, increased mean ADC suggests that vasogenic edema is more prominent over cytotoxic edema in our model. At 12 weeks post-TBI, we observed parenchymal atrophy correlating with a directional change in midline shift, increased mean ADC likely due to cystic formation and/or gliosis, and improved albeit abnormal CBF compared to baseline. Furthermore, TBI lead to a sustained disruption in white matter integrity. These tissue-level deficits measured through MRI correlated to progressive neuronal loss, neuroinflammation, gliosis, and oligodendrocyte pathology. Taken together, the injury indicators outlined here could be applied to the clinical

setting as a baseline for treatment efficacy indicators in the future, augmenting the translational capacity of current preclinical models as well as the probability of a successful clinical trial.

Human clinical studies have consistently demonstrated that midline shift is a strong indicator of abnormal intracranial pressure, and shift magnitude is associated with poor patient outcomes [36, 38]. T2-weighted images revealed parenchymal swelling that shifted the cerebral midline approximately 1.2 mm at 24 hours post-TBI which, when the difference in brain size is considered, equates to approximately a 4.5 mm shift in the human brain. In both the Marshall and Rotterdam CT classifications, a midline shift of 5 mm is considered the major turning point of increased mortality rate after TBI [39]. However, clinical studies of TBI have concluded that there is no distinct cut-off value for the degree of midline shift in relation to clinical outcome, and the authors recommended that midline shift should rather be viewed as a continuous variable for outcome prediction [32, 40]. Jacobs et al. found that patients with favorable outcomes had an average midline shift of 4.9 mm, which correlates with our study in which pigs demonstrated 0% mortality and 100% favorable outcome long term [32].

We demonstrate that TBI in our piglet model leads to early disruptions in white matter integrity that is sustained for 12 weeks post-TBI. White matter integrity was quantified through fractional anisotropy (FA) which measures the degree of anisotropic diffusion, or the directionality of water molecules in specific regions of the cerebrum [41, 42]. Areas with a high anisotropic diffusion like the corpus callosum or internal capsule are characterized by high FA values and appear bright on FA maps whereas areas with low anisotropic diffusion like the CSF or gray matter are characterized by low FA values and are dark on FA maps [43]. White matter is comprised of myelinated and unmyelinated axon bundles which foster communication between neurons in different gray matter compartments, and white matter disruption has been shown to

lead to motor dysfunction and cognitive impairment [44]. Preclinical animal models have documented white matter disruption after TBI through DTI and/or histological measures; however, the majority of these studies are carried out in the rodent which only has about 14% of the relative white matter volume of humans thus may not be directly translatable to white matter injury in the human [28, 29, 44-48]. Clinical studies have documented decreased FA in the corpus callosum in the chronic stages after TBI with focal lesions having a lower FA than non-focal lesions, which correlates with our finding that FA impairment is sustained between 24 hours and 12 weeks post-TBI [26, 49, 50]. Although deficits in white matter integrity were documented 12 weeks post-TBI, histological analysis revealed an increase in oligodendrocyte number at this time point. Oligodendrocytes are the myelinating cells of the CNS and after initial oxidative stress-induced apoptosis, their progenitors have been shown to proliferate in response to neural injury [51-53]. Similarly, we demonstrate reduced oligodendrocyte numbers 1 and 4 weeks post-TBI followed by oligodendrocyte proliferation 12 weeks post-TBI, which indicates that oligodendrocyte lineage precursors may be facilitating endogenous repair processes to remyelinate damaged axons and restore white matter integrity.

ADC is a measure of the overall magnitude of the apparent water diffusion, thus areas with a high rate of diffusion will appear hyperintense and have a high ADC value and areas with restricted diffusion will appear hypointense and have a low ADC value [43]. As a consequence, the assessment of ADC changes in a cerebral lesion can be used as a marker of tissue damage and can help delineate between the formation of vasogenic and cytotoxic edema accumulation, respectively [22]. In the acute phase of TBI, it is widely accepted that both cytotoxic and vasogenic edema accumulate in the damaged territory, often leading to signal heterogeneity on ADC maps [21, 22, 28, 54]. We found increased mean ADC 24 hours post-TBI, indicating that

vasogenic edema is prominent over cytotoxic edema in our model, with progressive increases in ADC by 12 weeks post-TBI. Similar to our finding, other preclinical models of focal injury documented an increase in mean ADC by 24 hours post-TBI indicative of BBB breach and thus vasogenic edema [27, 28, 47, 55, 56]. However, there is discrepancy in the longitudinal pattern with some studies reporting a progressive increase in ADC and others finding ADC values returning to baseline within a few days. A clinical study by Marmarou et al. documented increased mean ADC in patients presenting with focal TBI containing a contusion core and surrounding hyperdensity comparable to our injury model [57]. In contrast, other studies found only transient increases in ADC with decreased values by 24 hours post-TBI indicative of prominent cytotoxic edema, which eventually return to baseline levels [20, 22, 24]. Progressive increases in ADC between 24 hours and 12 weeks post-TBI, as documented here, can be initially attributed to vasogenic edema followed by neuron collapse, dissolved lesioned tissue, and/or gliosis [27, 56]. Indeed, we found a 7-fold increase in astrogliosis between 24 hours and 12 weeks post-TBI and significant tissue atrophy, which is consistent with these previous observations. Similarly, Mac Donald et al. documented sustained increases in GFAP+ astrocytes post-TBI which correlated to increased mean ADC one month post-TBI [47]. Taken together, changes in ADC after TBI over time seems to be highly variable depending on TBI type and severity.

Successful acquisition of MR spectra demonstrated that it is feasible to monitor cellular TBI changes utilizing ^{1}H MRS in our porcine model. However, without an accurate internal standard combined with varying total creatine concentrations, relative concentration changes were the most reliable from our ^{1}H MRS data. Given the additional challenges of ^{1}H MRS acquisition in the porcine model of TBI including smaller cerebral volume and subsequently

lower metabolite concentrations relative to humans, increased lipid layer near the skull, and respiration during scanning, further studies are needed to optimize ^{1}H MRS in this model. The preliminary results from this case study involving one animal revealed that neurometabolism was impaired 24 hours post-TBI with deficits in the abundance of NAA, Cho, Cr, Ins, and Glx along with increased Lac which correlates to the observed cerebral lesioning on T2-weighted images. Similar to our findings, previous studies have documented decreased NAA abundance within 24 hours post-TBI which has been attributed to impaired NAA synthesis in neuronal mitochondria [24, 25, 58, 59]. However, there was a temporal discrepancy between decreased abundance of the neuronal marker NAA at 24 hours post-TBI and a loss of NeuN+ neurons at 1 week post-TBI. Therefore, our findings correlate with others in that deficits in NAA does not directly correlate to neuronal death but rather metabolically endangered neurons, providing a potential indicator of at-risk tissue that could benefit from therapeutics that enhance mitochondria function [24, 25, 58, 59].

We demonstrated that TBI resulted in decreased CBF utilizing ASL, which is a contrast-free MRI method that employs magnetically labeled blood water as a flow tracer to quantify CBF on a voxel-by-voxel basis [60]. CBF did not return to normal levels in our study likely due to substantial tissue necrosis, we found that CBF was significantly recovered 12 weeks post-TBI compared to 24 hours post-TBI. To our knowledge, this is the first study to longitudinally monitor CBF utilizing ASL in a large animal TBI model with substantial white matter structures, which have been shown to possess different microvasculature anatomy compared to gray matter [61]. Although further optimization of ASL collection in a porcine model is needed, these results demonstrate that ASL could be a valuable tool in assessing CBF recovery longitudinally after therapeutic intervention in a translational large animal model.

Conclusion

In conclusion, we correlate longitudinal multiparametric MRI and ^{1}H MRS approaches with distinct histological changes to characterize long-term TBI pathology in a translational large animal model. TBI pathology illustrated a distinct time course with TBI-induced tissue and cellular level deficits up to 12 weeks after injury. These findings can be used as a platform to further study critical TBI injury mechanisms, deficits and recovery for application to the clinical setting.

Acknowledgements

We would like to thank Richard Utley and Kelly Parham for their animal assistance; Vivian Lau and Lisa Reno for their surgical expertise and support; and our amazing team of undergraduate researchers that helped us with all aspects of the animal work. Financial support was provided by the University of Georgia Office of the Vice President for Research.

The authors have no conflicts of interest

References

1. Langlois, J.A., Rutland-Brown, W., Thomas, K.E., *Traumatic brain injury in the United States: Emergency deparment visits, hospitalizations, and deaths.* Atlanta, GA: Centers for Disease Control and Prevention, National Center for Injury Prevention and Control, 2006.
2. Werner, C. and K. Engelhard, *Pathophysiology of traumatic brain injury.* Br J Anaesth, 2007. **99**(1): p. 4-9.
3. Winkler, E.A., et al., *Cerebral Edema in Traumatic Brain Injury: Pathophysiology and Prospective Therapeutic Targets.* Neurosurg Clin N Am, 2016. **27**(4): p. 473-88.
4. Jain, K.K., *Neuroprotection in traumatic brain injury.* Drug Discov Today, 2008. **13**(23-24): p. 1082-9.
5. Xiong, Y., A. Mahmood, and M. Chopp, *Animal models of traumatic brain injury.* Nat Rev Neurosci, 2013. **14**(2): p. 128-42.
6. Dobbing, J. and J. Sands, *Comparative aspects of the brain growth spurt.* Early Hum Dev, 1979. **3**(1): p. 79-83.
7. Dickerson, J.W. and J. Dobbing, *Prenatal and postnatal growth and development of the central nervous system of the pig.* Proc R Soc Lond B Biol Sci, 1967. **166**(1005): p. 384-95.
8. Conrad, M.S., R.N. Dilger, and R.W. Johnson, *Brain growth of the domestic pig (Sus scrofa) from 2 to 24 weeks of age: a longitudinal MRI study.* Dev Neurosci, 2012. **34**(4): p. 291-8.
9. Mudd, A.T. and R.N. Dilger, *Early-Life Nutrition and Neurodevelopment: Use of the Piglet as a Translational Model.* Adv Nutr, 2017. **8**(1): p. 92-104.

10. Gieling, E.T., R.E. Nordquist, and F.J. van der Staay, *Assessing learning and memory in pigs.* Anim Cogn, 2011. **14**(2): p. 151-73.

11. Lind, N.M., et al., *The use of pigs in neuroscience: modeling brain disorders.* Neurosci Biobehav Rev, 2007. **31**(5): p. 728-51.

12. Paredes, M.F., et al., *Extensive migration of young neurons into the infant human frontal lobe.* Science, 2016. **354**(6308).

13. Costine, B.A., et al., *The subventricular zone in the immature piglet brain: anatomy and exodus of neuroblasts into white matter after traumatic brain injury.* Dev Neurosci, 2015. **37**(2): p. 115-30.

14. Flynn, T.J., *Developmental changes of myelin-related lipids in brain of miniature swine.* Neurochem Res, 1984. **9**(7): p. 935-45.

15. Fairbairn, L., et al., *The mononuclear phagocyte system of the pig as a model for understanding human innate immunity and disease.* J Leukoc Biol, 2011. **89**(6): p. 855-71.

16. Conrad, M.S. and R.W. Johnson, *The domestic piglet: an important model for investigating the neurodevelopmental consequences of early life insults.* Annu Rev Anim Biosci, 2015. **3**: p. 245-64.

17. Saatman, K.E., et al., *Classification of traumatic brain injury for targeted therapies.* J Neurotrauma, 2008. **25**(7): p. 719-38.

18. Chastain, C.A., et al., *Predicting outcomes of traumatic brain injury by imaging modality and injury distribution.* J Neurotrauma, 2009. **26**(8): p. 1183-96.

19. Duhaime, A.C., et al., *Magnetic resonance imaging studies of age-dependent responses to scaled focal brain injury in the piglet.* J Neurosurg, 2003. **99**(3): p. 542-8.

20. Van Putten, H.P., et al., *Diffusion-weighted imaging of edema following traumatic brain injury in rats: effects of secondary hypoxia.* J Neurotrauma, 2005. **22**(8): p. 857-72.

21. Marmarou, A., et al., *Traumatic brain edema in diffuse and focal injury: cellular or vasogenic?* Acta Neurochir Suppl, 2006. **96**: p. 24-9.

22. Barzo, P., et al., *Contribution of vasogenic and cellular edema to traumatic brain swelling measured by diffusion-weighted imaging.* J Neurosurg, 1997. **87**(6): p. 900-7.

23. Detre, J.A. and D.C. Alsop, *Perfusion magnetic resonance imaging with continuous arterial spin labeling: methods and clinical applications in the central nervous system.* Eur J Radiol, 1999. **30**(2): p. 115-24.

24. Lescot, T., et al., *Temporal and regional changes after focal traumatic brain injury.* J Neurotrauma, 2010. **27**(1): p. 85-94.

25. Xu, S., et al., *Early microstructural and metabolic changes following controlled cortical impact injury in rat: a magnetic resonance imaging and spectroscopy study.* J Neurotrauma, 2011. **28**(10): p. 2091-102.

26. Farbota, K.D., et al., *Longitudinal diffusion tensor imaging and neuropsychological correlates in traumatic brain injury patients.* Front Hum Neurosci, 2012. **6**: p. 160.

27. Albensi, B.C., et al., *Diffusion and high resolution MRI of traumatic brain injury in rats: time course and correlation with histology.* Exp Neurol, 2000. **162**(1): p. 61-72.

28. Long, J.A., et al., *Multiparametric and longitudinal MRI characterization of mild traumatic brain injury in rats.* J Neurotrauma, 2015. **32**(8): p. 598-607.

29. Li, N., et al., *Evidence for impaired plasticity after traumatic brain injury in the developing brain.* J Neurotrauma, 2014. **31**(4): p. 395-403.

30. Grate, L.L., et al., *Traumatic brain injury in piglets of different ages: techniques for lesion analysis using histology and magnetic resonance imaging.* J Neurosci Methods, 2003. **123**(2): p. 201-6.

31. Manley, G.T., et al., *Controlled cortical impact in swine: pathophysiology and biomechanics.* J Neurotrauma, 2006. **23**(2): p. 128-39.

32. Jacobs, B., et al., *Computed tomography and outcome in moderate and severe traumatic brain injury: hematoma volume and midline shift revisited.* J Neurotrauma, 2011. **28**(2): p. 203-15.

33. Sauvigny, T., et al., *New Radiologic Parameters Predict Clinical Outcome after Decompressive Craniectomy.* World Neurosurg, 2016. **88**: p. 519-525 e1.

34. Provencher, S.W., *Estimation of metabolite concentrations from localized in vivo proton NMR spectra.* Magn Reson Med, 1993. **30**(6): p. 672-9.

35. Schneider, C.A., W.S. Rasband, and K.W. Eliceiri, *NIH Image to ImageJ: 25 years of image analysis.* Nat Methods, 2012. **9**(7): p. 671-5.

36. Kramer, A.H., et al., *Decompressive Craniectomy in Patients with Traumatic Brain Injury: Are the Usual Indications Congruent with Those Evaluated in Clinical Trials?* Neurocrit Care, 2016. **25**(1): p. 10-9.

37. Kawamata, T. and Y. Katayama, *Cerebral contusion: a role model for lesion progression.* Prog Brain Res, 2007. **161**: p. 235-41.

38. Kim, K.T., et al., *Comparison of the effect of decompressive craniectomy on different neurosurgical diseases.* Acta Neurochir (Wien), 2009. **151**(1): p. 21-30.

39. Chun, K.A., et al., *Interobserver variability in the assessment of CT imaging features of traumatic brain injury.* J Neurotrauma, 2010. **27**(2): p. 325-30.

40. Nelson, D.W., et al., *Extended analysis of early computed tomography scans of traumatic brain injured patients and relations to outcome.* J Neurotrauma, 2010. **27**(1): p. 51-64.

41. Alba-Ferrara, L.M. and G.A. de Erausquin, *What does anisotropy measure? Insights from increased and decreased anisotropy in selective fiber tracts in schizophrenia.* Front Integr Neurosci, 2013. **7**: p. 9.

42. Beppu, T., et al., *Measurement of fractional anisotropy using diffusion tensor MRI in supratentorial astrocytic tumors.* J Neurooncol, 2003. **63**(2): p. 109-16.

43. Huisman, T.A., *Diffusion-weighted and diffusion tensor imaging of the brain, made easy.* Cancer Imaging, 2010. **10 Spec no A**: p. S163-71.

44. Ahmad, A.S., et al., *Considerations for the Optimization of Induced White Matter Injury Preclinical Models.* Front Neurol, 2015. **6**: p. 172.

45. Hylin, M.J., et al., *Behavioral and histopathological alterations resulting from mild fluid percussion injury.* J Neurotrauma, 2013. **30**(9): p. 702-15.

46. Creed, J.A., et al., *Concussive brain trauma in the mouse results in acute cognitive deficits and sustained impairment of axonal function.* J Neurotrauma, 2011. **28**(4): p. 547-63.

47. Mac Donald, C.L., et al., *Diffusion tensor imaging reliably detects experimental traumatic axonal injury and indicates approximate time of injury.* J Neurosci, 2007. **27**(44): p. 11869-76.

48. Harris, N.G., et al., *Bi-directional changes in fractional anisotropy after experiment TBI: Disorganization and reorganization?* Neuroimage, 2016. **133**: p. 129-43.

49. Wu, T.C., et al., *Longitudinal changes in the corpus callosum following pediatric traumatic brain injury.* Dev Neurosci, 2010. **32**(5-6): p. 361-73.

50. Wilde, E.A., et al., *Diffusion tensor imaging in the corpus callosum in children after moderate to severe traumatic brain injury.* J Neurotrauma, 2006. **23**(10): p. 1412-26.

51. Flygt, J., et al., *Myelin loss and oligodendrocyte pathology in white matter tracts following traumatic brain injury in the rat.* Eur J Neurosci, 2013. **38**(1): p. 2153-65.

52. Dent, K.A., et al., *Oligodendrocyte birth and death following traumatic brain injury in adult mice.* PLoS One, 2015. **10**(3): p. e0121541.

53. Buffo, A., et al., *Expression pattern of the transcription factor Olig2 in response to brain injuries: implications for neuronal repair.* Proc Natl Acad Sci U S A, 2005. **102**(50): p. 18183-8.

54. Hou, D.J., et al., *Diffusion-weighted magnetic resonance imaging improves outcome prediction in adult traumatic brain injury.* J Neurotrauma, 2007. **24**(10): p. 1558-69.

55. Immonen, R.J., et al., *Distinct MRI pattern in lesional and perilesional area after traumatic brain injury in rat--11 months follow-up.* Exp Neurol, 2009. **215**(1): p. 29-40.

56. Wei, X.E., et al., *Dynamics of rabbit brain edema in focal lesion and perilesion area after traumatic brain injury: a MRI study.* J Neurotrauma, 2012. **29**(14): p. 2413-20.

57. Marmarou, A., et al., *Predominance of cellular edema in traumatic brain swelling in patients with severe head injuries.* J Neurosurg, 2006. **104**(5): p. 720-30.

58. Schuhmann, M.U., et al., *Metabolic changes in the vicinity of brain contusions: a proton magnetic resonance spectroscopy and histology study.* J Neurotrauma, 2003. **20**(8): p. 725-43.

59. Smith, D.H., et al., *Magnetic resonance spectroscopy of diffuse brain trauma in the pig.* J Neurotrauma, 1998. **15**(9): p. 665-74.

60. Telischak, N.A., J.A. Detre, and G. Zaharchuk, *Arterial spin labeling MRI: clinical applications in the brain.* J Magn Reson Imaging, 2015. **41**(5): p. 1165-80.

61. Nonaka, H., et al., *The microvasculature of the cerebral white matter: arteries of the subcortical white matter.* J Neuropathol Exp Neurol, 2003. **62**(2): p. 154-61.

Figure 4.1. CCI results in significant brain lesioning characterized by parenchymal swelling followed by atrophy. Representative T2-weighted images collected 24 hours (**A**) and 12 weeks (**B**) post-TBI displaying distinct brain lesion (arrows). Lesion size was quantified both 24 hours and 12 weeks post-TBI, and there was no difference in lesion size between the two time points (**C**). The percentage of measured tissue that was comprised of lesion was decreased 12 weeks post-TBI compared to 24 hours post-TBI (**D**). The volume of the left hemisphere (LH) and right hemisphere (RH) was calculated and expressed as a LH:RH ratio, which indicated parenchymal swelling 24 hours post-TBI followed by atrophy at 12 weeks post-TBI. Data are expressed as mean ± s.e.m. # indicates significance between time points ($p<0.05$). * indicates significance from a normal ratio of 1.0 ($p<0.05$).

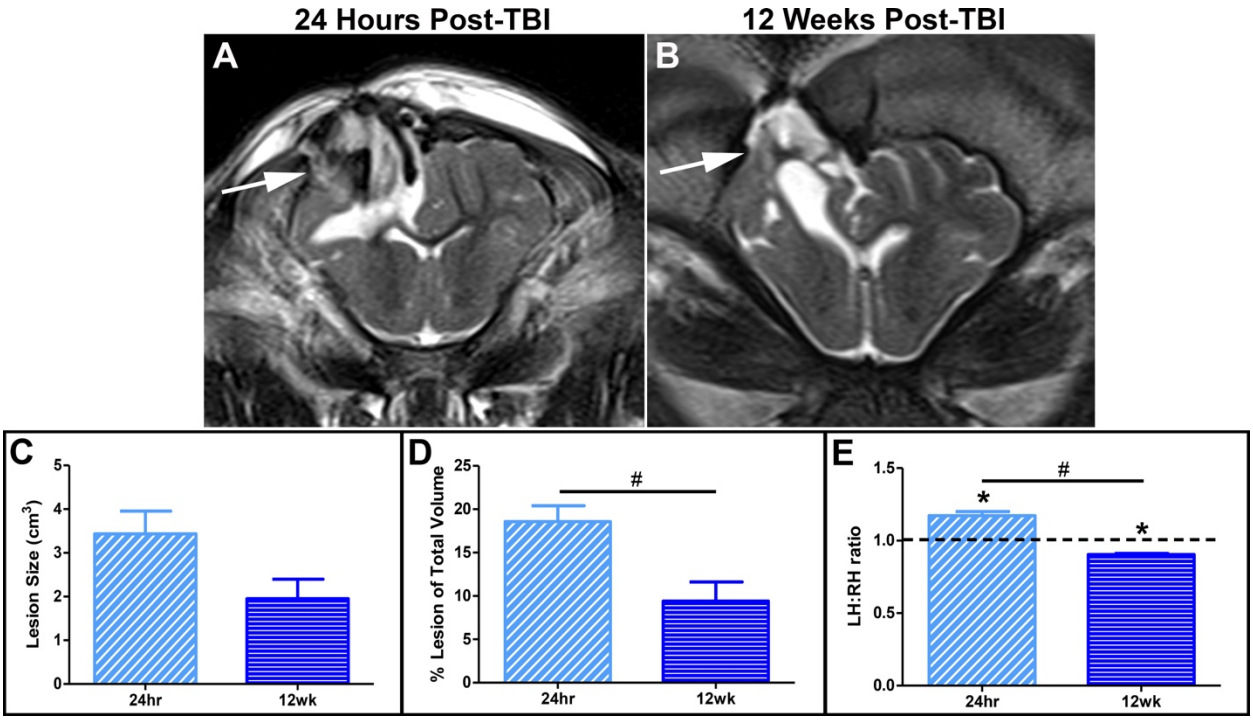
24 Hours Post-TBI
12 Weeks Post-TBI
A
B
C
Lesion Size (cm3)
5
4
3
2
1
0
24hr
12wk
D
% Lesion of Total Volume
25
20
15
10
5
0
#
24hr
12wk
E
LH:RH ratio
1.5
1.0
0.5
0.0
#
*
*
24hr
12wk

Figure 4.2. Directional change in midline shift supports observed brain atrophy at the lesion site. Representative T2-weighed images collected 24 hours (**A**) and 12 weeks (**B**) post-TBI displaying distinct midline shift by quantifying the width of the left hemisphere (red line) and right hemisphere (blue line) at the level of the septum pellucidum (yellow line). Midline was shifted away from the ipsilateral hemisphere 24 hours post-TBI while midline was shifted toward the ipsilateral hemisphere 12 weeks post-TBI (**C**). Data are expressed as mean ± s.e.m. # indicates significance between time points ($p<0.05$). * indicates significance from a normal midline (0.0) ($p<0.05$).

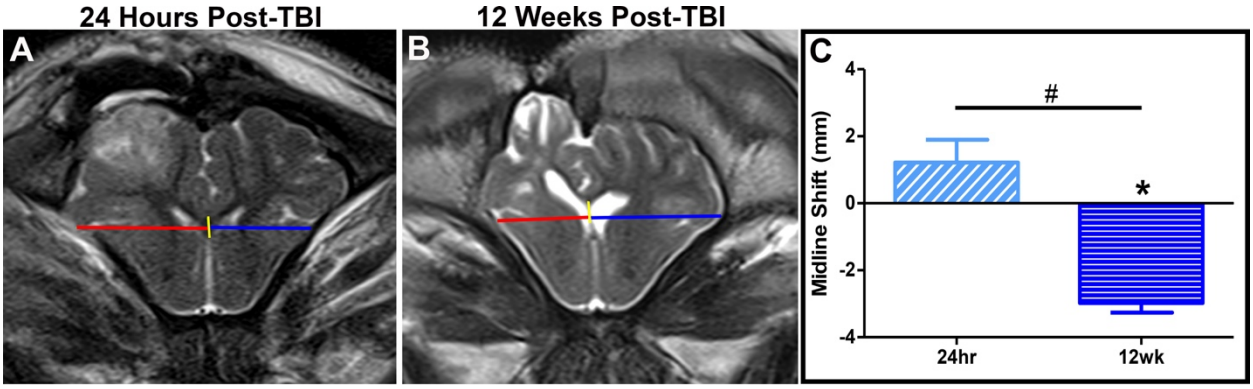
24 Hours Post-TBI
12 Weeks Post-TBI
A
B
C
Midline Shift (mm)
4
2
0
-2
-4
#
*
24hr
12wk

Figure 4.3. CCI leads to the accumulation of edema and disruption of white matter tracts.

Representative T2-weighted images and corresponding ADC maps collected at 24 hours (**A, B**) and 12 weeks (**C, D**) post-TBI. The ADC maps show heterogeneous contrast indicative of cytotoxic and vasogenic edema, but overall significant increases in mean ADC values were observed at 24 hours and 12 weeks post-TBI at the site of the lesion compared to the contralateral side and between time points (**I**). Representative FA maps and corresponding colored coded FA maps collected at 24 hours (**E, F**) and 12 weeks (**G, H**) post-TBI. A significant reduction in FA values were observed in the internal capsule and corpus callosum 24 hours and 12 weeks post-TBI indicative of white matter disruption (**J**). Data are expressed as mean ± s.e.m. # indicates significance between time points ($p<0.0001$). * indicates significance from the contralateral side ($p<0.05$).

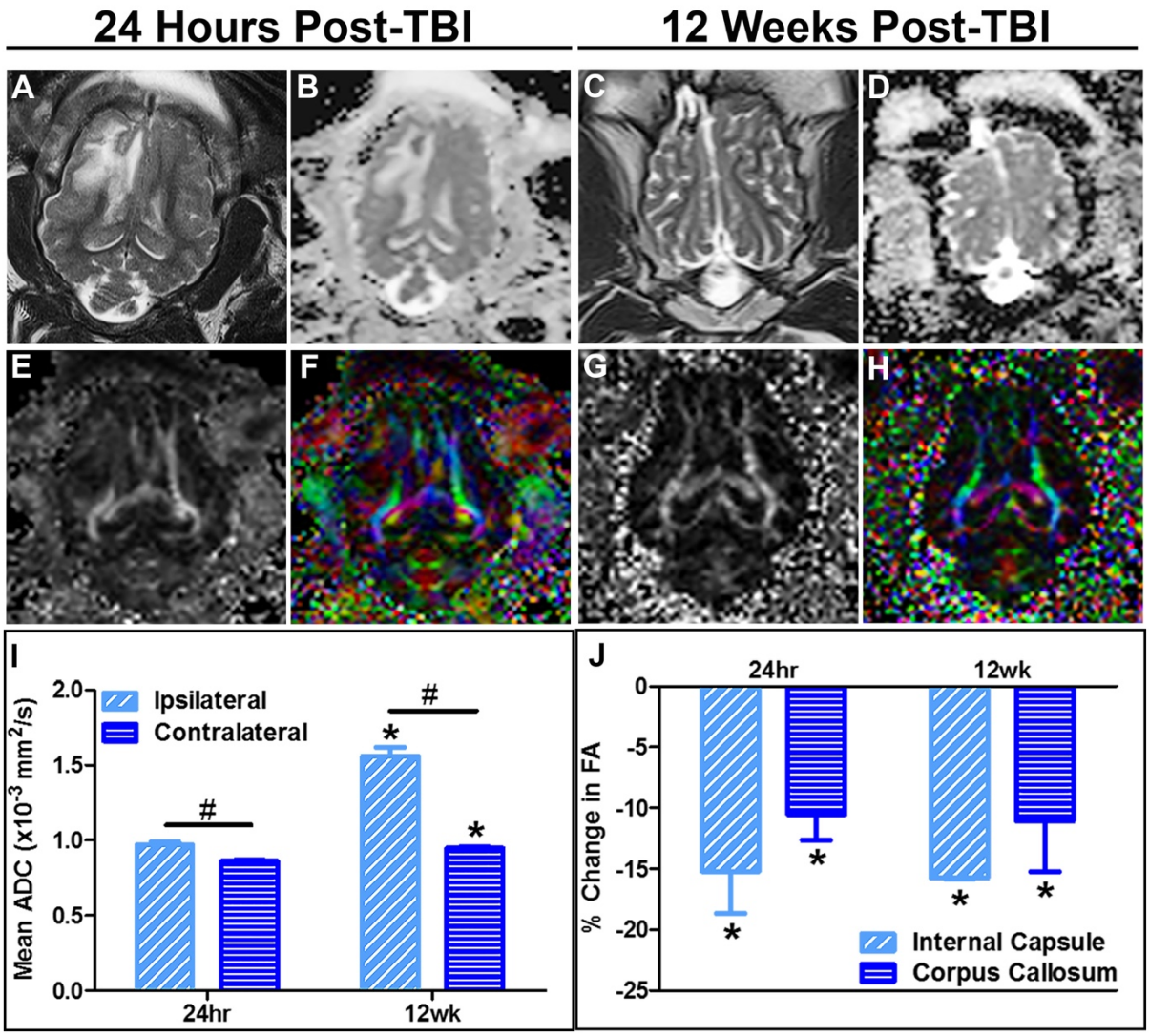
24 Hours Post-TBI
12 Weeks Post-TBI
A
B
C
D
E
F
G
H
I
Mean ADC (x10-3 mm2/s)
2.0
1.5
1.0
0.5
0.0
Ipsilateral
Contralateral
#
#
*
*
24hr
12wk
J
% Change in FA
0
-5
-10
-15
-20
-25
24hr
12wk
*
*
*
*
Internal Capsule
Corpus Callosum

Figure 4.4. CCI results in impaired cerebral blood flow. Representative ASL images taken 24 hours post-TBI illustrating hypointensity at the lesion site indicative of restricted blood flow (**A**, color coded in **B**). A significant decrease in cerebral blood flow was observed both 24 hours and 12 weeks post-TBI while a significant improvement was documented at 12 weeks post-TBI compared to 24 hours post-TBI (**C**). Data are expressed as mean ± s.e.m. # indicates significance between time points. * indicates significance from the contralateral side.

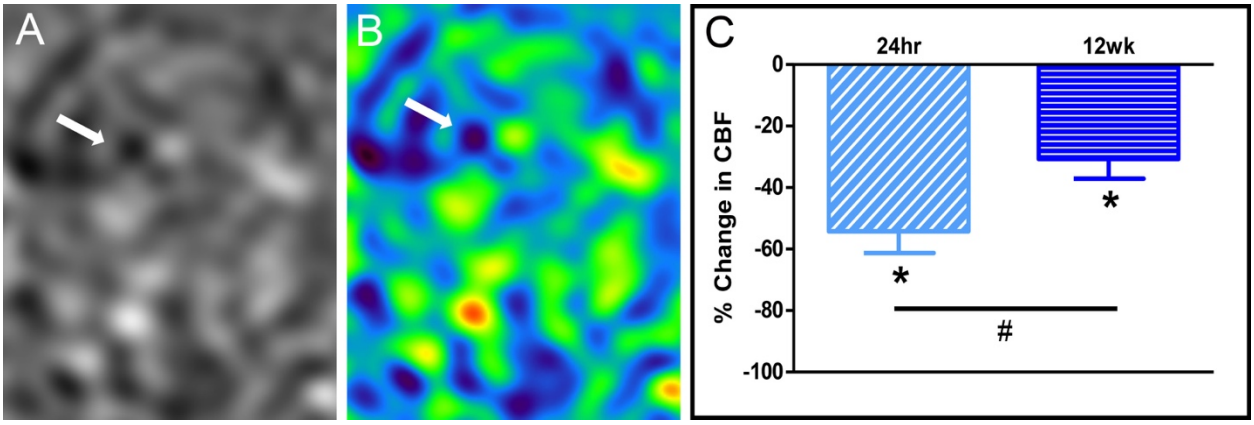
A
B
C
24hr
12wk
0
-20
-40
-60
-80
-100
% Change in CBF
*
*
#

Figure 4.5. MRS can be utilized to track changes in brain metabolites after controlled cortical impact in a piglet model. Sample MR spectra acquired from contralateral (**A**) and ipsilateral (**B**) voxels in a single subject at 24 hours post-TBI. Compared to the contralateral side, the ipsilateral side demonstrates decreased Ins, NAA, Cho, Cr, and Glx as well as increased Lac at 24 hours post-TBI (**B**).

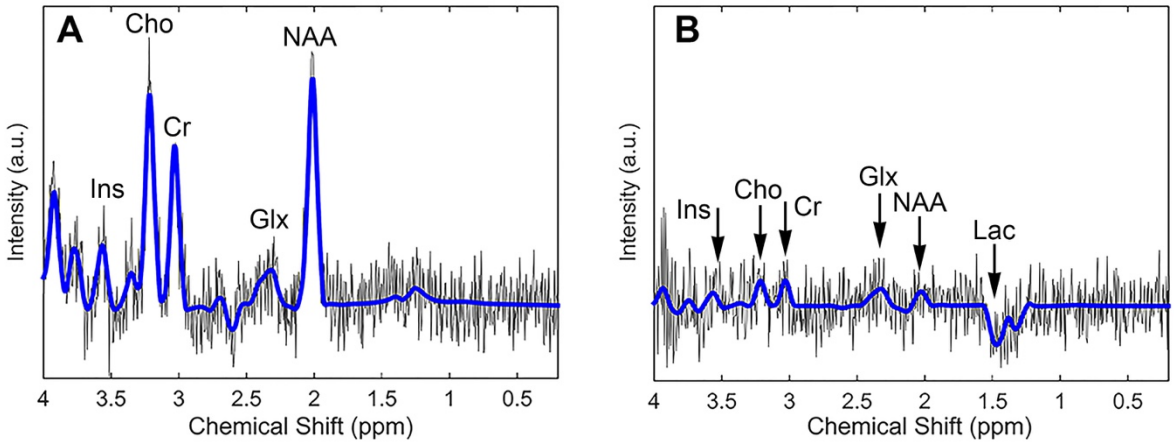
A
Cho
NAA
Cr
Ins
Glx
Intensity (a.u.)
4
3.5
3
2.5
2
1.5
1
0.5
Chemical Shift (ppm)
B
Ins
Cho
Cr
Glx
NAA
Lac
Intensity (a.u.)
4
3.5
3
2.5
2
1.5
1
0.5
Chemical Shift (ppm)

Figure 4.6. CCI results in longitudinal changes in neurons, astrocytes, oligodendrocytes, and microglia in the perilesional area. Representative image of NeuN+ neurons in the perilesional area in normal control animals (**A**), 24 hours post-TBI (**B**), and 12 weeks post-TBI (**C**). The percentage of NeuN+ neurons relative to normal control animals at 24 hours, 1, 4, and 12 weeks-post-TBI (**D**). Representative image of GFAP+ astrocytes in the perilesional area in normal control animals (**E**), 24 hours post-TBI (**F**), and 12 weeks post-TBI (**G**). The percentage of GFAP+ area relative to normal control animals at 24 hours, 1, 4, and 12 weeks-post-TBI (**H**). Representative image of Olig2+ oligodendrocytes in the perilesional area in normal control animals (**I**), 24 hours post-TBI (**J**), and 12 weeks post-TBI (**K**). The percentage of Olig2+ oligodendrocytes relative to normal control animals at 24 hours, 1 week, 4 weeks, and 12 weeks post-TBI (**L**). Representative image Iba1+ microglia in the perilesional area in normal control animals (**M**), 24 hours post-TBI (**N**), and 12 weeks post-TBI (**O**). The percentage of Iba1+ area relative to normal control animals (**P**). Data are expressed as mean ± s.e.m. # indicates significance between time points ($p<0.05$). ***** indicates significance from normal control animals ($p<0.05$).

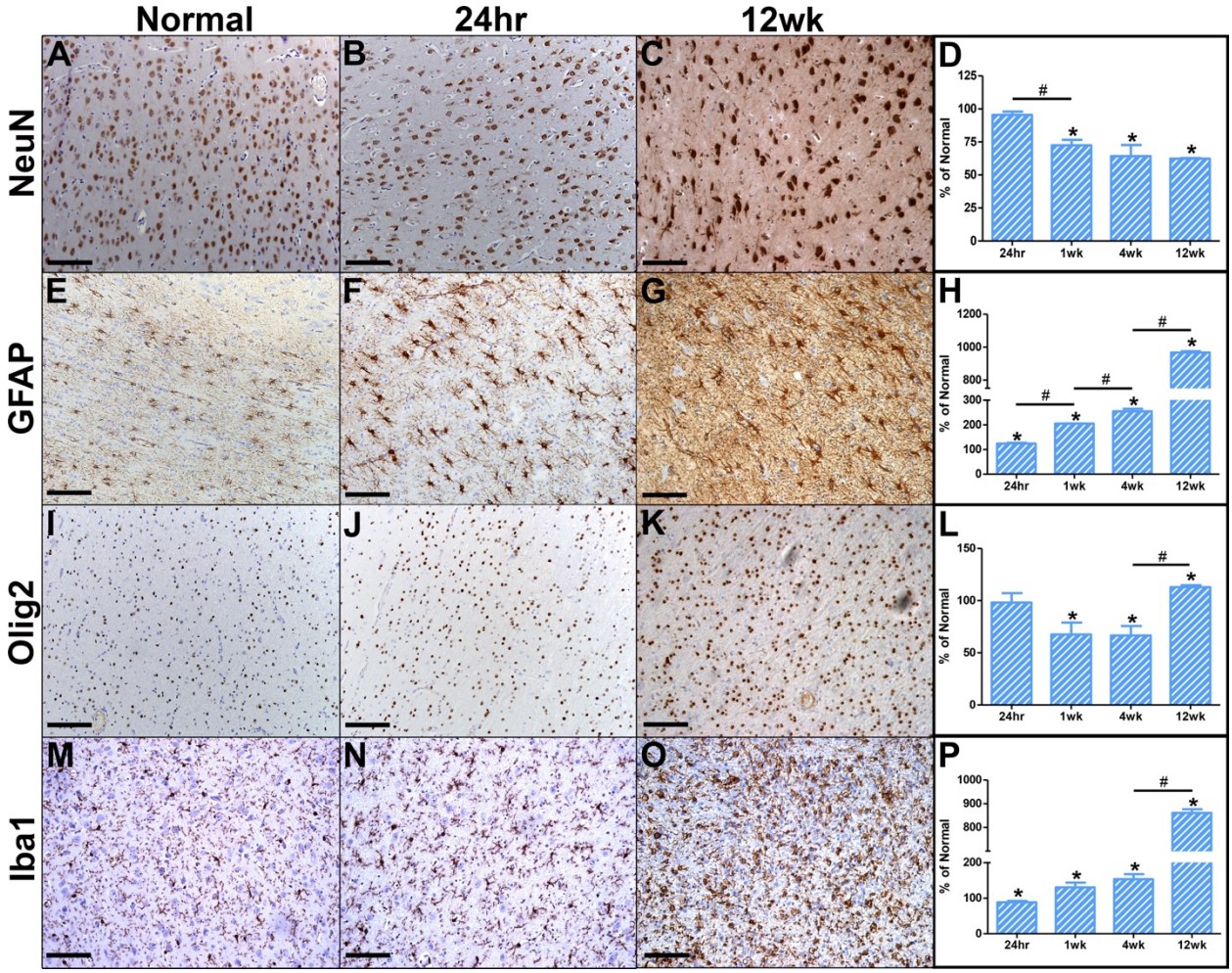
Normal
24hr
12wk
NeuN
GFAP
Olig2
Iba1
A
B
C
D
E
F
G
H
I
J
K
L
M
N
O
P
% of Normal
24hr
1wk
4wk
12wk

CHAPTER 5

A COMPREHENSIVE ASSESSMENT OF LEARNING, MEMORY, AND BEHAVIOR IN A PIGLET MODEL[1]

[1]Kinder, H.A., Baker, E.W., and West, F.D. Submitted to *Physiology and Behavior,* 08/26/2016

Abstract

The use of the piglet in neurobehavioral research has become of increased interest due to similarities in brain structure and development to toddler-aged children. However, further assessment of existing behavioral tests and development of new behavioral tests for pigs is needed. The present study evaluated the ability of four week old piglets to perform open field, object recognition, 3 chamber social recognition, and spatial T-maze tests to assess different aspects of cognition. In open field testing, piglets were placed in an open arena and monitored for motor, exploratory, and anxiety behaviors. Piglets initially exhibited significantly more exploratory behaviors and anxiety behaviors but over time explored fewer zones and became less ambulatory. For the object recognition test, piglets were exposed to two similar objects in a sample trial and then exposed to one familiar and one novel object in a test trial. Piglets explored the novel object significantly more than the familiar object in the test trial. In a novel 3 chamber social recognition test, piglets were exposed to an unfamiliar pig and a novel object in a sociability trial and then exposed to a familiar pig and a novel pig in a social memory trial. Piglets spent significantly more time with the unfamiliar pig in the sociability trial than the novel object and spent significantly less time with the familiar pig in the social memory trial compared to the previous sociability trial. Finally, for the spatial-T maze test, piglets learned to locate a food reward at a constant place in space by using extra-visual cues, despite starting the task at alternating locations. Piglets were significantly faster at making a reward arm choice by Day 4 and reached a performance criterion of at least 80% correct reward arm choices by Day 4. Taken together, these tests provide an ideal platform with which to continue behavioral testing in future studies using a more translational piglet model.

Introduction

Pigs possess a number of cognitive, anatomical, and physiological characteristics that make them a desirable translational animal model for use in neurobehavioral research [1-3]. In recent years, several important studies have revealed the cognitive capacity of pigs and their likeness to human cognition. Pigs are capable of performing different types of behavioral tests that range from operant conditioning and discrimination learning tasks to complex maze and recognition tests that assess different memory processes [4-10]. For example, pigs, similar to humans, appear to possess the ability to form both non-declarative and declarative memories [11]. Episodic memory, a type of declarative memory, involves the ability to recall an experience, details like objects and faces, as well as the temporal and spatial context in which the experience occurred [12, 13]. Only a limited number of behavior tests have been developed to assess episodic-like memory in pigs [7, 14]. In addition, pigs are inherently inquisitive of their environment, form strong social connections with other pigs, and, as foragers, are easily motivated to seek food rewards [11]. Pig brains are more similar to human brains in size, structure, and composition as compared to rodent brains [1-3]. Further, the piglet brain has been found to be comparable to human pediatric brains and generally mirrors a similar pattern of development in regards to myelination, neurogenesis, and electrical activity [11, 15-19].The maturation level and brain weight of 1 month old piglets are proportionally similar to that of the human toddler stage of 1-4 years [2, 20]. The anatomical and physiological similarity of pigs to humans in conjunction with their cognitive capacity has led to the development of an array of behavior tests that can be applied to multiple facets of translational research [1, 11].

Pig neurobehavioral research is an emerging field, particularly in piglet models, while rodent neurobehavioral research is extensive and thus well validated and standardized [21-26].

Most behavior tests developed for pigs have been adapted from rodent models. Behavior tests span multiple facets of cognition and chiefly serve to assess different modalities of learning, memory, and behavior [27-29]. Given that toddler-aged children are at a critical stage of brain development during which they are just beginning to consolidate skills and knowledge, it is important to utilize piglet models of comparable age for learning and memory studies as their memory processes may be more similar to that of children [17, 30]. Several behavior tests have been successfully adapted for use in pigs such as foraging tests, maze tests, social cognition tests, and object recognition tests, but their application remains low, especially in piglet models [11]. The improvement and expansion of these tests is a logical next step to better understand how the pig brain mirrors the human brain in responding to cognitive factors such as lifestyle (chronic life stress, malnutrition), neural disorders (schizophrenia), neural diseases (Parkinson's disease, Alzheimer's disease), or after neural injury (traumatic brain injury, stroke), and, further, to assess the effectiveness of novel therapies at the functional level [31-38].

Given the number of similarities between pigs and humans, recent years have seen a heightened interest in developing and utilizing behavior tests that are able to assess very specific aspects of cognition as a means to measure functional changes in a more translatable model. Abnormal behaviors, impairments in episodic memory formation, social cognition, and spatial memory formation are common after neural injury or disease, and humans serve to benefit from the continued study of these aspects of cognition in animal models [39-43]. The open field test, for example, is a simple assessment of the motor, sensory, and exploratory behaviors of pigs in a controlled environment and provides a platform with which to measure and compare normal behaviors to abnormal behaviors [37, 44]. The novel object recognition test assesses the formation of spontaneous object memories, or memories formed without training [14]. The 3

chamber social recognition test is a measure of social cognition, particularly sociability, or the affinity to seek a social stimulus, and social memory, or the ability to distinguish an individual as novel or familiar [45]. The spatial T-maze test assesses learning, working and reference memory, and, given the plus shape of the maze, extends this test to include a measure of spatial memory [46]. In an effort to expand the current knowledge of porcine cognitive abilities, our group performed a comprehensive assessment of learning, memory, and behavior using these four behavioral tests- open field, novel object recognition, 3 chamber social recognition, and spatial T-maze- in a normal piglet model.

In this report, we demonstrated that normal piglets displayed typical pig exploratory behaviors in an open field test, were able to distinguish a novel object from a familiar object in an object recognition test, were able to distinguish a familiar pig from a novel pig in a 3 chamber social recognition test, and were able to acquire a spatial T-maze test to seek a food reward. These results strengthen the utility of the piglet model for neurobehavioral assessment. To our knowledge, this is the first time the 3 chamber social recognition test has been adapted from rodent models and performed in a piglet model. In addition, these results represent the first time these four tests have been performed together in a piglet model, and demonstrate their promising utility to assess neurobehavioral outcomes in a multitude of different translational piglet models.

Materials and Methods

All work performed in this study was done in accordance with the University of Georgia Institutional Animal Care and Use Committee guidelines.

Animals, Housing, and Feeding

Two commercially bred pregnant Landrace-cross sows were housed in commercial farrowing crates and farrowed naturally. At weaning, 4 piglets 3 weeks of age from one litter were chosen at random and assigned to the test piglet group. These piglets underwent habituation, training, and testing for all behavioral tests described below. In addition, 4 piglets were chosen at random from the other litter and assigned to the stimulus piglet group. These pigs were used as the social stimuli for the 3 chamber social recognition test. Each litter was group housed in separate pens and fed a nutritionally complete pelleted starter diet ad libitum. Both litters of pigs were kept separate and were restricted from having physical or visual contact with one another. Room temperature was maintained at 26°C with a 12h light/dark cycle and an overhead heat lamp provided supplemental heat.

Handling and Habituation

In an effort to reduce anxiety and non-compliance during testing, all piglets were handled 2-3 times a day with initial handling starting the day after birth. Before weaning, handlers removed the entire litter from their mother and took them to a separate pen where they handled (touched, picked-up, held, etc.) each litter for 30- 45 minutes. At one week of age, handlers introduced the piglets to milk replacer (Sav-a-Calf Grade A Ultra 24 Multispecies Milk Replacer, Milk Products LLC). Milk replacer was prepared via package instructions and was offered twice a day until the start of behavior testing. Starting at 2 weeks of age, pigs from both the test and the stimulus groups were habituated to the open field arena and T-maze arenas once a day for 5 minutes each for two weeks. Piglets were habituated to the arenas individually in an effort to reduce stress, social anxiety and non-compliance during testing.

Experimental Design

Behavior testing took place over 10 days starting at 4 weeks of age **(Figure 5.1)**. Pigs underwent T-maze acquisition testing on Days 1-6 followed by T-maze reversal testing on Days 7-10. On Days 2 and 7 pigs underwent open field and object recognition testing and on Days 3 and 8 piglets underwent social recognition testing.

Design of Open Field Arena

The open field arena was used for 3 different behavioral tasks: the open field test, the object recognition test, and the 3 chamber social recognition test. The open field arena was slightly altered for each of the different behavior tests. The open field arena measured 14'x 16' and was constructed using pig paneling positioned over black rubber mats. White curtains were hung around the maze to reduce visual distractions during testing (**Figure 5.2A-B)**. During open field testing, the arena was divided into 8 zones that were visible to handlers only. During object recognition testing, objects were fixed to opposite corners at pig eye level. For the social recognition test, the open field arena was split into three separate chambers using removable panels, with two small openings to either of the outer chambers (**Figure 5.2C-D**). Two 5' panels on opposing sides created a start/exit area in the middle chamber at both the north and south ends to avoid starting the piglets at the same location each trial. Both outer chambers contained smaller metal enclosures, or social stimulus boxes (4' x 5'), for the stimulus pigs. This allowed the test pigs to be separated from the stimulus pigs while still allowing for visual, auditory, olfactory and tactile interactions. Any urination or defecation was wiped down with 70% ethanol between each trial as necessary to reduce olfactory bias. The arena was wiped down with 70%

ethanol between each pig as well to reduce olfactory cues across pigs. This process was repeated for all behavior tests.

Design of Spatial T-maze Arena

The design of the spatial T-maze arena and testing procedure was adapted from Elmore et al. [46]. Briefly, a plus-shaped T-maze was constructed using pig paneling, positioned over black rubber mats (**Figure 5.2E)**. North and south arms measured 7' x 4' and east and west arms measured 8' x 4' (**Figure 5.2F)**. Two removable barriers were fitted to both the north and south ends of the plus-maze. One end served as a start box and the other remained blocked off during testing to create a traditional T-maze shape. The start box alternated between the north and south ends during testing according to a pseudorandom pattern, where the same start arm could not be used for more than two successive trials during 10 total trials. White curtains were hung around the maze in order to reduce visual distractions during testing and additionally, were used to attach extra-maze visual cues (4 posters of different design, one in each corner) (**Figure 5.2E-F)**. A stationary reward bowl was placed at the far ends of the east and west arms. Both bowls contained a milk replacer food reward to reduce bias from olfactory cues. One bowl contained a perforated but secure cap that prevented the pigs from accessing the reward while the other remained open and accessible and could be opened using an inherent rooting motion.

Open Field Test

For the open field test, piglets were placed in the open field arena for 10 minutes. During this time, handlers observed and recorded specific, pre-defined behaviors. Behaviors measured included: zones entered/epoch, percent epochs sniffing/exploring, percent epochs escape

behaviors, and percent stationary/moving. Zones entered/epoch was determined by counting the total number of zones the pigs entered in one minute intervals. Percent epochs sniffing/exploring was determined by marking exploratory behaviors such as sniffing the walls or floors, and rooting motions as either present/absent in 10 second intervals. Percent epochs escape behaviors was measured by marking escape behaviors such as standing up on entrance gates as either present/absent in 10 second intervals. Percent stationary was calculated by recording the total amount of time the pig spent stationary during the 10 minute testing period. Percent moving was calculated by taking the difference from the time spent stationary during the 10 minute testing period.

Object Recognition Test

The object recognition test was comprised of three separate trials: habituation, sample trial, and test trial. The 10 minute habituation period for this test was used in conjunction as the open field test so as to reduce testing time for each pig. In the sample trial, two similar objects of the same color were attached to opposing sides of the open field arena (the northwest and southeast corners). The same set of two similar objects were used for all pigs for the first day of object recognition testing (Day 2) and then a different set of two similar objects were used for all pigs on the second day of object recognition testing (Day 7). All pigs were given 10 minutes to explore the arena and objects. Piglets were then removed from the arena for an inter-phase delay of 10 minutes. The similar object in the southeast corner was replaced with a novel object on the first day of testing (Day 2) and the similar object in the northwest corner was replaced with a novel object on the second day of testing (Day 7). The same novel object was used for all pigs on Day 2 of testing and then a different novel object was used for all pigs on Day 7 of testing. Pigs

were then placed back into the arena for an additional 10 minutes and allowed to explore the arena and objects. Pigs were placed in the arena at alternating north and south start locations for each trial. Time spent with each of the objects in both the sample and test trials was recorded. In addition, zones entered/epoch were measured by averaging the number of zones the piglets entered per 1 minute interval for each trial. Data collected from Day 2 and Day 7 was combined together for analysis.

3 Chamber Social Recognition Test

The 3 chamber social recognition test was comprised of three separate trials: habituation, sociability trial, and social memory trial. In the habituation trial, piglets were placed into the start/exit chamber at either the north or south start locations. Pigs were given 10 minutes to freely explore the arena. For the sociability trial, piglets were briefly removed from the arena while an unfamiliar stimulus piglet was placed into a social stimulus enclosure and a novel object was attached to the front of the opposing social stimulus enclosure. The pigs were then placed back into the arena and allowed to explore the arena, unfamiliar stimulus pig, and novel object freely for 10 minutes. For the social memory trial, the pigs were removed from the arena for an inter-phase interval of 10 minutes. The novel object was removed and a novel stimulus pig was brought into the arena and placed into a social stimulus enclosure. The unfamiliar pig from the sociability trial remained in the arena and thus became a familiar pig for the social memory trial. The test piglets were then placed back into the arena for an additional 10 minutes and allowed to explore the arena, the familiar pig, and the novel pig for 10 minutes. The time spent in each chamber for the sociability trial (start/exit chamber, unfamiliar pig chamber, novel object chamber) and for the social memory trial (start/exit chamber, familiar pig chamber, novel pig

chamber) were recorded. In addition, time spent interacting with the unfamiliar pig and novel object in the sociability trial, or familiar pig and novel pig in social memory trial, was recorded. The location of the unfamiliar pig and novel object was randomized where the unfamiliar pig and the novel object rotated between the east and west locations for each sociability trial. Additionally, locations of the novel pig in the social memory trial rotated between east and west locations for each social memory trial. The same novel object was used for all pigs on the first day of social recognition testing (Day 3) and a different novel object was used for all pigs on the second day of social recognition testing (Day 8). All social stimuli were randomized such that each pig was an unfamiliar pig, familiar pig, and novel pig throughout all trials to reduce a possible novelty affect where one pig could potentially be more memorable than the others. Data collected from Day 3 and Day 8 was combined together for analysis.

Spatial T-maze Test

Piglets began spatial T-maze testing after a nightly 6-h food deprivation to increase motivation for the milk replacer food reward. Pigs were placed in the start box in either the north or south arm (starting position changed according to a pseudorandom pattern). Piglets started in alternating north and south arms to ensure that they did not solve the task using a striatum-dependent, egocentric mechanism whereby muscle memory plays a role in reward selection, such as always turning the body to the left or right. Instead, pigs learned to solve the task using a hippocampal-dependent, allocentric mechanism whereby pigs use extra-visual cues to create spatial memories. Recording began once the barrier of the start box was opened. The pigs had 60 seconds to find the correct arm that contained the food reward. If correct, the pigs were able to access the milk replacer food reward. After consuming the reward, the pigs were placed in the

start box and the next trial began. For the first two days, if the pigs chose the incorrect arm they were corrected and were shown the correct arm. After two days, if the pigs chose the incorrect arm, they were returned to the start box for the next trial without any reward. A performance criterion of 80% correct was applied, which when reached, indicated that the pig had successfully acquired the task. After 6 days of acquisition testing, a reversal phase followed for 4 days in which the food reward arm was switched, but visual cues remained the same. Pigs completed 10 trials/day. Latency to choice for each piglet started once the start barrier was removed and stopped once the piglets reached the food reward, whether correct or incorrect. Handlers also recorded whether the piglets chose the correct or incorrect reward. If piglets made no choice within 60 seconds, the piglet was considered non-compliant for that trial.

Statistical Analysis

Behavior data was analyzed using a two-way ANOVA (SAS version 9.3; Cary, NC) followed by Tukey's LSD post-hoc test to determine significant differences between groups. Statistically significant differences were defined at the 95% confidence index ($p<0.05$). Data shown as means ± standard error of the mean.

Results

Piglets demonstrate high exploratory interest and habituation over time in an open field test

In the open field test, piglets were placed into an empty arena for 10 minutes. We observed that pigs entered an average of 7.98 ± 1.28 zones/one minute epoch on Day 2 and an average of 7.15 ± 0.70 zones/one minute epoch on Day 7 (**Figure 5.3A**) suggesting that piglets spent a great deal of time moving around and exploring their environment on both testing days.

Although piglets spent significantly ($p < 0.05$) more time stationary than mobile on both Days 2 and 7 (57.25 ± 2.79% vs. 65.25 ±2.87%, **Figure 5.3B**), we often observed that stationary behaviors were accompanied with sniffing/rooting behaviors. To that end, we observed that piglets spent approximately 74% epochs sniffing/exploring their environment on Day 2 of testing which is consistent with reports that suggest that normal piglets are highly inquisitive and exploratory (**Figure 5.3C)**. Although we did observe a significant ($p<0.05$) decrease in sniffing/exploring behaviors on Day 7 of testing compared to Day 2 (46.75 ± 5.54% epochs), these results suggest that the piglets became habituated to their environment over time. Finally, piglets exhibited more escape behaviors on Day 2 compared to Day 7 (7.25 ± 3.77% epochs vs. 0.75 ± 0.75% epochs, **Figure 5.3D)**. These results show trending ($p=.14$) differences between Day 2 and 7 although not significant. This suggests that piglets initially were highly anxious on the first day of testing, likely as a result of being separated from their littermates, but that on the second day of testing they were more habituated and comfortable being alone. Overall, these results indicate that pigs, when placed in a novel open field environment, display behaviors consistent with normal pig behavior such as high exploratory activity which generally decreases over time, likely as a result of habituation to the testing arena.

Piglets form spontaneous object memories of a familiar object in an object recognition test

The object recognition test assesses a pig's ability to form spontaneous trial-unique memories. These memories are analogous to human episodic memories, or memories that are formed spontaneously, without training. For this test, pigs first underwent a 10 minute habituation trial. Then pigs underwent a sample trial where they were exposed to two similar objects (Object A and Object B), then were removed from the arena for a 10 minute inter-phase

interval, and then finally underwent a test trial where they were exposed to one familiar object (Object A') and one novel object (Object C).

A comparison of average number of zones entered/epoch across all trials showed that pigs entered significantly ($p<0.05$) fewer zones in the test trial as compared to the habituation period (7.56 ± 0.69 zones vs. 4.83 ± 0.59 zones, **Figure 5.4A**). These results suggest that pigs entered fewer zones over time as an indication of habituation to the testing arenas, or that pigs were expressing greater exploratory interest towards the novel object, thus reducing their time spent moving about the arena. In the sample trial, there was no significant difference between exploration times of the two similar objects, Object A and Object B (71.63 ± 10.60s vs. 49.63 ± 7.11s, **Figure 5.4B**). In the test trial, pigs explored the novel object, Object C, significantly ($p<0.05$) more than the familiar object, Object A' (81.13 ± 12.23s vs. 40.25 ± 10.05s, **Figure 5.4C**). A comparison between time spent exploring the familiar object in the test trial as compared to exploration time of the same object in the sample trial demonstrates that pigs spent significantly ($p<0.05$) less time with familiar object in the test trial than the sample trial (71.63 ± 10.60s vs. 40.25 ± 10.05s, **Figure 5.4D**). These results indicate that normal pigs express an innate ability to distinguish and seek novelty and can form spontaneous object memories of a familiar object that can be recalled over a 10 minute period.

Piglets seek a social stimulus over a novel object and can recognize a familiar piglet in a 3 chamber social recognition test

The 3 chamber social recognition test assesses a piglet's affinity to seek a social stimulus as well as the ability to form a social memory of a familiar piglet and thus seek a novel piglet. Piglets first underwent a 10 minute habituation period in an empty arena. Next pigs were

exposed to an unfamiliar pig and a novel object in a sociability trial, then removed from the arena for a 10 minute inter-phase interval, and then finally exposed to a familiar pig from the sociability trial and a new pig in a social memory trial.

In the sociability trial, a comparison of total time spent in either the start/exit chamber, the unfamiliar pig chamber, or the novel object chamber showed that pigs spent significantly ($p<0.01$) more time in the unfamiliar pig and object chambers than the start/exit chamber (355.38 ± 27.37s and 185.25 ± 25.39s vs. 58.13 ± 22.82s, respectively), and additionally, pigs spent significantly ($p<0.001$) more time in the unfamiliar pig chamber than the object chamber (355.38 ± 27.37s vs. 185.25 ± 25.39s, **Figure 5.5A**). A measure of direct interaction with either the unfamiliar pig or the novel object demonstrated that pigs spent significantly ($p<0.01$) more time with an unfamiliar pig than a novel object (211.13 ± 32.68s vs. 70.38 ± 16.52s, **Figure 5.5B**). Taken together these results suggest that pigs, as social animals, prefer to seek the company of an unfamiliar pig rather than interact with a novel object.

In the social memory trial, a direct comparison of time spent in either the start/exit chamber, novel pig chamber, or familiar pig chamber shows that piglets spent significantly ($p<0.01$) more time in the novel pig chamber than the start/exit chamber (286.00 ± 42.49s vs. 124.88 ± 25.64s, **Figure 5.6A**). Additionally, test piglets showed a trending increase in the time directly interacting with the novel pig rather than the familiar pig (142.63 ± 35.86s vs. 69.25 ± 21.28s, **Figure 5.6B),** although this data did not reach significance ($p=0.10$). A comparison of the time spent exploring the familiar pig in the social memory trial as compared to the same pig in the sociability trial demonstrates that pigs spent significantly ($p<0.01$) less time with the familiar pig in the social memory trial, which suggests that pigs were able to form a social memory of the familiar pig (69.25 ± 21.28 vs. 211.12 ± 32.68, **Figure 5.6C**). Taken together, the

results indicate that piglets tend to seek interaction with a novel piglet over a familiar piglet, can form a social memory of a familiar piglet, and once again, prefer to be in closer proximity with a novel piglet in the testing arena.

Piglets can form spatial memories to seek a food reward in a plus-shaped spatial T-maze test

In a spatial T-maze task, piglets were trained to locate a food reward at a constant place in space. To promote the formation of spatial memories using an allocentric mechanism, which is hippocampal-based, rather than an egocentric mechanism, which is striatum-based, the start location varied from north to south in a pseudorandom order and visual cues were placed around the testing arena in fixed locations. Pigs underwent 6 days of acquisition testing followed by 4 days of reversal testing.

During the initial days of testing, one piglet was non-compliant for approximately 5% of trials on day 1 of acquisition and another piglet was non-compliant for approximately 7.5% of trials on day 3 (0.05± 0.05 and 0.075 ± 0.075, **Figure 5.7A**), but no significant differences were observed. However, once the piglets learned to navigate the maze and obtain the food reward, non-compliance ceased completely and piglets were actually eager to navigate the maze to the food reward. Latency to choice, or the time it took for pigs to reach a food reward bowl regardless of accuracy, improved significantly over time. Latency to choice was significantly (p<0.01) faster by Day 4 of acquisition as compared to Day 1 of acquisition, and remained significant throughout the duration of testing (7.30 ± 0.61s vs. 13.60 ± 1.20s, **Figure 5.7B**). Latency to choice was not affected by reversal testing as this parameter does not take into account accuracy of choice; therefore pigs still understood the objective of the task and continued to make quick reward arm decisions despite reversal of the reward. Finally, pigs

reached a performance criterion of at least 80% correct choices by Day 4 of acquisition, and the proportion of trials correct was significantly (p<0.0001) greater by Day 4 of acquisition as compared to Day 1 and remained significant for the duration of testing (0.80 ± .08 vs. 0.15 ± 0.05, **Figure 5.7C**). After reward reversal, proportion correct choices was significantly decreased (p<0.01) on Day 1 of reversal compared to Day 6 of acquisition (0.58 ± 0.06 vs. 0.90 ± .04), although piglets did continue to make significantly (p<0.001) more correct choices after Day 1 of reversal as compared to Day 1 of acquisition (0.58 ± 0.06 vs. 0.15 ± 0.05, **Figure 5.7C**). However, they made significantly (p<0.001) more correct choices by Day 4 of reversal as compared to Day 1 of reversal (0.95 ± 0.03 vs. 0.58 ± 0.06, **Figure 5.7C**) suggesting they were capable of forming new spatial memories. Overall, these results indicate that pigs can learn to navigate a spatial T-maze arena and can form and use spatial memories to locate a food reward at a constant place in space, despite alternating the starting location of the test.

Discussion

In this study we present for the first time a comprehensive, quantitative assessment of learning, memory, and behavior using four separate behavior tests performed by a single group of piglets. Piglets demonstrated several key exploratory and anxiety behaviors in an open field test and showed the ability to form object, social, and spatial memories in an object recognition test, social recognition test, and spatial T-maze test, respectively. While piglets have been tested in the open field test, spatial T-maze test, and object recognition test by other groups, further validation of these tests are needed [37, 46, 47]. However, we present for the first time individual assessment of piglet sociability behaviors and social memory in a 3 chamber social recognition test. This test has been used extensively in rodent models and, due to their social

nature, was easily adapted for use in pigs [45]. Comprehensive assessments of cognition in porcine models, and particularly in piglet models, are limited. Margulies et al. performed a comprehensive assessment of learning, memory, and behavior after rotational head injury in 3-5 day old piglets using an open field test, mirror task, glass barrier task, food cover task, and T-maze test [37, 48]. We present for the first time a comprehensive behavioral assessment using an open field test, object recognition test, 3 chamber social recognition test, and spatial T-maze test in a piglet model.

In the open field test, piglets were found to be highly exploratory of their environment. Exploratory behaviors were observed to decline with time as a result of habituation. Further, piglets were found to exhibit anxiety/escape behaviors on the first day of testing but by day 7 were mostly absent. This pattern of piglet behavior is expected based on the knowledge of inherit characteristics of pigs [44, 49, 50]. Wild boars, the ancestor of the domestic pig, are scavenging omnivores who commonly use their snouts to root and dig for food. Additionally, wild boars typically live in small herds with a stable hierarchy [11]. These characteristics have been passed down to domestic pigs, and when placed in a novel environment such as in the open field test, pigs are likely to display remnants of several of these behaviors. Pigs are inquisitive by nature and when placed in a novel environment will typically spend a great deal of time moving about their environment and use an inherent rooting motion to explore and test their environment. Additionally, as piglets are social animals that prefer to remain with their littermates than alone, escape and anxiety behaviors are often common when pigs are placed into a novel environment alone [51]. The results of this study are consistent with previous reports of piglet open field behavior [44, 50, 52]. Given the social nature of piglets, separation from their littermates may account for an increase in anxiety and escape behaviors during open field testing. Pigs in our

study showed increased levels of habituation over time as indicated by a decrease in observed exploratory and anxiety behaviors. There is strong evidence to support the idea of a 'habituation response' that can occur as a result of repeated exposure to a novel environment whereby a pig becomes less reactive to their environment as their stress and fear decline and they become more acclimated to change and social isolation [50, 53, 54]. The open field test has been used in agricultural research to assess factors such as weaning methods, early postnatal social isolation, tail biting, and barren/enriched housing on piglet behavior [31, 49, 55, 56]. Given its utility, this test provides an ideal means to assess changes in characteristic behaviors of pigs that may be sensitive to disruption in future biomedical research.

The object recognition test is based on the principle of inquisitive exploration where a behavioral response occurs as a result of an environmental change but not necessarily as a result of a stimulus [57]. The introduction of either familiar or novel objects to a testing environment have been found to elicit a behavioral response, such that piglets were found to explore a novel object more than a familiar one [57]. This innate tendency to seek novelty has been utilized to assess object recognition memory using the spontaneous object recognition test which requires no training and provides a direct measure of trial-unique memory of both familiar and novel objects [14]. Piglets in this study showed no preference for either of the similar objects in the sample trial. However, they spent significantly more time with a novel object over a familiar object in the test trial. The object recognition test has also been suggested to provide an assessment of episodic-like memory in pigs [58]. Extensions of this test that include recall of different what/where/which modalities of episodic memory where object memory is tested in different spatial and/or temporal contexts may provide a more stringent measurement of human episodic-like memory [7]. Manipulation of the duration of the initial exposure of the objects in

the sample trial or of the inter-phase delay has been hypothesized affect object recognition memory. In the present study, a 10 minutes sample trial was followed by a 10 minute inter-phase delay and animals showed significant object recognition abilities. Previous reports assent that object recognition is clearly evident after a 10 minute sample trial followed by a 10 minute inter-phase delay. However, Moustgaard et al. found evidence for object recognition after 1 hour while Kornum et al. did not observe object recognition after a 1 hour or 24 hour delay [14, 58]. Gifford et al. found that 5 week old piglets did not display a novelty preference after a 10 minute sample trial after either a 1 hour, 3 hours, or 6 day delay but piglets did display a novelty preference after a 2 hour sample trial and a 3 hour and 5 day delay [47]. However, piglets were tested in pairs and objects for the sample trial were placed into the home pen which may have influenced their observed testing outcomes. Further investigation of the relationship between sample trial exposure and inter-phase delay is needed in both piglet and adult pigs to better elucidate their capacity for object recognition memory.

The 3 chamber social recognition test provides a measure of sociability behaviors and social recognition memory. In the sociability trial piglets spent significantly more time in the unfamiliar pig chamber and spent significantly more time with an unfamiliar pig than a novel object. Pigs are highly social by nature and prefer to live in stable social groups [11]. Social isolation has been found to be highly stressful for pigs and may contribute to long-term negative consequences in cognition and overall welfare [51, 59]. Although piglets exhibited considerable interest in interacting with a novel object, our results suggest that social novelty surmounts object novelty during spontaneous exploration. While this is the first pig study to utilize the 3 chamber social recognition test, rodent studies consistently observe an affinity for social interaction over object interaction in normal animals [60, 61]. In the social memory trial, we

observed that pigs spent significantly more time in the novel pig chamber and tended to spend more time with a novel pig over a familiar pig (significance trending, p=0.10). However, we found a significant decrease in exploration when comparing the amount of time spent with the familiar pig during the social memory trial and the same pig during the previous sociability trial. These results suggest that piglets are capable of forming social memories and are thus able distinguish a familiar pig from a novel pig, similar to observed outcomes in rodents [60, 61]. A number of studies have utilized different methods to assess social recognition memory in pigs. Kristensen et al. and McLeman et al. utilized a Y-maze test to assess social recognition and found that pigs are able to use different sensory modalities such as visual, auditory, or olfactory cues to identify familiar pigs from unfamiliar pigs [62-64]. However, in order to isolate each of the sensory modalities during testing, a complex Y-maze apparatus was designed to allow for precise control of these factors [62, 63]. Zanella et al. designed an oval arena separated in the center by flexible netting located between two farrowing crates that allowed for two litters of piglets to have physical contact but prevented mixing and potential aggression between the two litters during a familiarization procedure [65]. The piglets were familiarized both as a full litter and in pairs and then assessed for social recognition in pairs. The authors reasoned that testing in pairs would prevent stress resulting from social isolation [65]. While Zanella et al. did assess social recognition with a younger cohort (12 days of age), we demonstrate here that sufficient individual habituation with piglets approximately 4-5 weeks of age prior to testing can sufficiently reduce social isolation stress so social recognition memory can be assessed in individual piglets without the distraction of other littermates. Our results provide promising evidence of the utility of the 3 chamber social recognition test for future pig studies in that the

set-up is simple and it provides a straightforward assessment of sociability and social memory in individual pigs.

The spatial T-maze test assesses the ability of piglets to learn the location of a food reward at a constant place in space based on extra-maze visual cues. Piglets begin the task at alternating north and south start arms and must therefore learn to navigate the maze using a hippocampal-dependent allocentric mechanism. This spatial memory test was recently developed by Elmore, Dilger, and Johnson for 2-3 week old piglets based on rodent 'place' and/or 'direction' learning T-maze tasks and to our knowledge has not yet been reproduced by other pig groups [46]. We made minor adjustments to their experimental design and reduced acquisition testing from 9 days to 6 days and increased reversal testing from 3 days to 4 days. Here, we confirm the successful acquisition of this task using 4-5 week old piglets. The time to select a reward arm steadily decreased over time as piglets acquired the task and latency to choice was significantly faster by Day 4 and remained significant throughout the direction of acquisition testing. Given that latency to choice reflects both correct and incorrect choices, we observed no significant changes in latency to choice after reversal. Elmore et al. observed a similar decrease in latency to choice over time and reported a significant decreased by Day 9 compared to Day 1. However they report a significant increase in latency to choice after reversal that was not observed in this study [46]. We also report that piglets made significantly more correct choices by Day 4 of testing that persisted through the acquisition phase. However, proportion trials correct was significantly decreased after Day 1 of reversal but recovered by Day 4 of reversal. The successful acquisition of a greater than 80% performance criterion for this test suggests that piglets were able to create a spatial map of the testing arena and surrounding environment and use an allocentric mechanism to identify the location of a food reward. These results are similar

to Elmore et al. who report a significant increase in proportion trials correct by Day 9 of acquisition as well as a significant decrease in proportion trials correct after reversal but a recovery in performance after 3 days of reversal [46]. We report no significant changes in proportion trials non-compliant. There are a number of other behavior tests such as the Morris Water maze, the eight arm radial maze, and the cognitive holeboard task that have been adapted for pigs to assess spatial memory [4, 5, 66, 67]. They are based on a similar concept that require pigs to use extra-maze visual cues to either escape to safety, as in the case of the Morris Water maze, or locate hidden food rewards, as in the case of the eight arm radial maze and the cognitive holeboard task. However, a number of limitations such as arena design and size, training requirements, and testing duration are significant hurdles with respect to these tests, making them less appealing tests of spatial memory in pigs. We found the spatial plus T-maze to be relatively easy to build and most importantly, piglets were easily trained to acquire this test with only 10 trials/day and the inter-trial interval was less than one minute/pig. This allowed us to easily test multiple piglets per day in combination with our other behavior tests.

Conclusion

In this study, a comprehensive assessment of normal piglet cognition was assessed using four behavior tests. Piglets exhibited normal motor and exploratory behaviors in an open field test. They used object memories to differentiate between a familiar and novel object in an object recognition test. In a social recognition test, piglets exhibited normal sociability behaviors and were able to form social memories of a familiar piglet. Finally, piglets were able to use spatial memories to successfully acquire a spatial T-maze test. These findings demonstrate that a combined approach using four behavior tests is an ideal method to assess different aspects of

piglet learning, memory, and behavior, thus supporting their potential to be used in future agricultural and biomedical studies to assess changes in cognition.

Acknowledgments and Disclosures

We would like to thank Kimberly Straub, Brooke Salehzadeh, Abby Howell, Joette Crews, Aleia Hollands, Kathryn Sellman, Jessica Gladney, Caroline Coleman, Sarah Shaver, Shelley Tau, and Jennifer Roveto for their indispensable help with all aspects of pig work from socializing the piglets to assisting with behavior testing. We would also like to thank Rick Utley and Kelly Parham at the UGA Swine Unit for their pig expertise and for providing us with piglets. Lastly, we would like to thank Randy Nation for his help in designing and building our behavior testing arenas. This work was supported by The University of Georgia Research Foundation.

The authors have no conflicts of interest.

References

1. Lind, N.M., et al., *The use of pigs in neuroscience: modeling brain disorders.* Neurosci Biobehav Rev, 2007. **31**(5): p. 728-51.
2. Thomas, J.M. and J.L. Beamer, *Age-weight relationships of selected organs and body weight for miniature swine.* Growth, 1971. **35**(3): p. 259-72.
3. Watanabe, H., et al., *MR-based statistical atlas of the Gottingen minipig brain.* Neuroimage, 2001. **14**(5): p. 1089-96.
4. Dilger, R.N. and R.W. Johnson, *Behavioral assessment of cognitive function using a translational neonatal piglet model.* Brain Behav Immun, 2010. **24**(7): p. 1156-65.
5. Arts, J.W., F.J. van der Staay, and E.D. Ekkel, *Working and reference memory of pigs in the spatial holeboard discrimination task.* Behav Brain Res, 2009. **205**(1): p. 303-6.
6. Held, S., et al., *Foraging behaviour in domestic pigs (Sus scrofa): remembering and prioritizing food sites of different value.* Anim Cogn, 2005. **8**(2): p. 114-21.
7. Kouwenberg, A.L., et al., *Episodic-like memory in crossbred Yucatan minipigs (Sus scrofa).* Applied Animal Behaviour Science, 2009. **117**(3-4): p. 165-172.
8. Moustgaard, A., et al., *Discriminations, reversals, and extra-dimensional shifts in the Gottingen minipig.* Behav Processes, 2004. **67**(1): p. 27-37.
9. Baldwin, B.A., *Study of Behaviour in Pigs.* British Veterinary Journal, 1969. **125**(6): p. 281-&.
10. Baldwin, B.A., *Operant Studies on the Behavior of Pigs and Sheep in Relation to the Physical-Environment.* Journal of Animal Science, 1979. **49**(4): p. 1125-1134.
11. Kornum, B.R. and G.M. Knudsen, *Cognitive testing of pigs (Sus scrofa) in translational biobehavioral research.* Neurosci Biobehav Rev, 2011. **35**(3): p. 437-51.

12. Dere, E., et al., *The case for episodic memory in animals.* Neurosci Biobehav Rev, 2006. **30**(8): p. 1206-24.

13. Allen, T.A. and N.J. Fortin, *The evolution of episodic memory.* Proc Natl Acad Sci U S A, 2013. **110 Suppl 2**: p. 10379-86.

14. Moustgaard, A., et al., *Spontaneous object recognition in the Gottingen minipig.* Neural Plast, 2002. **9**(4): p. 255-9.

15. Niblock, M.M., et al., *Comparative anatomical assessment of the piglet as a model for the developing human medullary serotonergic system.* Brain Res Brain Res Rev, 2005. **50**(1): p. 169-83.

16. Fang, M., et al., *Myelination of the pig's brain: a correlated MRI and histological study.* Neurosignals, 2005. **14**(3): p. 102-8.

17. Dobbing, J. and J. Sands, *Comparative aspects of the brain growth spurt.* Early Hum Dev, 1979. **3**(1): p. 79-83.

18. Pampiglione, G., *Some aspects of development of cerebral function in mammals.* Proc R Soc Med, 1971. **64**(4): p. 429-35.

19. Flynn, T.J., *Developmental changes of myelin-related lipids in brain of miniature swine.* Neurochem Res, 1984. **9**(7): p. 935-45.

20. Coppoletta, J.M. and S.B. Wolbach, *Body Length and Organ Weights of Infants and Children: A Study of the Body Length and Normal Weights of the More Important Vital Organs of the Body between Birth and Twelve Years of Age.* Am J Pathol, 1933. **9**(1): p. 55-70.

21. Sharma, S., S. Rakoczy, and H. Brown-Borg, *Assessment of spatial memory in mice.* Life Sciences, 2010. **87**(17-18): p. 521-536.

22. Vorhees, C.V. and M.T. Williams, *Value of water mazes for assessing spatial and egocentric learning and memory in rodent basic research and regulatory studies.* Neurotoxicol Teratol, 2014. **45**: p. 75-90.

23. Bengoetxea, X., M. Rodriguez-Perdigon, and M.J. Ramirez, *Object recognition test for studying cognitive impairments in animal models of Alzheimer's disease.* Front Biosci (Schol Ed), 2015. **7**: p. 10-29.

24. Fujimoto, S.T., et al., *Motor and cognitive function evaluation following experimental traumatic brain injury.* Neurosci Biobehav Rev, 2004. **28**(4): p. 365-78.

25. Kas, M.J., et al., *Assessing behavioural and cognitive domains of autism spectrum disorders in rodents: current status and future perspectives.* Psychopharmacology (Berl), 2014. **231**(6): p. 1125-46.

26. Dudchenko, P.A., *An overview of the tasks used to test working memory in rodents.* Neurosci Biobehav Rev, 2004. **28**(7): p. 699-709.

27. Morris, R.G., *Episodic-like memory in animals: psychological criteria, neural mechanisms and the value of episodic-like tasks to investigate animal models of neurodegenerative disease.* Philos Trans R Soc Lond B Biol Sci, 2001. **356**(1413): p. 1453-65.

28. Pickens, C.L. and P.C. Holland, *Conditioning and cognition.* Neurosci Biobehav Rev, 2004. **28**(7): p. 651-61.

29. Paul, C.M., G. Magda, and S. Abel, *Spatial memory: Theoretical basis and comparative review on experimental methods in rodents.* Behav Brain Res, 2009. **203**(2): p. 151-64.

30. Bremner, J.G. and A. Fogel, *Blackwell handbook of infant development*. Blackwell handbooks of developmental psychology. 2001, Malden, MA: Blackwell Pub. xii, 780 p.

31. Kanitz, E., et al., *Consequences of repeated early isolation in domestic piglets (Sus scrofa) on their behavioural, neuroendocrine, and immunological responses.* Brain Behav Immun, 2004. **18**(1): p. 35-45.

32. Ng, K.F. and S.M. Innis, *Behavioral responses are altered in piglets with decreased frontal cortex docosahexaenoic acid.* J Nutr, 2003. **133**(10): p. 3222-7.

33. Lind, N.M., et al., *Prepulse inhibition of the acoustic startle reflex in pigs and its disruption by d-amphetamine.* Behav Brain Res, 2004. **155**(2): p. 217-22.

34. Holm, I.E., A.K. Alstrup, and Y. Luo, *Genetically modified pig models for neurodegenerative disorders.* J Pathol, 2016. **238**(2): p. 267-87.

35. Mikkelsen, M., et al., *MPTP-induced Parkinsonism in minipigs: A behavioral, biochemical, and histological study.* Neurotoxicol Teratol, 1999. **21**(2): p. 169-75.

36. Sondergaard, L.V., et al., *Determination of odor detection threshold in the Gottingen minipig.* Chem Senses, 2010. **35**(8): p. 727-34.

37. Friess, S.H., et al., *Neurobehavioral functional deficits following closed head injury in the neonatal pig.* Exp Neurol, 2007. **204**(1): p. 234-43.

38. Tanaka, Y., et al., *Experimental model of lacunar infarction in the gyrencephalic brain of the miniature pig: neurological assessment and histological, immunohistochemical, and physiological evaluation of dynamic corticospinal tract deformation.* Stroke, 2008. **39**(1): p. 205-12.

39. Lockhart, S.N., et al., *Episodic memory function is associated with multiple measures of white matter integrity in cognitive aging.* Front Hum Neurosci, 2012. **6**: p. 56.

40. Anderson, V., et al., *Predictors of cognitive function and recovery 10 years after traumatic brain injury in young children.* Pediatrics, 2012. **129**(2): p. e254-61.

41. Anderson, V., et al., *Functional plasticity or vulnerability after early brain injury?* Pediatrics, 2005. **116**(6): p. 1374-82.

42. Benz, B., A. Ritz, and S. Kiesow, *Influence of age-related factors on long-term outcome after traumatic brain injury (TBI) in children: A review of recent literature and some preliminary findings.* Restor Neurol Neurosci, 1999. **14**(2-3): p. 135-141.

43. Schwartz, L., et al., *Long-term behavior problems following pediatric traumatic brain injury: prevalence, predictors, and correlates.* J Pediatr Psychol, 2003. **28**(4): p. 251-63.

44. Lind, N.M., et al., *Open field behaviour and reaction to novelty in Gottingen minipigs: Effects of amphetamine and haloperidol.* Scandinavian Journal of Laboratory Animal Science, 2005. **32**(2): p. 103-112.

45. Tang, G., et al., *Loss of mTOR-dependent macroautophagy causes autistic-like synaptic pruning deficits.* Neuron, 2014. **83**(5): p. 1131-43.

46. Elmore, M.R., R.N. Dilger, and R.W. Johnson, *Place and direction learning in a spatial T-maze task by neonatal piglets.* Anim Cogn, 2012. **15**(4): p. 667-76.

47. Gifford, A.K., S. Cloutier, and R.C. Newberry, *Objects as enrichment: Effects of object exposure time and delay interval on object recognition memory of the domestic pig.* Applied Animal Behaviour Science, 2007. **107**(3-4): p. 206-217.

48. Naim, M.Y., et al., *Folic acid enhances early functional recovery in a piglet model of pediatric head injury.* Dev Neurosci, 2010. **32**(5-6): p. 466-79.

49. Reimert, I., et al., *Responses to novel situations of female and castrated male pigs with divergent social breeding values and different backtest classifications in barren and straw-enriched housing.* Applied Animal Behaviour Science, 2014. **151**: p. 24-35.

50. Donald, R.D., et al., *Emotionality in growing pigs: is the open field a valid test?* Physiol Behav, 2011. **104**(5): p. 906-13.

51. Herskin, M.S. and K.H. Jensen, *Effects of different degrees of social isolation on the behaviour of weaned piglets kept for experimental purposes.* Animal Welfare, 2000. **9**(3): p. 237-249.

52. Sullivan, S., et al., *Improved behavior, motor, and cognition assessments in neonatal piglets.* J Neurotrauma, 2013. **30**(20): p. 1770-9.

53. Zebunke, M., B. Puppe, and J. Langbein, *Effects of cognitive enrichment on behavioural and physiological reactions of pigs.* Physiol Behav, 2013. **118**: p. 70-9.

54. van der Staay, F.J., et al., *The d-amphetamine-treated Gottingen miniature pig: an animal model for assessing behavioral effects of antipsychotics.* Psychopharmacology (Berl), 2009. **206**(4): p. 715-29.

55. Dantzer, R. and P. Mormede, *[Influence of weaning method on the behavior and the hypophyseal-adrenal axis activity in the piglet].* Reprod Nutr Dev, 1981. **21**(5A): p. 661-70.

56. Ursinus, W.W., et al., *Tail Biting in Pigs: Blood Serotonin and Fearfulness as Pieces of the Puzzle?* PLoS One, 2014. **9**(9).

57. Woodgush, D.G.M. and K. Vestergaard, *The Seeking of Novelty and Its Relation to Play.* Animal Behaviour, 1991. **42**: p. 599-606.

58. Kornum, B.R., et al., *The effect of the inter-phase delay interval in the spontaneous object recognition test for pigs.* Behav Brain Res, 2007. **181**(2): p. 210-7.

59. Ruis, M.A., et al., *Adaptation to social isolation. Acute and long-term stress responses of growing gilts with different coping characteristics.* Physiol Behav, 2001. **73**(4): p. 541-51.

60. Yang, M., J.L. Silverman, and J.N. Crawley, *Automated three-chambered social approach task for mice.* Curr Protoc Neurosci, 2011. **Chapter 8**: p. Unit 8 26.

61. Kaidanovich-Beilin, O., et al., *Assessment of social interaction behaviors.* J Vis Exp, 2011(48).

62. Kristensen, H.H., et al., *The use of olfactory and other cues for social recognition by juvenile pigs.* Applied Animal Behaviour Science, 2001. **72**(4): p. 321-333.

63. McLeman, M.A., et al., *Discrimination of conspecifics by juvenile domestic pigs, Sus scrofa.* Animal Behaviour, 2005. **70**: p. 451-461.

64. McLeman, M.A., et al., *Social discrimination of familiar conspecifics by juvenile pigs, Sus scrofa: Development of a non-invasive method to study the transmission of unimodal and bimodal cues between live stimuli.* Applied Animal Behaviour Science, 2008. **115**(3-4): p. 123-137.

65. Souza, A.S., et al., *A novel method for testing social recognition in young pigs and the modulating effects of relocation.* Applied Animal Behaviour Science, 2006. **99**(1-2): p. 77-87.

66. Siegford, J.M., G. Rucker, and A.J. Zanella, *Effects of pre-weaning exposure to a maze on stress responses in pigs at weaning and on subsequent performance in spatial and fear-related tests.* Applied Animal Behaviour Science, 2008. **110**(1-2): p. 189-202.

67. Wang, B., et al., *Dietary sialic acid supplementation improves learning and memory in piglets.* Am J Clin Nutr, 2007. **85**(2): p. 561-9.

Figure 5.1. Schematic of experimental design. Behavior testing took place over a 10 day period. T-maze acquisition testing occurred on Days 1-6 and T-maze reversal testing occurred on Days 7-10. Open Field (OF) and Object Recognition (OR) testing took place on Days 2 and 7, and Social Recognition (SR) testing took place on Days 3 and 8.

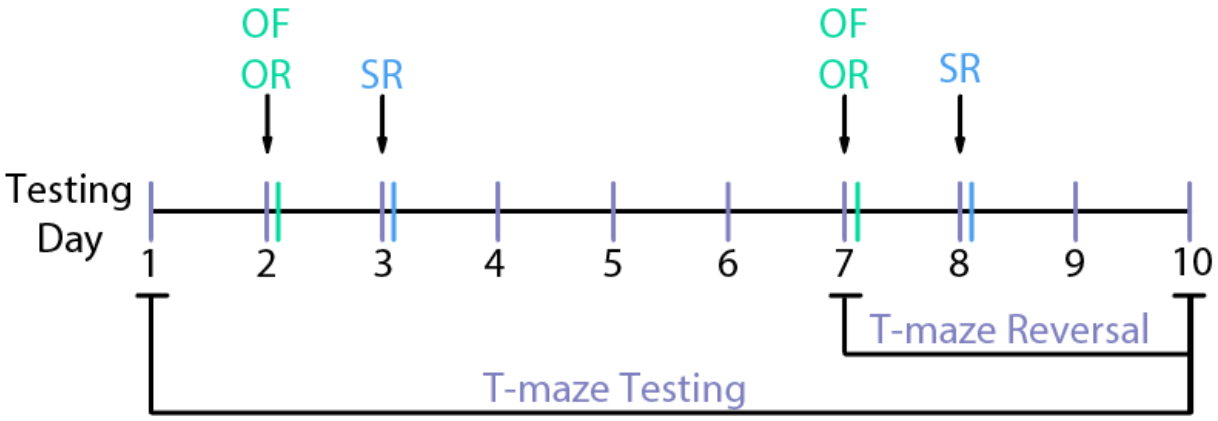
OF
OR
SR
OF
OR
SR
Testing
Day
1
2
3
4
5
6
7
8
9
10
T-maze Reversal
T-maze Testing

Figure 5.2. Photograph and schematic of open field, social recognition, and T-maze arenas. Photograph (**A**) and schematic (**B**) of the open field arena. Photograph (**C**) and schematic (**D**) of the 3 chamber social recognition arena which is comprised of two outer chambers that each contain a social stimulus enclosure as well as a center start/exit chamber. Photograph (**E**) of T-maze depicts a start box in the south and the north arm closed off to restrict access to the north arm. 4 posters were placed around the perimeter of the arena to serve as visual cues. Schematic (**F**) of T-maze arena represents the location of the reward bowls and visual cues as well as the two possible start configurations. In a south start configuration, a removable panel is used to create a start box in the south and a second removable panel closes off the north arm (grey dotted lines). In a north start configuration, a removable panel is used to create a start box in the north and a second removable panel closes off the south arm (red dotted lines).

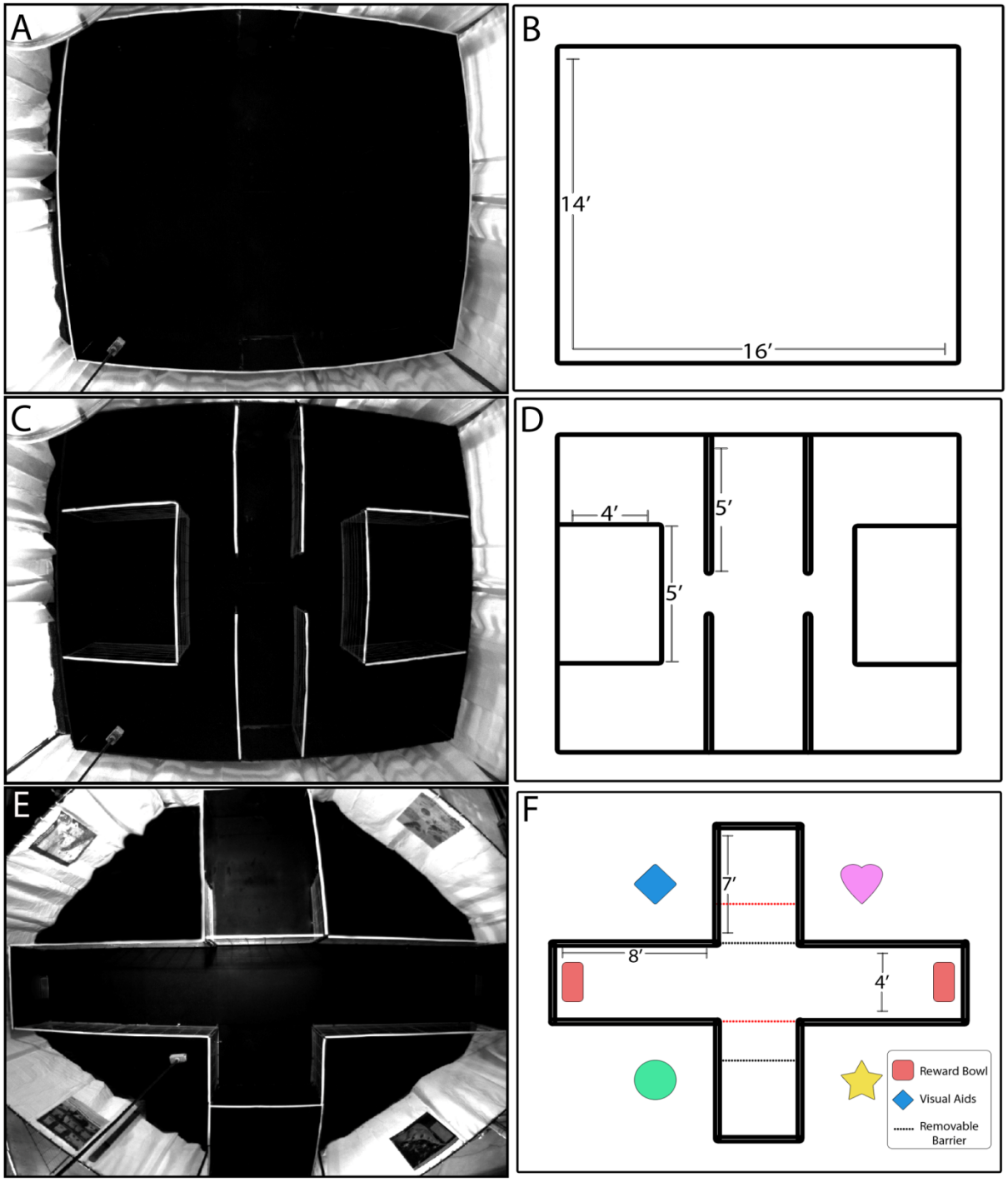
A
B
14′
16′
C
D
4′
5′
5′
E
F
7′
8′
4′
Reward Bowl
Visual Aids
Removable Barrier

Figure 5.3. Piglets demonstrate exploratory behaviors in an open field test. Piglets showed no significant difference in zones entered on Day 2 vs. Day 7 of testing (**A**). Pigs were significantly ($p<0.05$) more stationary than mobile on both Day 2 and Day 7 (**B**). Piglets spent significantly ($p<0.05$) fewer percent epochs sniffing and exploring the open field arena on Day 7 vs. Day 2 (**C**). Pigs generally exhibited fewer escape behaviors on Day 7 vs. Day 2, although not significant (**D**). *= statistically significant difference with a p-value <0.05.

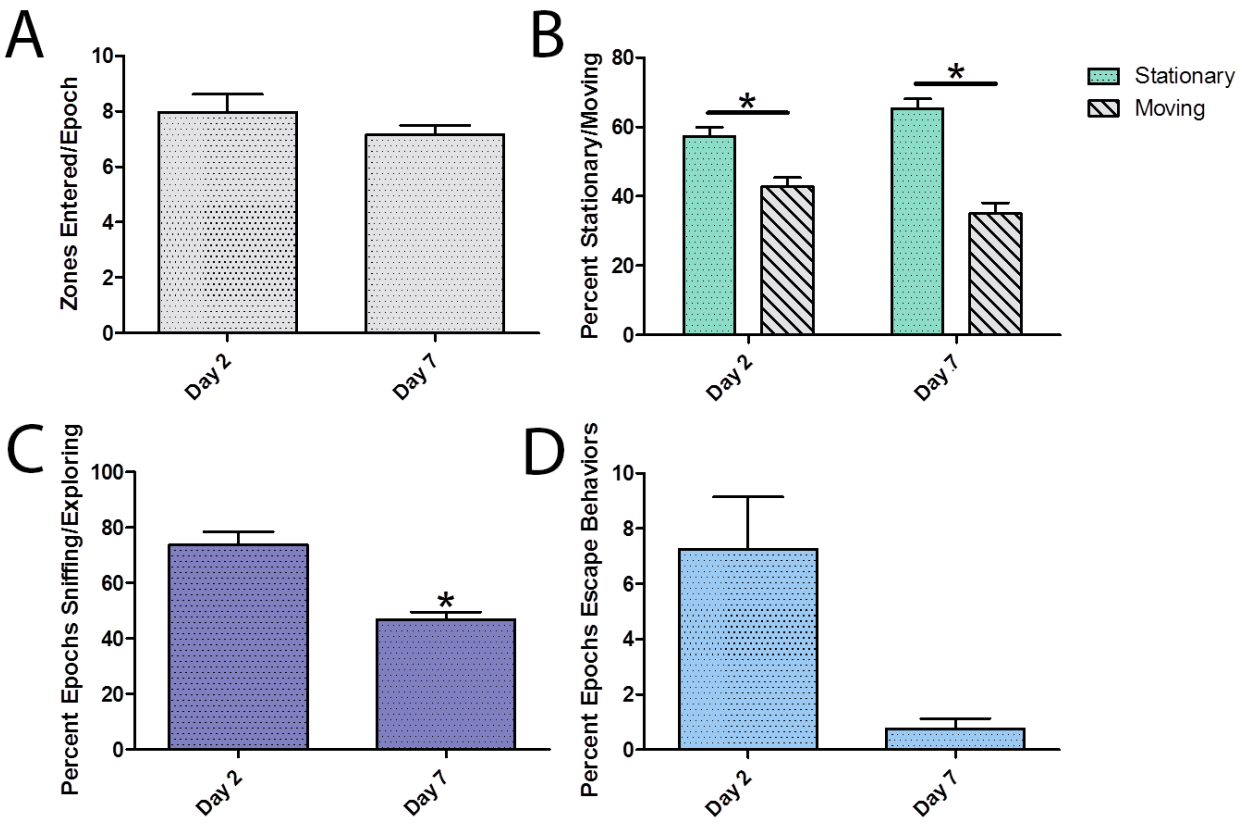
A
Zones Entered/Epoch
10
8
6
4
2
0
Day 2
Day 7
B
Percent Stationary/Moving
80
60
40
20
0
*
*
Day 2
Day 7
Stationary
Moving
C
Percent Epochs Sniffing/Exploring
100
80
60
40
20
0
*
Day 2
Day 7
D
Percent Epochs Escape Behaviors
10
8
6
4
2
0
Day 2
Day 7

Figure 5.4. Piglets demonstrate the ability to form spontaneous object memories of a familiar object. Pigs entered significantly ($p<0.05$) fewer zones in the test trial than the initial habituation trial (**A**). Pigs explored two similar, unfamiliar objects (Objects A and B) equally in the sample trial (**B**). Pigs explored a novel object (Object C) significantly ($p<0.05$) more than a familiar object (Object A') in the test trial (**C**). A comparison of the exploration time of the unfamiliar object (Object A) in the sample trial and of the same object as the familiar object (Object A') in the test trial showed pigs spent significantly ($p<0.05$) less time exploring the familiar object (Object A') (**D**). *= statistically significant difference with a p-value <0.05.

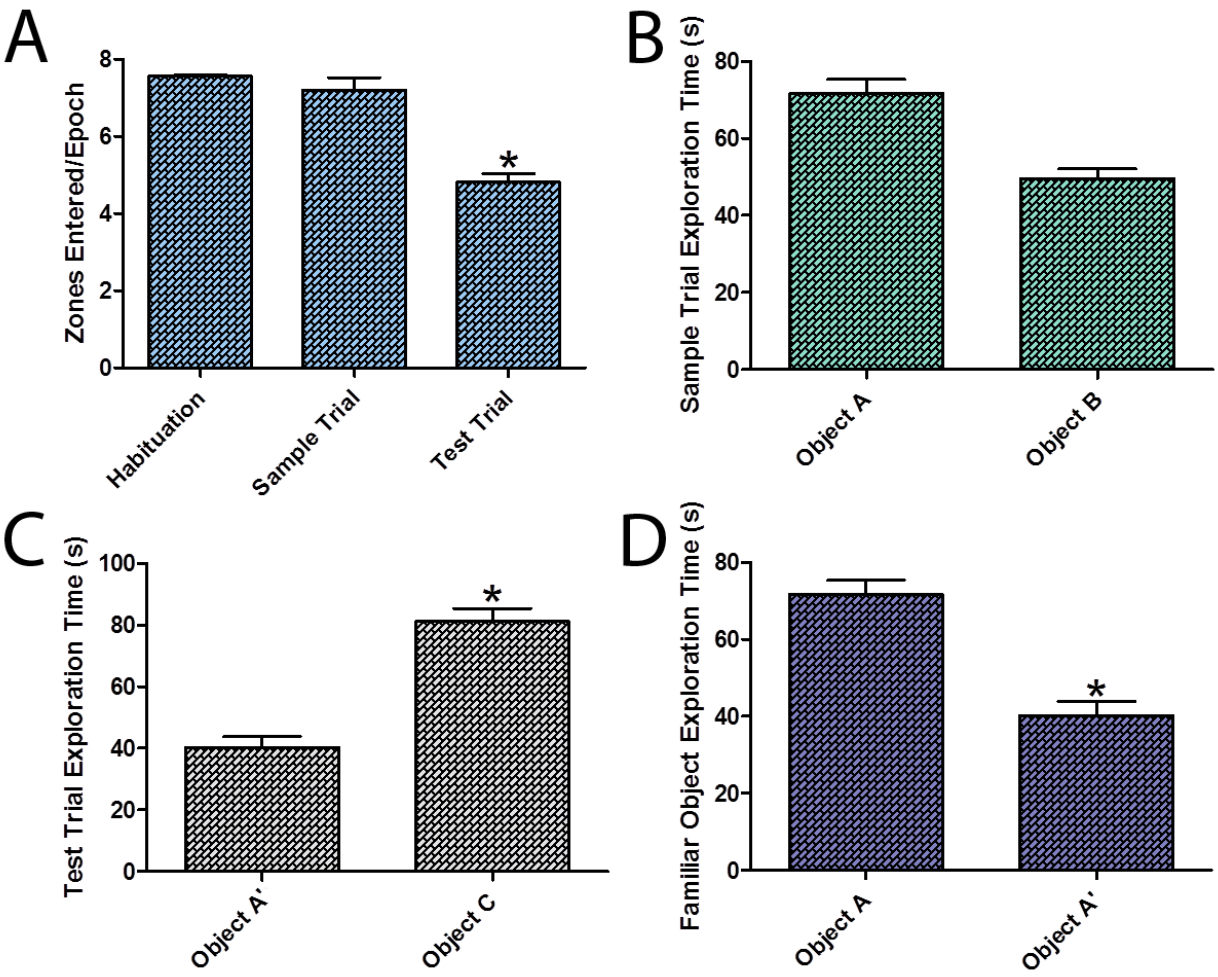
A
Zones Entered/Epoch
0
2
4
6
8
*
Habituation
Sample Trial
Test Trial
B
Sample Trial Exploration Time (s)
0
20
40
60
80
Object A
Object B
C
Test Trial Exploration Time (s)
0
20
40
60
80
100
*
Object A'
Object C
D
Familiar Object Exploration Time (s)
0
20
40
60
80
*
Object A
Object A'

Figure 5.5. Piglets spent significantly more time investigating an unfamiliar pig than a novel object in a sociability trial. In a sociability trial, piglets spent significantly (p<0.01) more time in the unfamiliar pig and object chambers than in the start/exit chamber and spent significantly (p<0.01) more time in the unfamiliar pig chamber than the object chamber (**A**). *= statistically significant difference with a p-value <0.01 when comparing time spent in start/exit chamber to unfamiliar pig and object chambers. #= statistically significant difference with a p-value <0.01 when comparing the time spent in the unfamiliar pig and object chambers. Pigs spent significantly (p<0.01) more time exploring an unfamiliar pig than a novel object, demonstrating pigs inherent inclination to explore a social target (**B**). *= statistically significant difference with a p-value <0.01 when comparing to the time spent in the unfamiliar pig and object chambers.

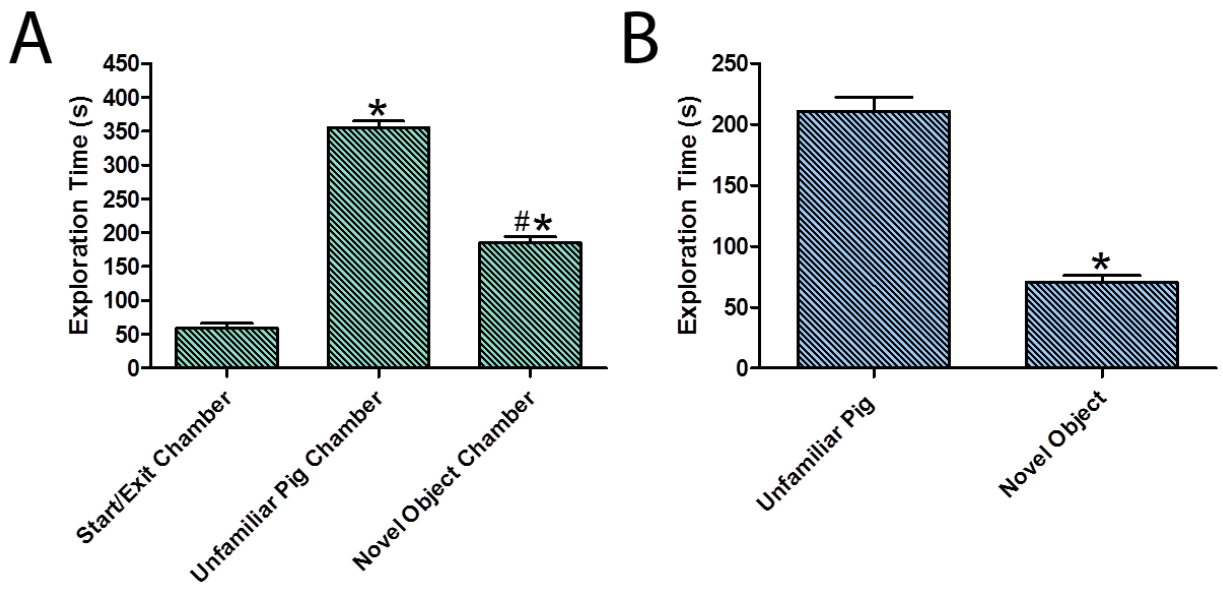
A
Exploration Time (s)
450
400
350
300
250
200
150
100
50
0
*
#*
Start/Exit Chamber
Unfamiliar Pig Chamber
Novel Object Chamber
B
Exploration Time (s)
250
200
150
100
50
0
*
Unfamiliar Pig
Novel Object

Figure 5.6. Piglets spent significantly less time exploring a familiar pig in a social memory trial relative to a sociability trial. In a social memory trial, pigs spent significantly (p<0.01) more time in the novel pig chamber than the start/exit chamber (**A**). *= statistically significant difference with a p-value <0.01 when comparing time spent in the start/exit chamber and novel pig chambers. Pigs generally spent more time with a novel pig than a familiar pig in the social memory trial, although this data only showed trending significance (p=0.10) (**B**). A comparison of the exploration time of the familiar pig in the social memory trial and with the same pig in the previous sociability trial shows that piglets spent significantly (p<0.01) less time exploring the familiar pig in the social memory trial (**C**). *= statistically significant difference with a p-value <0.05 when comparing familiar pig exploration time in sociability and social memory trials.

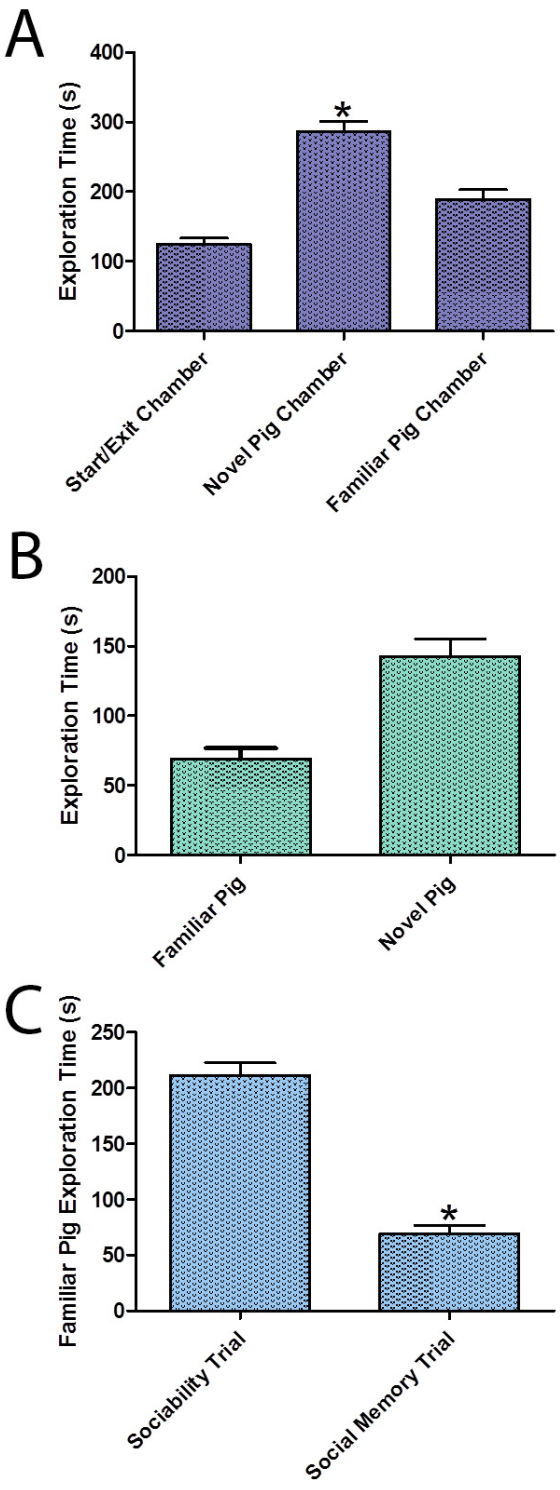
A
Exploration Time (s)
400
300
200
100
0
*
Start/Exit Chamber
Novel Pig Chamber
Familiar Pig Chamber
B
Exploration Time (s)
200
150
100
50
0
Familiar Pig
Novel Pig
C
Familiar Pig Exploration Time (s)
250
200
150
100
50
0
*
Sociability Trial
Social Memory Trial

Figure 5.7. Piglets performed significantly faster and reached a performance criterion of 80% by day 4 of acquisition in a spatial T-maze test. Piglets demonstrated initial low levels of non-compliance the first three days of T-maze testing (**A**). Piglets were significantly ($p<0.01$) faster at navigating the T-maze by Day 4 of acquisition testing (**B**). Pigs reached a performance criterion of at least 80% correct arm choices and made significantly ($p<0.0001$) more correct arm choices by Day 4 of acquisition (**C**). However, after reversal piglets made significantly ($p<0.01$) fewer correct choices on Day 1 of reversal compared to Day 6 of acquisition. Ultimately, piglets significantly ($p<0.001$) improved their performance outcome by Day 4 of reversal testing compared to Day 1 of reversal. *= statistically significant difference with a p-value <0.01 relative to A1 in latency to choice (**B**) and proportion trials correct (**C**). $= statistically significant difference with a p-value <0.01 relative to A6 in proportion trials correct (**C**). #= statistically significant difference with a p-value <0.001 relative to R1 in proportion trials correct (**C**).

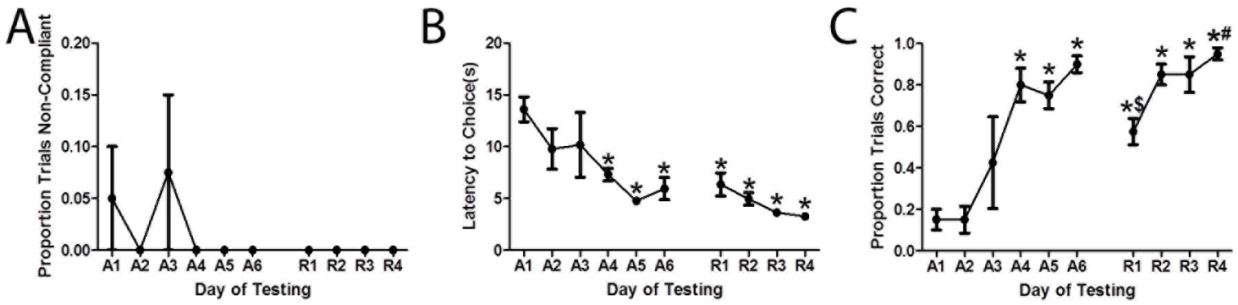
A
Proportion Trials Non-Compliant
0.20
0.15
0.10
0.05
0.00
A1 A2 A3 A4 A5 A6 R1 R2 R3 R4
Day of Testing
B
Latency to Choice(s)
20
15
10
5
0
A1 A2 A3 A4 A5 A6 R1 R2 R3 R4
Day of Testing
C
Proportion Trials Correct
1.0
0.8
0.6
0.4
0.2
0.0
A1 A2 A3 A4 A5 A6 R1 R2 R3 R4
Day of Testing

CHAPTER 6

COGNITIVE, MOTOR FUNCTION, AND HISTOLOGICAL CHANGES IN A PIGLET CONTROLLED CORTICAL IMPACT TRAUMATIC BRAIN INJURY MODEL[1]

[1]Kinder, H.A., Baker, E.W., Howerth, E.W., Wendzik, M.N., Duberstein, K.J., West, F.D. To be submitted to *Journal of Neurotrauma.*

Abstract

Traumatic brain injury (TBI) is a leading cause of death and disability in the United States with children who sustain a TBI having a greater risk of developing long-lasting cognitive, behavioral, and motor function deficits. This has led to increased interest in utilizing more human-like, large animal models to study pathophysiologic and functional changes after injury in hopes of identify novel therapeutic targets. In the present study, a controlled cortical impact (CCI) piglet TBI model was utilized to evaluate cognitive, motor, and histopathologic outcomes. CCI injury (4m/s velocity, 9mm depression, 400ms dwell time) was induced at the parietal cortex. Compared to normal pigs, TBI-affected pigs exhibited appreciable cognitive deficiencies, including significantly impaired spatial memory in spatial T-maze testing and a significant decrease in exploratory behaviors followed by marked hyperactive exploration in open field testing. Additionally, gait analysis revealed significant increases in cycle time and stance percent, significant decreases in hind reach, and a shift in the total pressure index from the front to the hind limb on the affected side; suggesting TBI impairs gait and balance. Lastly, TBI lead to a significant decrease in neurons and a significant increase in microglia activation and gliosis at the perilesional area, a significant loss in neurons at the dorsal hippocampus, and significantly increased neuroblast proliferation at the subventricular zone. These data demonstrate a strong correlation between TBI-induced cellular changes and functional outcomes in our piglet TBI model that lay the framework for future studies that assess the ability of therapeutic interventions to contribute to functional improvements.

Introduction

Traumatic brain injury (TBI) continues to be a leading cause of death and disability in children. Young children between the ages of 0 and 4 have are the age group most likely to sustain a TBI as a result of a concussive injury from a fall and have the highest rate of TBI-related emergency department visits (1,256 per 100,000 population) [1]. Despite the perception that children's brains are potentially more 'plastic' at a younger age, recent research findings suggest that the immature brain may be more vulnerable to early insult [2, 3]. Injury severity plays an important role in neurocognitive outcomes, where mild TBI results in few, if any, cognitive impairments, but moderate to severe TBI can lead to robust and significant impairments in cognition that persist over time [4, 5].

Disruptions in cognition can emerge in the acute and/or chronic phases of TBI [6]. Severe cognitive impairments in young children in the acute phase after TBI have been found to worsen rather than recover over time, suggesting that acute cognitive impairments may be a sensitive predictor of long-term outcomes [7]. Consequently, moderate to severe TBI is thought to disrupt existing neural networks and interfere with normal development, impeding the learning process and putting children developmentally and cognitively behind their peers even years after injury [5]. Similarly, TBI has been found to contribute to impairments in motor function that correlate with injury severity [8, 9]. Although the majority of children who sustain a severe TBI regain independent ambulation, balance and speed of ambulation can remained impaired [10]. Like cognitive deficits, TBI at a young age is not associated with better long-term recovery in gait which may be attributed to disruption of normal developmental processes [10, 11].

Animal models of TBI have played a crucial role in elucidating the pathophysiology and functional outcomes associated with injury. The controlled cortical impact (CCI) model has

gained popularity in recent years because it allows for precise control of injury location and severity, making it an ideal model with which to recapitulate the human condition of a focal TBI [12]. A number of studies have examined cognitive and motor function deficits and associated histological changes in rodents CCI models [13-16]. More recently, interest in juvenile rodent CCI models have expanded in response to recent evidence that that the immature brain may respond differently to injury than the mature brain [17, 18]. Furthermore, TBI in juvenile rats has been shown to lead to cognitive deficits that persist into adulthood [18-20]. Significant credit can be attributed to pre-clinical rodent TBI studies for creating the framework of knowledge of TBI pathophysiology, functional responses, treatment strategies, and therapeutic targets. However, the lack of effective therapies to treat TBI has led to increased interest in utilizing large animal models to study TBI.

The juvenile piglet has been implicated as an ideal model to study the effect of early life insults on neurodevelopment and to study the potential of novel therapeutic interventions [21]. Given its numerous similarities to humans in terms of brain size, growth, time-course of myelination, and innate immunity, the pig has emerged as a front-runner in terms of large animal models [22-26]. As such, a number of recent studies have established the pig as an excellent model of TBI in both adults and juveniles. The piglet brain has been found to have a maturation-dependent response to injury and, similar to human infants, evidence of neuroblast proliferation and migration from the subventricular zone after injury [27-29]. In addition, the pig has been well validated as an excellent model to study cognition and neurobehavioral disorders [30]. Cognitive and gross motor deficits have been observed in a non-impact axial rotation TBI piglet model, but to date, no study has been performed that examines the effects of CCI on cognition or motor function in a piglet model [31, 32].

The purpose of this study was to assess the cognitive, motor, and corresponding histopathologic effects of CCI in a piglet TBI model. For evaluation of cognitive and neurobehavioral deficits after injury, the spatial T-maze test was utilized to measure hippocampal-dependent spatial memory, the 3 chamber social recognition test was used to assess sociability behaviors and social memory, and the open field test was utilized to measure exploratory behaviors after injury. In addition, gait analysis was performed using a GAITFour pressure mat to assess changes in pressure and spatiotemporal gait parameters after TBI. Finally, histopathologic analysis included the evaluation of neuronal cell death, microglia activation, and reactive gliosis in the perilesional cortex, neuronal cell death at the hippocampus, and neuroblast proliferation at the subventricular zone.

Materials and Methods

All work in this study was performed in accordance with the University of Georgia Institutional Animal Care and Use Committee guidelines.

Animals

Two commercially bred pregnant Landrace-cross sows were housed in commercial farrowing crates and farrowed naturally. Each litter was removed from the farrowing crates 2-3 times per day starting immediately after birth for socialization with handlers until weaning. Socialization included holding and stroking the piglets and giving them milk replacer (Sav-a-Calf Grade A Ultra 24 Multispecies Milk Replacer, Milk Products LLC) as a treat. Preliminary studies showed that socialization was critical to reduce anxiety and increase compliance during handling and testing procedures. At weaning (3 weeks of age), 5 male piglets from each litter

were chosen at random, group housed by litter, and fed a nutritionally complete pelleted starter diet ad libitum for the duration of the study. Room temperature was maintained at 26°C with a 12h light/dark cycle and an overhead heat lamp provided supplemental heat.

Experimental Design

Starting at two weeks of age, all piglets were habituated individually on the gait track twice a day to acclimate the piglets to a new environment and to being socially isolated. After weaning at 3 weeks of age, all piglets underwent gait track training for 3-4 days, then baseline gait analysis was collected on 3 separate days before the start of the study. At 4 weeks of age, each litter was randomly assigned to a treatment group- normal control (n=5) or TBI (n=5). At the start of the study, TBI pigs underwent controlled cortical impact (CCI) surgery. Gait analysis was performed 1, 3, 7, 14, and 28 days post-TBI. The Open Field test was performed 1, 7, 14, and 28 days post-TBI. The 3 chamber social recognition test was performed 15 days post-TBI. The spatial T-maze test was performed between 16-25 days post-TBI. Normal controls pigs underwent gait analysis collection, open field, social recognition, and spatial T-maze testing at corresponding time-points, but no TBI surgery was performed at the start of the study. All animals were sacrificed at 28 days for histological analysis of brain tissues.

Surgical Preparation and Controlled Cortical Impact

Piglets were initially anesthetized with 5% vaporized isoflurane mixed with oxygen using a nose cone until non-responsive to stimulation. For the duration of surgery, anesthesia was maintained within 2.5%-3% isoflurane and vitals were monitored every 5-10 minutes. The surgical site was prepared in a routine manner using Betadine and 70% ethanol and covered with

a sterile drape. A 4cm, left-sided incision was made at the top of the cranium to expose the underlying skull. A 20mm craniectomy was performed using an air drill (Brasseler USA; Savannah, GA) at the left posterior junction of the coronal and sagittal sutures to exposure the underlying dura.

Pigs were secured in a controlled cortical impactor device (University of Georgia Instrument Design and Fabrication Shop; Athens, GA) designed specifically for pigs. The impactor tip (15mm diameter) was centered over the exposed dura and a TBI was induced with the following parameters: 4m/s velocity, 9mm depth of depression, and 400ms dwell time. The injury site was flushed with sterile saline and then the overlying skin was re-apposed with surgical suture. Anesthesia was discontinued and piglets were allowed to breath oxygen until recovered. Banamine (2.2mg/kg, MERCK Animal Health; USA) and Butorphanol (0.2mg/kg, Pfizer; New York, NY) were administered for analgesia and Oxytetracycline (19.8mg/kg, Norbrook Inc. USA; Overland Park, KS) was administered as an antibiotic during surgery and for an additional 4 days post-surgery. Once piglets were completely ambulatory, they were placed back in their home pens and monitored daily for health.

Spatial T-maze Test

The design of the spatial T-maze arena and testing procedure was adapted from Elmore et al. [33]. Briefly, a plus-shaped T-maze was constructed using metal grid paneling positioned over black rubber mats (**Figure 6.1A**). North and south arms measured 2.1m x 1.2m and east and west arms measured 2.4m x 1.2m. A white shower curtain encircled the maze to reduce visual distractions and extra-maze environmental cues. Two reward bowls (University of Georgia Instrument Design and Fabrication Shop; Athens, GA) were fixed to the east and west arms.

Reward bowls were filled with equal volumes of milk replacer to provide identical olfactory cues to both arms of the maze. One reward bowl was accessible and could be opened by the pigs using an inherent rooting motion and the other inaccessible reward bowl was secured shut. During initial days of testing, if pigs chose the correct reward bowl but were unable to open the lid, handlers manually opened the lid until the skill was mastered. Extra-maze visual cues (blue rectangle, gray circle, black triangle, red plus-sign) were attached to the white shower curtain. Visual cues were rotated around the arena to account for the location of the reward such that the red plus-sign was always located to the left of the reward, the blue rectangle to the right, the circle to the left of the incorrect reward, and the triangle to the right. In order to allow for alternating starting locations in the north and south arms, removable panels were constructed that could create a start box in the north arm and block off the south arm for "north start" configuration or a start box in the south arm and block off the north arm for a "south start" configuration (**Figure 6.1B**).

Piglets began spatial T-maze testing after a 6 hour food deprivation to increase motivation for the milk replacer food reward. The spatial T-maze test consisted of 6 days of acquisition testing in which the reward was assigned to either the east or west arms and 4 days of reversal testing where the reward arm was moved to the opposite arm. The extra-maze visual cues did not move during reversal testing. The reward location was assigned for each pig by running a spatial bias test on day 1 of acquisition (A1). Pigs underwent 5 trials in which the reward was not accessible in either arm. The reward location was assigned to the arm visited least frequently by the animal to account for potential spatial bias. As such, 8/10 pigs for both TBI (n=4) and normal (n=4) groups exhibited a bias for the west arm and were therefore assigned to the east reward arm. 2/10 pigs for the TBI (n=1) and normal (n=1) groups exhibited a

bias for the east arm and were therefore assigned to the west reward arm. The starting location for each trial alternated from north to south in a pseudo-random order where no pig could start from one arm more than twice in a row. Alternating north and south arms encouraged pigs to solve the task using a hippocampal-dependent, allocentric mechanism whereby pigs use extra-maze visual cues to create spatial memories rather than a striatum-dependent, egocentric mechanism whereby muscle memory plays a role in reward selection, such as always turning the body to the left or right. Pigs underwent 10 trials per day and had a maximum of 60 seconds to reach the reward. If the pig exceeded 60 seconds without choosing a reward, the pig was deemed non-compliant for that trial. For the first two days, if the pigs chose the incorrect arm they were corrected and taken to the correct arm. After two days, if the pigs chose the incorrect arm, they were returned to the start box for the next trial without any reward. Between each trial, any defecation and/or urination was removed and the entire arena was wiped down with 70% ethanol to remove any olfactory cues from trial to trial. In addition, the starting boxes were blacked out such that the pigs were unable to see the handlers refill the reward bowl between trials. An automatic tracking software (EthoVision, Noldus; Wageningen, The Netherlands) was used to measure latency to choice and proportion trials correct. Latency to choice was started manually once the removable panel was opened in the start box and automatically stopped once the piglet's nose-point entered a zone around a reward bowl, whether correct or incorrect. Proportion trials correct was measured as the proportion correct/total trials. The entire maze was cleaned between each pig to reduce olfactory bias.

3 Chamber Social Recognition Test

The 3 chamber social recognition arena was constructed using metal grid paneling positioned over black rubber mats and is comprised of 3 chambers (**Figure 6.1C**). The center chamber is the start/exit chamber made up of 2 panels attached to the north wall of the arena and 2 panels attached to the south wall of the arena, each 1.5m in length. Both the north and south walls of the start/exit chamber contain doors that allow the pigs to enter/exit at alternating locations of arena. Two openings in the start/exit chamber lead into the two outer chambers. Each outer chamber contains a smaller social stimulus box (1.5 x 1.2m) that can hold a single stimulus pig (**Figure 6.1D**). The bars of the social stimulus box allowed nose contact between the test and stimulus pigs, but prevented direct social interactions that might lead to aggression. Stimulus pigs were of identical age, were from a separate litter, and had not seen or interacted with the test piglets previously. Stimulus pigs (n=5) used for TBI pigs were different from stimulus pigs (n=5) used for normal control pigs. All stimulus pigs were randomized such that each pig was an unfamiliar pig, familiar pig, and novel pig throughout all trials to reduce a possible novelty affect where one pig could potentially be more memorable than the others. In addition, in lieu of a social stimulus pig, a novel object could be securely attached to the front of either social stimulus box to measure object exploration. 5 different objects were randomly assigned to TBI and to normal control pigs. No object bias for any objects used in this test were found (data not shown). White curtains were hung around the maze to reduce visual distractions during testing**.**

The 3 chamber social recognition test was comprised of three separate trials: habituation, sociability trial, and social memory trial. In the habituation trial, piglets were placed into the start/exit chamber at either the north or south start locations and given 10 minutes to freely

explore the arena. For the sociability trial, piglets were briefly removed from the arena while an unfamiliar stimulus piglet was placed into a social stimulus enclosure and a novel object was attached to the front of the opposing social stimulus box. The pigs were then placed back into the arena and allowed to explore the arena, the unfamiliar stimulus pig, and the novel object freely for 10 minutes. For the social memory trial, the pigs were removed from the arena for an inter-phase interval of 10 minutes. The novel object was removed and a novel stimulus pig was brought into the arena and placed into a social stimulus box. The unfamiliar pig from the sociability trial remained in the arena and thus became a familiar pig for the social memory trial. The test piglets were then placed back into the arena for an additional 10 minutes and allowed to explore the arena, the familiar pig, and the novel pig for 10 minutes. The location of the unfamiliar pig, novel object, and familiar pig alternated between east and west chambers for the sociability and social memory trials between animals. The automatic tracking software EthoVision was used to measure the amount of time spent with the unfamiliar pig and novel object in the sociability trial and the amount of time spent exploring the novel pig and familiar pig in the social memory trial. Time spent exploring a stimulus pig in either the sociability or social memory trials was measured as the time at which the nose-point of the test pig was in the zone immediately surrounding the social stimulus box. The time spent exploring a novel object was measured as the time during which the nose-point of the test pig was in the zone surrounding the novel object. Any urination or defecation in the arena was wiped down with 70% ethanol between each trial as necessary to reduce olfactory bias. The arena was wiped down with 70% ethanol between each pig as well to reduce olfactory cues across pigs.

Open Field Test

The open field arena measures 4.3x 4.9m and was constructed using metal grid paneling positioned over black rubber mats (**Figure 6.1E-F**). White curtains were hung around the maze to reduce visual distractions during testing. For the open field test, pigs were placed into the arena from alternating north and south start/exit gates and allowed to freely explore the arena for 10 minutes. The exploratory behaviors distance traveled and velocity of the center point of the pig were measured using the automatic tracking software EthoVision for the duration of the test.

Gait Analysis

The gait analysis track was constructed of metal grid paneling with an adjustable, straight chute approximately 6.7m x 0.5m with circular turn around pens at either end approximately 2.1m in diameter, giving the track a "dog bone" shape. A gait pressure mat (GAITFour, CIR Systems Inc, Franklin, NJ) was placed down the length of the chute and covered with a protective no-slip, adhesive mat. After approximately one week of individual acclimation to the gait track, pigs were trained to travel back and forth across the track at a consistent pace using milk replacer as a reward. Two handlers, one in each of the holding pens, rewarded the pig if the animal crossed the entire length of the mat at a consistent 2-beat trotting gait without stopping or breaking into a run (or 3-beat gait) until 5 valid runs were collected. The pressure mat recorded the footfalls of the pig as it traveled across the mat and calculated the following spatial-temporal and pressure gait biomechanical parameters: cycle time (time elapsed between the first two contacts of two consecutive limb strikes of the same limb, i.e. left front to left front), stance percent (percentage of time spent in stance phase of one stride cycle), hind reach (distance from the heel center of the hind limb to the heel center of the previous front limb on the same side),

and total pressure index (TPI) (the percent of weight distribution across all four limbs, where most quadrupeds carry 60% of their weight on their forelimbs and 40% of their weight on their hind limbs).

Histology

Pigs were euthanized at 28 days. After euthanasia, brains were removed and fixed whole in 10% buffered formalin for immunohistochemical analysis. After fixation, brains were sectioned into 5mm slices using a coronal pig-specific brain sectioner. Slices with both injured cortex and dorsal and ventral hippocampus at approximately the same level were routinely processed, embedded in formalin, and stained with antibodies specific for NeuN (Millipore, 1:500), GFAP (Biogenex, 1:4000), Iba1 (Wako, 1:8000), and doublecortin (DCX; Abcam, 1:2000). Heat induced antigen retrieval was performed for all antibodies using citrate buffer at pH6 (DAKO). Detection was performed utilizing biotinylated antibodies and a streptavidin label (4plus Streptavidin HRP, Biocare) followed by an HRP label and DAB chromagen (DAKO). All sections were lightly counterstained with hematoxylin. Microscopic inspection and imaging was performed on a Nikon Eclipse TE300 inverted microscope utilizing SPOT Imaging v5.2 software (Sterling Heights, MI) at the perilesional area at 200X, at the dorsal polymorphic layer of the dentate gyrus at 200X, and at 5 consecutive fields at the ventricular subventricular zone (vSVZ) at 20X. For quantification, a region of interest (ROI) was drawn around the perilesional area and the polymorphic layer of the dentate gyrus and NeuN+ cells were manually counted using the cell counter plugin on ImageJ 2.0 and expressed as cells/mm^2. For semiquantitative analysis of GFAP and Iba1, the total area of immunoreactivity corresponding to increased optical density was measured by ImageJ software at the perilesional area. Finally, a ROI was drawn around the

vSVZ and DCX+ neuroblasts were manually counted using ImageJ 2.0 and expressed as cells/mm^2.

Statistics

For the spatial T-maze test, open field test, and gait analysis, data analysis was conducted using the proc MIXED procedure as a two way (treatment x day) repeated measures ANOVA using Statistical Analysis software (SAS Version 9.1; Cary, NC). Post-hoc comparisons using Pdiff were made to further examine significant effects. For the social recognition test and histological analysis, data analysis was conducted using a two-tailed T-test with SigmaPlot. Statistical significance was accepted at $p<0.05$ and statistical trends at $p<0.10$. Data are presented as mean ± standard error.

Results

TBI-affected piglets exhibit spatial memory deficits in a spatial T-maze test.

Spatial T-maze testing was initiated 16 days post-TBI. On acquisition day 1 (A1), both normal and TBI-affected piglets were unfamiliar with the maze and thus exhibited a longer latency to choice indicative of a lengthier, less direct track to the reward bowl (**Figure 6.2A**). However, latency to choice was significantly ($p<0.05$) reduced by A2 for normal and TBI-affected animals (**Figure 6.2A-B**). Latency to choice continued to decrease throughout acquisition and remained unaffected by reward reversal for normal and TBI-affected animals (**Figure 6.2B**). For proportion trials correct, TBI-affected piglets made significantly ($p<0.05$) fewer correct reward choices than normal piglets from A1 through A4 (**Figure 6.2C**). In addition, compared to the first day of testing on A1, normal piglets made significantly ($p<0.05$)

more correct choices by A2, while TBI-affected piglets took one day longer and made significantly more correct choices on A3 (**Figure 6.2C**). Both normal and TBI-affected pigs showed a temporary significant ($p<0.05$) decrease in correct choices on reversal day 1 (R1). Together, this data suggests that TBI leads to spatial memory deficits that affect acquisition of the reward location in a spatial T-maze.

TBI-affected piglets show disruptions in sociability behaviors and social memory formation in a 3 Chamber Social Recognition Test

Pigs were tested in a 3 chamber social recognition test on day 15 post-TBI. In sociability trials, both normal and TBI-affected pigs exhibited a strong preference for an unfamiliar pig over a novel object. However, TBI-affected piglets overall spent less time with the unfamiliar pig than the novel object compared to normal controls (0.875 ± 0.034 vs. 0.950 ± 0.014, respectively), but significance was trending ($p=0.079$) (**Figure 6.3A-B**). In social memory trials, normal pigs spent more time with the novel pig than the familiar pig while TBI-affected pigs spent more time with the familiar pig than the novel pig (0.592 ± 0.121 vs. 0.444 ± 0.140, respectively), however there was no significant difference between treatment groups (**Figure 6.3A,C**). This data suggests that TBI may potentially disrupt sociability and social memory behaviors, but no significant effects on these behaviors were detected.

TBI-affected piglets show reduced exploration immediately after TBI followed by a period of hyperactivity in an open field test.

Piglets were tested in an open field test 1 day, 7 days, 14 days, and 26 days post-TBI. TBI-affected piglets traveled significantly ($p<0.05$) less distance 1 day post-TBI compared to

normal controls (**Figure 6.4A-B**). Normal pigs showed the highest exploration and traveled the greatest distance on day 1, and, as expected, became habituated to the testing arena (**Figure 6.4A**). As a result, distance traveled generally decreased over time and was significantly ($p<0.05$) reduced by day 14 (**Figure 6.4B**). However, for TBI-affected pigs, distance traveled generally increased over time and was significantly ($p<0.05$) increased by 26 days post-TBI (**Figure 6.4A-B**). Similarly, TBI-affected piglets moved at a significantly ($p<0.05$) slower velocity 1 day post-TBI compared to normal controls (**Figure 6.4C**). Normal pigs showed the highest interest in their environment and greatest velocity on day 1 that generally decreased over time and was significantly ($p<0.05$) reduced by day 14 (**Figure 6.4C**). However, for TBI-affected pigs, velocity generally increased over time and was significantly ($p<0.05$) greater on days 14 and 26 post-TBI compared to 1 day post-TBI. Additionally, the velocity of TBI piglets was significantly ($p<0.05$) higher than normal pigs 14 days post-TBI (**Figure 6.4C**). This data suggests that TBI leads to an immediate decrease in exploratory behaviors that is followed by a period of hyperactivity in the weeks following TBI.

TBI-affected piglets demonstrate transient deficits in gait, evident by increased cycle time and stance percent

Changes in the gait parameter cycle time was assessed by comparing each time-point to pre-TBI for the left front, right front, left hind, and right hind limbs. TBI-affected pigs showed a significant ($p<0.05$) increase in cycle time in all limbs 1 and 3 days post-TBI compared to pre-TBI and a significant increase in cycle time 1 day post-TBI compared to normal controls for all limbs (**Figure 6.5A-D**). No change in cycle time was observed on days 1 and 3 in normal control pigs compared to pre-TBI, however from days 7 through 28 a significant increase in cycle time

was observed for all limbs that is indicative of normal changes associated with growth of the pig (**Figure 6.5A-D**). TBI-affected animals showed normal changes in cycle time at 7 and 14 days post-TBI for all limbs, but no significant change in cycle time was observed 28 days post-TBI, likely as a result of an overall preference for TBI-affected pigs to move at a faster velocity than normal animals at this time-point (**Figure 6.5A-D**).

Changes in the gait parameter stance percent was assessed by comparing each time-point to pre-TBI for the left and right front limbs. TBI-affected pigs showed a significant ($p<0.05$) increase in stance percent 1 and 3 days post-TBI compared to pre-TBI for the left and right front limbs (**Figure 6.5E-F**). In addition, a significant ($p<0.05$) increase in stance percent was observed 1 day post-TBI for the left front limb and 1 and 3 days post-TBI compared to normal controls for the right front limb (**Figure 6.5E-F**). Similar to cycle time, no change in stance percent was observed on days 1 and 3 in normal control pigs compared to pre-TBI, however from days 7 through 28 a significant ($p<0.05$) increase in stance percent was observed for the left and right front limbs that is indicative of normal changes associated with growth of the pig (**Figure 6.5E-F**). TBI-affected animals showed normal changes in stance percent on 7 and 14 days post-TBI for all limbs, but no significant change in stance percent was observed 28 days post-TBI, likely as a result of an overall faster velocity than normal animals at this time-point (**Figure 6.5E-F**). This data suggests that TBI contributes to transient changes in cycle time and stance percent that alter normal gait.

TBI-affected piglets demonstrate transient gait impairments that result in increased hind reach and a shift in weight carriage from the front to the hind contralateral limb.

Changes in the gait parameter hind reach, which provides a measure of pig stability and balance, was assessed by comparing each time-point to pre-TBI for the left and right hind limbs. TBI-affected animals showed a significant ($p<0.05$) increase in hind reach 1 and 3 days post-TBI compared to pre-TBI for the left and right hind limbs (**Figure 6.6A-B**). In addition, a significant ($p<0.05$) increase in hind reach was observed 1 day post-TBI for the left hind limb and 1 and 3 days post-TBI compared to normal controls for the right hind limb (**Figure 6.6A-B**). No change in hind reach was observed on days 1, 3, and 7 in normal control pigs compared to pre-TBI, however from days 14 through 28 a significant decrease in stance percent was observed for the left and right hind limbs that can be attributed to growth of the pig (**Figure 6.6A-B**). TBI-affected animals show normal changes in hind reach 7, 14, and 28 days post-TBI for the left hind limb, but at 14 days post-TBI hind reach was significantly reduced for the right hind limb compared to normal control pigs. Changes in right hind reach returned to normal by 28 days post-TBI (**Figure 6.6A-B**).

Changes in the gait parameter TPI was assessed by comparing each time-point to pre-TBI for the left front, right front, left hind, and right hind limbs. A significant ($p<0.05$) decrease in TPI in the right front and a corresponding significant ($p<0.05$) increase in TPI in the right hind was observed 1 day post-TBI compared to pre-TBI, and no change in TPI was observed in the left front or hind limbs (**Figure 6.6C-F**). Although significant ($p<0.05$) changes in TPI are observed in the right front limb starting at 7 days but not in the left limb until 28 days in normal pigs, overall, TPI appears to decrease in the both front limbs over time as the animal ages (**Figure 6.6C-F**). Furthermore, significant ($p<0.05$) changes in TPI are observed in the left hind

limb starting at 7 days but not in the right hind limb until 28 days in normal pigs, thus overall, TPI appears to increase in both hind limbs over time (**Figure 6.6C-F**). This data suggests that hind reach on the contralateral right side may be affected for up for 14 days post-TBI but that changes in TPI are transient and affect weight carriage only immediately after TBI.

TBI leads to neuronal loss at the perilesional area and the hippocampus, increased microglial activation and astrogliosis, and proliferation of neuroblasts at the subventricular zone.

Parenchymal tissues were assessed for cellular changes at the perilesional site, hippocampus, and vSVZ 28 days after TBI. A significant ($p<0.05$) loss of NeuN+ neurons was detected at the perilesional site for TBI-affected pigs compared to normal control pigs (51.055 ± 13.129 cells/mm^2 vs. 94.907 ± 4.272 cells/mm^2, respectively, **Figure 6.7A-C**). In addition, a significant ($p<0.05$) loss of NeuN+ neurons were observed at the polymorphic layer of the dorsal dentate gyrus in TBI-affected pigs compared to normal control pigs (44.369 ± 2.154 cells/mm^2 vs. 52.901 ± 1.943 cells/mm^2, respectively, **Figure 6.7D-F**). A significant ($p<0.05$) increase in Iba1+ microglia was observed at the perilesional site in TBI-affected pigs compared to normal control pigs (25.211 ± 3.218 cells/mm^2 vs. 16.353 ± 1.306 cells/mm^2, respectively, **Figure 6.7G-I**). There was a significant ($p<0.05$) increase in GFAP+ astrocytes at the perilesional site in TBI-affected pigs compared to normal control pigs (36.217 ± 5.736 cells/mm^2 vs. 17.880 ± 2.279 cells/mm^2, respectively, **Figure 6.7J-L**). Finally, significant ($p<0.05$) recruitment in DCX+ neuroblasts was observed at the vSVZ in TBI-affected pigs compared to normal control pigs (2.136 ± 0.306 cells/mm^2 vs. 0.937 ± 0.239 cells/mm^2, respectively, **Figure 6.7M-O**). Taken together, this data suggests that TBI contributes a number of cellular changes at the perilesional site as well as at more remote zones such as the hippocampus and vSVZ.

Discussion

In the present study, we have shown that experimental TBI using CCI in a piglet model induces cognitive, motor, and histopathological deficits pathologically consistent with features found in human patients. TBI-affected piglets exhibited spatial memory deficits, evident by an impaired ability to locate a food reward in a spatial T-maze test. Trending evidence of disruption of normal sociability and social memory behaviors was observed in TBI-affected pigs in a 3 chamber social recognition test. In an open field test, TBI-affected pigs showed reduced exploratory behaviors immediately after TBI that was followed by a period of hyperactivity that persisted over time. In addition, transient gait impairments in cycle time, stance percent, hind reach, and TPI were observed between 1-3 days post-TBI. Histological analysis revealed loss of neurons in the cortex and hippocampus, an increase in microglia activation and astrogliosis, and stimulation of endogenous neuroblast populations at the SVZ. To our knowledge, this is the first report that uses a piglet CCI model to quantitatively measure histopathological changes and functional deficits using a comprehensive battery of behavior tests and gait analysis.

In this study, pigs performed a spatial T-maze test, originally adapted from rodents for pigs by Elmore et al., to measure spatial memory deficits [33, 34]. This test has been well validated as a means to measure early life insults on cognition, specifically hippocampal-based spatial memory formation in pigs [33, 35-37]. This is important to study because children who sustain a severe TBI have shown evidence of spatial learning and cognitive mapping deficits initially after TBI and even 4 years later [38, 39]. The spatial T-maze test was performed 16 days post-TBI to avoid potential confounds with motor function deficits in the first days after injury [15]. All pigs acquired the “rules” of this task exceedingly fast; both normal and TBI-affected pigs showed similar significant improvements in latency to choice as soon as A2.

Motivation for seeking the reward was high given that milk replacer had been used previously as a reward for gait analysis training and the animals were feed restricted the night prior to testing. Latency to choice continually decreased for all pigs throughout acquisition testing and remained mostly unchanged after reward reversal. These results suggest that both normal and TBI-affected animals easily acquired how to navigate the maze to seek a reward. However, TBI-affected pigs showed significant impairments in choosing the correct reward location. For the first 4 days of acquisition testing, TBI-affected pigs performed significantly worse than normal animals, making significantly fewer correct reward choices. Within treatment groups, normal pigs made significantly more correct choices compared to the first day of testing as soon as A2, quickly learning how to navigate the maze to seek the correct reward. On the contrary, TBI-affected animals took until A3 to make significantly more correct choices compared to the first day of testing. The underlying principle of this test assesses the pigs' ability to use a spatial memory-based, allocentric mechanism to learn location of a fixed reward, despite alternating the starting position between trials, by using extra-maze cues [33, 40, 41]. Allocentric navigation is hippocampal-based and is characterized by the ability to navigate using distal cues. This is in contrast to egocentric navigation which is striatal-based and is characterized by the ability to navigate using internal cues [42]. This type of navigation is employed in standard T-maze tests without alternating starting positions. Taken together, we show that, compared to normal controls, TBI impedes allocentric navigation and spatial memory formation in a spatial T-maze test.

Children affected by moderate to severe TBI are also at risk for social impairment [43]. Social participation, or the intensity of participation in social activities, has been found to be vulnerable to TBI [44]. In addition, TBI at a young age may lead to impairments in recognition

memory such as facial recognition memory [45]. Evidence of long-term social dysfunction after pediatric TBI has garnered recent interest in incorporating social behavior tests in experimental animal models of brain injury [46-48]. Here, we report the use of a 3 chamber social recognition test to assess sociability behaviors and social memory after TBI. To our knowledge, this is the first time this test has been utilized to assess social behaviors in a pig or piglet TBI model. We found trending evidence of diminished sociability behaviors. TBI-affected pigs showed a preference for an unfamiliar pig over a novel object, but compared to normal control pigs, social preference for the unfamiliar pig was diminished, although significance was not reached. TBI-affected pigs on average spent more time with the familiar pig than the novel pig, suggesting social memory impairments, but significance was not reached. Our results differ from Semple et al. who also utilized a 3 chamber social recognition test to assess sociability behaviors and social memory after TBI in juvenile mice over time [49]. Sham and TBI mice showed a comparable preference for sociability and no social memory deficits during adolescence. However, differences in species, injury severity, or injury location could also account for differences between studies. In addition, social processing is highly complex, involving numerous brain structures that together help shape social behavior [50]. The hippocampus has been implicated in mediating social recognition [51]. Hitti et al. found that the hippocampal CA2 region plays a functional role in social memory [52]. However, further studies are needed to fully elucidate the role of the hippocampus and other brain structures in social memory formation.

Evaluation of the effect of TBI on open field testing revealed an initial reduction in exploratory behaviors 1 day post-TBI followed by marked hyperactive exploration in the weeks after TBI. Characteristic hyperactivity behaviors, increased velocity and distance traveled, were elevated starting at 7 days post-TBI and reached significance by 14 and 28 days post-TBI,

respectively. This is in contrast to normal animals who showed a marked decrease in distance traveled and velocity over time, indicative of a habituation effect due to repeated testing [53]. A decrease in exploratory behaviors immediately after TBI has been reported in other experimental animal models [54-56]. These changes may be attributed to anxiety or depressive symptoms, or a loss in exploratory interest [18, 57]. Increased hyperactive exploration of the open field arena is frequently reported in rodent CCI studies at the parietal cortex [16, 58-61]. Although the precise mechanism of TBI contribution to a hyperactive phenotype has not yet been fully elucidated, a study by Li et al. suggested that deficits in spatial and working memory reflect impairments in habituation and the ability to form and retrieve spatial maps, leading to hyperactivity [62]. Furthermore, the parietal cortex and dorsal hippocampus, both regions affected in this study, have been shown to be part of a complex control system that modulates and suppresses a basally hyperactive locomotor tone [63]. Disruption to this system by TBI would therefore lead to increased locomotor activity. Clinically, human patients often display depressive symptoms shortly after sustaining a TBI that may coexist with anxiety disorders [64, 65]. Children who sustain a TBI at a young age are three times more likely to develop attention-deficit hyperactivity disorder (ADHD) than their peers [66]. Behavioral problems and disorders that often accompany pediatric TBI continue to be both prevalent and long-term problems in affected individuals, highlighting the need for additional studies that further define TBI-induced behavioral changes [67].

Currently, no studies have correlated cognitive deficits to hippocampal histopathology in pigs after CCI. Here we report a loss of NeuN+ neurons in the dorsal polymorphic layer of the dentate gyrus. The polymorphic layer of the dentate gyrus is comprised of a number of different neuronal cell types that give rise to ipsilateral associational projections that innervate the

molecular layer as well as commissural projections that innervate the contralateral polymorphic layer [68]. Disruption of mossy fibers or neurons within the polymorphic layer can result in disruption of normal hippocampal function [69]. Therefore, TBI, likely as a result of mechanical energy transfer at the time of injury or through secondary injury mechanisms, may interrupt normal dentate gyrus function, leading to cognitive impairments [70].

In particular, the dorsal dentate gyrus showed a deleterious response with a significant loss of neurons post-TBI. Recent evidence suggests that there may be a gradient of function in the hippocampal long axis [71]. The ventral (or anterior hippocampus in humans) has been implicated in episodic-memory formation and emotional processes and the dorsal (or posterior hippocampus in humans) has been implicated in spatial memory formation [34, 72-74]. Insults to the dorsal hippocampus as a result TBI have been found to result in spatial memory deficits that are dependent on injury severity [75]. A number of adult and juvenile rodent TBI studies have correlated spatial memory deficits with histological analysis of the dorsal hippocampal region, noting loss of neurons [14], morphological changes [76], synaptic reorganization [17], and a reduction in hippocampal volume [15, 19, 20, 77].

Children who sustain a TBI at a young age are also at risk for acquiring motor function deficits, particularly those relating to balance and gait [78]. Analysis of spatiotemporal gait variables in children after TBI have shown an increase in step cycle time and a corresponding decrease in gait velocity [9, 11]. In this study, pigs showed a similar increase in cycle time in all limbs 1 and 3 days post-TBI compared to normal control pigs. A corresponding increase in stance percent for left front limb 1 day post-TBI and 1 and 3 days post-TBI for the right limb was observed. Reports of changes in stance percent are varied in children, with some studies reporting no change in overall stance percent and others that show an increase in stance percent

in the unaffected limb (ipsilateral to TBI) but no change in stance percent in the affected limb [9, 79]. Here, stance percent is increased overall in both front limbs, but compared to normal controls, stance percent in the right, affected limb was more prominently altered than the left, unaffected limb. Pigs are quadrupeds as opposed to bipeds, therefore variations in gait may account for these differences. Duberstein et al. showed that, contrary to stroke patients, stroked pigs exhibited increased stance percent of the affected limb and suggested this may be due to either lack of propulsive forces of the affected limb or an effort to maintain ground contact of the affected limb in order to better stabilize weight distribution on the affected side [80].

TBI-affected pigs also showed an increase in hind reach for the left and right hind limbs 1 and 3 days post-TBI coupled with a decreased in TPI in the right front limb and a corresponding increase in TPI in the right hind limb 1 day post-TBI. These results suggest that TBI-affected pigs brought their hind limbs more underneath of their body, tracking up closer to their front limbs, and in conjunction, shifted their weight from the front to the hind limbs on the affected side, likely in an effect to better stabilize their gait and improve balance. Recently, rodent TBI studies utilizing a Catwalk imaging method have found similar responses in stance percent, relative paw placement (hind reach), and intensity (TPI) acutely but not long-term [81-83]. Here we report only transient gait deficits that persist for only a few days after TBI, likely a result of TBI location and severity. A recently study by Schwerin et al. observed only early gait deficits in ferrets after severe CCI injury to the somatosensory cortex, which they note is separate from but intimately connected with the motor cortex and could explain transient, but not long-term motor function deficits [56]. Liu et al. acknowledged the disadvantage of traditional CCI models with restricted spatial acuity and thus developed a semicircular CCI model in which a semicircular

impactor tip covered both the motor and somatosensory cortices and was able to elicit both long-term motor and cognitive deficits in mice [15].

A small number of pig CCI studies have both qualitatively and quantitatively analyzed immunohistological changes after TBI. Duhaime et al. described cell loss at the lesion site and gliosis adjacent to the lesion [27]. Manley et al. showed loss of MAP-2+ and NeuN+ neurons and an increase in Fluoro-Jade B+ degenerating neurons near the injury site [84]. Only one group has performed behavior and motor function tests in a piglet TBI model, however TBI was induced using a closed head rotational injury, and histological analysis consisted of quantitative analysis of axonal injury area indicated by positive β-amyloid precursor protein (β-APP) staining [32, 85, 86]. Here we show a loss of NeuN+ neurons and an increase in Iba1+ and GFAP+ area at the perilesional site. These results are consistent with reports from other experimental CCI studies [14, 56, 87, 88]. Cell loss following both experimental and clinical TBI has been correlated with poor prognosis and cognitive deficits [89]. In addition, astrocyte and microglial dysfunction following TBI can secrete pro-inflammatory cytokines that can alter synaptic plasticity mechanisms, contributing to functional deficits like memory loss or motor function deficits [90, 91]. Lastly, we observed a significant increase in DCX+ neuroblasts at the vSVZ following TBI. Costine et al. was the first to identify the neurogenesis of DCX+ neuroblasts at the SVZ in a TBI piglet model and note that the long-term outcomes of alterations in normal neuroblast migration are unknown, but that they could potentially play role in repair or remodeling mechanisms in the developing brain [28].

Conclusion

We have developed a clinically relevant piglet TBI model that demonstrates functional deficits with corresponding histological changes. Neuronal loss at the hippocampus and cortex and presence of astrogliosis and microglia activation at the perilesional site suggest a possible mechanism for the progression of cognitive, behavioral, and motor function impairments after injury. The piglet brain is more similar to the human brain in terms of size, structure, and white matter composition, and responds similarly to injury, making it an ideal pre-clinical animal model. This model can be utilized in future studies to help elucidate the effects of early life insult on development in the young gyrencephalic brain and to target and test novel therapeutics that lead to functional improvements.

Acknowledgements and Disclosures

We would like to thank Shelley Tau, Kayla Hargrove, Jaime Certusi, Sarah Lewis, Olivia Fuller, Caroline Coleman, Kathryn Sellman, Alex Ross, Natalie Bishop, Julianne Gillis, and Andrea Kuehndorf for their significant and integral involvement in all pig work; Kelly Scheulin, Neil Doshi, and Sonal Dugar for their help with immunohistochemistry; We would also like to thank Rick Utley and Kelly Parham at the UGA Swine Unit for their pig expertise and for providing us with piglets. Lastly, we would like to thank Randy Nation for his help in designing and building our behavior testing arenas. This work was supported by The University of Georgia Research Foundation.

The authors have no conflicts of interest.

References

1. Langlois, J.A., Rutland-Brown, W., Thomas, K.E., *Traumatic brain injury in the United States: Emergency deparment visits, hospitalizations, and deaths.* Atlanta, GA: Centers for Disease Control and Prevention, National Center for Injury Prevention and Control, 2006.
2. Anderson, V., et al., *Functional plasticity or vulnerability after early brain injury?* Pediatrics, 2005. **116**(6): p. 1374-82.
3. Anderson, V.A., et al., *Understanding predictors of functional recovery and outcome 30 months following early childhood head injury.* Neuropsychology, 2006. **20**(1): p. 42-57.
4. Anderson, V.A., et al., *Recovery of memory function following traumatic brain injury in pre-school children.* Brain Inj, 2000. **14**(8): p. 679-92.
5. Babikian, T. and R. Asarnow, *Neurocognitive outcomes and recovery after pediatric TBI: meta-analytic review of the literature.* Neuropsychology, 2009. **23**(3): p. 283-96.
6. Lajiness-O'Neill, R., L. Erdodi, and E.D. Bigler, *Memory and learning in pediatric traumatic brain injury: a review and examination of moderators of outcome.* Appl Neuropsychol, 2010. **17**(2): p. 83-92.
7. Anderson, V.A., et al., *Functional memory skills following traumatic brain injury in young children.* Pediatr Rehabil, 1999. **3**(4): p. 159-66.
8. Kuhtz-Buschbeck, J.P., et al., *Analyses of gait, reaching, and grasping in children after traumatic brain injury.* Arch Phys Med Rehabil, 2003. **84**(3): p. 424-30.
9. Beretta, E., et al., *Assessment of gait recovery in children after Traumatic Brain Injury.* Brain Inj, 2009. **23**(9): p. 751-9.

10. Katz-Leurer, M., et al., *Balance abilities and gait characteristics in post-traumatic brain injury, cerebral palsy and typically developed children.* Dev Neurorehabil, 2009. **12**(2): p. 100-5.

11. Kuhtz-Buschbeck, J.P., et al., *Sensorimotor recovery in children after traumatic brain injury: analyses of gait, gross motor, and fine motor skills.* Dev Med Child Neurol, 2003. **45**(12): p. 821-8.

12. Osier, N.D., J.R. Korpon, and C.E. Dixon, *Controlled Cortical Impact Model*, in *Brain Neurotrauma: Molecular, Neuropsychological, and Rehabilitation Aspects*, F.H. Kobeissy, Editor. 2015: Boca Raton (FL).

13. Hamm, R.J., et al., *Cognitive deficits following traumatic brain injury produced by controlled cortical impact.* J Neurotrauma, 1992. **9**(1): p. 11-20.

14. Smith, D.H., et al., *A model of parasagittal controlled cortical impact in the mouse: cognitive and histopathologic effects.* J Neurotrauma, 1995. **12**(2): p. 169-78.

15. Liu, N.K., et al., *A semicircular controlled cortical impact produces long-term motor and cognitive dysfunction that correlates well with damage to both the sensorimotor cortex and hippocampus.* Brain Res, 2014. **1576**: p. 18-26.

16. Tucker, L.T., A.H. Fu, and J.T. McCabe, *Performance of male and female C57BL/6J mice on motor and cognitive tasks commonly used in pre-clinical traumatic brain injury research.* J Neurotrauma, 2015.

17. Card, J.P., et al., *Plastic reorganization of hippocampal and neocortical circuitry in experimental traumatic brain injury in the immature rat.* J Neurotrauma, 2005. **22**(9): p. 989-1002.

18. Ajao, D.O., et al., *Traumatic brain injury in young rats leads to progressive behavioral deficits coincident with altered tissue properties in adulthood.* J Neurotrauma, 2012. **29**(11): p. 2060-74.

19. Kamper, J.E., et al., *Juvenile traumatic brain injury evolves into a chronic brain disorder: behavioral and histological changes over 6months.* Exp Neurol, 2013. **250**: p. 8-19.

20. Amoros-Aguilar, L., et al., *Traumatic brain injury in late adolescent rats: effects on adulthood memory and anxiety.* Behav Neurosci, 2015. **129**(2): p. 149-59.

21. Conrad, M.S. and R.W. Johnson, *The domestic piglet: an important model for investigating the neurodevelopmental consequences of early life insults.* Annu Rev Anim Biosci, 2015. **3**: p. 245-64.

22. Dobbing, J. and J. Sands, *Comparative aspects of the brain growth spurt.* Early Hum Dev, 1979. **3**(1): p. 79-83.

23. Dickerson, J.W. and J. Dobbing, *Prenatal and postnatal growth and development of the central nervous system of the pig.* Proc R Soc Lond B Biol Sci, 1967. **166**(1005): p. 384-95.

24. Conrad, M.S., et al., *Magnetic resonance imaging of the neonatal piglet brain.* Pediatr Res, 2012. **71**(2): p. 179-84.

25. Flynn, T.J., *Developmental changes of myelin-related lipids in brain of miniature swine.* Neurochem Res, 1984. **9**(7): p. 935-45.

26. Fairbairn, L., et al., *The mononuclear phagocyte system of the pig as a model for understanding human innate immunity and disease.* J Leukoc Biol, 2011. **89**(6): p. 855-71.

27. Duhaime, A.C., et al., *Maturation-dependent response of the piglet brain to scaled cortical impact.* J Neurosurg, 2000. **93**(3): p. 455-62.

28. Costine, B.A., et al., *The subventricular zone in the immature piglet brain: anatomy and exodus of neuroblasts into white matter after traumatic brain injury.* Dev Neurosci, 2015. **37**(2): p. 115-30.

29. Paredes, M.F., et al., *Extensive migration of young neurons into the infant human frontal lobe.* Science, 2016. **354**(6308).

30. Gieling, E.T., et al., *The pig as a model animal for studying cognition and neurobehavioral disorders.* Curr Top Behav Neurosci, 2011. **7**: p. 359-83.

31. Friess, S.H., et al., *Neurobehavioral functional deficits following closed head injury in the neonatal pig.* Exp Neurol, 2007. **204**(1): p. 234-43.

32. Sullivan, S., et al., *Improved behavior, motor, and cognition assessments in neonatal piglets.* J Neurotrauma, 2013. **30**(20): p. 1770-9.

33. Elmore, M.R., R.N. Dilger, and R.W. Johnson, *Place and direction learning in a spatial T-maze task by neonatal piglets.* Anim Cogn, 2012. **15**(4): p. 667-76.

34. Packard, M.G. and J.L. McGaugh, *Inactivation of hippocampus or caudate nucleus with lidocaine differentially affects expression of place and response learning.* Neurobiol Learn Mem, 1996. **65**(1): p. 65-72.

35. Rytych, J.L., et al., *Early life iron deficiency impairs spatial cognition in neonatal piglets.* J Nutr, 2012. **142**(11): p. 2050-6.

36. Radlowski, E.C., et al., *A neonatal piglet model for investigating brain and cognitive development in small for gestational age human infants.* PLoS One, 2014. **9**(3): p. e91951.

37. Liu, H., et al., *Early supplementation of phospholipids and gangliosides affects brain and cognitive development in neonatal piglets.* J Nutr, 2014. **144**(12): p. 1903-9.

38. Lehnung, M., et al., *Children's spatial behavior is differentially affected after traumatic brain injury.* Child Neuropsychol, 2001. **7**(2): p. 59-71.

39. Lehnung, M., et al., *Recovery of spatial memory and persistence of spatial orientation deficits after traumatic brain injury during childhood.* Brain Inj, 2003. **17**(10): p. 855-69.

40. Lanke, J., et al., *Spatial memory and stereotypic behaviour of animals in radial arm mazes.* Brain Res, 1993. **605**(2): p. 221-8.

41. Morris, R.G.M., *Spatial Localization Does Not Require the Presence of Local Cues.* Learning and Motivation, 1981. **12**(2): p. 239-260.

42. Vorhees, C.V. and M.T. Williams, *Assessing spatial learning and memory in rodents.* ILAR J, 2014. **55**(2): p. 310-32.

43. Rosema, S., L. Crowe, and V. Anderson, *Social function in children and adolescents after traumatic brain injury: a systematic review 1989-2011.* J Neurotrauma, 2012. **29**(7): p. 1277-91.

44. Anaby, D., et al., *Predictors of change in participation rates following acquired brain injury: results of a longitudinal study.* Dev Med Child Neurol, 2012. **54**(4): p. 339-46.

45. Lowther, J.L. and J. Mayfield, *Memory functioning in children with traumatic brain injuries: a TOMAL validity study.* Arch Clin Neuropsychol, 2004. **19**(1): p. 105-18.

46. Wells, R., P. Minnes, and M. Phillips, *Predicting social and functional outcomes for individuals sustaining paediatric traumatic brain injury.* Dev Neurorehabil, 2009. **12**(1): p. 12-23.

47. Ryan, N.P., et al., *Predictors of very-long-term sociocognitive function after pediatric traumatic brain injury: evidence for the vulnerability of the immature "social brain".* J Neurotrauma, 2014. **31**(7): p. 649-57.

48. Bondi, C.O., et al., *Found in translation: Understanding the biology and behavior of experimental traumatic brain injury.* Neurosci Biobehav Rev, 2015. **58**: p. 123-46.

49. Semple, B.D., S.A. Canchola, and L.J. Noble-Haeusslein, *Deficits in social behavior emerge during development after pediatric traumatic brain injury in mice.* J Neurotrauma, 2012. **29**(17): p. 2672-83.

50. Adolphs, R., *The social brain: neural basis of social knowledge.* Annu Rev Psychol, 2009. **60**: p. 693-716.

51. Maaswinkel, H., et al., *Roles of the basolateral amygdala and hippocampus in social recognition in rats.* Physiol Behav, 1996. **60**(1): p. 55-63.

52. Hitti, F.L. and S.A. Siegelbaum, *The hippocampal CA2 region is essential for social memory.* Nature, 2014. **508**(7494): p. 88-92.

53. Russell, P.A. and D.I. Williams, *Effects of repeated testing on rats' locomotor activity in the open-field.* Anim Behav, 1973. **21**(1): p. 109-11.

54. Mychasiuk, R., H. Hehar, and M.J. Esser, *A mild traumatic brain injury (mTBI) induces secondary attention-deficit hyperactivity disorder-like symptomology in young rats.* Behav Brain Res, 2015. **286**: p. 285-92.

55. O'Connor, C., et al., *Effects of daily versus weekly testing and pre-training on the assessment of neurologic impairment following diffuse traumatic brain injury in rats.* J Neurotrauma, 2003. **20**(10): p. 985-93.

56. Schwerin, S.C., et al., *Establishing the ferret as a gyrencephalic animal model of traumatic brain injury: Optimization of controlled cortical impact procedures.* J Neurosci Methods, 2017.

57. Qu, W., et al., *Automated monitoring of early neurobehavioral changes in mice following traumatic brain injury.* Neural Regen Res, 2016. **11**(2): p. 248-56.

58. Pullela, R., et al., *Traumatic injury to the immature brain results in progressive neuronal loss, hyperactivity and delayed cognitive impairments.* Dev Neurosci, 2006. **28**(4-5): p. 396-409.

59. Budinich, C.S., et al., *Short and long-term motor and behavioral effects of diazoxide and dimethyl sulfoxide administration in the mouse after traumatic brain injury.* Pharmacol Biochem Behav, 2013. **108**: p. 66-73.

60. Schwarzbold, M.L., et al., *Effects of traumatic brain injury of different severities on emotional, cognitive, and oxidative stress-related parameters in mice.* J Neurotrauma, 2010. **27**(10): p. 1883-93.

61. Yu, F., et al., *Lithium ameliorates neurodegeneration, suppresses neuroinflammation, and improves behavioral performance in a mouse model of traumatic brain injury.* J Neurotrauma, 2012. **29**(2): p. 362-74.

62. Li, S., et al., *Transient versus prolonged hyperlocomotion following lateral fluid percussion injury in mongolian gerbils.* J Neurosci Res, 2006. **83**(2): p. 292-300.

63. Viggiano, D., *The hyperactive syndrome: metanalysis of genetic alterations, pharmacological treatments and brain lesions which increase locomotor activity.* Behav Brain Res, 2008. **194**(1): p. 1-14.

64. Kirkwood, M., et al., *Prevalence and correlates of depressive symptoms following traumatic brain injuries in children.* Child Neuropsychol, 2000. **6**(3): p. 195-208.

65. Max, J.E., et al., *Depression in children and adolescents in the first 6 months after traumatic brain injury.* Int J Dev Neurosci, 2012. **30**(3): p. 239-45.

66. Schachar, R., et al., *Attention deficit hyperactivity disorder symptoms and response inhibition after closed head injury in children: do preinjury behavior and injury severity predict outcome?* Dev Neuropsychol, 2004. **25**(1-2): p. 179-98.

67. Li, L. and J. Liu, *The effect of pediatric traumatic brain injury on behavioral outcomes: a systematic review.* Dev Med Child Neurol, 2013. **55**(1): p. 37-45.

68. Amaral, D.G. and M.P. Witter, *The three-dimensional organization of the hippocampal formation: a review of anatomical data.* Neuroscience, 1989. **31**(3): p. 571-91.

69. Laurberg, S. and J. Zimmer, *Lesion-induced sprouting of hippocampal mossy fiber collaterals to the fascia dentata in developing and adult rats.* J Comp Neurol, 1981. **200**(3): p. 433-59.

70. Meaney, D.F. and D.H. Smith, *Biomechanics of concussion.* Clin Sports Med, 2011. **30**(1): p. 19-31, vii.

71. Strange, B.A., et al., *Functional organization of the hippocampal longitudinal axis.* Nat Rev Neurosci, 2014. **15**(10): p. 655-69.

72. Burgess, N., E.A. Maguire, and J. O'Keefe, *The human hippocampus and spatial and episodic memory.* Neuron, 2002. **35**(4): p. 625-41.

73. Kuhn, S. and J. Gallinat, *Segregating cognitive functions within hippocampal formation: a quantitative meta-analysis on spatial navigation and episodic memory.* Hum Brain Mapp, 2014. **35**(4): p. 1129-42.

74. Chang, Q. and P.E. Gold, *Intra-hippocampal lidocaine injections impair acquisition of a place task and facilitate acquisition of a response task in rats.* Behav Brain Res, 2003. **144**(1-2): p. 19-24.

75. An, C., et al., *Severity-Dependent Long-Term Spatial Learning-Memory Impairment in a Mouse Model of Traumatic Brain Injury.* Transl Stroke Res, 2016. **7**(6): p. 512-520.

76. Casella, E.M., et al., *Traumatic brain injury alters long-term hippocampal neuron morphology in juvenile, but not immature, rats.* Childs Nerv Syst, 2014. **30**(8): p. 1333-42.

77. Adelson, P.D., et al., *Morris water maze function and histologic characterization of two age-at-injury experimental models of controlled cortical impact in the immature rat.* Childs Nerv Syst, 2013. **29**(1): p. 43-53.

78. Stephens, J., et al., *Subtle Motor Findings During Recovery from Pediatric Traumatic Brain Injury: A Preliminary Report.* J Mot Behav, 2017. **49**(1): p. 20-26.

79. Ochi, F., et al., *Temporal-spatial feature of gait after traumatic brain injury.* J Head Trauma Rehabil, 1999. **14**(2): p. 105-15.

80. Duberstein, K.J., et al., *Gait analysis in a pre- and post-ischemic stroke biomedical pig model.* Physiology & Behavior, 2014. **125**: p. 8-16.

81. Neumann, M., et al., *Assessing gait impairment following experimental traumatic brain injury in mice.* J Neurosci Methods, 2009. **176**(1): p. 34-44.

82. Wang, Y., et al., *Fluoxetine increases hippocampal neurogenesis and induces epigenetic factors but does not improve functional recovery after traumatic brain injury.* J Neurotrauma, 2011. **28**(2): p. 259-68.

83. Schonfeld, L.M., et al., *Long-Term Motor Deficits after Controlled Cortical Impact in Rats Can Be Detected by Fine Motor Skill Tests but Not by Automated Gait Analysis.* J Neurotrauma, 2017. **34**(2): p. 505-516.

84. Manley, G.T., et al., *Controlled cortical impact in swine: pathophysiology and biomechanics.* J Neurotrauma, 2006. **23**(2): p. 128-39.

85. Naim, M.Y., et al., *Folic acid enhances early functional recovery in a piglet model of pediatric head injury.* Dev Neurosci, 2010. **32**(5-6): p. 466-79.

86. Sullivan, S., et al., *Behavioral deficits and axonal injury persistence after rotational head injury are direction dependent.* J Neurotrauma, 2013. **30**(7): p. 538-45.

87. Fox, G.B., et al., *Sustained sensory/motor and cognitive deficits with neuronal apoptosis following controlled cortical impact brain injury in the mouse.* J Neurotrauma, 1998. **15**(8): p. 599-614.

88. Huh, J.W. and R. Raghupathi, *Chronic cognitive deficits and long-term histopathological alterations following contusive brain injury in the immature rat.* J Neurotrauma, 2007. **24**(9): p. 1460-74.

89. Wakade, C., et al., *Delayed reduction in hippocampal postsynaptic density protein-95 expression temporally correlates with cognitive dysfunction following controlled cortical impact in mice.* J Neurosurg, 2010. **113**(6): p. 1195-201.

90. Walker, K.R. and G. Tesco, *Molecular mechanisms of cognitive dysfunction following traumatic brain injury.* Front Aging Neurosci, 2013. **5**: p. 29.

91. Kou, Z. and P.J. VandeVord, *Traumatic white matter injury and glial activation: from basic science to clinics.* Glia, 2014. **62**(11): p. 1831-55.

Figure 6.1. Photographs and schematics of the behavior testing arenas. Photograph of the T-maze arena depicts a start box in the south arm and restricted access to the north arm. 4 extra-maze visual cues were located around the perimeter of the arena (**A**). Schematic of the T-maze arena represents the location of the two possible start configurations, the reward bowls, and the visual cues. In a south start configuration, a removable panel is used to create a start box in the south arm of the maze, and an additional removable panel restricts access to the north arm (grey dotted lines). In a north start configuration, a removable panel is used to create a start box in the north arm of the maze, and an additional removable panel restricts access to the south arm (red dotted lines) (**B**). Photograph (**C**) and schematic (**D**) of the 3 chamber social recognition arena which is comprised of a start/exit chamber and two outer chambers that each contain a social stimulus pen. Schematic (**E**) and photograph (**F**) of the open field arena.

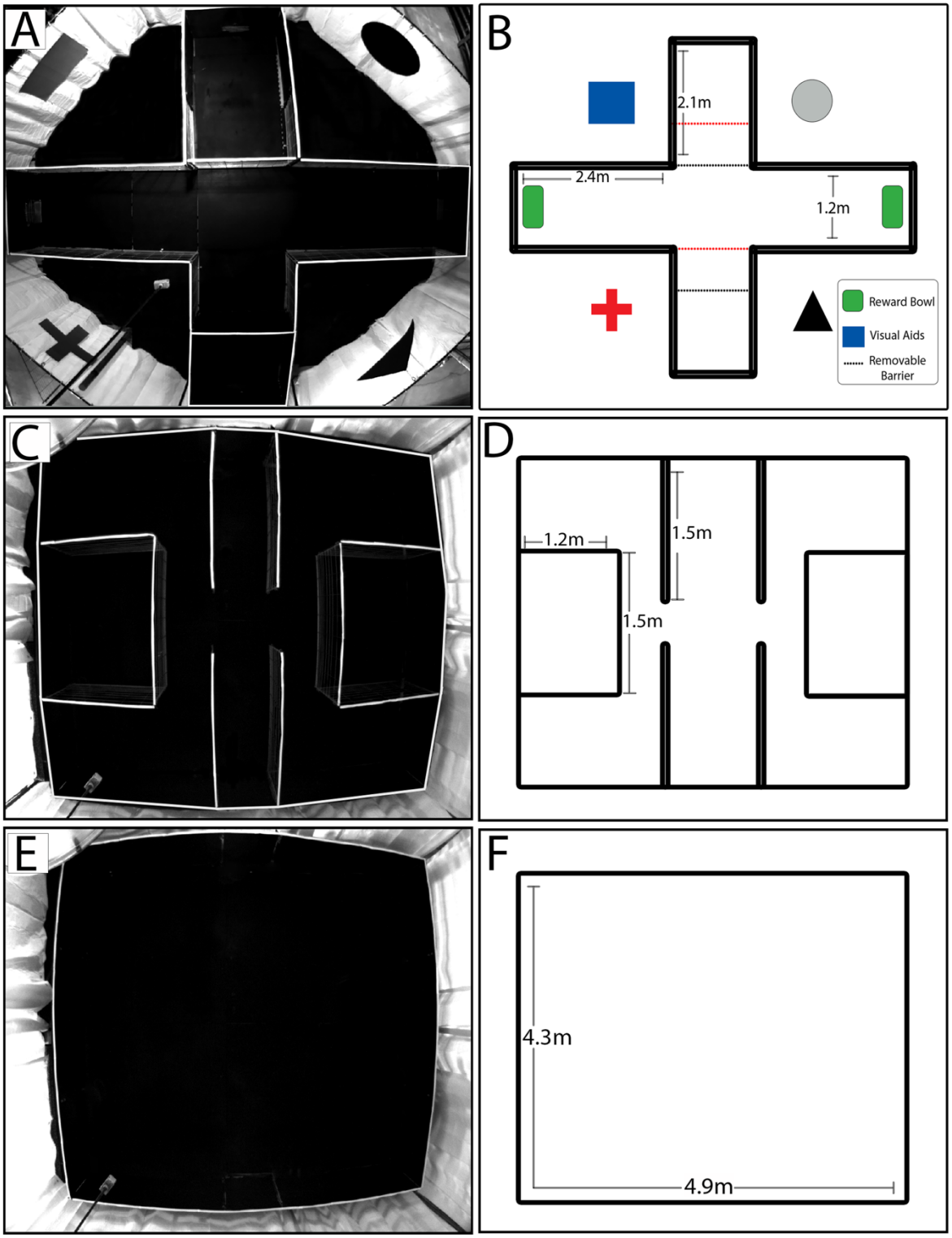
A
B
2.1m
2.4m
1.2m
Reward Bowl
Visual Aids
Removable Barrier
C
D
1.2m
1.5m
1.5m
E
F
4.3m
4.9m

Figure 6.2. TBI impairs spatial memory formation in a spatial T-maze test. Representative nose point tracks of normal and TBI piglets on A1 compared to A2 during T-maze testing. Open gray circles represent the correct reward, crossed circles represent the incorrect reward (**A**). Both normal and TBI piglets demonstrated a significantly faster latency to choice by A2 compared to A1 that persisted through the duration of testing (**B**). TBI piglets made significantly fewer correct reward choices compared to normal piglets from A1 through A4. In addition, compared to A1, normal piglets made significantly more correct choices by A2 while TBI piglets did not make significantly more correct choices until A3 (**C**). Data are expressed as mean ± S.E.M. *= statistically significant difference between time-points compared to A1 within normal controls for latency to choice and proportion trials correct ($p<0.05$). # indicates statistically significant difference between time-points compared to A1 within TBI-affected animals for latency to choice and proportion trials correct ($p<0.05$). $ indicates statistically significant difference within time-points between treatment groups ($p<0.05$).

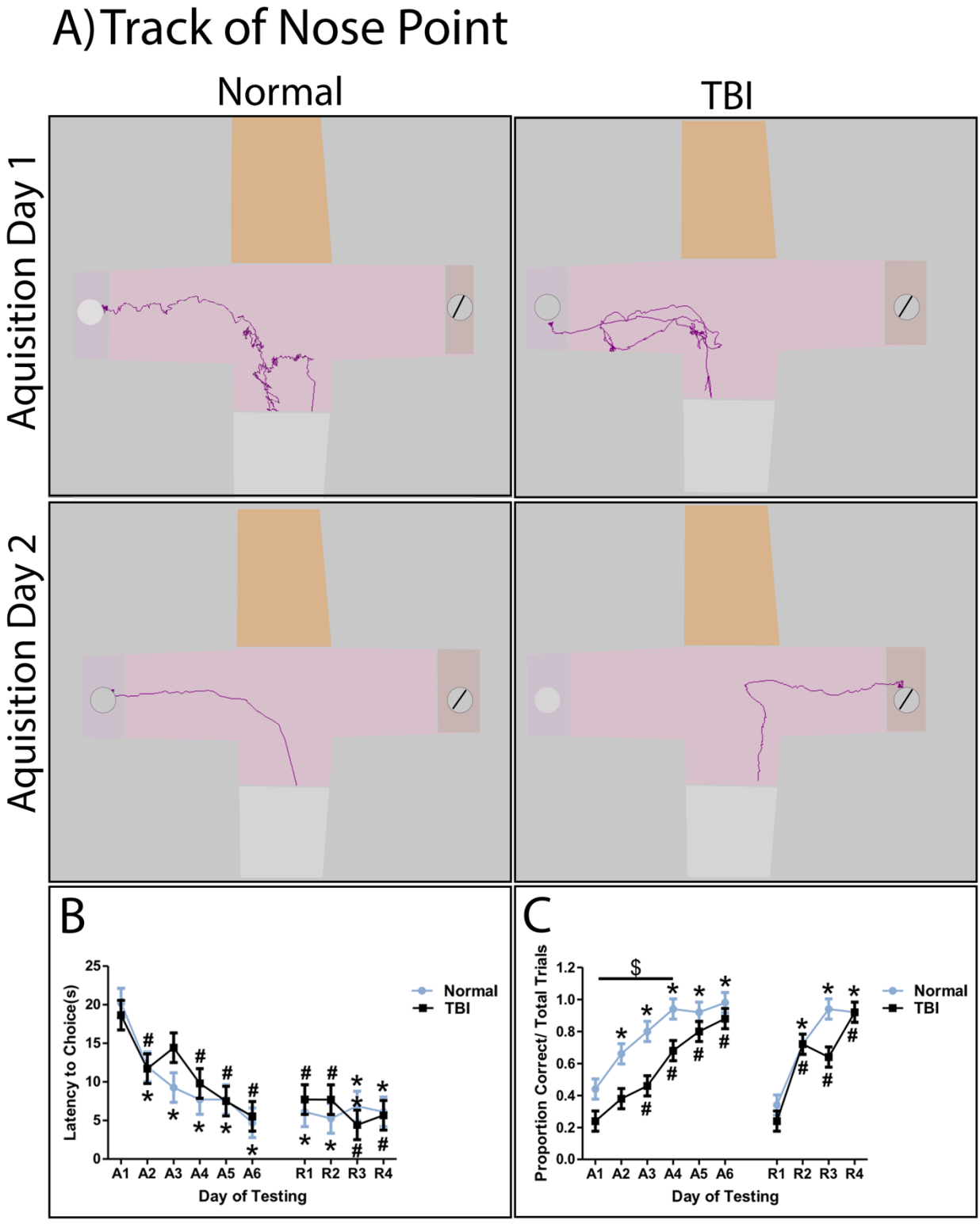
A) Track of Nose Point
Normal
TBI
Aquisition Day 1
Aquisition Day 2
B
Latency to Choice(s)
Day of Testing
A1 A2 A3 A4 A5 A6 R1 R2 R3 R4
Normal
TBI
C
Proportion Correct/ Total Trials
$
Day of Testing
A1 A2 A3 A4 A5 A6 R1 R2 R3 R4
Normal
TBI

Figure 6.3. TBI reduces sociability-seeking behavior and disrupts social memory in a 3 chamber social recognition test. Representative nose point tracks of sociability and social memory trials for normal and TBI-affected pigs (**A**). In sociability trials, red lines indicate when the nose-point was located in the zone around the unfamiliar pig. Yellow lines indicate the position of the nose-point in the object zone (blue open circle) or around the chambers of the arena. In social memory trials, red lines indicate when the nose-point was located in the zone around the novel pig. Yellow lines indicate the position of the nose-point is in the zone around the unfamiliar pig or around the chambers of the arena. For sociability trials, normal and TBI-affected pigs exhibited a high degree of exploration of an unfamiliar pig compared to a novel object. However, comparatively, TBI pigs overall exhibited a lower exploration ratio of the familiar pig, but significance was trending (**B**). For social memory trials, TBI piglets showed a preference for exploring the familiar pig more than the unfamiliar pig (**C**). Dotted lines represent an exploration ratio of 0.5 which indicates no preference.

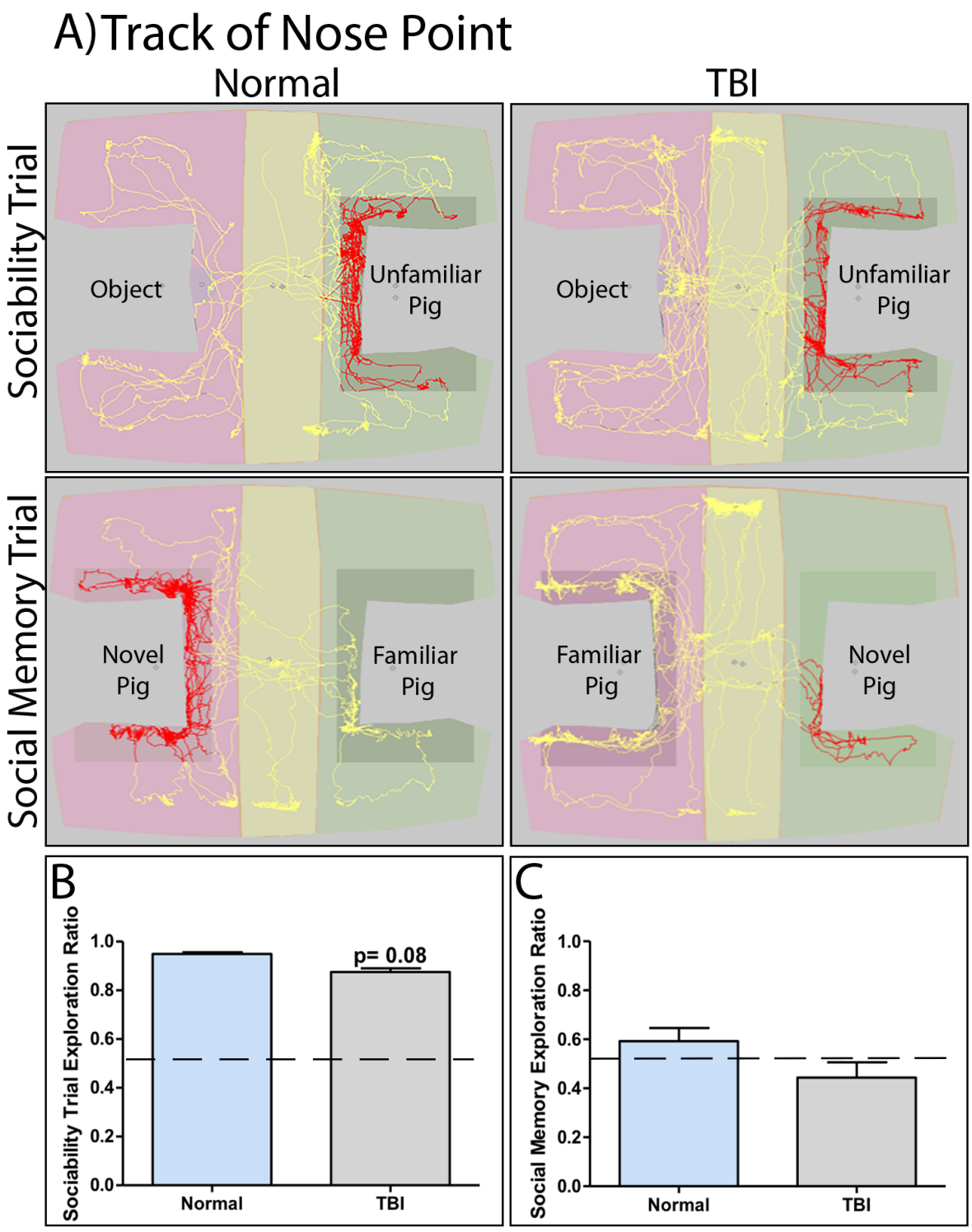
A) Track of Nose Point
Normal
TBI
Sociability Trial
Social Memory Trial
Object
Unfamiliar Pig
Novel Pig
Familiar Pig
B
Sociability Trial Exploration Ratio
p= 0.08
C
Social Memory Exploration Ratio
Normal
TBI

Figure 6.4. TBI results in a transient period of reduced exploratory behavior followed by a period of hyperactivity in an open field test. Representative center point tracks of normal and TBI-affected pigs 1, 7, 14, and 26 days post-TBI (**A**). Normal pigs become habituated to the arena over time while TBI-affected pigs showed an initial decrease in exploratory behaviors immediately after TBI followed by increased exploration of the open field arena over time. TBI piglets traveled significantly less distance 1 day post-TBI compared to normal controls. A comparison across time-points showed that TBI-affected piglets increased their exploration over time and traveled significantly more distance 28 days post-TBI compared to 1 day post-TBI. However, normal piglets are observed traveling significantly less distance in the open field arena by 14 days (**B**). TBI-affected piglets traveled at a significantly slower velocity 1 day post-TBI compared to normal controls. A comparison across time-points showed that TBI-affected piglets increased their velocity over time and traveled at a significantly faster velocity by 14 and 28 days post-TBI compared to 1 day post-TBI. However, the velocity of normal piglets was significantly decreased at 14 days compared to TBI-affected animals and compared to day 1 (**C**). Data are expressed as mean ± S.E.M. * indicates significant difference between time-points within treatment group compared to 1 day post for distance traveled and velocity ($p<0.05$). # indicates significant difference between treatment groups within time-points for distance traveled and velocity ($p<0.05$).

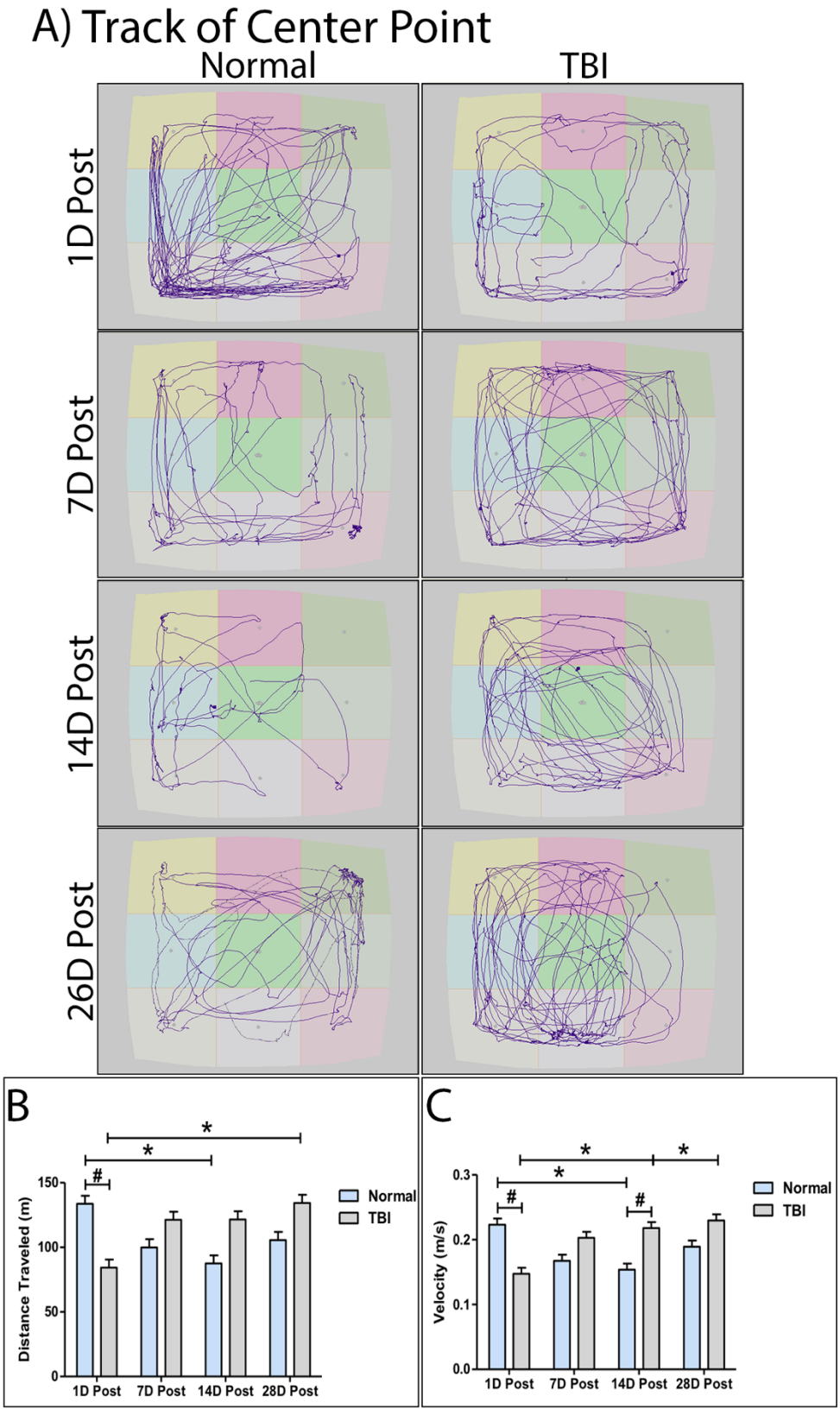
A) Track of Center Point
Normal
TBI
1D Post
7D Post
14D Post
26D Post
B
Distance Traveled (m)
150
100
50
0
1D Post
7D Post
14D Post
28D Post
Normal
TBI
C
Velocity (m/s)
0.3
0.2
0.1
0.0
1D Post
7D Post
14D Post
28D Post
Normal
TBI

Figure 6.5 TBI leads to significant gait impairments in cycle time and stance percent.

Significant increases in cycle time were observed 1 and 3 days post-TBI in the left front (**A**), right front (**B**), left hind (**C**), and right hind (**D**) compared to pre-TBI and between treatment groups at 1 day post-TBI. Significant increases in stance percent were observed 1 and 3 days post-TBI in the left front (**E**) and right front (**F**) compared to pre-TBI and between treatment groups at 1 day post-TBI for the left front and at both 1 and 3 days post-TBI for the right front. Data are expressed as mean ± S.E.M. * indicates significant difference within time-points within treatment group compared to pre-TBI ($p<0.05$). # indicates significant difference within time-points between treatment groups ($p<0.05$).

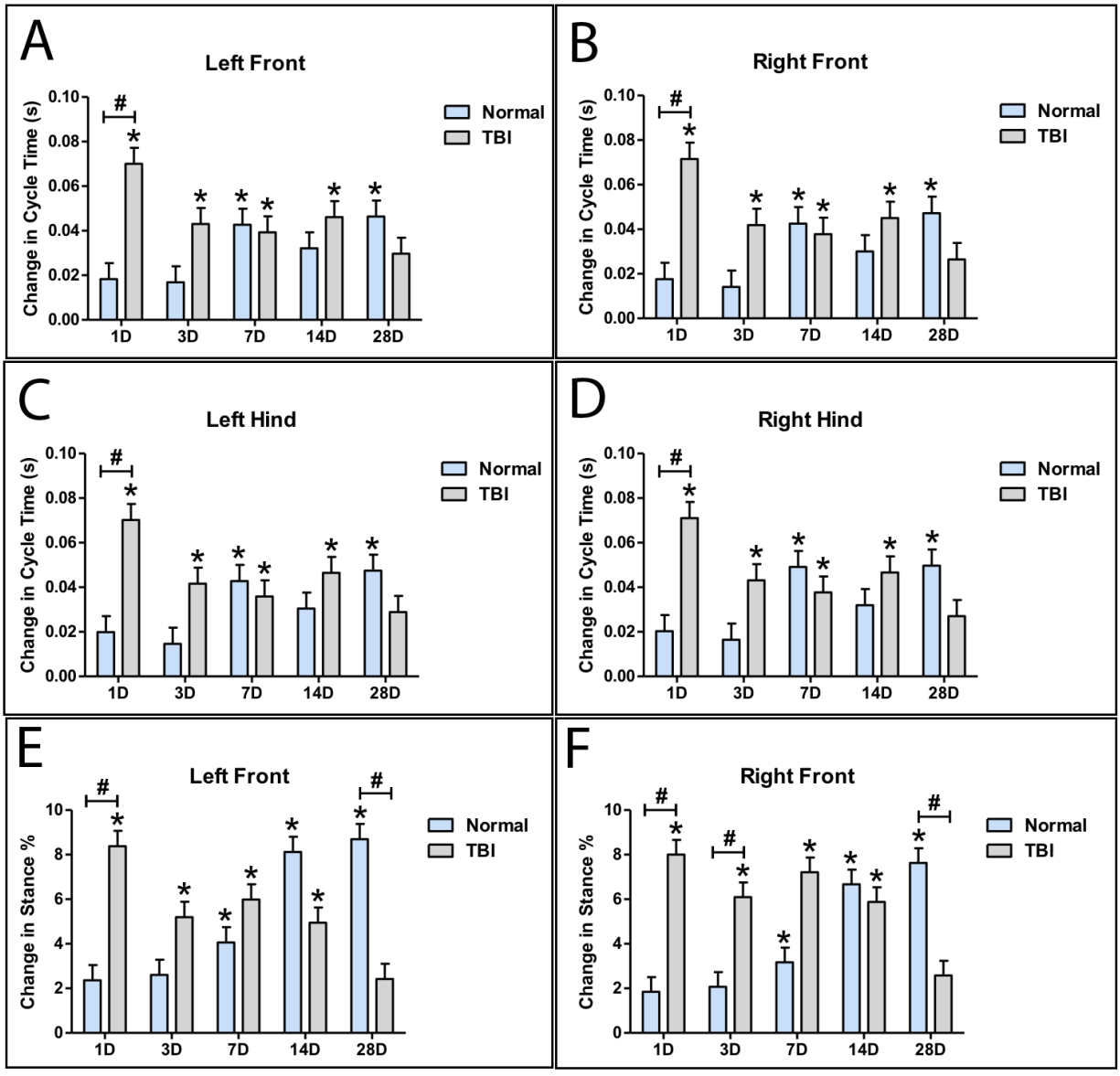
A
Left Front
Change in Cycle Time (s)
0.10
0.08
0.06
0.04
0.02
0.00
1D
3D
7D
14D
28D
Normal
TBI
B
Right Front
C
Left Hind
D
Right Hind
E
Left Front
Change in Stance %
10
8
6
4
2
0
F
Right Front

Figure 6.6. TBI results in significant gait impairments in hind reach and total pressure index. Significant increases in hind reach were observed at 1 and 3 days post-TBI in the left hind (**A**) and right hind (**B**) compared to pre-TBI and between treatment groups at 1 day post-TBI for the left hind and at 1 and 3 days post-TBI for the right hind. Slight decreases in TPI were observed for normal and TBI affected animals in the left front limb (**C**) while a significant decrease in TPI was observed at 1 day post-TBI compared to pre-TBI and between treatment groups for the right front (**D**). Corresponding increases in TPI were observed in the left hind (**E**) and right hind (**F**). A significant increase in TPI was observed 1 day post-TBI in the right hind 1 day post-TBI compared to pre-TBI and between treatment groups. Data are expressed as mean ± S.E.M. * indicates significant difference from pre-TBI or pre-start of study within time-point ($p<0.05$). # indicates significant difference between treatment groups within time-points ($p<0.05$).

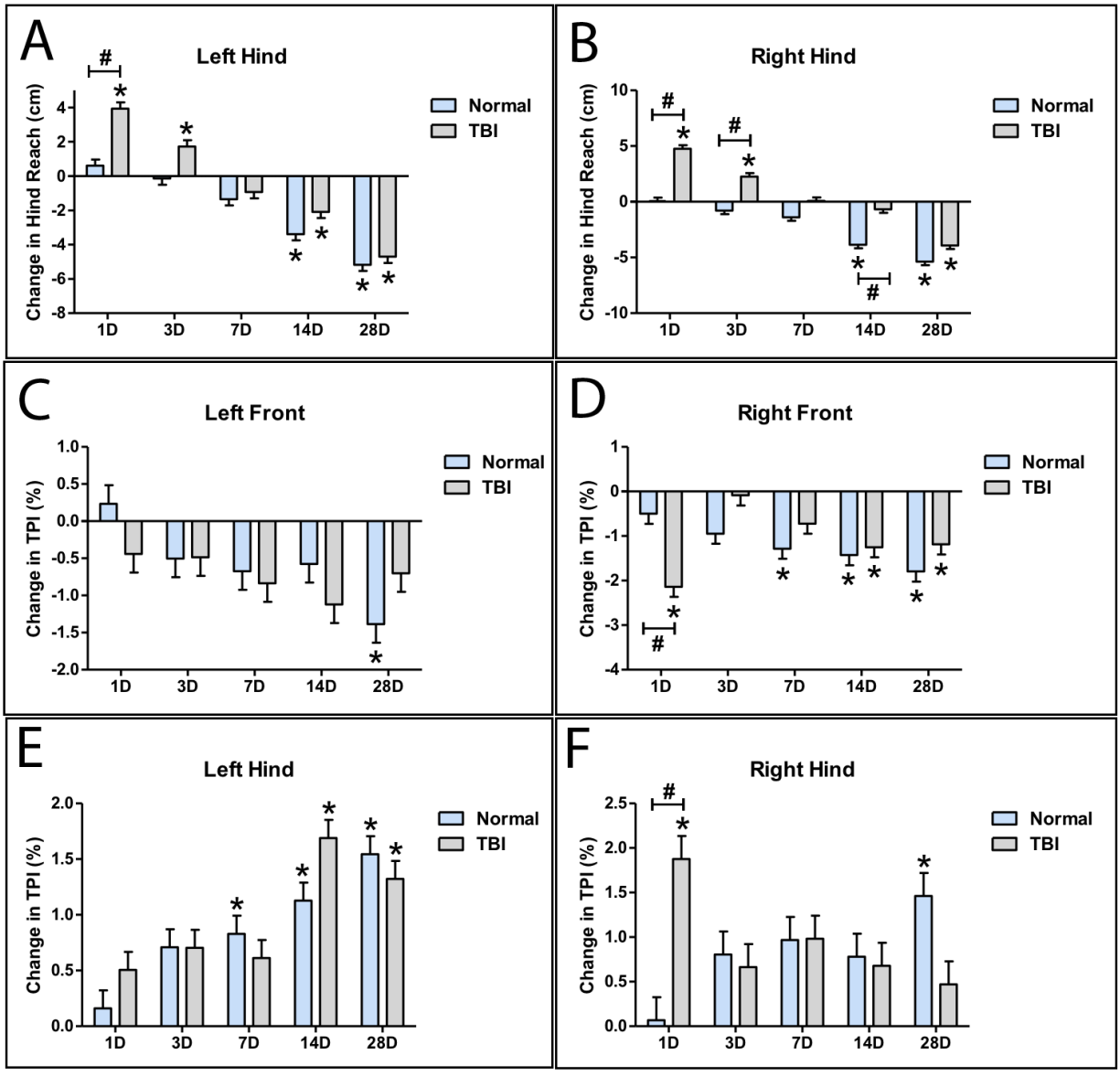
A
Left Hind
Change in Hind Reach (cm)
Normal
TBI
1D
3D
7D
14D
28D
B
Right Hind
Change in Hind Reach (cm)
Normal
TBI
C
Left Front
Change in TPI (%)
D
Right Front
Change in TPI (%)
E
Left Hind
Change in TPI (%)
F
Right Hind
Change in TPI (%)

Figure 6.7. TBI leads to neuronal loss, microglial activation, astrogliosis, and neuroblast proliferation. Representative image of NeuN staining at the cortex in normal (**A**) and TBI-affected (**B**) pigs. A significant loss of neurons was observed in TBI-affected animals compared to normal controls (**C**). Representative image of NeuN staining at the dentate gyrus in normal (**D**) and TBI-affected (**E**) pigs. A significant decrease in neurons was observed in TBI-affected animals compared to normal controls in the polymorphic layer of the dentate gyrus (**F**). Representative image of Iba1 staining at the cortex in normal (**G**) and TBI-affected (**H**) pigs. A significant increase in Iba1 expression was observed in TBI-affect animals compared to normal controls (**I**). Representative image of GFAP staining at the cortex in normal (**J**) and TBI-affected (**K**) pigs. A significant increase in GFAP expression was observed in TBI-affected animals compared to normal controls (**L**). Representative image of DCX staining at the vSVZ in normal (**M**) and TBI-affected (**N**) pigs. A significant increase in DCX+ neuroblasts was observed in TBI-affected animals compared to normal controls (**O**). NeuN, Iba1, and GFAP images were acquired at 4X. DCX images were acquired at 20X. Data are expressed as mean ± S.E.M. * indicates significant difference from normal control animals ($p<0.05$).

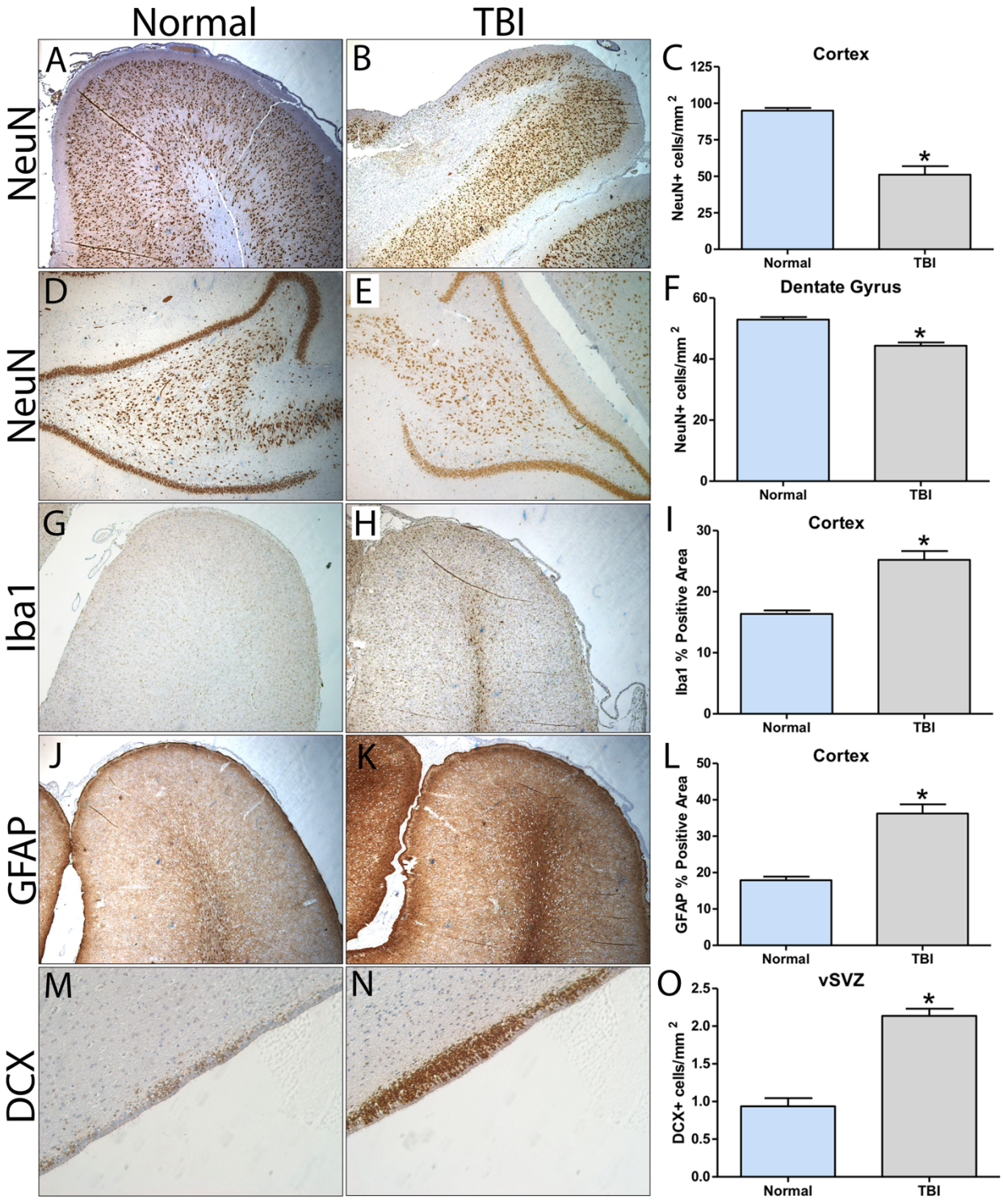
Normal
TBI
A
B
C
Cortex
NeuN
NeuN+ cells/mm 2
125
100
75
50
25
0
*
Normal
TBI
D
E
F
Dentate Gyrus
NeuN
NeuN+ cells/mm 2
60
40
20
0
*
Normal
TBI
G
H
I
Cortex
Iba1
Iba1 % Positive Area
30
20
10
0
*
Normal
TBI
J
K
L
Cortex
GFAP
GFAP % Positive Area
50
40
30
20
10
0
*
Normal
TBI
M
N
O
vSVZ
DCX
DCX+ cells/mm 2
2.5
2.0
1.5
1.0
0.5
0.0
*
Normal
TBI

CHAPTER 7

CONCLUSION

The impact of TBI both in the United States and worldwide is significant, affecting millions of people each year. Children in particular are at high risk for developing long-term neurological deficits that can even persist into adulthood [1]. Despite the prevalence and high cost of TBI, there is currently no effective treatment that offers neuroprotection or regeneration of damaged brain tissue in a clinical setting [2]. Preclinical animal models of TBI have been developed to more closely study the pathophysiology and functional impairments, to identify potential therapeutic targets, and to test the safety and efficacy of potential neuroprotective therapies [3]. Although a number of neuroprotective strategies have been regarded as highly successful in animal models, lack of translatability from a preclinical to clinical setting has long plagued the field [4]. Although the inherent heterogeneity of TBI makes it difficult to fully recapitulate experimentally, one possible explanation for the lack of effective therapies may be attributed to the type of animal most commonly used to model TBI and assess potential treatments- the rodent. The utility and contribution of rodent models in characterizing TBI sequelae and identifying potential treatment targets should certainly not be diminished, but the translational power of these models may be impeded by a number of significant physiologic and morphologic differences between rodent and humans [5].

The pig may be an ideal large animal model of human TBI given several key similarities between humans and pigs. Pigs and humans share a similar developmental time course with regards to brain growth, neurogenesis, and myelination [6-8]. Furthermore, pig and human brains

are gyrencephalic and are similar in size and composition [9]. Perhaps most importantly, pigs and humans each have significantly more white matter than gray matter, a characteristic that makes modeling TBI, which often causes significant damage to major white matter tracks in the brain, a top priority [10]. TBI in humans often leads to significant impairments in cognition, behavior, and motor function. Pigs are highly intelligent and trainable and are amenable to performing behavior and motor testing paradigms [11]. This makes pigs an ideal candidate to measure functional outcomes after TBI and more importantly, the ability for therapeutic interventions to improve functional deficits after injury. However, further testing is needed to fully characterize the predictive power of pigs as a preclinical large animal for TBI. Therefore, the overall goal of these studies was to develop and characterize a highly translational piglet controlled cortical impact (CCI) model with measureable pathophysiologic changes at the tissue and cellular level that corresponded with impaired functional outcomes.

In these studies, we first developed a scaled pig TBI model by manipulating CCI impact velocity and depth of depression and characterized the corresponding histopathological and functional responses to injury. We found that lesion volume increased as a function of injury severity. Histopathologically, we observed increases in neuronal cell loss, astrogliosis, hemorrhage, and white matter degeneration that correlated with impact parameters. Quantitative gait biomechanic analysis revealed progressive impairments in motor function that corresponded with TBI severity as well. The results from this study demonstrated that both TBI pathology and functional outcomes are progressively worsened by increasing injury severity in pigs, consistent with reports of human TBI [12].

Next, we utilized multiparametric magnetic resonance imaging (MRI) and magnetic resonance spectroscopy (^{1}HMRS) combined with histological analysis to longitudinally assess

TBI pathology. At 24 hours post-TBI, we observed presence of heterogeneous edema accumulation in the brain parenchyma that consisted of both cytotoxic and vasogenic edema, but was mainly dominated by vasogenic edema, a hallmark of human TBI [13, 14]. As a consequence, the volume of the ipsilateral hemisphere increased, resulting in a midline shift. We also found evidence of white matter disruption, decreased cerebral blood flow (CBF), and metabolic dysfunction. At 12 weeks post-TBI, we noted a significant decrease in the volume of the ipsilateral hemisphere and thus a directional shift in the midline as a result of tissue necrosis. Additionally, we found evidence of potential cyst formation at the injury site as well as sustained disruption of white matter integrity and CBF. Deficits observed with MRI and ^{1}HMRS were found to correlate with longitudinal histological analyses that showed significant neuronal loss, neuroinflammation, gliosis, and oligodendrocyte pathology. The results from this study showed the utility of using clinically relevant, non-invasive MRI to longitudinally track TBI pathophysiology in a large animal model as well as demonstrate the potential of this approach to monitor recovery after therapeutic interventions.

Then, in order to provide a platform with which to assess cognitive and behavioral deficits incurred from TBI, we developed a series of quantitative behavioral tests that each assessed different aspects of learning, memory, and behavior. We found that normal piglets demonstrated several key behaviors in an open field test, namely high exploratory interest of their environment, presence of anxiety behaviors due to social isolation, as well as habituation to the open field arena after repeated exposure. In a novel object recognition test, we found that piglets spent significantly more time with a novel object than a familiar object, demonstrating a preference for novelty and the ability to form object memories. In a 3 chamber social recognition test, we found that piglets exhibited normal sociability behaviors, spending more time with a

social stimulus over a novel object. Piglets also showed a preference for a novel pig over a familiar pig, demonstrating the ability to form social memories. Piglets also demonstrated the ability to form spatial memories by learning how to navigate a plus-shaped T-maze by using extra-maze cues. The results from this study showed that a combined approach using four behavior tests provided a comprehensive assessment of piglet learning, memory, and behavior that may have promising utility for studying functional changes in pig neural injury models.

In our final study, we used a combined approach to study functional outcomes and corresponding histopathological changes after TBI in piglets. We found that TBI-affected pigs exhibited spatial memory deficits in a spatial T-maze test and showed trending evidence of disruption of sociability and social memory deficits in a 3 chamber social recognition test. TBI-affected pigs also showed reduced exploratory behavior immediately after TBI that was followed by significant hyperactivity behaviors that persisted for up to 4 weeks post-TBI. Using a quantitative gait pressure mat system, we also observed transient but significant deficits in gait. Corresponding histopathological analysis revealed a significant neuronal loss, microglia activation, and astrogliosis at the perilesional site at the cortex. In addition, significant neuronal loss was observed at the dorsal hippocampus, which may explain the presence of cognitive and behavioral deficits. We also noted stimulation of endogenous neuroblast populations at the subventricular zone. The results of this study provided evidence of both cognitive and motor function deficits in response to TBI that correlated with observed histopathology. These results provide important implications for future studies aimed at studying functional responses of TBI and as a means to test the predictive power of potential therapeutics to yield functional recovery and to restore of quality of life.

Challenges and Future Studies

Although the results reported in these preclinical studies have made significant contributions to the current understanding of focal TBI sequelae in a more translational pig model, several issues should be considered in future studies to maximize the translational potential of this model. First, a few overarching issues were observed in all studies. Although CCI induced TBI generally produces focal, highly reproducible injuries that are very similar across all animals, we observed a fair amount of injury heterogeneity between animals possibly due to individual brain size, anatomical, and vascular differences. Given the small number of animals in each of these studies, high variability between animals presents a challenge in identifying significant tissue, cellular, and functional responses. However, a similar phenomenon is observed in other pig CCI models [15]. Future studies will benefit from an increase in cohort sizes to better account for variability between animals. In these studies, we also utilized males only for all studies. We recognize this is a significant limitation in modeling TBI given that clinically this type of injury affects both males and females. Future studies should include animals from both sexes to account for potential sex differences in response to TBI. Furthermore, CCI is induced in anesthetized animals after performing a craniectomy. Anesthetics, such as isoflurane, have been shown to have neuroprotective properties [16] and a decompressive craniectomy is performed clinically as a means to reduce intracranial pressure [17]. Future studies should include both sham and normal controls to assess the effect of anesthesia and craniectomy on pathological and functional outcomes.

We found that increasing CCI velocity and depth of depression increased injury severity and subsequently led to a scaled response in lesion size, neuronal loss, inflammation, and motor function deficits. In a clinical setting, the Glasgow Coma Scale is the primary means for injury

severity classification and follows a strict neurological scoring system to classify TBI as either mild, moderate, or severe [18]. Although in these studies we found evidence of mild, moderate, and severe responses to TBI in our pig model, no common neurological scoring system with strict scoring guidelines has been developed for pigs that allows us to classify it as such.

MRI studies allow for non-invasive, longitudinal measurements of TBI outcomes like lesion size, midline shift, edema accumulation, white matter integrity, cerebral blood flood, and metabolic changes, but they are accompanied by a number of significant challenges. First, given the differences in brain size between humans and pigs, the resolution of MRI scans in the pig is much lower than that of the human. This is especially true for voxel-based sequences such as ^{1}HMRS in which voxel size is much smaller in pigs than humans. This presents a challenge since the signal-to-noise ratio is directly proportional to the voxel size [19]. Added challenges for ^{1}HMRS included respiration during scanning, small cerebral volume, increased lipid layer near the skull, and substantial hemorrhage at the lesion site which prevented quantitative comparisons between ipsilateral and contralateral hemispheres in our model. Total creatine is often used as an internal standard, however we noted significant changes in total creatine levels in our model. Additional optimization studies utilizing ^{1}HMRS are needed to develop a different internal standard, like internal water, to better normalize spectra and to improve the resolution of voxel placement. The presence of substantial hemorrhage at the lesion site also provided a challenge in identifying areas of vasogenic edema, identified as areas of hyperintensity on ADC maps derived from diffusion weighted sequences, since both hemorrhage and vasogenic edema present as hyperintensities on ADC maps [20]. It may be of interest in future studies to generate T2-weighted sequences that correspond with ADC maps to help delineate between vasogenic edema and hemorrhage.

In these studies, we utilized two different modalities of assessing motor function deficits. First, we used high speed cameras to record spatiotemporal changes in gait. Video data was analyzed manually using Kinovea software, opening the door for human error involving potential subjective errors regarding footfall placement and timing. Video gait analysis is also limited to assessment of spatiotemporal gait parameters only (e.g. stride time, stance time, and support phase). However, our next study addressed some of these issues by utilizing a gait pressure mat system. The gait pressure mat can assess both spatiotemporal parameters and changes in footfall pressure, like total pressure index that measure the amount of pressure on the front limbs compared to the hind limbs. Analysis of changes in gait is semi-automatic using the gait pressure mat system, reducing potential human error. However, the gait pressure mat still presents with a number of challenges, namely that even normal pig gait can have a high degree of variability between animals and pigs must be well-trained to travel across the mat at a consistent velocity or runs are unable to analyzed. Future studies will benefit from increased number of animals and improved training techniques.

We also utilized a number of behavior testing paradigms to assess pig cognition and behavior in both normal and TBI-affected animals. Although these tests were shown to provide reliable information regarding pig cognition and behavior in normal animals, a number of limitations exist in their use. The spatial T-maze test for example, provides an excellent measure of spatial memory formation in pigs and was found to be sensitive enough to detect spatial memory deficits in TBI-affected animals. However, we observed that although TBI-affected pigs had difficult acquiring the test in the first few days, they eventually caught up to normal pigs in their performance after only 5 days. Although it appears that these spatial memory deficits are only transient in this case, it's quite possible this this test is not sensitive enough to detect more

subtle, long-term deficits in cognition. For example, for this test, pigs have a 50/50 chance of choosing the correct reward, making it inherently easier for them to learn to solve the maze over time. Future studies may benefit from additional testing using more sensitive measures of spatial memory, such as the holeboard discrimination task where the pig must find the location of multiple food rewards among many incorrect food rewards, rather than just a single correct reward and a single incorrect reward as in the T-maze test. For the 3 chamber social recognition test, we were unable to reach significant results for the social memory test, despite a clear trend for TBI-affected pigs to seek the familiar pig over the novel pig. These results can most likely be attributed to a low number of animals used in these studies. For the open field test, our measurements were limited only locomotor activities in normal and TBI-affected animals. While we did find significant differences in locomotor activity between these animals, it would be of interest to expand on the number of behaviors measured to include additional behaviors such as anxiety, depression, or abnormal locomotor behaviors such as circling or backing up.

In conclusion, we have developed a highly translational piglet TBI that exhibits similar pathophysiologic and functional responses to humans. We have also developed a number of exciting gait and behavior testing modalities never before used in pig TBI models that can detect even subtle and transient changes in motor function and cognition after TBI in pigs. The future implications for this model are exciting as we move forward towards our goal of developing treatment strategies that have the potential to vastly improve the lives of the millions affected by TBI each year.

References

1. Hessen, E., K. Nestvold, and V. Anderson, *Neuropsychological function 23 years after mild traumatic brain injury: a comparison of outcome after paediatric and adult head injuries.* Brain Inj, 2007. **21**(9): p. 963-79.
2. Loane, D.J. and A.I. Faden, *Neuroprotection for traumatic brain injury: translational challenges and emerging therapeutic strategies.* Trends Pharmacol Sci, 2010. **31**(12): p. 596-604.
3. Johnson, V.E., et al., *Animal models of traumatic brain injury.* Handb Clin Neurol, 2015. **127**: p. 115-28.
4. Xiong, Y., A. Mahmood, and M. Chopp, *Neurorestorative treatments for traumatic brain injury.* Discov Med, 2010. **10**(54): p. 434-42.
5. Briones, T.L., *Chapter 3 animal models of traumatic brain injury: is there an optimal model that parallels human brain injury?* Annu Rev Nurs Res, 2015. **33**: p. 31-73.
6. Dobbing, J. and J. Sands, *Comparative aspects of the brain growth spurt.* Early Hum Dev, 1979. **3**(1): p. 79-83.
7. Dickerson, J.W.T. and J. Dobbing, *Prenatal and Postnatal Growth and Development of the Central Nervous System of the Pig.* Proceedings of the Royal Society of London. Series B. Biological Sciences, 1967. **166**(1005): p. 384-395.
8. Flynn, T.J., *Developmental changes of myelin-related lipids in brain of miniature swine.* Neurochem Res, 1984. **9**(7): p. 935-45.
9. Gieling, E.T., et al., *The pig as a model animal for studying cognition and neurobehavioral disorders.* Curr Top Behav Neurosci, 2011. **7**: p. 359-83.

10. Zhang, K. and T.J. Sejnowski, *A universal scaling law between gray matter and white matter of cerebral cortex.* Proc Natl Acad Sci U S A, 2000. **97**(10): p. 5621-6.

11. Gieling, E.T., R.E. Nordquist, and F.J. van der Staay, *Assessing learning and memory in pigs.* Anim Cogn, 2011. **14**(2): p. 151-73.

12. Andriessen, T.M., B. Jacobs, and P.E. Vos, *Clinical characteristics and pathophysiological mechanisms of focal and diffuse traumatic brain injury.* J Cell Mol Med, 2010. **14**(10): p. 2381-92.

13. Marmarou, A., et al., *Traumatic brain edema in diffuse and focal injury: cellular or vasogenic?* Acta Neurochir Suppl, 2006. **96**: p. 24-9.

14. Kawamata, T. and Y. Katayama, *Cerebral contusion: a role model for lesion progression.* Prog Brain Res, 2007. **161**: p. 235-41.

15. Duhaime, A.C., et al., *Magnetic resonance imaging studies of age-dependent responses to scaled focal brain injury in the piglet.* J Neurosurg, 2003. **99**(3): p. 542-8.

16. Statler, K.D., et al., *Comparison of seven anesthetic agents on outcome after experimental traumatic brain injury in adult, male rats.* J Neurotrauma, 2006. **23**(1): p. 97-108.

17. Allen, K.A., *Pathophysiology and Treatment of Severe Traumatic Brain Injuries in Children.* J Neurosci Nurs, 2016. **48**(1): p. 15-27; quiz E1.

18. Teasdale, G. and B. Jennett, *Assessment of coma and impaired consciousness. A practical scale.* Lancet, 1974. **2**(7872): p. 81-4.

19. Hoyer, C., et al., *Advantages and challenges of small animal magnetic resonance imaging as a translational tool.* Neuropsychobiology, 2014. **69**(4): p. 187-201.

20. Wei, X.E., et al., *Dynamics of rabbit brain edema in focal lesion and perilesion area after traumatic brain injury: a MRI study.* J Neurotrauma, 2012. **29**(14): p. 2413-20.